TIME AND SCALE EFFECTS ON THE SHAFT FRICTION OF DISPLACEMENT PILES IN SAND

by

Jit Kheng LIM

B.Eng. (Hons), M.Eng.

This thesis is presented for
the degree of Doctor of Philosophy of
The University of Western Australia

School of Civil and Resource Engineering
2013

DECLARATION

I hereby declare that, except where specific reference is made to the work of others, the contents of this dissertation are original and have not been submitted in whole or in part for consideration for any other degree of qualification at this, or any other, university.

Jit Kheng LIM

September 2013

ABSTRACT

The phenomenon of pile set-up (i.e. increase in pile shaft friction with time) in sand has been reported for decades but the observations are highly scattered and the mechanisms giving rise to set-up are poorly understood. The capacity gain with time, if successfully justified with greater understanding of its governing mechanisms, has major cost benefits for foundations and for the re-use of existing foundations. This thesis describes a series of laboratory and field experiments designed to track the changes of shaft resistance up to a maximum of 72 days after installation. The laboratory-scale pile tests were conducted in a pressure chamber, taking into account the interfering sample ageing effect, to study the relative influence of several important factors on pile set-up. The field tests employing three sizes of reduced-scale model piles (D = 65, 100 and 135 mm), each equipped with a surface stress transducer (SST), were installed and subsequently load-tested statically in tension at three sand sites of different mineralogy and groundwater conditions. The results, combined with other well-documented case histories, are examined to gain further insights on this longstanding contentious issue. Evidence shows that it is more appropriate to describe the phenomenon of pile set-up as a recovery process (rather than a gain) following the disturbance induced by pile installation. Set-up in the medium and longer term varies with the logarithm of time but involves a *delay* during the initial period and a *limit* after stress equilibration is reached, which can be better represented using a newly proposed expression. The measurements of SSTs reveal that the increases in stationary radial effective stress (σ'_{rs}) over the ageing period are relatively small but considerable changes in the increases in radial effective stress during shearing ($\Delta\sigma'_{rd}$) are evident. The observation suggests that the major underlying mechanism of pile set-up in sand is that of constrained dilation due to an increase in the shear stiffness of the surrounding soil following installation disturbance. To assess how model pile test results can be extrapolated to full-scale conditions, the thesis examines scale effects using a database of tension load tests comprising pile diameters which vary by more than two orders of magnitude. The UWA-05 design method, which is adopted as a base calculation approach in the assessment, indicates that the prediction of full-scale offshore piles is reasonable but the capacity of small-scale model piles required a more complex representation of the shear stiffness of the sand mass surrounding the pile shaft.

ACKNOWLEDGEMENTS

First, I would like express my sincere gratitude to my supervisor, Professor Barry Lehane, for all his time and support throughout this study. I appreciate that you always make yourself available whenever I need some advice and guidance and always respond promptly and positively with many invaluable review comments on my work. I have benefited from the knowledge not only on my research topic but also on many aspects of geotechnical engineering in general for working with you in the past 4 years.

I would like to thank Professor Mark Randolph for welcoming my interest in pursuing PhD at UWA and introducing me to a variety of interesting research topics. I am grateful to Dr Schneider and Dr Xu, Professor White, Professor Jardine and Dr Standing, and Dr Kelly who are willing to share many useful data and references related to this research topic. Professor Briaud, Dr Fiona, Dr Bowman, Dr Tan, Dr Gavin, together with Ray (UWA librarian) who assisted me in locating an old technical report are acknowledged, although the report is still (somehow) unfound.

I am indebted to Jim, Harry, Neil, Frank, Alby, Nandish and Andrew (from Civil and Mechanical workshop); John, Phil, Shane, Khin and Wayne (from Electronic workshop); Don, Bart and Manuel (from Centrifuge); and Binaya, Claire and Alex (from Soil laboratory) for the enthusiastic technical support and assistance in making the experimental work possible. The permission from COFS to use the actuator and testing facilities, the contribution of Brian and crew from Probedrill to perform the pile installation and site investigation, and the efforts of UWA final year students, Daniel, Tom, Halda, Elaine, Liam and Tim who helped out in the field and chamber testings are gratefully acknowledged.

I am grateful to the geotechnical research community in UWA, all the academics, colleagues and visitors, past and present, for many drinks and discussions during the past 4 years. Special thanks to Yusuke, Fauzan, Stefanus, Ariel, Wen, Guoyang and many others for sharing bits and pieces on research and having some great time together over the years. I am also thankful to David and Harold who showed me around and helped me in finding a temporary accommodation when I first arrived in Perth.

I would like to acknowledge the financial support from Malaysian government through Universiti Teknologi MARA (UiTM) for my scholarship, an ARC grant which funded the research, top-up scholarship from Barry, and PhD Completion Scholarship and Graduate Research Student Travel Award from UWA.

Finally, I would like to thank my family for their endless love and constant support. This thesis is dedicated to all of you: Mum, Dad, my sister Brenda and brother-in-law Francis, my wife Sandy and my two boys Daniel and Tate.

TABLE OF CONTENTS

LIST OF FIGURES

LIST OF TABLES

SYMBOLS AND ABBREVIATIONS

Roman

a	correction factor for pile end condition (ICP-05); empirical parameter that represents the effects of soil displacement (UWA-05)
A	set-up factor ($\neq B$)
A_{rs}	effective area ratio
b	empirical parameter that represents the degree of plugging
B	set-up factor ($\neq A$)
c	empirical parameter that represents the effects of friction fatigue
c_{ij}	calibration coefficients of SST
C_u	coefficient of uniformity
C_c	compression index
C_D	empirical parameter that reflects the effects of densification or disturbance induced (e.g. by vibration, blasting)
C_α	secondary compression index; creep coefficient
D	pile diameter
D_{50}	mean particle size
D_c	cone diameter
D_i	pile inner diameter
D_o	pile outer diameter
D_r	relative density
e	mean thickness of interface shear band
e_{max}	maximum void ratio
e_{min}	minimum void ratio
E_D	dilatometer modulus
f/f_c	correction factor for loading direction
FR	friction ratio
F_r	normalised friction ratio
f_s	sleeve friction
n-g	n times of gravitational acceleration

G	shear stiffness; shear modulus
G_o	small-strain shear modulus
h	vertical distance from pile tip
I_c	soil behaviour type index
I_D	material index
k	empirical parameter that controls the rate of recovery
k_n	normal stiffness
K	constant
K_0	coefficient of lateral earth pressure at-rest
K_D	horizontal stress index
K_G	empirical parameter that reflects the ageing and cementation of sand
L	pile length
L/D	pile slenderness ratio
n	empirical parameter used as a stress exponent
N_b	number of hammer blows in pile driving
N_{cyc}	number of loading-unloading cycles during installation
N_d	empirical parameter that reflects the degree of disturbance imparted during pile installation
N_{qc}	normalised change in q_c per log cycle of time
p'	mean effective stress
p_0	DMT lift-off pressure
p_1	DMT expansion pressure
p_a	atmospheric pressure (taken as 100 kPa)
P_J	final jacking force
P_{ult}	ultimate pile capacity
q	deviatoric stress
q_b	pile end resistance
q_c	cone tip resistance
$q_{c\text{-}avg}$	average cone tip resistance
q_{c1N}	dimensionless normalised cone tip resistance ($\neq Q_{tn}$)
q_{cR}	reference cone tip resistance

q_t	total cone tip resistance ($\approx q_c$ in sand)
Q	pile capacity
Q_o	initial (reference) pile capacity
Q_b	pile end resistance
Q_c	calculated pile capacity
Q_m	measured pile capacity
Q_n	normalised cone tip resistance
Q_R	reference pile capacity
Q_s	pile shaft capacity
Q_{so}	initial (reference) pile shaft capacity
Q_{sc}	pile shaft capacity in compression
Q_{st}	pile shaft capacity in tension
Q_{tn}	dimensionless normalised cone tip resistance ($\neq q_{c1N}$)
Q_u	ultimate pile capacity after 100% of set-up has been realised
Q_{UWA}	predicted pile shaft capacity using UWA-05
r	radial distance from centreline of pile
R	pile radius
R^*	modified pile radius
r^2	coefficient of determination
R_i	pile inner radius
R_o	pile outer radius
R_{cla}	centre-line average roughness
R_n	relative roughness
s	pile head displacement
s_p	minimum spacing between piles
s_w	minimum spacing between pile and wall boundary
t	time
t_o	initial (reference) time
T_{50}	time required for 50% of set-up to realise
t_{max}	maximum set-up period
t_R	reference time

t_w	thickness of pile wall
u	porewater pressure
u_o	ambient porewater pressure; hydrostatic pressure
V_i	input voltage
V_o	output voltage
V_s	shear wave velocity
z	depth
Z	normalised depth

Greek

α_s	coefficient of unit shaft friction
δ_{cv}	constant volume interface friction angle (critical state)
δ_f	interface friction angle at failure
δh	radial displacement of shear band along pile shaft
Δh_p	incremental change in plug height
Δq	increment of deviatoric stress
Δr	radial displacement of interface shear zone (= δh)
$\Delta \sigma'_r$	change of radial effective stress during shearing
$\Delta \sigma'_{rd}$	change of radial effective stress during shearing (due to interface slip dilation)
$\Delta \sigma'_{rp}$	change of radial effective stress during shearing (due to rotation of principal stress directions)
Δz_b	incremental increase in embedment depth
γ'	effective unit weight
η	dimensionless normalised cone tip resistance (= q_{c1N})
ρ	total soil density
σ_r	radial stress; radial total stress
σ_v	total vertical stress
σ'_h	effective horizontal stress
σ'_{hoop}	circumferential or hoop stress
σ'_n	normal stress

σ'_r	radial effective stress
σ'_{rc}	equilibrium radial effective stress
σ'_{rf}	radial effective stress at failure
σ'_{rmax}	maximum radial effective stress
σ'_{ro}	reference stationary radial effective stress
σ'_{rs}	stationary radial effective stress ($\approx \sigma'_{rc}$)
σ'_v	effective vertical stress
σ'_{vo}	effective overburden stress
τ_o	initial (reference) average shaft shear stress at failure
τ_{avg}	average shaft shear stress at failure
$\tau_{avg\text{-}install}$	average shaft shear stress at failure during last installation push
$\tau_{avg\text{-}test}$	average shaft shear stress at failure during tension load test
τ_d	dilation component of shaft shear stress
$\tau_{d\text{-}avg}$	average shaft shear stress of the dilation component
τ_f	local shear stress at failure
τ_{ICP}	predicted average pile shaft resistance using ICP-05
τ_{lim}	limit pile shaft resistance estimated using UWA-05
τ_{peak}	peak shaft shear stress
τ	shaft shear stress
τ_s	stationary component of shaft shear stress
$\tau_{s\text{-}avg}$	average shaft shear stress of the stationary component
τ_{UWA}	predicted average pile shaft resistance using UWA-05

Abbreviations

ALC	axial load cell
API	American Petroleum Institute
ARC	Australian Research Council
ASCE	American Society of Civil Engineers
BC	boundary condition
BOR	beginning of restrike

C	closed-ended
C-T	tension re-test preceded by a compression load test
CAPWAP	Case pile wave analysis programme
CDG	completely decomposed granite
CEP	closed-ended pile
CNL	constant normal load
CNS	constant normal stiffness
CoV	coefficient of variation
CPT	cone penetration test
CPTu	piezocone penetration test
DLT	dynamic load test
DSA	direct shear apparatus
EOID	end of initial driving
EU	European Union
FHWA	Federal Highway Administration, US
FORM	first-order reliability method
HSDPT	high-strain dynamic pile testing
IAC	intact ageing characteristic
ICL	Imperial College London, UK
ICP	Imperial College instrumented pile
ICP-05	ICP pile design method
IFR	incremental filling ratio
ISSMGE	International Society of Soil Mechanics and Geotechnical Engineering
KTH	Royal Institute of Technology, Sweden
LC	load cell
LRFD	load and resistance factor design
LVDT	linear displacement transducer
NGI	Norwegian Geotechnical Institute
NGI-05	NGI pile design method
O	open-ended

O-cell	Osterberg cell
OCR	overconsolidation ratio
OD	outer diameter
OEP	open-ended pile
PCPT	centrifuge piezocone penetration test
PIV	particle image velocimetry
RSA	residual stress analysis; ring shear apparatus
SBT	soil behaviour type
SBPMT	self-boring pressuremeter test
SCPT	seismic cone penetration test
SDMT	seismic dilatometer test
SLT	static load test
SPT	standard penetration test
SSA	simple shear apparatus
SST	surface stress transducer
T-T	tension re-test preceded by a tension load test
TC	technical committee
UCD	University College Dublin, Ireland
UF	University of Florida, US
UWA	The University of Western Australia, Australia
UWA-05	UWA pile design method

CHAPTER 1. INTRODUCTION

1.1 BACKGROUND

Displacement piles have been used as foundations to support structures for thousands of years and continue to dominate the foundation market both onshore and offshore due to their time and cost effectiveness. Advancements in construction material and piling technology have allowed large and long piles to be constructed in line with a variety of modern developments. Consequently, shaft friction, which used to be neglected with an emphasis on achieving a pile 'set', emerges as an important element governing the economies of the foundations.

The mechanisms controlling shaft friction of displacement piles are complex and changes in stress and fabric due to installation processes, for instance, are not accounted for in conventional design approaches. Improvements require proper consideration of the physical processes during installation, equilibration and loading through scientific approaches (Randolph, 2003). In sand, major advances have been achieved in the last two decades and were incorporated in recent CPT-based pile design methods (e.g. ICP-05 and UWA-05) that were shown to outperform the conventional API design method (Lehane *et al.*, 2005c). Nevertheless, these methods only provide an estimation of the medium-term pile capacity.

It is now well-documented that the shaft capacity of displacement piles in sand, similar to that in clay, increases with time after installation (Chow *et al.*, 1998; Axelsson, 2000). However, in contrast to piles in clay where the majority of time-dependent changes can be explained by consolidation theory (Soderberg, 1962; Randolph *et al.*, 1979), the excess pore pressures generated in sand during pile installation are negligible and dissipate very quickly. As a result, the long-term time effects in sand are generally perceived as a creep-induced 'ageing' phenomenon, but the underlying mechanisms and many other details remain unclear.

Although evidence of increases in pile shaft friction in sand are compelling, the observations are highly scattered and a well-defined trend line cannot be established with confidence levels required for its full incorporation in routine practice. The

majority of published data related to ageing of shaft friction in sand are from dynamic restrikes and suffer from various uncertainties. Poor understanding, inappropriate characterisation and controversial hypothesised mechanisms prompt a further investigation into the subject matter urgently.

1.2 SIGNIFICANCE

The capacity gain with time, if successfully justified with greater understanding of its governing mechanisms, will provide major cost benefits for foundation construction. This is because the application of full design loads (from superstructure) on the completed pile foundation usually takes months, whilst pile designs are generally based on static or dynamic load tests which are conducted shortly after installation when the capacities are the lowest.

Another area of major relevance of long-term capacities relates to the re-use of existing foundations. Foundation re-use is now a major consideration in many urban cities around the world, where the lifespan of typical office buildings is often less than 30 years. Chapman *et al.* (2001) anticipated that re-use of foundations would be the only practical and economical solution in the future on urban redevelopment with congested underground services and infrastructure.

1.3 APPROACH

The best way to approach such a unique and complex phenomenon is by performing careful experimental research. Instrumented full-scale pile testing, while generally perceived as the most convincing method, is rather costly. As an alternative, attempts are made to employ smaller, reduced-scale, field piles equipped with high quality of instrumentation in the investigation – similar to the well-known pile research programme undertaken at Imperial College, London.

A great advantage of the Imperial College pile test programme is that the piles incorporated a surface stress transducer (SST), which allows for the measurements of both radial and shear stresses acting on the pile shaft simultaneously. In this research, three sizes of model piles, each equipped with a SST, are installed at three different sand sites of varying mineralogy and groundwater conditions to investigate the changes of pile shaft friction over time. To avoid damages and malfunctions of the instruments

due to harsh impact driving, the model piles were installed using incremental jacking procedures that mimic the pile driving process (in terms of resultant cyclic shearing effects). Pile tests at Shenton Park capitalised on another driven pile testing programme conducted by a previous PhD candidate at the same site.

The results from these tests require detailed examination of the influence of pile diameter to allow extrapolation to full-scale conditions. At present, the scale effects are poorly understood and the compensating diameter dependency incorporated in the ICP-05 and UWA-05 formulations has not been investigated rigorously, especially over the range of small-scale diameter piles in laboratory model studies. An assessment is performed by examining the shaft friction of driven piles over a wide range of diameters (≈ 10 to 1000 mm) to gain a broader view of the expected scale and diameter effects.

Some of the limitations in the field investigation above can be complemented by employing laboratory models since the experiments are performed in a well-controlled environment and each variable can be altered more easily, which is ideal for parametric studies. Nevertheless, it is noted that there are modelling constraints such as scale effects and that associated with long-term time effects (e.g. unscaled creep factor, sample ageing), which require proper consideration in the experimental setup and testing procedures. This research employs a pressure chamber test that allows for multiple insertions of piles in one sample (as in centrifuge testing) to increase the efficiency and sample consistency.

Findings from these field and laboratory experiments, which compose the largest database of first-time loaded aged piles of varying diameters and tested under different conditions, would shed more light on the phenomenon of pile set-up. In addition, high quality sensors that trace the shaft stresses throughout the entire ageing periods could reveal valuable information of stress evolution that takes place on the pile shafts over time. Detailed analyses and careful interpretation, in conjunction with previous reported observations, are likely to provide further insights on this complex phenomenon.

1.4 THESIS OUTLINE

Chapter 2 reviews the literature relating to current-state-of-art and practice of pile set-up in sand. Particular attention is given to the uncertainties involved in quantifying set-up characteristics, which exist in the majority of the reported case histories. Instead of expanding a doubtful database, a selected body of field evidence and limited number of model studies are elaborated. Hypotheses on set-up mechanisms and empirical relationships proposed to describe the set-up behaviour are presented, as is the difference between jacked and driven piles.

Reviews on several other relevant issues are presented separately, for example: laboratory modelling constraints in Chapter 3, laboratory interface tests devices in Chapter 5 and scale effects of pile shaft friction in Chapter 7.

Chapter 3 describes a laboratory-scale model test designed to simulate the ageing effects of pile shaft friction in sand. Challenges, considerations and limitations of modelling the time-dependent phenomenon are discussed and an appropriate experimental setup and procedures are proposed. A series of tests (of varying ageing period, installation method, pile diameter, pile surface roughness, stress level) were performed and the results are presented which provide qualitative indications of the relative influence of a variety of parameters on pile set-up.

Chapter 4 describes a series of field test programmes performed at three sand sites of differing mineralogy and groundwater regimes to investigate the effects of pile set-up in sand. Three different diameters of reduced-scale model piles, each equipped with a surface stress transducer, are employed in the investigation. Recorded global and local measurements during installation, equilibration and load testing are analysed to reveal the tendency of pile set-up and the possible underlying mechanisms.

Chapter 5 further elaborates the shaft stresses measured by the surface stress transducers equipped on the model piles during the course of installation. The measurements from three separate sand sites of different mineralogy and groundwater conditions and involving different pile diameters were examined in the context of laboratory interface tests that are commonly used to model the pile shaft's response. Three instances of

brittleness of shaft shear stress observed are highlighted and the corresponding plausible mechanisms are discussed.

Chapter 6 contrasts the results of two different investigation programmes on time effects. Both were performed at the same sand site but each employed a different pile installation method. The investigation reveals a significant influence of installation disturbance on a pile's subsequent set-up behaviour. Existing methods that characterise the effects of set-up were explored and are shown to perform unsatisfactorily. A new characterisation approach is proposed which considers the phenomenon of pile set-up as a recovery process following the disturbance induced by pile installation.

Chapter 7 examines the scale and diameter effects of shaft friction on driven piles, employing the UWA-05 design method as the base calculation approach. A database comprising reliable pile tests that involve a wide range of pile scales was compiled for assessment. Necessary amendments were made by taking into account varying ageing and installation effects (due to different sources of test data) which lead to a consistent diameter dependency of pile shaft friction. The UWA-05 method was shown to predict shaft capacity of full-scale offshore piles reasonably well but the capacity of small-scale model piles was over-predicted.

Chapter 8 summarises the main conclusions from this thesis and makes suggestions for future research.

Supplementary information is provided in the appendices:

Appendix A details the calibration of SST and its performance.

Appendix B presents the results of instrumented pile tests at Ledge Point, which have been published as: Lehane, B.M., Schneider, J.A., Lim, J.K., and Mortara, G. (2012). Shaft friction from instrumented displacement piles in an uncemented calcareous sand. *Journal of Geotechnical and Geoenvironmental Engineering*, Vol. 138, No. 11, pp 1357-1368.

Appendix C describes the ICP-05 and UWA-05 pile design methods, which were employed in the analysis and interpretation in this thesis.

Appendix D presents the results of numerical integration on the UWA-05 method to disclose its diameter dependency.

CHAPTER 2. LITERATURE REVIEW

2.1 INTRODUCTION

There is a growing body of evidence from field tests showing that the capacity of driven pile in sand increases substantially after installation. The reported capacity gains (set-up), however, are widely scattered and their underlying mechanisms are poorly understood. In fact, many practitioners remain highly sceptical believing that time-dependent changes in free-draining granular materials should be very small and that those reported set-up effects are partly a result of site variability and inaccurate testing procedures.

This chapter presents a literature review on the phenomenon of pile set-up in sand. The review focuses on our current understanding based on field observations. A short list of what the author believes to be reliable field tests, together with some laboratory-based studies, are reviewed with the aim of presenting the current state-of-the-art. Existing hypotheses on set-up mechanisms and empirical relationships proposed to describe the set-up characteristics are presented and a small section is included to explore if comparable set-up effects can be anticipated for the jacked piles.

2.2 PILE SET-UP IN SAND

2.2.1 Definition

The capacities of driven piles have been reported to increase with time following installation. This phenomenon is commonly known as pile 'set-up' or 'freeze'. Field tests indicate that set-up occurs predominantly through an increase in shaft resistance (e.g. Axelsson, 2000). In clay, this has been explained by consolidation theory where excess pore pressures induced during pile installation dissipate, accompanied by an increase in lateral effective stress acting on the pile shaft (Soderberg, 1962; Randolph *et al.*, 1979). In contrast, as sand is a free draining material, excess pore pressures generated during installation are negligible and hence no appreciable gain in shaft capacity with time is expected. For that reason, set-up in sand is generally perceived as an 'ageing' effect, for which various mechanisms have been hypothesised but no consensus is reached to date.

2.2.2 General Observations

It must be noted that the general observations of pile set-up in sand as listed in the following are synthesised from previous assessments by others and are largely based on the results of dynamic load tests (some uncertainties will be discussed in Section 2.3):

- Pile set-up in sand has been reported on driven piles, regardless of pile type (e.g. concrete, steel, timber) and shape (e.g. square, circular, H, tapered), but has not been observed for bored piles. This suggests that the phenomenon is closely related to the installation disturbance.

- Set-up has been recorded in both dry and saturated sand sites (Holm, 1992; Svinkin *et al.*, 1994). Although it is difficult to isolate the effects of water when comparing one site to another, the extreme environmental changes such as the severe regular scouring effects as observed at Jamuna bridge (Tomlinson, 1996) is believed to have accelerated the set-up process.

- Set-up appears to be more pronounced at locations on the pile shaft closer to the pile base, as indicated by the strain gauges from static load tests (e.g. Chow *et al.*, 1998; Fellenius *et al.*, 2000; Kolk *et al.*, 2005b) and CAPWAP dynamic analyses (e.g. Samson and Authier, 1986; Seidel and Kalinowski, 2000; Komurka, 2004). The observations generally imply a greater tendency of set-up over the high stress regime near the pile tip.

- A few studies have suggested a greater set-up factor for soil with smaller average grain size and higher fines content (Rausche *et al.*, 1997). The relationship between particle angularity and mineralogy with set-up is not clear due to limited observations and the fact that comparison is usually complicated by other issues such as particle damage during pile driving.

- There have been a few reported case histories where the total pile capacity has reduced and not increased. The soil conditions for these case histories have generally been saturated dense silt or fine sand (e.g. Parsons, 1966; Yang, 1970; York *et al.*, 1994) and the phenomenon, which is commonly known as ‘relaxation’, has been explained as the tendency for dilatancy associated with the

development of negative pore pressures during pile driving (Peck *et al.*, 1974). The phenomenon is believed as a short-term response after driving particularly on the closely spaced pile groups.

2.2.3 Existing Databases

Chow *et al.* (1998) were the first to collate a number of well-documented case histories of pile set-up in sand. Despite some significant scatter, an average trend of 50% increase per log cycle of time or a doubling of the initial pile capacity after 100 days was deduced (Figure 2.1). The high degree of scatter was explained as being attributable to the differences in:

- The definition of initial (reference) capacity: In most cases, these capacities were measured dynamically at the end of initial driving (EOID), which involved the short-term pore pressure effects, whereas static load tests are usually performed a few days after installation.

- The types of pile load tests: Pile bearing capacity determined from dynamic and static load tests are not distinguished; not only among projects but those within the same test series. The same grouping issue applies for the shaft capacities derived from tension and compression load tests.

- The loading failure criterion: The ultimate pile capacities are determined using different failure criterion in the static load tests.

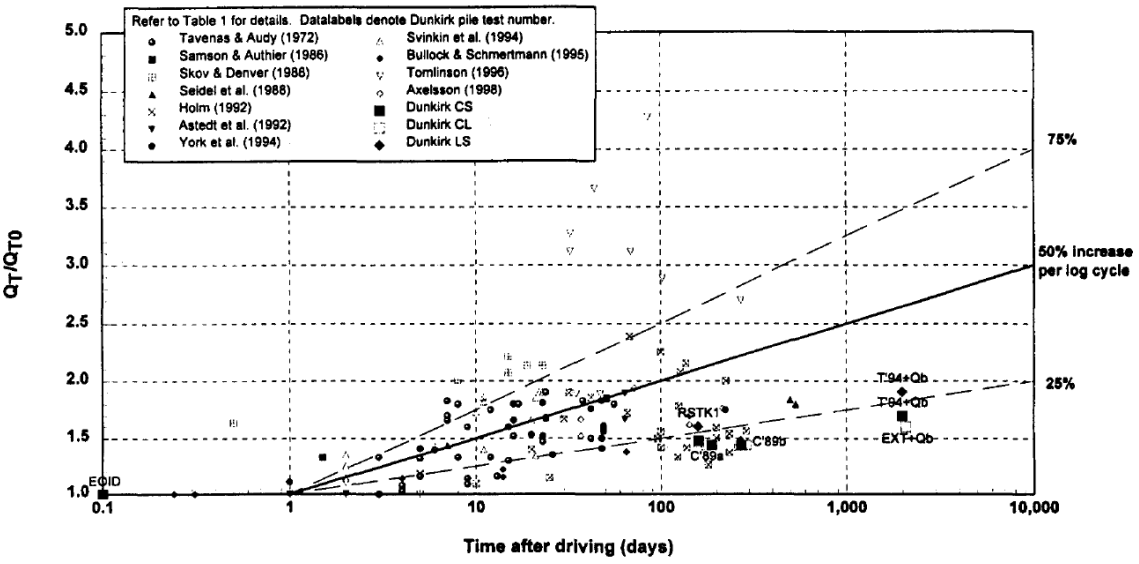

Notes: Datapoints from Bullock & Schmertmann (1995) and Tomlinson (1996) are for changes in shaft capacity only.
The potential base contributions, Q_b, in the Dunkirk 1994 tests were estimated assuming they remained the same as in C'89b.

(a)

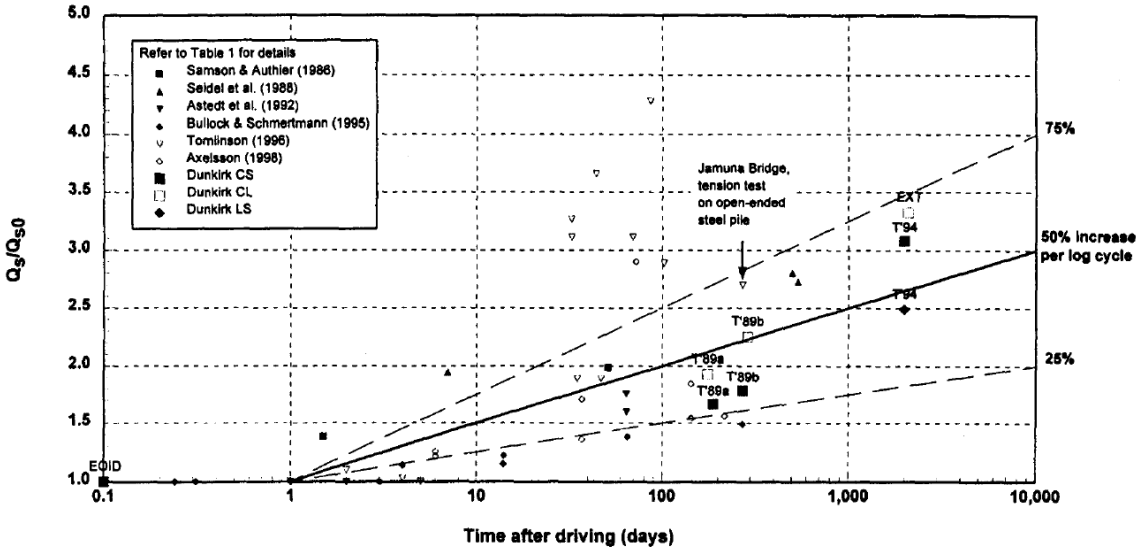

Note: The compression shaft capacities at Jamuna Bridge (Tomlinson 1996) were estimated using Chin analyses.

(b)

Figure 2.1. Increases in pile capacity with time: (a) total pile capacity; (b) shaft capacity alone (Chow *et al.*, 1998)

Axelsson (2000) revised the database by eliminating those cases for which the reference capacity was measured less than 12 hours after driving and included a few more cases mainly from European countries. A refined increasing trend line of 40 ± 25% per log time cycle was proposed and showed a good agreement with the results of his pile tests. He clarifies some other deficiencies of the existing database (besides those stated above) as follows:

- The capacities derived from dynamic load tests may not be fully mobilised if the permanent set is small. Some of the suspected cases were omitted from his database.

- Pile shaft capacity cannot be determined accurately from the measured total pile capacity without instrumentation, which is not readily available in most cases. Assumptions were made by taking a maximum of one third of the total capacity.

Others who attempted to expand the database of pile set-up in sand include Long *et al.* (1999), Komurka *et al.* (2003), Yang and Liang (2009) and Alawneh *et al.* (2009). It is noteworthy that many of the case histories are the same as those given in Chow *et al.* (1998) and the new cases included were all assessed from dynamic load tests that suffer from the limitations described above.

Table 2.1 summarises the cases considered in the existing databases mentioned above. It is noted that the majority of the case histories reported in the literature were derived from dynamic load tests and essentially all cases are based on re-tested capacities. There are a handful of recent cases of pile set-up in sand that can be traced from the literature (e.g. Axtell *et al.*, 2004; Erbland and McGillivray, 2004; Kolk *et al.*, 2005b; Shek *et al.*, 2006; Kuo *et al.*, 2007; Lee *et al.*, 2010) but these mostly have the same limitations.

Table 2.1. Summary of the type of pile load test results considered in the existing databases

Reference	Database [#]	Pile load test [Static/Dynamic]	Test condition [Fresh/Re-test]
Tavenas and Audy (1972)	1, 2, 3, 5	Static	Re-test
Samson and Authier (1986)	1, 3, 5	Dynamic	Re-test
Ng *et al.* (1988) [+]	1	Static	Re-test
Skov and Denver (1988)	1, 2, 3, 5	Dynamic	Re-test
Seidel *et al.* (1988)	1, 2, 5	Dynamic	Re-test
Holm (1992)	1	Dynamic	Re-test
Åstedt *et al.* (1992)	1	Dynamic	Re-test
York *et al.* (1994)	1, 2, 4, 5, 6	Dynamic	Re-test
Svinkin *et al.* (1994)	1, 2, 3, 4, 5, 6	Dynamic	Re-test
Bullock *et al.* (2005a) *	1, 4, 5	Static, Dynamic	Re-test
Tomlinson (1996)	1, 4	Dynamic	Re-test
Axelsson (2000) *	1, 3, 4, 5, 6	Static, Dynamic	Re-test
Chow *et al.* (1998)	1, 4, 5	Static	Re-test
Zai (1988)	2, 5	Dynamic	Re-test
Fellenius *et al.* (1989)	3, 6	Dynamic	Re-test
Eriksson *et al.* (1993) [+]	3	Dynamic	Re-test
Åstedt *et al.* (1994) [+]	3	Dynamic	Re-test
Foyn and Alstad (1999) [+]	3	Dynamic	Re-test
Attwooll *et al.* (1999)	4	Dynamic	Re-test
Koutsoftas (2002)	4	Dynamic	Re-test
Preim *et al.* (1989)	5	Dynamic	Re-test
Tan *et al.* (2004)	5	Dynamic	Re-test
Hussein *et al.* (2002)	6	Dynamic	Re-test
Fellenius and Altaee (2002)	6	Dynamic	Re-test
Svinkin (2002)	6	Dynamic	Re-test
Komurka (2004) *	6	Dynamic	Re-test
Saxena (2004)	6	Dynamic	Re-test

[#] Databases 1 – 6 refer accordingly to Chow *et al.* (1998), Long *et al.* (1999), Axelsson (2000), Komurka *et al.* (2003), Yang and Liang (2009) and Alawneh *et al.* (2009).

[+] Original document could not be located, hence secondary reference was made to Axelsson (2000).

* A later version of the document was referred to.

2.2.4 Incorporation in Design Practice

Despite large uncertainties and poor understanding of the underlying mechanisms, the effects of pile set-up have now been incorporated in some design practices. Rausche *et al.* (1997) recommend some general set-up factors based on the predominant soil type along the pile shaft as presented in Table 2.2. The set-up factor was defined as the static capacity at failure divided by the end-of-drive wave equation capacity from a database of 99 test piles from 46 sites. The recommendation has been included in the FHWA Manual on the Design and Construction of Driven Pile Foundations (Hannigan *et al.*, 1997).

Table 2.2. Pile set-up factors (Rausche *et al.*, 1997)

Predominant Soil Type Along Pile Shaft	Range in Set-up Factor	Recommended Set-up factor *	Number of Sites (Percentage of Database)
Clay	1.2 – 5.5	2.0	7 (15%)
Silt – Clay	1.0 – 2.0	1.0	10 (22%)
Silt	1.5 – 5.0	1.5	2 (4%)
Sand – Clay	1.0 – 6.0	1.5	13 (28%)
Sand – Silt	1.2 – 2.0	1.2	8 (18%)
Fine Sand	1.2 – 2.0	1.2	2 (4%)
Sand	0.8 – 2.0	1.0	3 (7%)
Sand – Gravel	1.2 – 2.0	1.0	1 (2%)

* Confirmation with local experience recommended.

Komurka (2004) demonstrated how set-up was incorporated in the design of pile foundations of a bridge project in Milwaukee, Wisconsin. A site-specific set-up distribution was first established by performing CAPWAP analyses at EOID and during restrike (at 70 days after installation), which then combined with the Case Method initial-drive capacity from dynamic monitoring results. By taking into account the effects of pile set-up, significant cost and time saving were shown by having production piles of smaller sections and shorter lengths, which could be installed using smaller hammers.

Based on the results of a pile test programme that was performed at five different sites in North Florida, Bullock *et al.* (2005b) argue that set-up does not seem to vary significantly with soil type. The programme utilised a comprehensively instrumented test pile, which was tested dynamically in the first hour and later tested statically up to a maximum of about 5 years. They recommend a default minimum set-up factor of A = 0.1 (A as defined by Skov and Denver (1988) but with t_o = 1 day; see Section 2.7.1) to be considered in the routine pile design without additional testing.

Yang and Liang (2009), whose database is included in the summary in Table 2.1, attempted to incorporate the set-up effect into a reliability-based load and resistance factor design (LRFD) of driven piles in sand. The statistical analysis shows that a lognormal distribution can be used to describe the probabilistic characteristics of pile set-up capacity. Separate resistance factors were derived to account for different degrees of uncertainties associated with measured short-term capacity and the predicted capacity gain with time using the first-order reliability method (FORM).

2.3 UNCERTAINTIES IN QUANTIFYING SET-UP

Instead of continue gathering more and more doubtful cases or leap onto the advanced probabilistic analyses based on poor quality of data, it is important to clarify the uncertainties that are involved in the assessment of pile set-up so that attention can be focused on some reliable cases, which may possibly shed more light on this complex phenomenon.

2.3.1 General Deficiencies of DLT

High-strain dynamic pile testing (HSDPT), more commonly referred to as dynamic load testing (DLT), has become an indispensable tool for installation and testing of driven piles due to its substantial savings in cost and time as compared to the conventional static load test (SLT). Dynamic load testing enables a larger proportion of piles to be tested giving rise to improved confidence in overall foundation performance. Although it has been accepted as an independent approach for pile testing in Australia (AS-2159, 2009), many design standards (EN-1997, 2009; ASTM-D4945, 2012) and piling handbooks (e.g. Tomlinson and Woodward, 2007; Fleming *et al.*, 2008) still

recommend that DLT has to be calibrated against SLT, which is recognised as the most reliable measure of static capacity.

The DLT, which involves the measurements of force and velocity near the pile head accompanied by a signal matching procedure to assess the static capacity, is known to have a number of intrinsic limitations. De Cock *et al.* (2003) contrast the typical key attributes of different types of pile tests and highlight the difficulties in converting the dynamically mobilised resistance into static resistance. Chambers and Lehane (2011) elaborated the deficiencies of DLT and show a significant degree of spread in the inference of static capacity from DLTs using a database of reported case histories. General uncertainties associated with DLTs were emphasised by Svinkin (2004), amongst others. Such uncertainties have the potential to lead to even greater uncertainties in the quantification of set-up from DLTs.

2.3.2 EOID of DLT as Reference

As noted earlier, the majority of the cases in the databases were assessed using DLTs, which, by default, offers the measured capacity at EOID as the initial reference. For pile set-up in sand, the main concern is whether the static capacity determined days after installation (as in a SLT) would continue to increase with time. Referencing at the EOID involves the short-term effects (e.g. excess pore pressure dissipation), which tends to indicate a higher set-up and mask the main objective of the study.

Another problem of taking EOID as the reference is the uncertainty in quantifying the corresponding reference time (t_o), which can be important in the characterisation of pile set-up behaviour. Svinkin *et al.* (1994) postulate an immediate response of set-up in sandy soils and consider EOID as the reference with $t_o \approx 0$. Chow *et al.* (1998) assume the t_o of EOID at 0.1 day, whereas Bullock *et al.* (2005a) approximate $t \approx 1$ min for EOID but suggest $t_o = 1$ day as a practical reference time.

2.3.3 Multiple Restrikes in DLT

DLTs are usually conducted by imparting numerous hammer blows (typically 2 – 10) on the pile head in an attempt to fully mobilise the pile bearing capacity. This practice may result in some unnecessary disturbance to the surrounding soils that affect the

subsequent evolution of set-up behaviour. For instance, Axelsson (2000) observed a reduction of the 37-day capacity for one pile (Pile A) from 1505 kN to approximately 900 kN between the first and third blow. The actual disturbance to the intact ageing behaviour could be worse since most of the case histories deployed multiple series of DLT restrikes over time in quantifying the pile set-up.

2.3.4 Under-mobilisation in DLT

As a rule of thumb, a permanent pile set between 2.5 mm and 10 mm per blow is presumed to have fully mobilised the pile capacity. If set-up is ignored and the same hammer as that used for installation is employed in the restrike testing, the resultant permanent set could be too small. This was pointed out by Axelsson (2000) and those case histories were removed from his database.

For large and/or long piles, full capacity may not be fully mobilised (to the required pile set) in a single blow at the full efficiency of hammer. Even if there is sufficient energy from the available hammer, care must be taken not to exert excessive driving stresses, which would affect the pile integrity. In this case, results from multiple blows are analysed together using a superposition method to project the full bearing capacity (Stevens, 2000; Hussein *et al.*, 2002). Rausche *et al.* (2008), however, emphasise that superposition is not a simple undertaking and is inclined to over-predict, and therefore should be avoided.

An example of set-up of a large diameter closed-ended pipe pile was reported by Mello and Galgoul (1992) who used the superposition technique in the CAPWAP analysis (Figure 2.2). It is noted from the figure that the profile at the beginning of redriving is dramatically different with that at the end of redriving (after superposition) in order to show a significant set-up along the entire pile shaft when contrasted with the profile at the end of continuous driving (EOID).

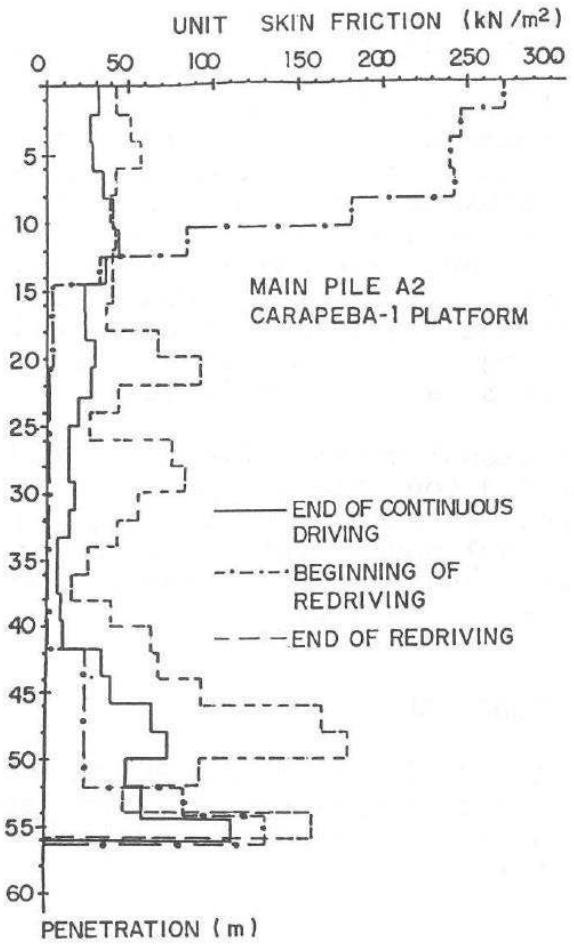

Figure 2.2. Results of CAPWAP analysis with superposition technique (Mello and Galgoul, 1992)

2.3.5 Inferred Shaft Friction from DLT

Previous research shows that set-up occurs predominantly along the pile shaft. While dynamic tests and analyses could provide reasonably accurate estimate of the total capacity in some cases, the separation of end bearing and shaft friction (and its distribution) is less reliable. The uncertainty was demonstrated by Seidel and Kalinowski (2000) through an example of set-up observed for an open-ended steel pipe pile which was driven into a dense to very dense sand layer. CAPWAP capacities at blow 2 and blow 6 during the 3rd restrike (22 days after installation) showed fairly consistent results of the total capacity (21.9 MN and 21.4 MN respectively) but contributions from the shaft and toe are quite different (21.4 and 0.5 MN for blow 2 and 17.4 and 4.0 MN for blow 6, respectively).

Another indication of some of the approximations made is provided by Bullock *et al.* (2005a), who adjusted the CAPWAP end bearing to an assumed constant and considered any changes in the measured total capacity over time are all resulted from shaft friction. In addition, the separation also depends on whether the option of residual stress analysis (RSA) was considered. A CAPWAP analysis using the RSA option usually results in less shaft friction and more toe resistance (with same total pile resistance) as compared to a non-RSA analysis (Komurka, 2004).

2.3.6 Combination of SLT and DLT

The inferences made from some of the case histories that used a combination of DLTs and/or SLTs (as presented by Chow *et al.* (1998) and others) may lead to unreliable/ inaccurate conclusions. In most cases, the SLT is a single testing event, which was combined with the results of DLTs (at EOID and/or BOR) that were performed at different ageing periods to assess set-up. It could be argued that a more consistent approach would use either DLTs or SLTs only – and not a combination of both.

A further reference highlighting the potential for discrepancies between DLT and SLT was reported by Axelsson (2000), who load tested an instrumented concrete pile (statically in compression followed by dynamically on the same day) five days after EOID. Load test results indicate that the CAPWAP total capacity overestimated the Davisson capacity by 36%. Moreover, the toe capacity from the CAPWAP analysis was clearly smaller than that measured by the toe cell (in spite of a relatively large permanent displacement of 14 mm being mobilised) resulting in significant discrepancy in the assessed shaft capacities.

2.3.7 Inferred Shaft Friction from SLT in Compression

It is almost impossible to infer accurately the shaft friction of an un-instrumented pile from a static compression load test. A rough inference can be made using some empirical approaches, such as the Chin method (Chin, 1970), which was employed by Tomlinson (1996) in quantifying the increases of pile shaft friction with time for Jamuna Bridge project. As a common rule, the Chin failure load is expected to be 20% to 40% greater than the Davisson limit as reported by Fellenius (1980). Limitations of Chin method were further discussed by Fleming (1992).

2.3.8 SLT in Compression Not Conducted to Full Failure

Even in cases where the total capacity is determined in a static compression load test, some ambiguity on the evaluation of set-up potential may exist if, for instance, the tests are not conducted to full failure. Fellenius (2002) replotted the results of static compression load tests performed by Axelsson (2000) at 1 day, 8 days, 4 months and 22 months after installation against the cumulative pile head movements (instead of a common origin for each re-test) and argues that the observed increases in pile capacity with time could be simply a continued mobilisation of its ultimate capacity (Figure 2.3).

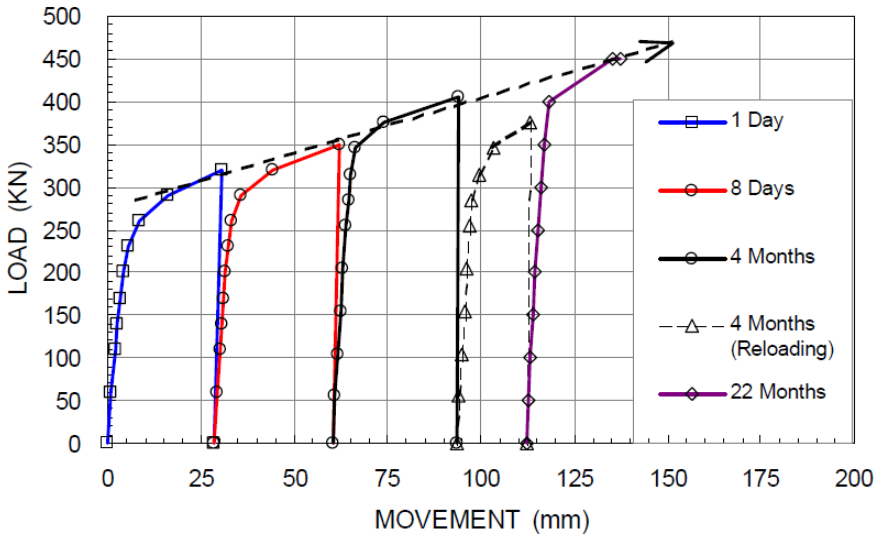

Figure 2.3. Results of static load tests on Pile D plotted against cumulative pile head movements (Replotted by Fellenius (2002) based on data from Axelsson (2000))

2.3.9 Tension Re-tests in SLT

As described earlier with reference to multiple restrikes in DLTs, there is also potential for errors associated with the inference of set-up of shaft friction from static tension re-tests of the same piles performed at specific ageing periods. For examples, Jardine *et al.* (2006) showed that in a full-scale pile test programme involving tension tests performed over a period of eight months (consists both first-time tested and re-tested aged piles), 'fresh' piles (i.e. those only subjected to load testing once) exhibited much greater capacity gain than those of previously failed piles. They refer to as the intact ageing characteristic (IAC) to describe the genuine ageing effect of driven piles, which appears

to be higher than the average trend derived from existing database (this is discussed further in Section 2.4.6).

2.3.10 Different Re-tests in SLT

Re-tested shaft capacities also vary with the loading histories. For example, the ultimate resistance measured in a tension re-test that follows from a compression load test (C-T) can differ from that if it had been subjected to an earlier tension load test (T-T). Chow (1997) observed a consistent reduction of shaft resistance together with a softer loading response when the shearing direction is reversed. It is even more complex if the pile is subjected to differing degrees of cyclic loading in between the assessment of set-up behaviour. While high level cycling inflicts damage, low level cycling leads to modest gain in tension capacity (Jardine *et al.*, 2006; Tsuha *et al.*, 2012).

2.3.11 Shaft Friction from Tension and Compression SLTs

Another issue that needs to be considered when inferring set-up from SLTs is the higher shaft friction of piles when tested in compression compared to that under tension loading. This effect has been observed in field tests (e.g. Beringen *et al.*, 1979; Lehane *et al.*, 1993) as well as model experiments (e.g. O'Neill and Raines, 1991; De Nicola and Randolph, 1999) but no such distinction appears to have been made when assessing set-up from databases. Lehane *et al.* (1993) suggest that the difference is partly due to the changes of mean effective stress associated with different rotation of the principal stress direction. Other potential mechanisms, including the Poisson effect, were addressed theoretically by De Nicola and Randolph (1993).

2.3.12 General Comment on Quantification of Set-up

In order to minimise the uncertainties in quantifying pile set-up, the ideal approach would be to compare a series of first-time loaded (fresh/virgin) ultimate pile shaft capacities through SLTs in tension in a homogeneous sand site at different ageing periods. This is certainly a very costly and time-consuming undertaking. The GOPAL project (Jardine *et al.*, 2006) complies to the requirements stated above, and hence is

one of very few field-scale case histories to provide an unambiguous reference for the set-up characteristics.

2.4 SELECTED FIELD EXPERIMENTS

Owing to various uncertainties that exist in the databases assembled to assess pile set-up in sand, it is important to re-examine the well-documented studies available in the literature. Priority is given to those case histories where pile capacities were assessed using reliable static load tests – preferably with instrumentation that measured the shaft friction distribution. Other information such as sand type and pile size are reported below so that any potential trend for a dependence of set-up on sand type and pile diameter can be explored. The selected case histories are presented in the following:

2.4.1 St Charles River, Quebec (Tavenas and Audy, 1972)

This case history reports an evidence of pile set-up on foundation piles for two 3.8 km long retaining walls constructed on both sides of the St Charles River in downtown Quebec City. The soil conditions are very uniform and consist of about 5 m of backfill overlying a thick deposit of fine to medium sand ($D_{50} \approx 0.28$ mm, < 10% fines). The groundwater table was about 5 m below ground level during the site investigation. Standard penetration tests (SPT) gave *N*-values that increased slightly with depth, with an average of about 23.

The precast concrete piles employed were hexagonal in shape, with an equivalent diameter of 320 mm and ranged from 8.5 m to 14.0 m in length. A total of 39 piles, driven at various locations on both shores of the river were selected for load testings. The results of static compression re-tests performed at different ageing periods indicate a substantial increase when compared to the ultimate bearing capacities of the corresponding piles previously measured at 12 hours after installation (Figure 2.4). A tentative trend line was proposed suggesting a potential 70% capacity gain in 15 to 20 days' time after installation, which remains constant thereafter.

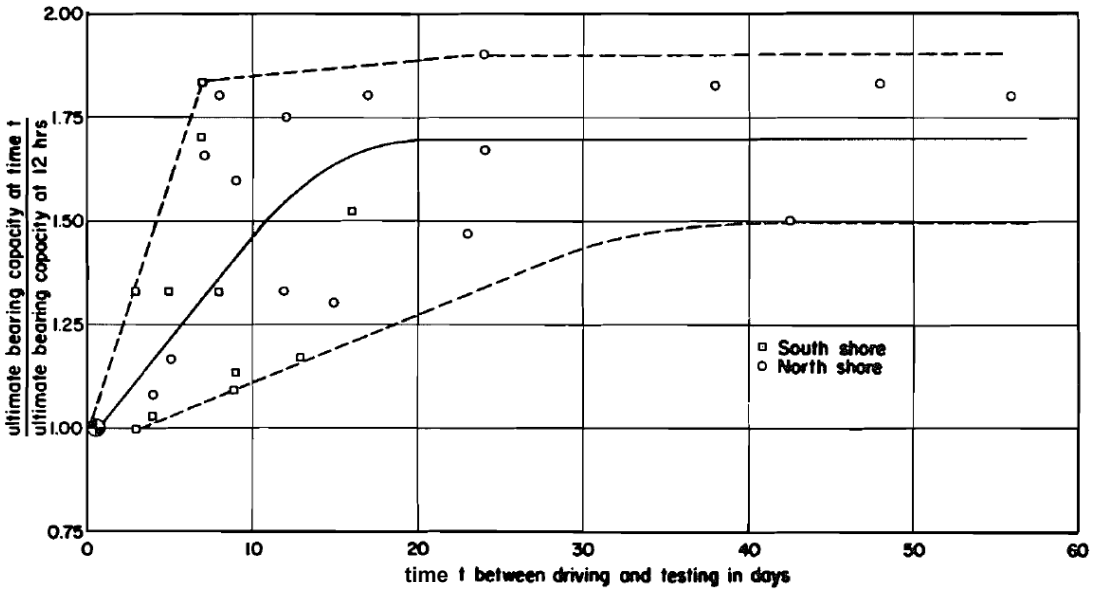

Figure 2.4. Increase in total pile capacity with time (Tavenas and Audy, 1972)

2.4.2 CLAROM (Chow, 1997; Chow *et al.*, 1998)

In the CLAROM project, four open-ended steel pipe piles (designated as CS, CL, LS and LL) of 324 mm outer diameter and 12.7 mm wall thickness (with a thicker internal shoe of 19.1 mm at the toe of CS and LS) were driven to the final embedded lengths of 11 m (CS and CL) and 22 m (LS and LL) in 1988. Partial plugging was observed with the plug heights measured at about half the embedded pile lengths. The short piles were fitted with thirty strain gauges distributed over ten levels for detailed investigation. All four piles were tested dynamically, and a series of static tension and compression load tests were performed on the short piles.

The test site is at Dunkirk, on the coast of northern France. The stratigraphy consists of about 30 m of medium to very dense (average D_r of 75%) marine Flandrian Sand overlain by 3 m of very dense hydraulic sand fill. The water table was 4 m below ground level. The Flandrian Sand is uniform, fine to medium, subrounded to rounded, with a mean particle size D_{50} of 0.25 mm and composed (on average) of 84% quartz, 8% feldspar and 8% calcium carbonate shell fragments.

Tension re-tests performed on CS in 1994 show that the average shaft resistance was 85% greater than that measured five years earlier in 1989 (Figure 2.5). A similar trend (without detail measurement) was also observed for the long pile CL. Local measurements from strain gauges reveal that the capacity gain mainly arose from the large increases in friction along lower length of the pile shafts (Figure 2.6).

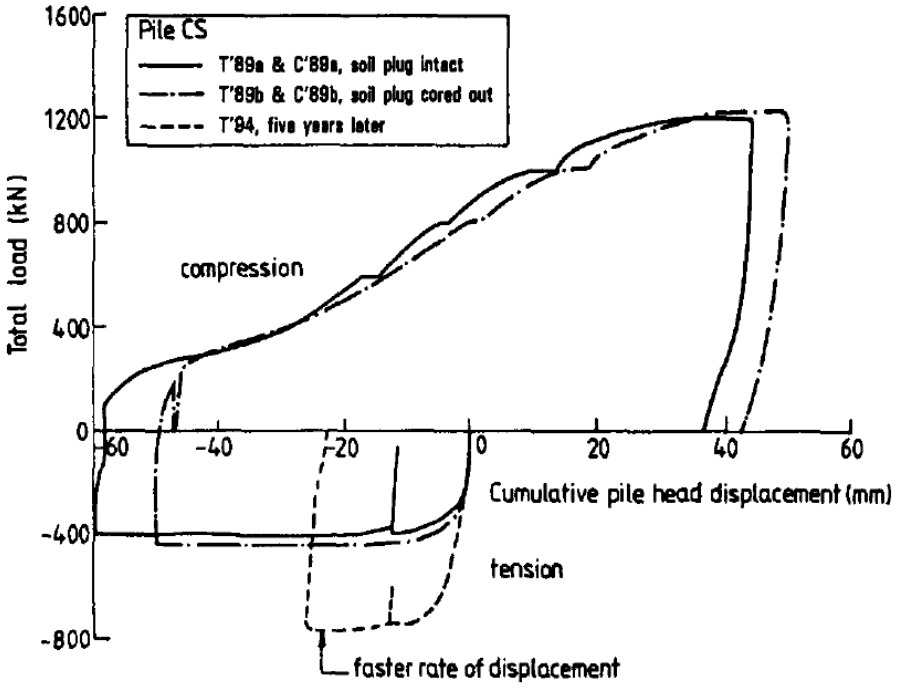

Figure 2.5. Load-displacement curves for Pile CS

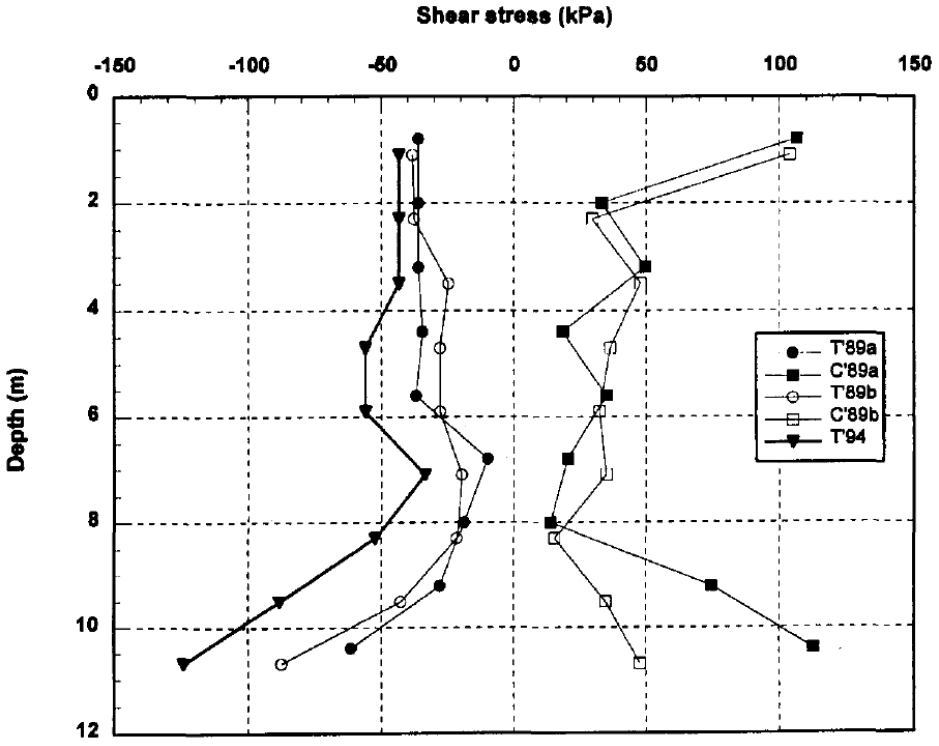

Figure 2.6. Shear stress distribution at failure for Pile CS

2.4.3 UF (Bullock, 1999; Bullock *et al.*, 2005a, b)

A research programme on side shear set-up of driven piles was initiated by researchers from University of Florida (UF) in 1994. Five 457 mm square prestressed concrete piles were driven into a variety of coastal plain soils at different sites in Florida, of which two composed primarily of sand: weakly cemented, loose to medium overlying dense fine sand at Buckman Bridge (BKM) and dense fine sand with different degrees of shell contents at Vilano Beach Bridge East (VLE). The test pile was heavily instrumented with Osterberg-cell, vibrating wire strain gauges, piezometers, Marchetti dilatometer total stress cells and telltale rods.

The piles at BKM and VLE were driven to embedded lengths of 9.16 m and 10.68 m, respectively, almost entirely below the groundwater surface. The piles were then 'staged' tested (re-tests) over time, first dynamically (at end of driving and about 20 minutes and 1 hour after installation) and subsequently statically using the O-cell test procedure (at pile age of approximately 6 hours, 3 days, 16 days, 66 days and 268 days; no data for VLE after 16 days).

Results of O-cell re-tests show that the measured increases in side shear resistance are much lower than those reported in the literature. The overall set-up factor A (A as defined by Skov and Denver (1988) but with t_o = 1 day; see Section 2.7.1) were found at 0.174 and 0.118 for BKM and VLE, respectively (Figure 2.7). The overall findings from this project should be read with caution since most of the summary statistics and many concluding remarks are based primarily on the observations from clay sites.

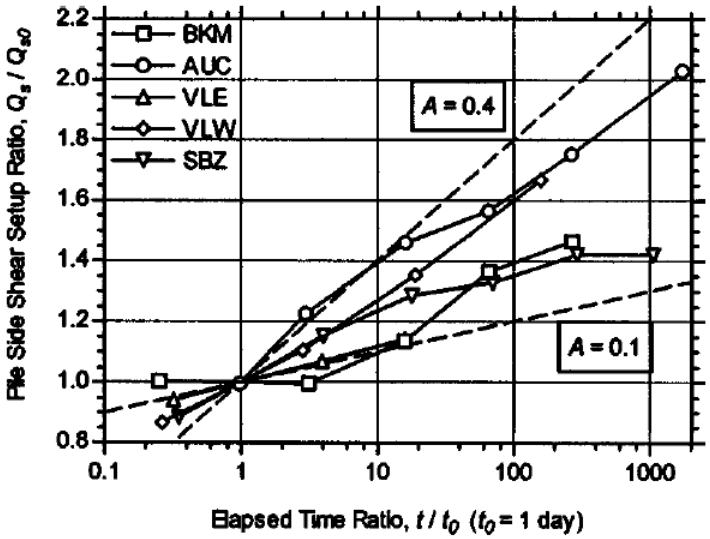

Figure 2.7. Pile side shear set-up ratio against elapsed time ratio (Bullock *et al.*, 2005a)

2.4.4 EURIPIDES (Zuidberg and Vergobbi, 1996; Kolk *et al.*, 2005b)

An extensive pile load test programme was initiated by a Joint Venture of Fugro Engineers B.V. (The Netherland) and Geodia S.A. (France) in 1995. An instrumented open-ended steel pipe pile of 0.76 m outer diameter was driven in very dense sands at Eemshaven, The Netherlands. The pile was extensively instrumented (particularly near the pile toe) with 95 sensors comprising axial and tangential strain gauges, total pressure cells, pore pressure cells, toe load cells and thermocouple mounted over the lower 27 m section. The site stratigraphy is typical of that in the southern North Sea, which consists of very dense (q_c ranges from 40 to 80 MPa), overconsolidated silica Pleistocene sand at depth, overlain by made ground and Holocene sand (average q_c of 5 MPa), which is about 22 m thick.

The instrumented pile was driven and tested statically in both compression and tension at the first location at three penetration depths (30.5 m, 38.7 m and 47.0 m). At the second location, the pile was driven and tested at the penetration depth of 46.7 m after 6 days and then re-tested after 1.5 years. Re-tests performed after ageing period of 533 days show remarkable increases in pile capacity of more than 64% and 48% compared to their initial capacities in tension and compression, respectively. Much higher set-up could have been proven if the loading system allowed application of the true ultimate capacity (Figure 2.8). The unit skin friction derived from the strain gauge measurements indicated that the set-up mainly occurred along the lower levels of the pile shaft (Figure 2.9).

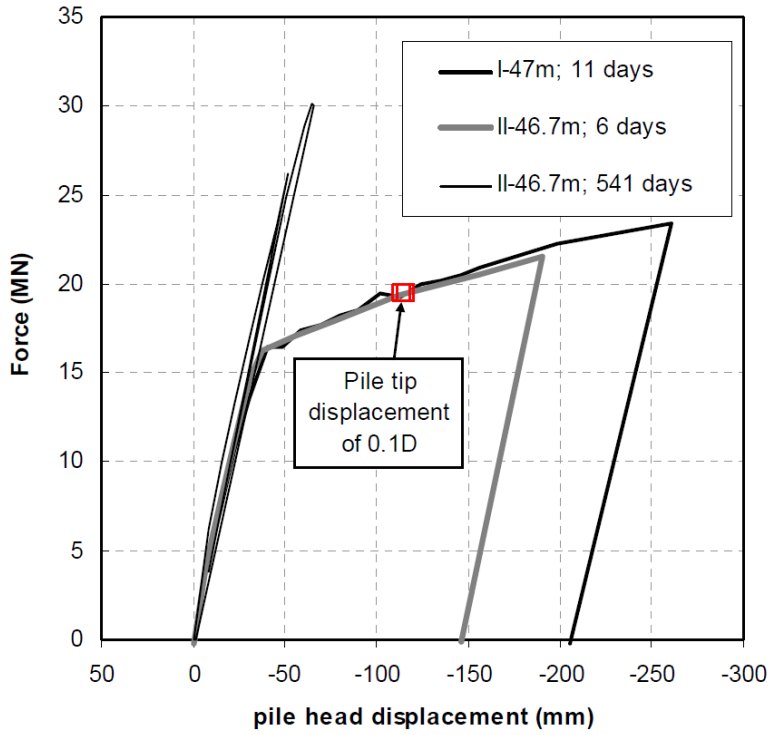

Figure 2.8. Load-displacement curves for EURIPIDES (Replotted by Schneider (2007) based on data from Kolk *et al.* (2005b))

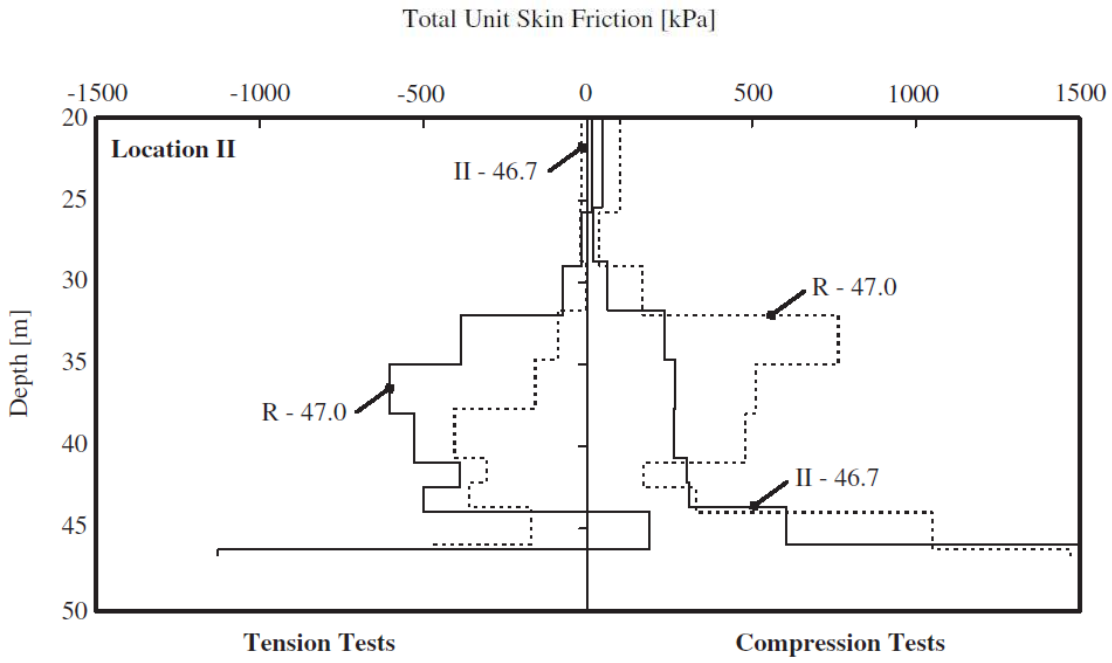

Figure 2.9. Distribution of total unit skin friction at 0.1*D* pile toe displacement for EURIPIDES (Kolk *et al.*, 2005b)

2.4.5 KTH (Axelsson, 2000)

From 1995 to 1999, two series of field experiments were conducted next to the Fittja Straits at Vårby, situated 20 km southwest of Stockholm, by researchers from the Royal Institute of Technology, Sweden (KTH). The stratigraphy at the test site consists of more than 40 m of well-graded, loose to medium dense (D_r estimated between 35-50%) glacial sand. The groundwater table lies approximately 2 m below ground level. Mineralogical investigation shows that the sand grains mainly composed of hard minerals such as quartz and feldspars.

The first series of experiments involved three 235 mm square concrete piles (Piles A, B and C), of which two (Pile A and C) were instrumented with earth pressure cells and piezometers on the shaft at various depths, driven to final penetration depth of 19.1 m and dynamically tested at various points of time. In the second series, an instrumented concrete pile of the same size as previous (denoted Pile D) was driven to a depth of 12.8 m and load tested statically in compression at 1, 8, 141 and 667 days after final installation.

The results of static load tests indicate that pile capacity increases linearly with the logarithm of time without any tendency to level off after 22 months (Figure 2.10). As revealed by the gauges, the capacity gain mainly took place along pile shaft and the majority of the increase (estimated at 65%) was attributed to an increase in dilatancy during shearing over time (Figure 2.11). Average stress paths on the pile shaft and the changes over time are illustrated in Figure 2.12.

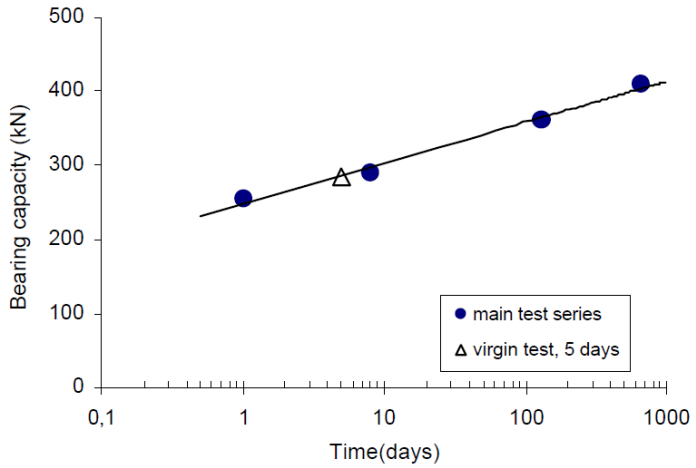

Figure 2.10. Increase in total pile capacity with time (Axelsson, 2000)

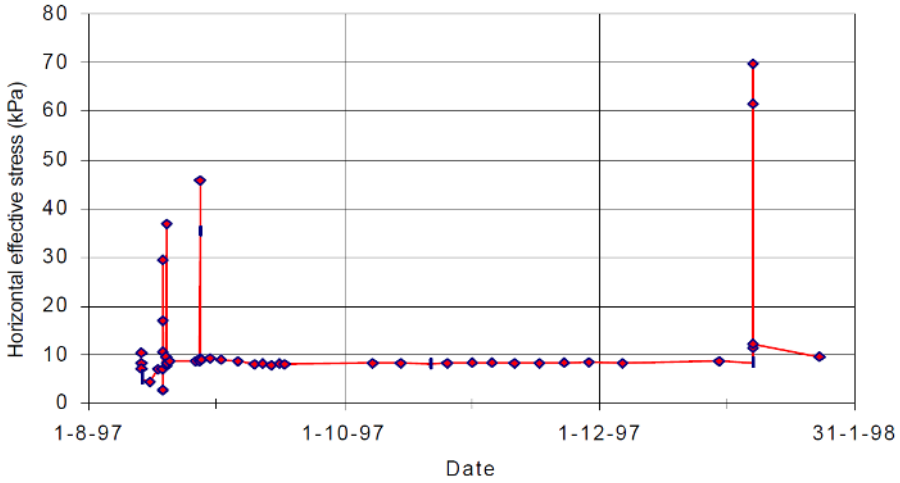

Figure 2.11. Measurements of horizontal stresses on pile shaft for cell D1 (Axelsson, 2000)

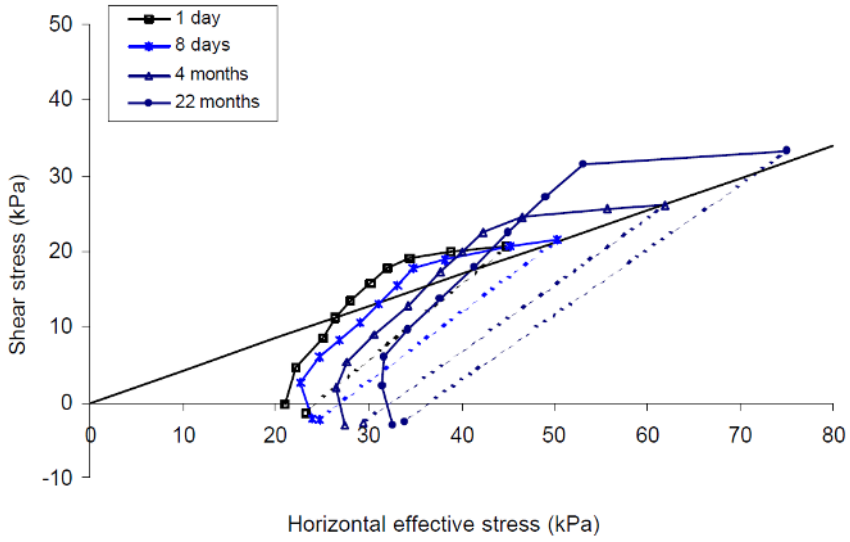

Figure 2.12. Changes of average stress paths on pile shaft over time (Axelsson, 2000)

2.4.6 GOPAL (Jardine and Standing, 2000; Jardine *et al.*, 2006)

In the EU-funded GOPAL project, which aimed to study the behaviour of piles enhanced by jet-grouting, a secondary programme was incorporated to investigate the time-dependent behaviour of driven piles in sand over a period of eight months beginning in 1998. The field tests were conducted within 70 m of the CLAROM project test site as described in Section 2.4.2 and hence share the similar ground conditions.

Six open-ended steel pipe piles (labelled as R1 to R6) of 457 mm outside diameter and 13.5 mm wall thickness (except a thicker 20 mm section over the upper 2.5 m) were driven to final penetrations of between 18.9 m and 19.4 m; these piles were installed as reaction piles for a main test pile. Internal soil plugs were measured during pile driving and found to occupy about 60% of the pile length. The piles were considered as 'fresh' or un-failed piles for subsequent static tension and cyclic loading tests over the eight-month period as they were not subjected to greater than 60% of their expected tension capacity during the main load test.

The main findings from the experiments on set-up are:

- The first-time tension load tests conducted on piles R1, R6 and R2 at 9, 81 and 235 days after installation (Figure 2.13) provide a unique set of long-term set-up data on 'fresh' piles and provides what Jardine *et al.* (2006) refer to as the intact ageing characteristic (IAC). The set-up effect for the IAC is significantly higher than existing trend line derived from database that comprises a mixture of first-time tests, re-tests and restrikes (Figure 2.14).

- The series of tension re-tests on pile R1, which were performed at 57 and 239 days after installation (without complex loading histories like others), in conjunction with its first-time tension test at 9 days, indicates a much lower capacities and slower growth rate compared to the dataset of 'fresh' piles described above. The capacity change follows a zigzag pattern with capacity decreasing during tests but subsequently increasing during the pause periods before subsequent re-tests (Figure 2.15).

- The piles that were subjected to tension re-tests show a brittle response as observed from their load-displacement curves (Figure 2.16). This brittleness is not apparent on the first-time tested 'fresh' piles (Figure 2.13).

- Tension re-tests on a pile that was subjected to a series of low-level cyclic loading one day before testing (pile R4) shows a much higher set-up effects than another identical pile of comparable ageing period but without cyclic loading (pile R3).

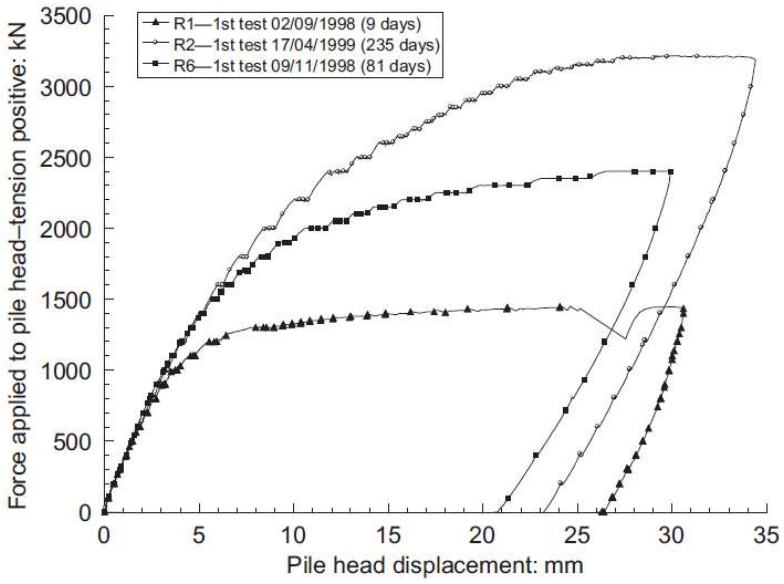

Figure 2.13. Load-displacement curves for first-time tension load tests (Jardine *et al.*, 2006)

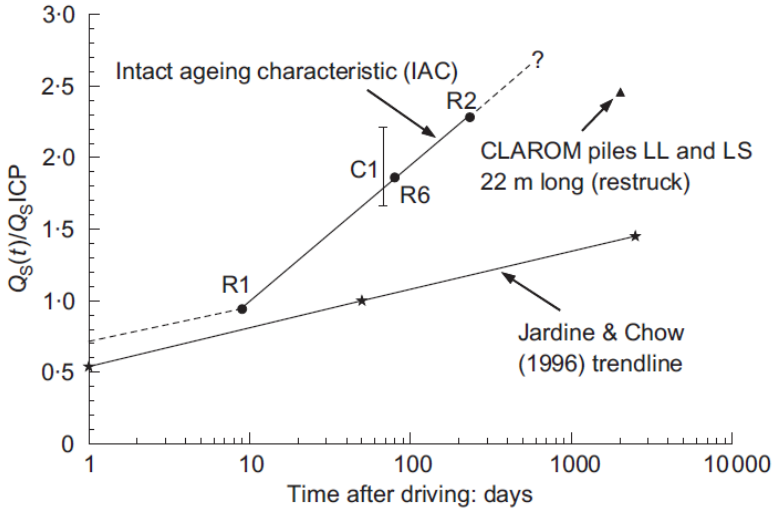

Figure 2.14. Normalised shaft capacities against time for the first-time tension load tests (set of R1, R6 and R2 that forms IAC) (Jardine *et al.*, 2006)

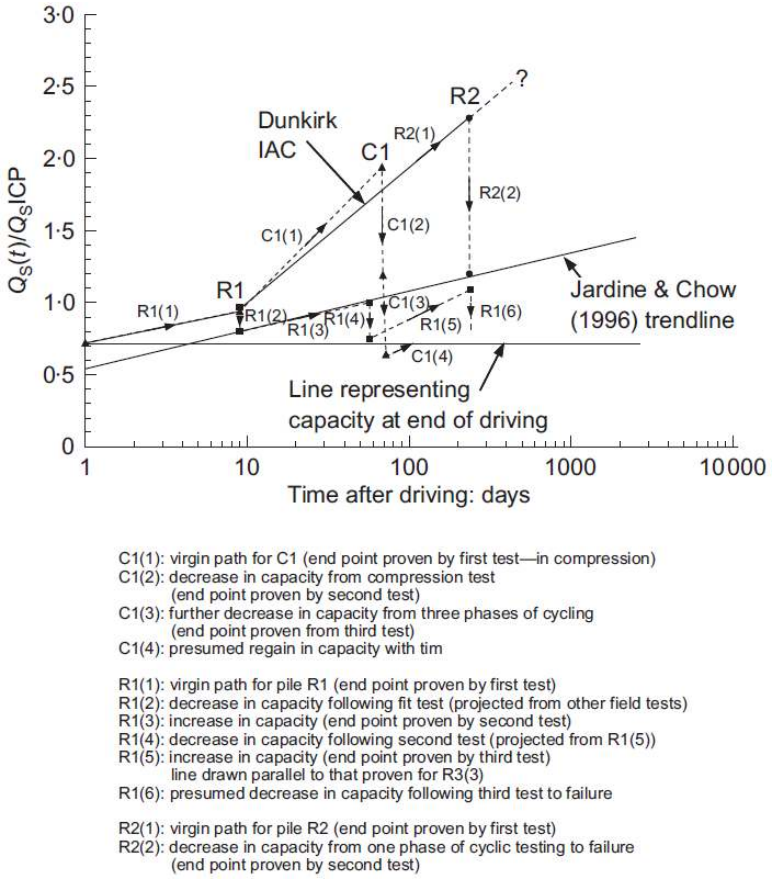

Figure 2.15. Changes of normalised shaft capacities with time for first-time and re-tested tension load tests (Jardine *et al.*, 2006)

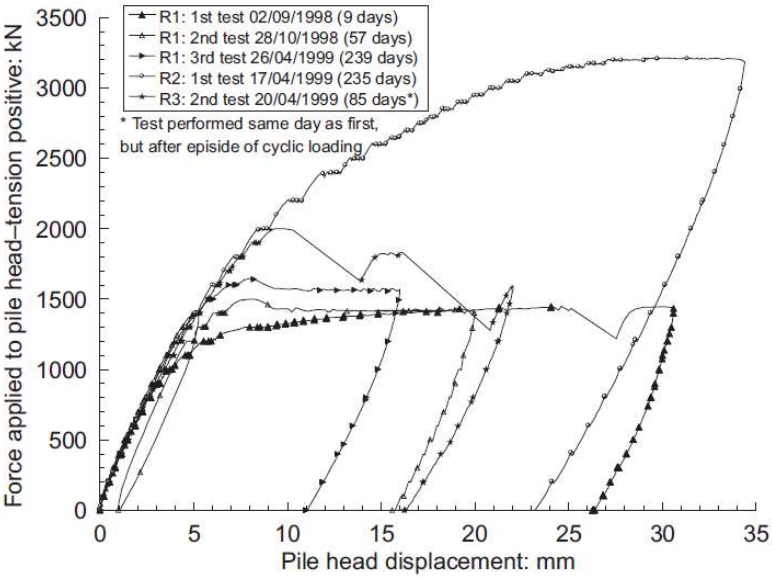

Figure 2.16. Selection of load-displacement curves for first-time and re-tested tension load tests (Jardine *et al.*, 2006)

2.4.7 UWA (Schneider, 2007)

In 2005, a pile test programme was conducted at The University of Western Australia (UWA) test bed site at Shenton Park. This area is categorised as Tamala Limestone formation of which the overlying stratum (ranges 4 to 14 m) is predominantly medium dense siliceous sand with mild traces of carbonates that provides very weak cementation and bonding between particle grains. The groundwater table is at the base of the sand stratum and the sand maintains a low level of saturation that varies slightly between wet and dry season. The sand is sub-angular to sub-rounded, uniformly graded with a mean particle size (D_{50}) of 0.42 mm and coefficient of uniformity (C_u) of about 2.

Twelve un-instrumented steel pipe piles (P01 to P12) of various configurations were driven to a maximum depth of 4 m and series of static tension re-tests over a period of 1 year were performed to study the behaviour of pile set-up in sand. The model piles are mostly open-ended (except P03 and P12), ranged from 33.7 mm to 114.3 mm outer diameter and were 2.5 m to 4 m long. Installation was performed by dropping a 25 kg mass (except P7 with a 10 kg mass) from a fall height of 0.5 m.

Results show a significant increase in pile shaft capacity with time in all cases. Closed-ended piles and the open-ended piles with higher effective area ratios were subjected to larger numbers of installation blows during installation and these piles tended to have higher rates of capacity gain with time (Figure 2.17). The increases are much higher (up to 12 times its initial capacity for P03) than previously observed in case histories.

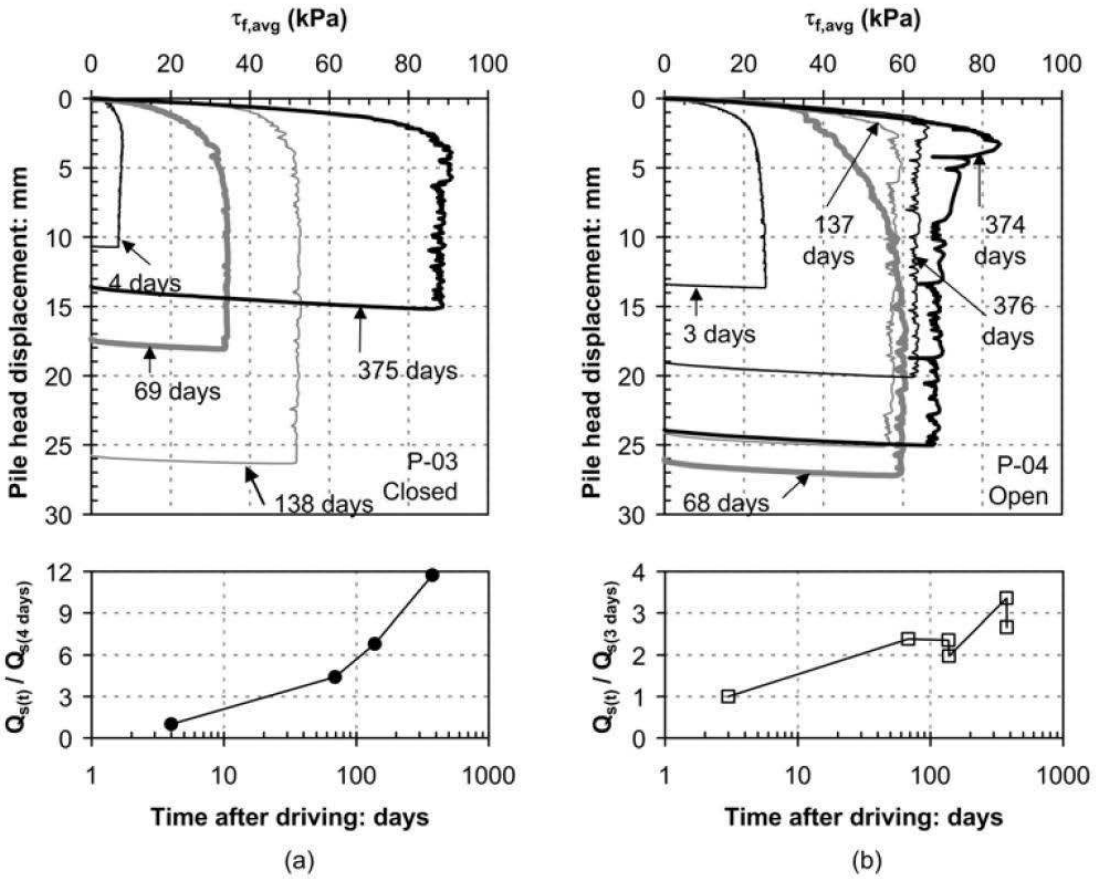

Figure 2.17. Typical load-displacement curves and set-up characteristics for (a) closed-ended piles and (b) open-ended piles at Shenton Park (Schneider, 2007)

2.4.8 UCD (Gavin *et al.*, 2013)

Most recently, a pile test programme investigating the ageing effects of piles in sand was conducted at the University College Dublin (UCD) test site located in Blessington, about 25 km southwest of Dublin city. The test site comprises very dense ($D_r \approx 100\%$), heavily overconsolidated, glacially deposited fine sand (D_{50} of 0.1 – 0.15 mm with 2 – 14% of fines). The groundwater table was well below the pile tip level and the sand deposits exhibited an in-situ water content of approximately 10% without seasonal effects.

The investigation employed four open-ended steel pipe piles (designated S2 to S5) with an outer diameter of 340 mm and wall thickness of 14 mm. Pile S5 was instrumented with miniature pressure gauges fixed at vertical distances above pile tip (h) of 1.5, 5.5, 10.5 and 17.5 times the pile diameter (D). The piles were driven to a final embedment of 7 m below ground level and first-time tension load tests were performed at 1 day, 12 days, 30 days and 220 days after installation.

Results show that the shaft capacity of piles increased by 185% over a period of 7 months after driving (Figure 2.18). The observed ageing effects compare reasonably well with the ICP-05 prediction in concert with intact ageing characterisation line proposed by Jardine *et al.* (2006). Nevertheless, the result of S4 (with relatively lower q_c and higher IFR) was ignored in the overall interpretation which resulted in a linear trend on the logarithmic time scale and without any tendency of lower set-up during the initial period.

The changes of the stationary radial stresses revealed by pressure gauges on the pile S5 over the ageing period of 220 days were reported to be small (decreased at h/D of 1.5 but increased at h/D of 5.5 and above). However, the increases in radial stresses during loading were noticeably large relative to the stationary values (Figure 2.19). No further interpretation is possible with a single set of data on an aged pile. Gavin *et al.* (2013) concluded that pile ageing is attributed to a combination of creep-induced increases of stationary radial effective stresses, enhanced dilation and increased interface roughness (due to observed sand bonding on S5 after 220 days) but did not evaluate their relative contributions.

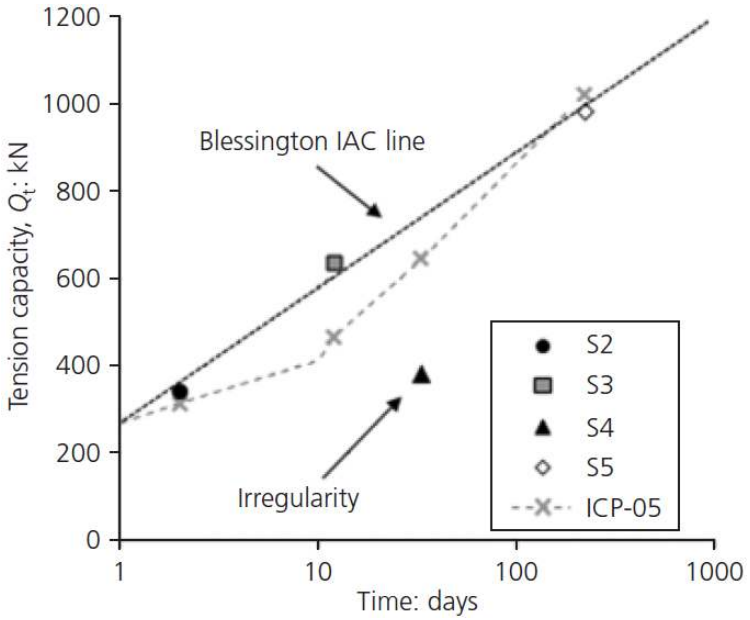

Figure 2.18. Increases in first-time tested shaft capacity with time (Gavin *et al.*, 2013)

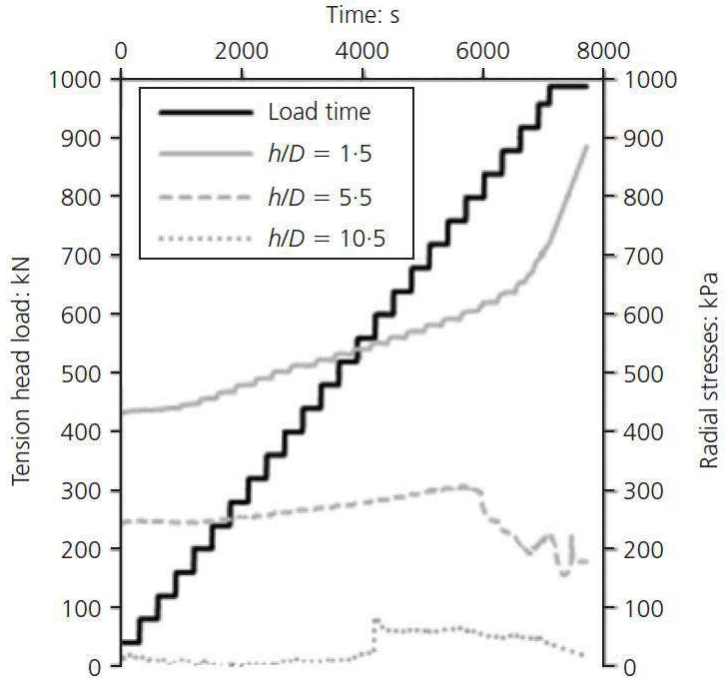

Figure 2.19. Variations of radial effective stress during load test on pile S5 (Gavin *et al.*, 2013)

2.4.9 General Comment on Field Experimentation

The field evidence provided in the preceding sections confirms the existence of pile set-up in sand, which occurs predominantly along the lower section of pile shafts. However, most case histories either comprised re-tested capacities or were un-instrumented, hindering further explanation of this complex phenomenon. For instance, the observed set-up remains very variable ranging from about 50% over the first year (Axelsson, 2000) to more than 1000% for the comparable ageing period (Schneider, 2007). In addition, other than IAC, there are other factors which may lead to significant set-up effects as indicated in some cases that involve re-testing (Tomlinson, 1996; Schneider, 2007).

2.5 LABORATORY EXPERIMENTS

Physical modelling is an important experimental technique commonly employed in geotechnical engineering. Great advances have been made over the last few decades following some improvements on modelling techniques and technology. However, some specific issues such as viscous behaviour, ageing characteristics and particle size effects remain problematic (Simpson and Tatsuoka, 2008). Attempts to model the phenomenon of pile set-up in sand in the laboratory were reported in the literature but no satisfactory results are obtained so far.

2.5.1 Bullock, 1999

An attempt to model pile set-up behaviour using a centrifuge facility was reported by Bullock (1999). A model pile was manufactured from a 420 mm long, high strength steel rod with a diameter of 9.52 mm. Sand specimens (typical Florida sand with D_{50} of 0.46 mm and C_u of 1.7) were prepared to loose, medium and dense consistencies by dry pluviation, followed by densification on a shaking table. The pile was driven to an embedded length of 254 mm at centrifuge acceleration of 50-*g* using a model pile driver, which could provide a variety of driving sequences and subsequently statically load test the pile in flight without the need to halt the centrifuge.

A series of static tension re-tests was performed to failure (without unloading the pile in between test stages) at 15 minutes, 2 hours and 4 hours after driving. Results indicated a minor loss of pile shaft friction at the beginning of each stage of testing (Figure 2.20).

The tests were repeated with the pile completely unloaded between stages and reduced the shear displacement to the minimum (4 – 5 mm) in order to minimise the discrepancy of contact area between tests. Test results up to a maximum elapsed time of 6 hours after driving confirm the earlier observation (Figure 2.21). It was concluded that centrifuge model testing does not accelerate pile set-up in dry sands.

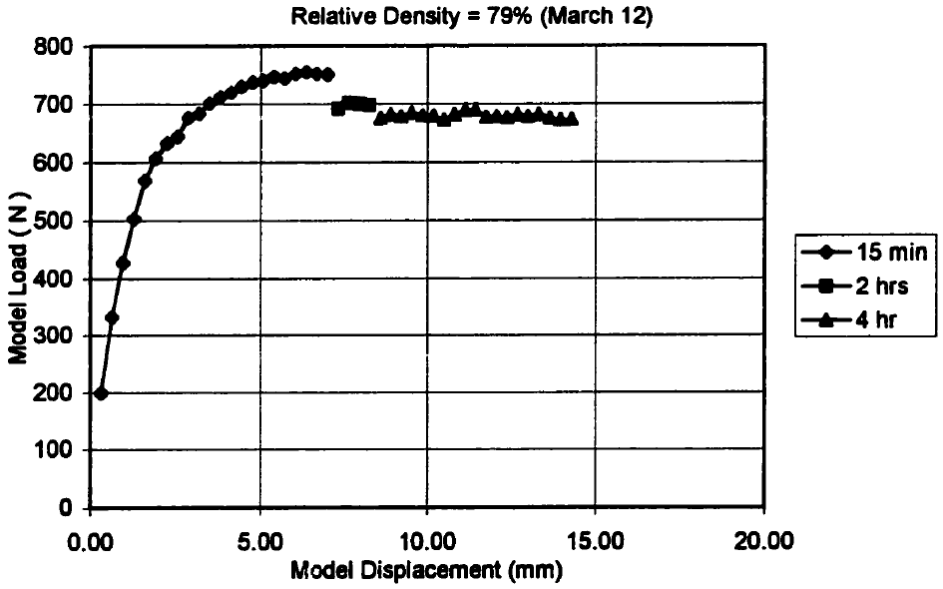

Figure 2.20. Results of staged tension tests: without unloading in between stages (Bullock, 1999)

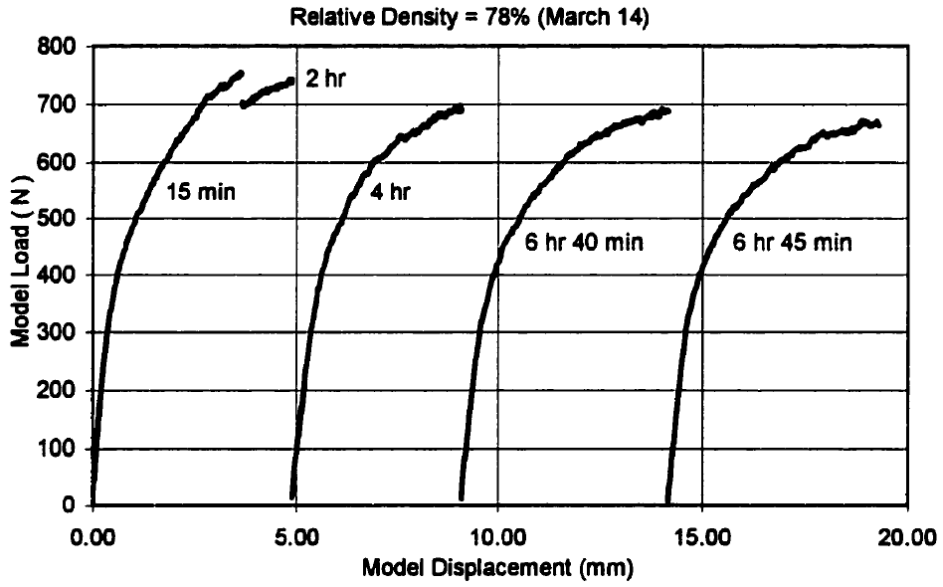

Figure 2.21. Results of staged tension tests: fully unloaded between stages (Bullock, 1999)

2.5.2 Axelsson, 2000

Axelsson (2000) initiated a series of laboratory studies that involved driving a 28 mm diameter model pile into a pressure chamber (outer diameter of 385 mm) filled with saturated medium dense sand. The pile was made of stainless steel and sandblasted to centre-line average roughness (R_{cla}) of about 9 – 13 μm. Well-graded postglacial silica sand (D_{50} = 0.65 mm and C_u = 4.7) was compacted in layers to an overall relative density in the range of 63 – 73%, saturated with water, and then pressurised and left for 24 hours before installation of the pile. The pile was driven to a final embedded length of 970 mm by a 10.1 kg hammer dropped from a height of 0.2 m. Tension load tests were conducted using a maintained load procedure and the uplift capacity was evaluated at a pile displacement (s) of 1.4 mm (s/D = 5%).

A total of nine chamber tests were conducted with confining pressure ranges from zero to a maximum of 30 kPa. For each chamber, three to five tension re-tests were performed at different time intervals over a period of about 1 week (except one occasion that was extended to 23 days). Results show that the increases in pile shaft capacity over time is greatly influenced by the applied lateral pressure, thus suggesting that pile set-up is stress-level dependent (Figure 2.22). The investigated set-up periods are rather short and the (reference) first-time uplift tests are mostly performed within one hour of driving.

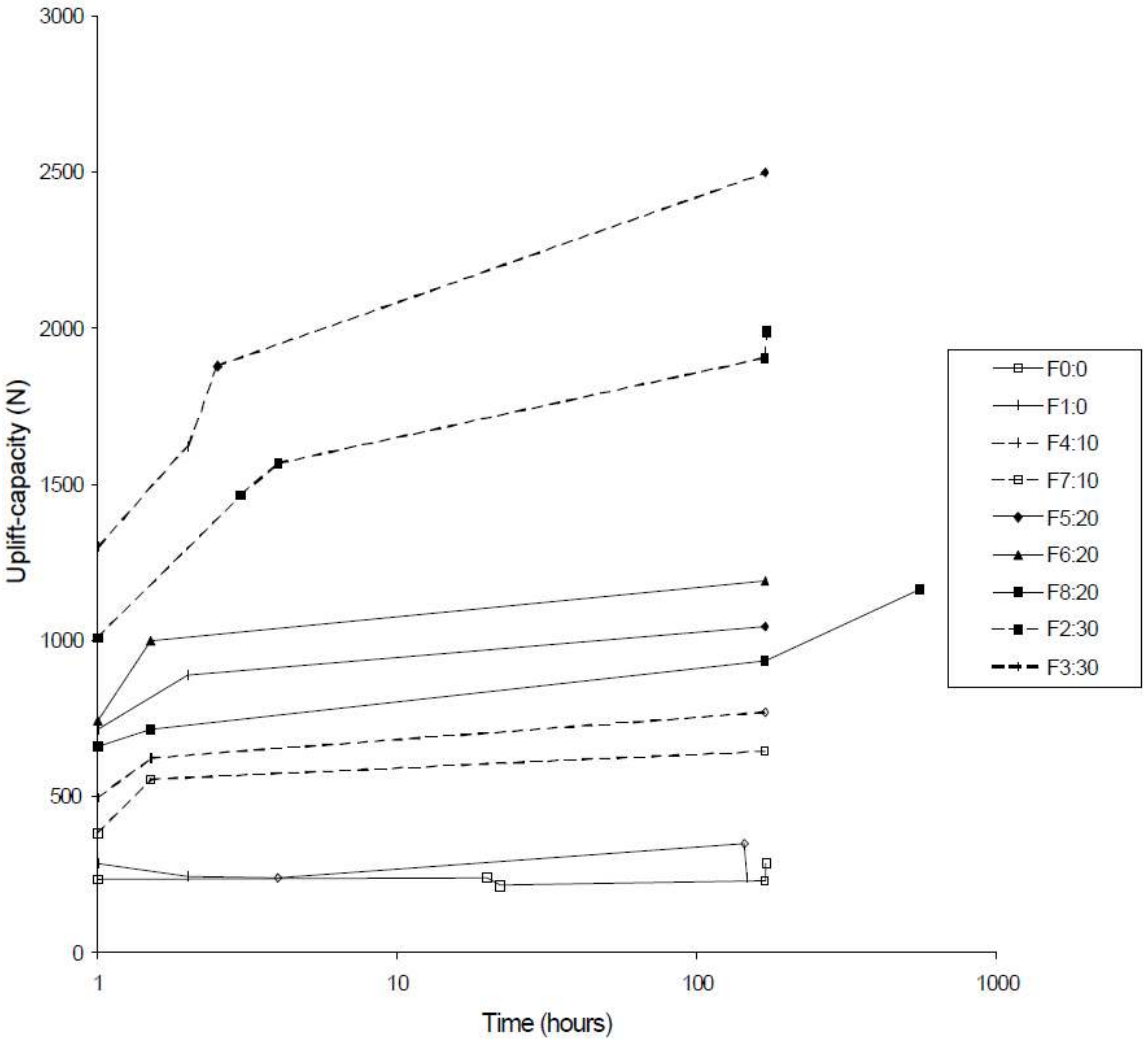

Figure 2.22. Increases of uplift capacity over time (Axelsson, 2000); the legend indicates chamber number follows by confining pressure (in kPa)

2.5.3 White & Zhao, 2006

White and Zhao (2006) performed a 1-*g* model-scale experiment in the laboratory by jacking multiple 10 mm diameter steel rods into two large chambers (850 mm diameter and 400 mm high) containing carbonate sand (Dog's Bay sand finer than 1.18 mm sieve) prepared by pluviation. One chamber was kept fully saturated while the other was subjected to a total of 15 cycles of water table fluctuations over the test period; the fluctuations involved lowering of the water level to the chamber base followed by its restoration back to the surface. The model piles were made from mild steel (except for an additional 4 piles made from stainless steel) and were smooth and un-instrumented. The piles were monotonically jacked to an embedded depth of 200 mm, keeping a minimum distance of about 150 mm (15 diameters) with adjacent piles, 200 mm to the wall and 130 mm from the base.

Displacement-controlled axial compression load tests were conducted by jacking the piles by a displacement of approximately 1 mm (10% of the pile diameter). The piles were re-tested after certain time intervals over a period up to 96 days. The observed apparent set-up on the mild steel piles was explained to be due to further mobilisation of the full pile capacity and a result of corrosion. The results on stainless steel piles show a negligible set-up effect (under this very low stress level) but that cycling of water table significantly increases the potential of pile set-up (Figure 2.23).

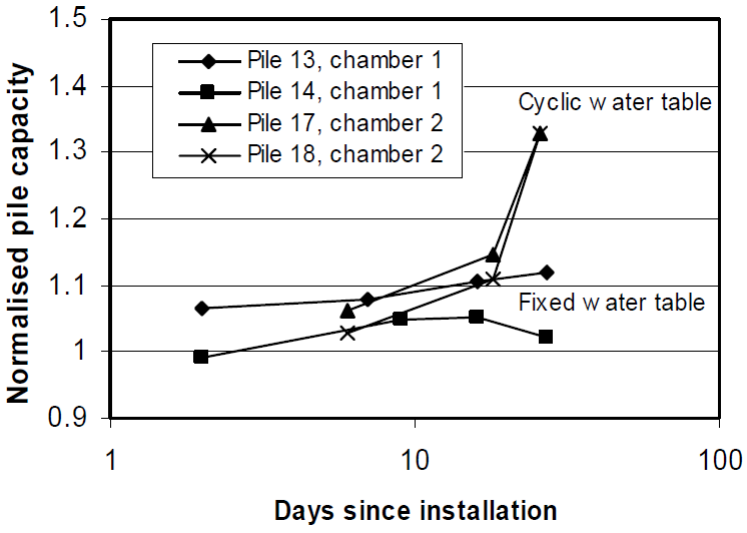

Figure 2.23. Changes of total pile capacity over time – stainless steel piles (White and Zhao, 2006)

2.5.4 Foray *et al.*, 2010; Rimoy *et al.*, 2012

A joint research programme between the Laboratoire 3S-R (Grenoble Institute of Technology) and Imperial College London was initiated in 2007 to investigate the effects of cyclic loading on time-dependent behaviour of pile shaft friction (Foray *et al.*, 2010; Rimoy *et al.*, 2012; Tsuha *et al.*, 2012). NE34 Fontainebleau sand (D_{50} = 0.21 mm, C_u = 1.53) was air-pluviated to a medium dense state ($D_r \approx 72\%$) in a 1.2 m diameter calibration chamber, which then imposed a constant vertical stress (σ'_v) of around 150 kPa that resulted in cone resistance (q_c) of about 23 ± 2 MPa. A 36 mm diameter highly instrumented mini-ICP (Jardine *et al.*, 2009), which comprises three instrument clusters respectively referred to as leading, following and trailing (A, B and C), was employed in the investigation. The pile was installed to a final embedment depth of 0.98 m by jacking at penetration rates between 0.5 mm/s and 2.0 mm/s with jack strokes of 5 mm, 10 mm and 20 mm in different installations and pause periods between jacking strokes.

After installation, extensive ageing periods were allowed (97 days for ICP1 and 139 days for ICP2) before the first-time compression and tension load tests were performed. The piles were then subjected to series of low level, one-way cyclic tests (load-controlled) and high level, two-way cyclic tests (both load- and displacement-controlled), each followed by a tension load test to contrast the effect of cyclic loading on pile shaft friction. Tension re-tests show that low-level cycling led to 10 – 20% gain in pile shaft capacity whereas high-level cycling inflicted considerable damage and reduced the tension capacity by half within a few tens of cycles (though testings were only conducted to 3 mm displacement, Figure 2.24). Results relating to time effects have yet to be published.

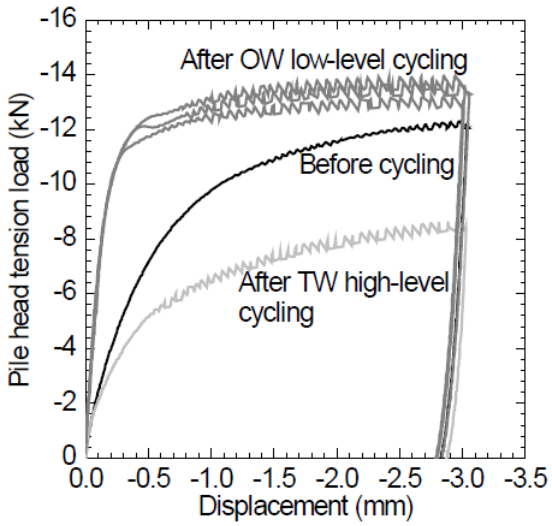

Figure 2.24. Tensile load-displacement curves of ICP2 (Rimoy *et al.*, 2012)

2.5.5 General Comment on Laboratory Experimentation

The foregoing review has highlighted some of the limitations associated with a study of pile ageing effects in the laboratory/centrifuge, although the attraction of having the well-controlled laboratory environment is clear – at least for parametric studies. Scale effects are clearly an important issue for small-scale laboratory/centrifuge tests and these need to be resolved if laboratory testing programmes are to be worthwhile.

It is evident from Bullock (1999) and the recommendation of ISSMGE-TC2 (Garnier *et al.*, 2007) that the creep time scaling factor in sand is unity, meaning that it has been generally uneconomic to study pile set-up effects in a centrifuge. Results from Axelsson (2000) and White and Zhao (2006) indicate the importance of stress similitude in the development of set-up behaviour, whereas existing experiments in calibration chambers (Axelsson, 2000; Rimoy *et al.*, 2012) have pointed to concerns about effects of sample ageing, the relative capacities of re-tested and fresh piles and associated time/costs if re-testing is not employed.

2.6 PROPOSED MECHANISMS

2.6.1 Basic Components of Pile Shaft Friction

To gain a better understanding of the possible mechanisms leading to pile set-up, it is instructive to revisit some recent developments of pile shaft friction in sand. Based on the results of advanced pile experiments conducted in loose to medium dense sand at Labenne, which employed an extensively instrumented Imperial College Pile (ICP), Lehane *et al.* (1993) show that the local shear stress at failure along the pile shaft (Figure 2.25) can be described by Mohr-Coulomb failure criterion as follows:

$$\tau_f = (\sigma'_{rc} + \Delta\sigma'_r) \tan \delta_f \qquad (2\text{-}1)$$

where σ'_{rc} is the equilibrium radial effective stress after installation and equalisation, $\Delta\sigma'_r$ is the increase in radial effective stress during pile loading, and δ_f is the interface friction angle.

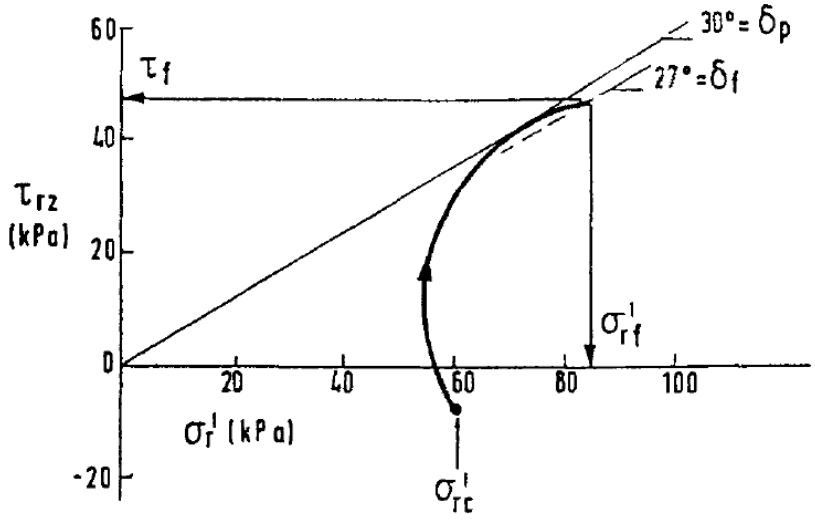

Figure 2.25. Stress path along pile shaft during load testing (Lehane *et al.*, 1993)

The σ'_{rc} was demonstrated to depend strongly on the initial in-situ conditions and the pile installation process. The initial conditions were described as a function of the pile end resistance (q_b) approximating CPT cone tip resistance (q_c), which is also a measure of sand relative density (D_r) and effective overburden stress (σ'_{vo}). The effect of

friction degradation following pile installation is reflected by the distance from the pile tip (h) normalised by the pile radius (R). The relationships are shown below:

$$\sigma'_{rc} = f\left(q_b, \frac{h}{R}\right) = f\left(D_r, \sigma'_{vo}, \frac{h}{R}\right) \quad (2\text{-}2)$$

The $\Delta\sigma'_r$ term can be subdivided into two components, i.e. an initial reduction in radial stress due to the Poisson effect (for tension loading) and rotation of the principal stress directions ($\Delta\sigma'_{rp}$) followed by a marked increase in radial stress due to interface slip dilation ($\Delta\sigma'_{rd}$). The value of $\Delta\sigma'_{rp}$ is expected to be more pronounced in tension loading and decreases with increasing relative density depending on the preferential orientation of sand grains and grain-to-grain contact forces (Symes, 1983). The effects vary along the pile shaft, which are difficult to quantify and are often assumed to be relatively insignificant.

The dilation component $\Delta\sigma'_{rd}$ is suggested as a result of radial displacement (δh) during shearing on a rough pile interface, of which a narrow shear band of a few grains thick tends to dilate moving radially so that slip may occur. Using a cavity expansion analogy, Boulon and Foray (1986) show that the radial stress change can be modelled by imposing a constant normal stiffness of k_n, which is a function of sand shear stiffness (G) and pile radius, on a modified interface shear apparatus (Figure 2.26). This relationship can be represented by the following expression:

$$\Delta\sigma'_{rd} = 2G\varepsilon_c = 2\delta h\frac{G}{R} = k_n\delta h \quad (2\text{-}3)$$

The interface friction angle at failure (δ_f) is the constant volume interface angle (δ_{cv}) at critical state. Based on the results of direct shear tests on a range of clean sands and a silica silt sheared against steel interface at initial average centre-line roughness (R_{cla}) between 6 and 10 μm, Jardine *et al.* (1992) show that δ_{cv} is independent of the initial relative density of the sand and increases with decreasing mean particle size (D_{50}) for a given interface roughness (Figure 2.27).

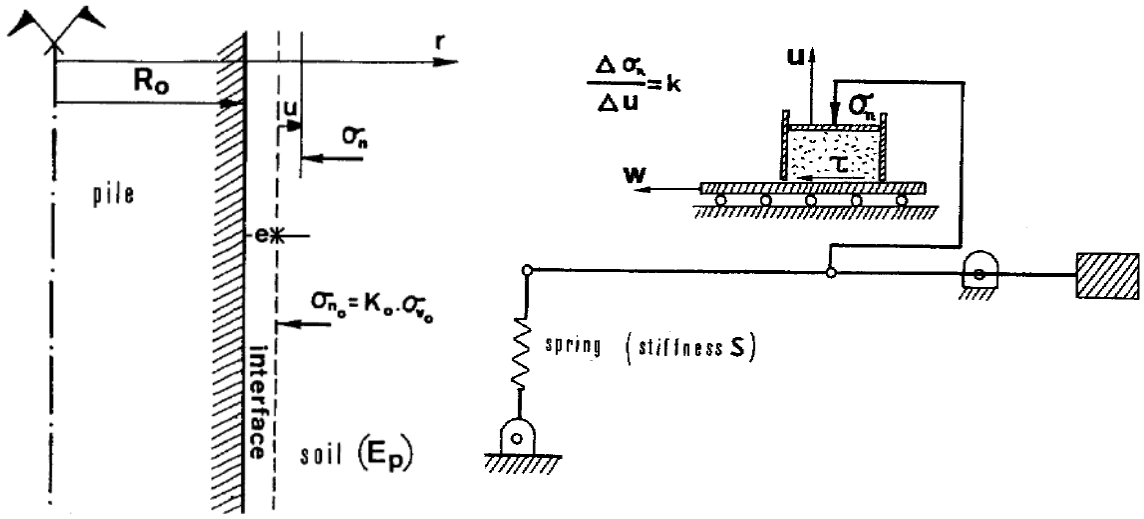

Figure 2.26. Analogy between local shear stress along pile shaft and an interface direct shear test with an imposed normal stiffness (Boulon and Foray, 1986)

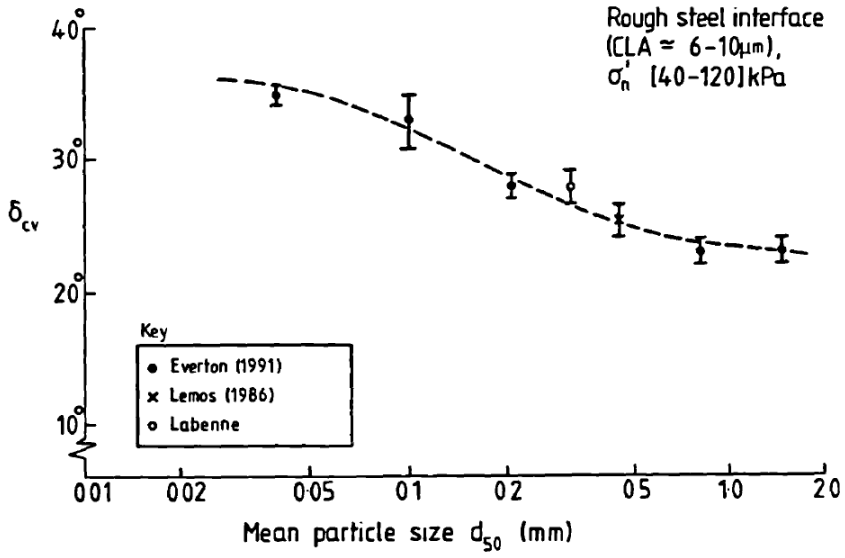

Figure 2.27. Variation of interface friction angle with mean particle size (Jardine *et al.*, 1992)

The design approach described above, which is summarised in Lehane and Jardine (1994), provides the basic framework for the later development of ICP-05 (Jardine *et al.*, 2005) and UWA-05 (Lehane *et al.*, 2005b) pile design methods which are now recognised as the most reliable approaches. In spite of the significant improvements provided by these methods compared to the conventional API method, Schneider *et al.*

(2008b) highlighted that none of the pile design methods explicitly takes into account the time-dependent behaviour of driven piles in sand.

Given the evidence of pile set-up in sand that occurs along pile shafts, it implies that at least one of the above-mentioned controlling parameters must be a function of time. Various hypotheses have been suggested but no consensus regarding the mechanism(s) leading to this phenomenon has been reached to date. The proposed mechanisms of pile set-up can be generally categorised into three (with reference to Equations (2-1) to (2-3) above):

1. An increase in radial effective stress (σ'_{rc}) acting on the pile shafts due to creep-induced relaxation of circumferential arching (hoop stress, σ'_{hoop}) established around the pile shafts during installation.

2. An increase in shear stiffness and dilatancy ($\Delta\sigma'_{rd}$) of the sand around the pile shafts due to ageing (chemical and/or mechanical) following disturbance from pile installation.

3. An increase in pile-sand interface friction angle (δ_f) due to corrosion or sand welding/bonding to the pile shaft.

2.6.2 Increase in Radial Effective Stress (σ'_{rc})

To explain the 85% increase in pile shaft capacity of the CLAROM pile measured at Dunkirk over an ageing period of five years, Chow *et al.* (1998) performed a critical appraisal of all three possible mechanisms above. They concluded that the increase in σ'_{rc} appears to be the most plausible dominant process leading to pile set-up – in line with the hypothesis proposed by Åstedt *et al.* (1992) (Figure 2.28). This inference was made in the light of observations by Robinsky and Morrison (1964), Allersma (1988) and Chong (1988), who suggest a formation of denser sand around the pile shaft following pile installation and the ability to sustain high hoop stresses (σ'_{hoop}) by arching. Over time, the circumferential arching would relax through creep, and allow for incremental increases in σ'_{rc}.

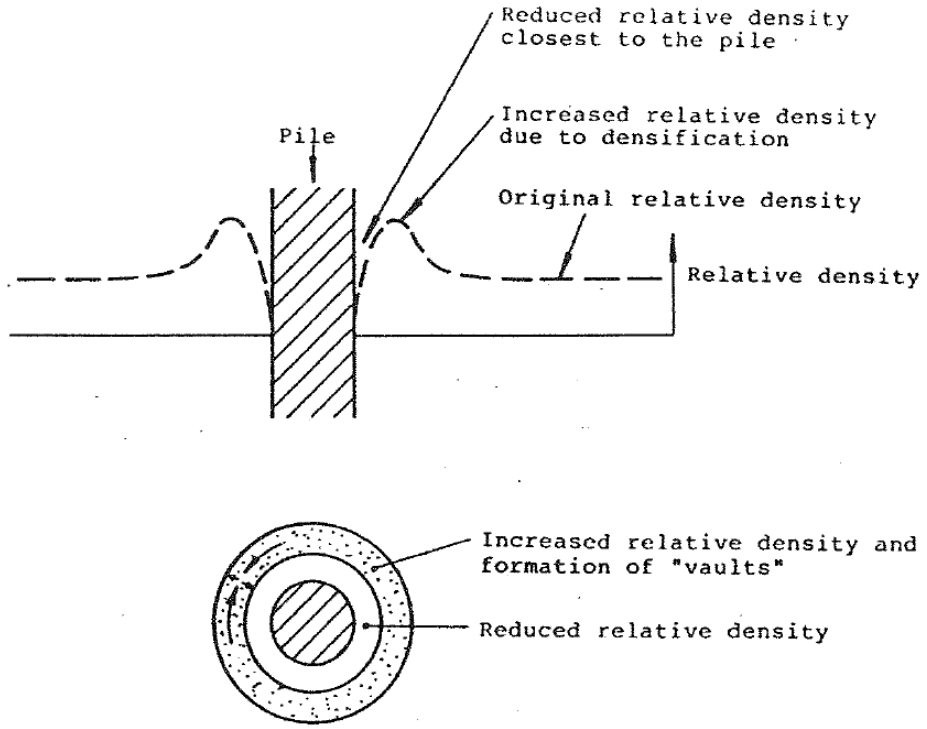

Figure 2.28. Arching mechanisms around pile shaft immediately after end of driving (Åstedt *et al.*, 1992)

Corrosive and chemical effects at the soil-structure interface which may increase the δ_f value were not thought to be the principal cause of pile set-up because the phenomenon is common to steel, concrete and timber piles in both carbonate and carbonate-free sand sites. In addition, the distribution of corrosion and sand bonding at the upper unsaturated oxygenated zone is at odds with the observed increases of shear stress measured at the lower sections of pile shafts.

2.6.3 Increase in Shear Stiffness and Dilatancy ($\Delta\sigma'_{rd}$)

Results of the direct interface shear tests on aged samples performed by Chow (1997) show that no changes in δ_{cv} were detected but increases in shear stiffness and dilation angles with ageing period were clearly observed (Figure 2.29); this observation agrees with that made by Daramola (1980) in triaxial compression tests. The interface tests were conducted under the most ageing conducive condition, which involved saturated dense Dunkirk sand samples (D_r = 85%) aged under normal stress (σ'_n) of 300 kPa for

up to 63 days before shearing against a stainless steel interface at $R_{cla} \approx 9.8$ μm. Her inference (assuming a doubling of δh and 50% increase of G over 5 years) was that only one-third of the measured capacity gain for CLAROM piles could be attributed to the dilatancy effects.

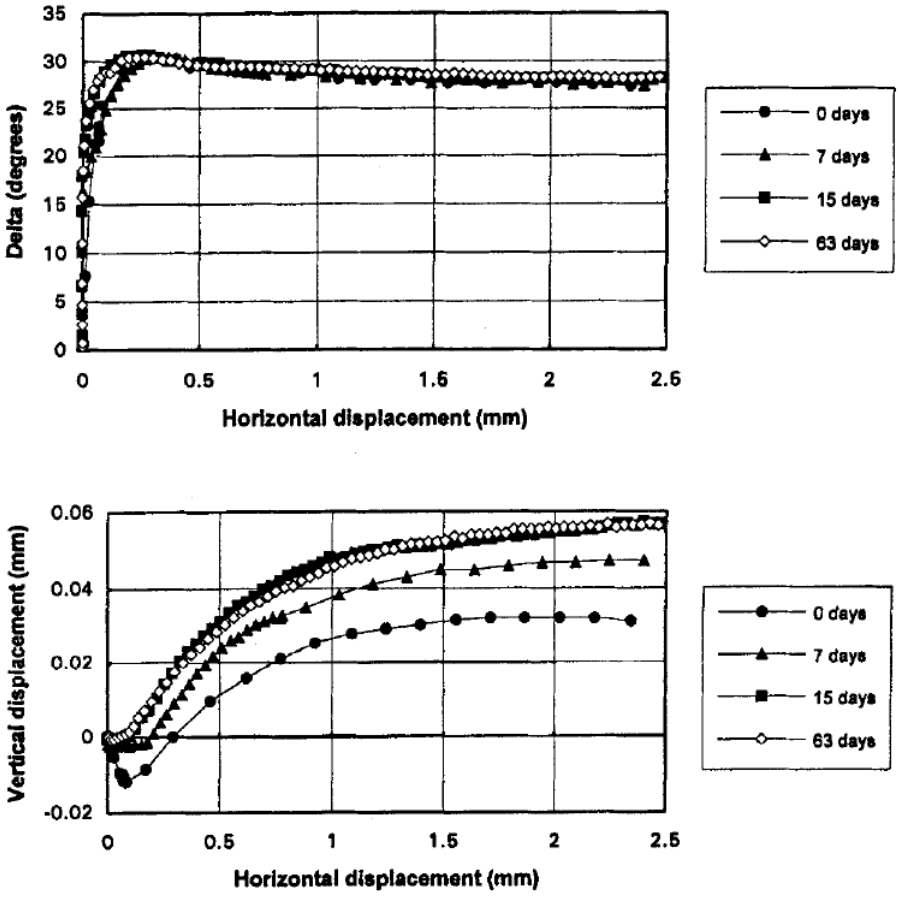

Figure 2.29. Effects of ageing on interface shear behaviour (Chow, 1997)

Axelsson (2000) observed a 60% increase in pile shaft capacity over a 22-month period in his study of pile set-up, which involved installation of an instrumented 235 mm square concrete pile driven into glacial sand to a depth of 12.8 m followed by static compression load re-tests at various ageing periods. Measurements of earth pressure cells reveal a nominal contribution of the horizontal stress at rest (σ'_{rc}) due to stress relaxation and preloading effects, and a remarkable increase in the horizontal stress change during loading ($\Delta\sigma'_{rd}$) due to increased dilatancy (estimated at 65%) over time (see Figure 2.12). A similar trend was observed in another of his pile test programmes

which involved similar instrumented concrete piles driven to deeper depths at an adjacent site but tested dynamically.

An instrumented full-scale concrete pile was driven into a sand site at Jacksonville, Florida in 1994 (Bullock, 1999). A series of static load re-tests performed up to 268 days after installation showed an average of 47% increase in pile shaft resistance. The total stress cells and piezometers measured very little changes in both σ'_{rc} and excess pore pressure during the monitoring period after pile installation and before each static re-tests. No measurement was made on the $\Delta\sigma'_{rd}$ during the O-cell static tests. Bullock *et al.* (2005b) postulate that the observed set-up is likely attributed to the mechanical ageing (due to increased dilatancy and interface friction angle) and some staged testing effects. Their conclusions broadly agree with those of Axelsson (2000).

2.6.4 Kinematics of Friction Fatigue

White and Bolton (2004) conducted an experimental study by using a plain-strain model pile jacked monotonically into siliceous and calcareous sands of various densities that were contained within a surcharged rectangular chamber. With the aid of particle image velocimetry (PIV) and close-range photogrammetry technique, they observed the displacement and strain paths induced during installation and suggest that friction fatigue (pile shaft friction degradation) emerges as a result of contractile interface zone adjacent to pile shaft following pile penetration (Figure 2.30). They hypothesise that the mechanism of interface contraction provides initial conditions for pile set-up. The lower radial stress (point B in Figure 2.31) on the pile shaft resulting from interface contraction is anticipated to gradually equalise with the higher surrounding stress field created during soil flow around the pile tip (towards point C) over time.

The idea was extended by incorporating the effect of friction fatigue (in the form of stress reduction in a cavity contraction stage) in the conventional cylindrical cavity expansion analysis (White *et al.*, 2005; White and Deeks, 2007). The effect of pile installation is modelled as a cavity expansion to some maximal value of σ'_{rmax} (comparable to q_b or q_c), then radially contracted to a value of $(q_c/a)(h/D)^{-c}$ (approximately 1% of the initial value σ'_{rmax}) to represent the soil flow around pile tip and subsequent friction fatigue. A smaller reduction of radial stress is assumed to occur

in the region of $3 < r/R < 6$ away from pile. The resulting lower σ'_{rc} and relatively higher σ'_{hoop} adjacent to pile shaft provide the initial conditions for set-up, which may equalise under the inward migration of high mean stress over time (Figure 2.32).

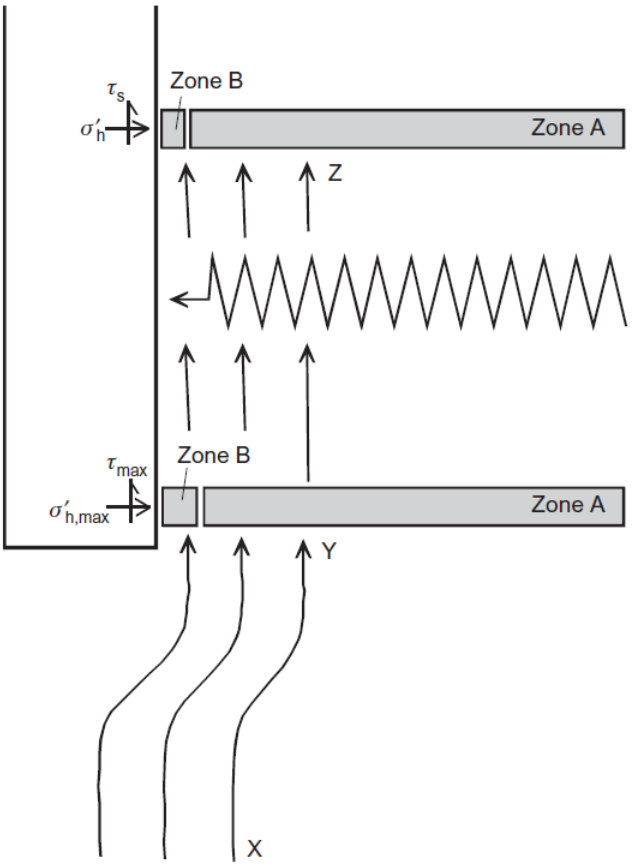

Figure 2.30. Kinematics of friction fatigue on pile shaft (White and Bolton, 2004)

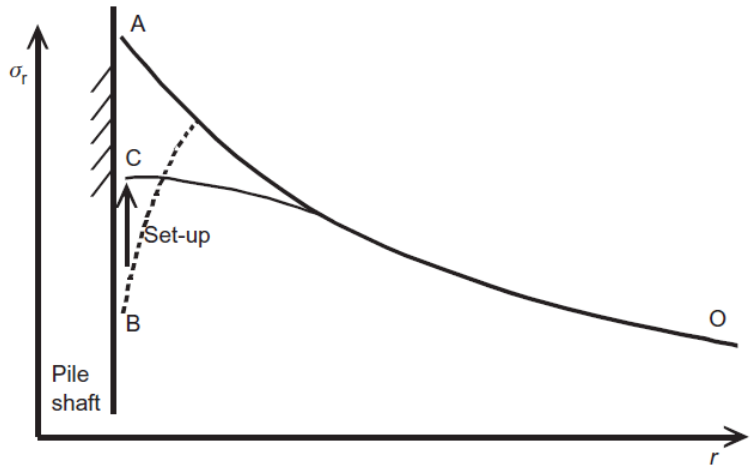

Figure 2.31. Radial stress distribution due to interface contraction (White and Bolton, 2004)

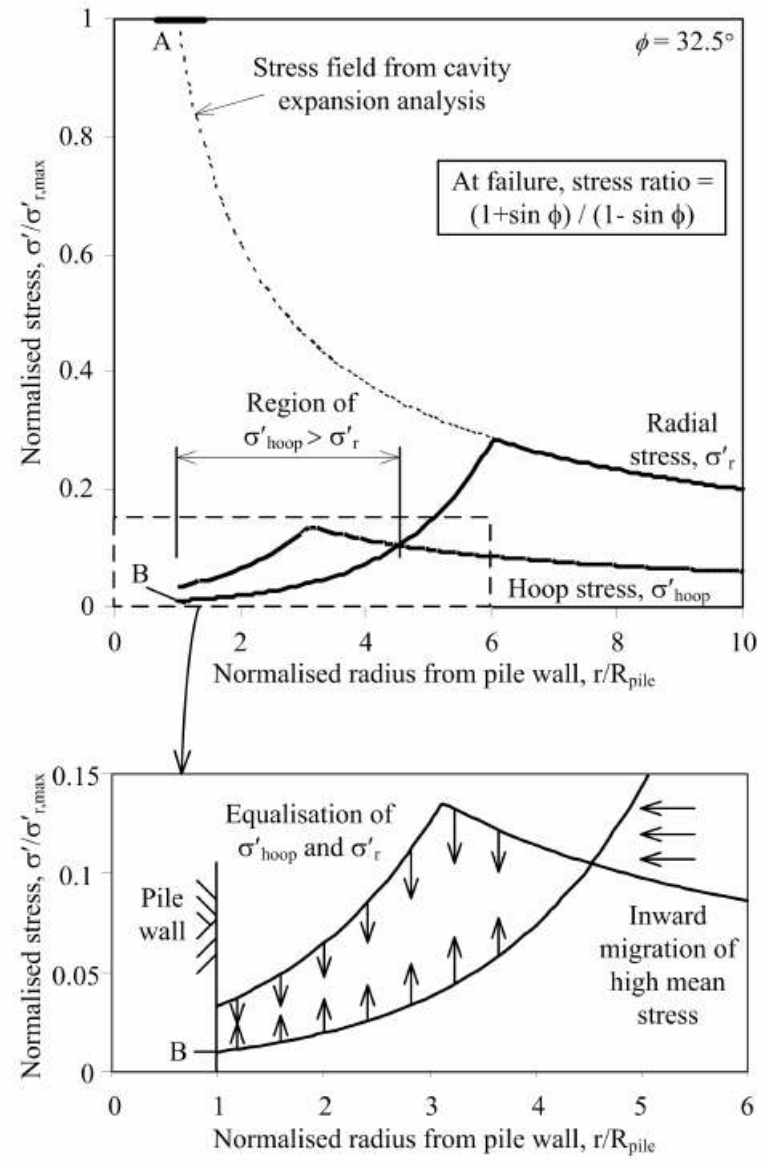

Figure 2.32. Hypothesised mechanism for creep-induced set-up based on stress fields from cavity expansion and contraction (White and Deeks, 2007)

2.6.5 Kinematically Restraint Dilatant Creep

An investigation of the mechanisms of displacement pile set-up in sand was performed by Bowman and Soga (2005) using a series of triaxial creep experiments. Three types of materials were tested: (*i*) standard clean laboratory Leighton Buzzard silica sand (type E); (*ii*) natural unwashed silica beach sand with shell fragments found at Montpellier (type M); and (*iii*) near-spherical glass beads (type G). Samples were pluviated to relative densities ranging from 54 to 75%, then saturated and finally subjected to a specific stress path before creep behaviours were monitored. The stress path was designed to mimic the loading history of a soil element adjacent to a displacement pile (i.e. first loading to p' = 600 kPa and q = 800 kPa and then unloading to p' = 100 kPa and q = -75 kPa at loading rate of 30 kPa/min).

The extension creep response (as indicated by local volumetric changes) may reflect the pile set-up tendency and this was seen to be contractive initially but then changed to become dilative as the sand particles rearranged themselves to redistribute stresses. The key findings from the main tests (i.e. series Y extension creep) include:

- Influence of material type (Figure 2.33): The weak angular particles (M_N) show greater contraction and longer contractive response before dilation than the strong angular particles (E_N). Also, the strong angular particles (E_N) show a faster rate of set-up than strong rounded particles (G_N). The trends were explained as a continued movement because of asperity yield and void collapse on angular particles (more for weak than strong), and the greater initial fabric anisotropy due to pluviation.

- Influence of relative density (Figure 2.34): The denser sample (E_N) develops dilatant characteristics within a shorter time, thus showing greater set-up than the looser sample (E_L). Loose sample simply contracts because of greater space available between the particles and greater asperity yield in a less stable structure (due to higher contact forces from fewer contacts between particles).

- Influence of cyclic loading (Figure 2.35; Figure 2.36): Application of load cycles tends to increase the tendency of strong angular particles to dilate (E_C vs E_N), while the dilatancy in weak angular particles is accompanied by a greater

contraction (M_C vs M_N). Extra care should be taken to ensure the magnitude of load cycles would not break down the existing contact force network or to cause substantial particle breakage.

- Influence of loading rate (Figure 2.37): The slow test (E_S) performed at 0.6 kPa/min (50 times slower) shows more contractive behaviour with longer contraction period than the normal rate test (E_N). The greater contractive response in the slow test was assessed to be because of the availability of more time for the particles to disengage and rotate, which may generate more collapsible void space and weaken the contacts.

Based on the triaxial creep responses, Bowman and Soga (2005) suggest another hypothesis for pile set-up, which they refer to as kinematically restrained dilatant creep under high stress ratio. The limitations of triaxial tests to model aspects of pile installation and pile-sand interaction are acknowledged by the authors. The results may not reflect the absolute magnitude and rate of pile set-up in real, but they certainly provide further insights into sand creep characteristics for different granular materials under various simulated conditions.

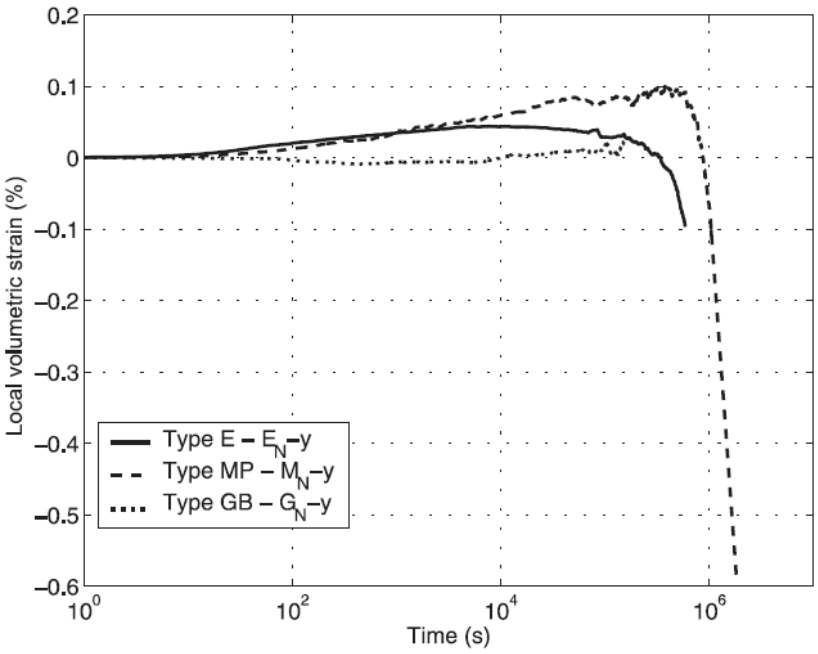

Figure 2.33. Comparison of creep behaviour of three materials (E, MP and GB) at similar relative density (Bowman and Soga, 2005)

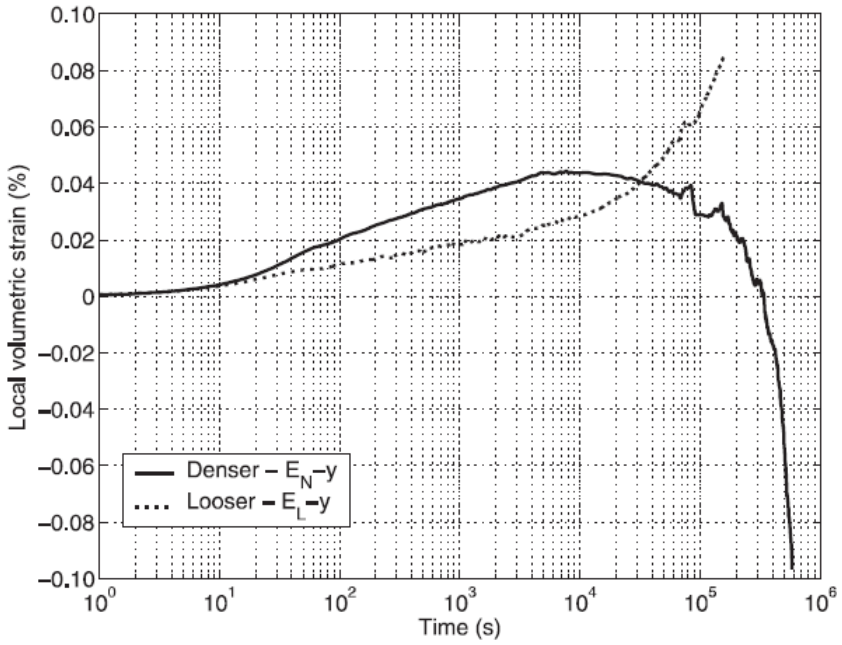

Figure 2.34. Effect of different relative density (soil type E) on creep strain development (Bowman and Soga, 2005)

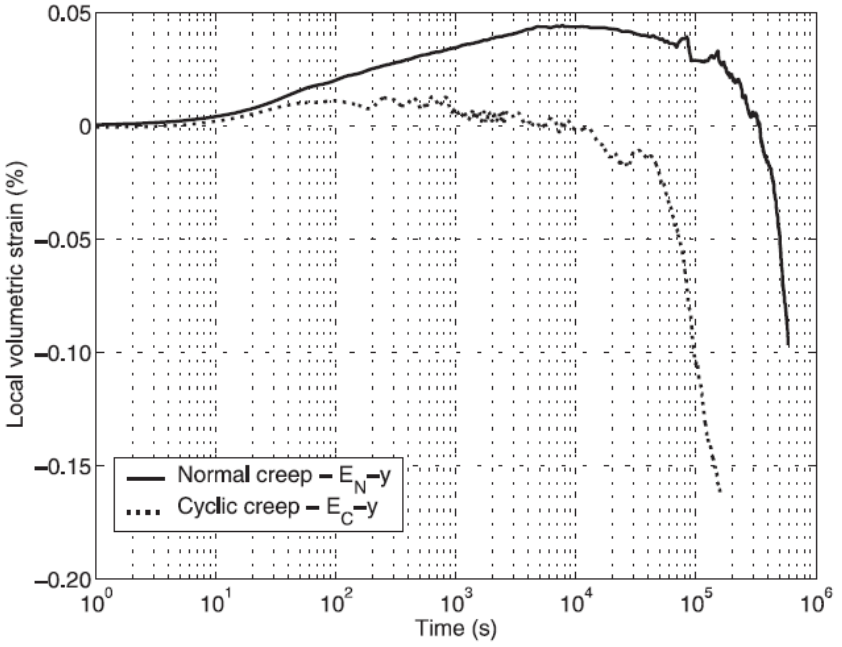

Figure 2.35. Influence of perturbations via load cycling (soil type E) at Δq = ±5 kPa during creep (Bowman and Soga, 2005)

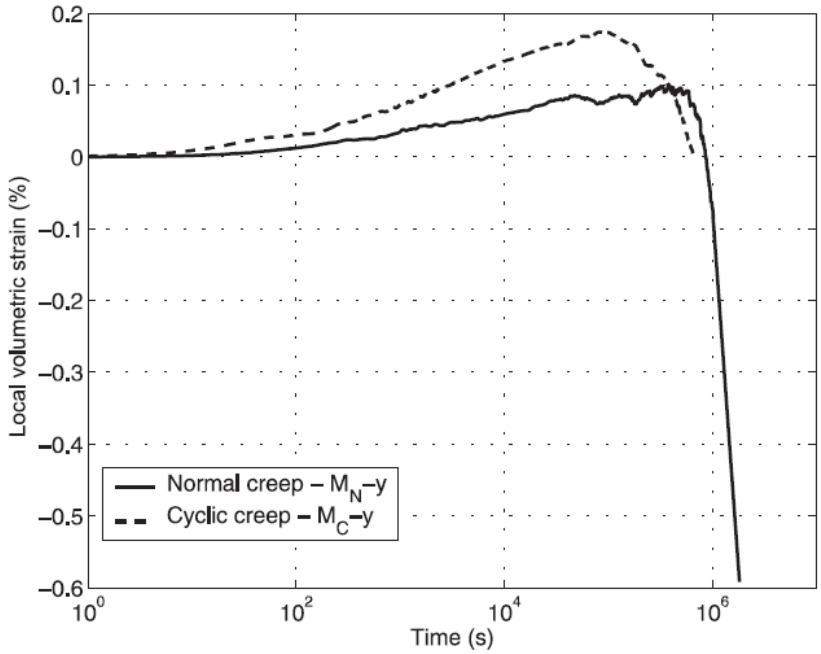

Figure 2.36. Influence of perturbations via load cycling (soil type MP) at Δq = ±5 kPa during creep (Bowman and Soga, 2005)

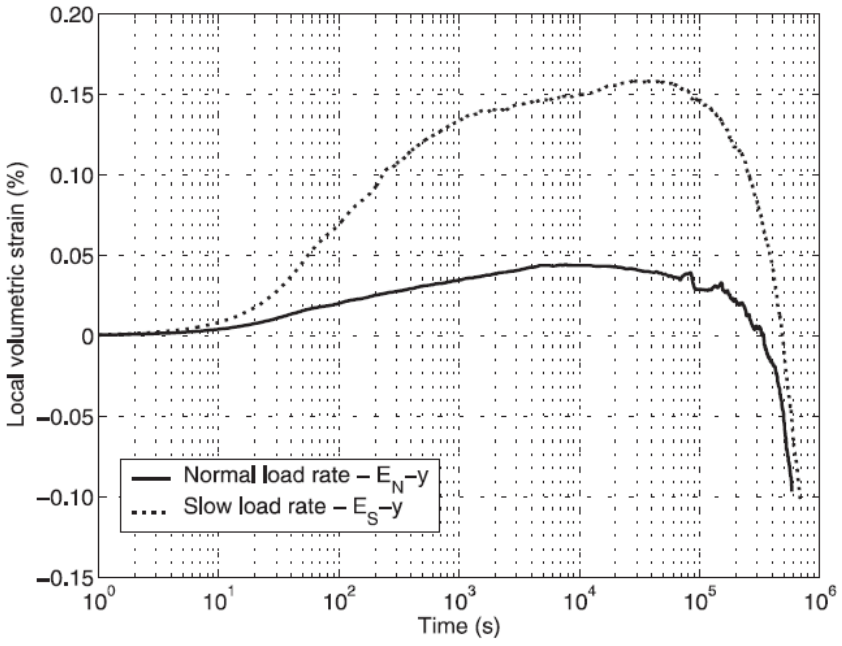

Figure 2.37. Comparison of creep behaviour after unloading (soil type E) at slow rate (-0.6 kPa/min) and at normal rate (-30 kPa/min) (Bowman and Soga, 2005)

2.6.6 Chemical Ageing

Sand ageing, which is a phenomenon on recently disturbed or freshly deposited sand that gains strength and stiffness over time at constant effective stress, is often linked up with pile set-up. While some basic mechanisms especially microscopic changes at particulate level may be similar, physical processes of a driven pile installation and boundary conditions that govern the pile shaft capacity are not directly comparable to that of a large deposit of densified sand. Mitchell (2008) in his recent state-of-the-art paper on sand ageing show a large variation of ageing behaviour from reported case histories and suggest that each case should be evaluated separately.

Increases in shear modulus with time under sustained pressure were observed in laboratory studies for a long time (Afifi and Woods, 1971; Anderson and Stokoe, 1978). The time-dependent behaviour of sand began to attract more attention after exposure of ground improvement (e.g. blasting and vibrocompaction) and hydraulic reclamation projects that show a significant increase in cone penetration resistance over time (Mitchell and Solymar, 1984; Thomann and Hryciw, 1992; Charlie *et al.*, 1993; Ng *et al.*, 1998).

Mitchell and Solymar (1984) postulate that the most probable cause of this sand ageing effect is cementation at particle contacts, through dissolution and precipitation of silica or other solution that may form a cementing agent. Mesri *et al.* (1990), and others, however doubt if significant chemical reactions can occur under nominal in-situ temperature and pressure over such short periods (weeks or months). In addition, there is some evidence of ageing in dry sands where chemical processes are likely to be slow.

Laboratory experiments conducted by Joshi *et al.* (1995) indicate that the measured increases in penetration resistance, besides that caused by particle rearrangement, could be partly attributed to a chemical mechanism. The study involves sand specimens from a local river and the Beaufort Sea, which were first prepared in dry conditions and submerged in distilled water and seawater, and then subjected to a constant vertical stress of 100 kPa throughout the 2-year testing period. Penetration resistances, which were measured at different ageing periods, show a larger increase in submerged sands than in dry specimens. The increases were related to the presence of precipitates at

grain contacts and the interspaces that were observed from the scanning electron micrograph images captured before and after the experiments.

More recently, Baxter and Mitchell (2004) designed an extensive laboratory testing programme to examine the changes of small-strain shear modulus, electrical conductivity, pore fluid chemistry and cone penetration resistance of sand up to a maximum of 118 days. Two different sands with various combinations of relative density, temperature and pore fluid composition were tested under well-controlled conditions. Despite some positive changes of the measurements of shear wave velocities, electrical conductivity and chemical analyses with time, there was no corresponding increase in penetration resistance. Based on the results and other evidence (to be discussed in next section), Baxter and Mitchell (2004) conclude that chemical reactions or cementation are unlikely to be the primary cause responsible for ageing effects in sand.

2.6.7 Mechanical Ageing

In response to Mitchell and Solymar (1984), Schmertmann (1987) suggested an alternative explanation to the increase in cone penetration resistance in clean sand as: (*i*) Time-dependent recovery increases in horizontal stresses; and (*ii*) frictional gain as a result of dispersive particle reorientation during secondary compression. Mesri *et al.* (1990) and Schmertmann (1991) believe drained ageing is closely related to secondary compression or creep, driven by in-situ effective stresses. Other than an increase in overall density, continued particles rearrangement would result in gradual increase in macro-interlocking between particles and micro-interlocking of particle surface roughness forming a more efficient packing. Mechanical processes as described above are now accepted as the main causes of sand ageing phenomenon.

2.6.8 Static Fatigue

Recently, the concept of static fatigue (or stress corrosion cracking) was evoked to explain time effects in sand such as the delayed increase in penetration resistance after dynamic compaction (Karimpour and Lade, 2010; Michalowski and Nadukuru, 2012). Brittle materials such as quartz and feldspar, under sustained loading, may fracture at stresses which are considerably smaller than their short-term strength through time-

dependent crack propagation. From a microscopic view, when sand particles come into contact, the surface asperities would first be loaded to considerable degree and prone to develop cracks. The micro-fracturing does not occur simultaneously at all contacts but depends on the distribution of force chains, hence leading to a time-delayed process.

Experiments on creep and stress relaxation in sand as conducted by Lade and Karimpour (2010) show that the time effects in granular materials, in the absence of strain rate effects, are attributed to grain crushing, which in turn is time-dependent. Michalowski and Nadukuru (2012) inspected the development of fractured asperities of sand grains under sustained load using scanning electron microscopy. Although major damage was observed shortly after application of loading, continuing fracturing over the following week was noticeable.

2.7 EMPIRICAL RELATIONSHIPS

2.7.1 Logarithmic Function (Skov and Denver, 1988)

Several empirical relationships were suggested to represent the trend and variation of pile set-up in sand. Among them, the linear relationship with logarithmic time function as proposed by Skov and Denver (1988) is most widely used:

$$\frac{Q}{Q_o} = 1 + A \log\left(\frac{t}{t_o}\right) \tag{2-4}$$

where Q_o is the initial (reference) pile capacity measured at time t_o, and Q is the pile capacity measured at time t after installation. The factor A is a function of soil type that represents the rate of capacity change whereas t_o is the time at which the capacity stabilises after initial driving, which is also a function of soil type.

For a driven pile in sand, Skov and Denver (1988) suggested A = 0.2 and t_o = 0.5 day. The expression has been employed by Chow *et al.* (1998) and Axelsson (2000) in their databases which indicated respective average A values of 0.5 and 0.4. Bullock *et al.* (2005b) recommend a default minimum A = 0.1 to be included in routine design.

2.7.2 Power-Law Function (Mesri *et al.*, 1990)

Based on an expression originally proposed for estimating the changes of post-densification penetration resistance with time in sand (Mesri *et al.*, 1990), Long *et al.* (1999) and later Mesri and Smadi (2001) modified the power-law function to suit the time-dependent changes of pile capacity in sand in the following format:

$$\frac{Q}{Q_R} = \left(\frac{t}{t_R}\right)^{C_D C_\alpha / C_c} \tag{2-5}$$

where Q is the pile capacity measured at time t after driving, and Q_R is the reference capacity corresponds to time t_R (taken as 1 day after driving). The parameter C_α/C_c is a fundamental soil constant with values in the range of 0.02 ± 0.01 for all granular soils and C_D is an empirical value used to reflect a potential for sand stiffness increase as well as the changes of stress regime surrounding the pile that results from pile installation.

The case histories presented by Chow *et al.* (1997) were replotted using the power-law function assuming $C_\alpha/C_c = 0.02$ and $C_D = 7$, and found to agree reasonably well with the average trend. Chow *et al.* (2001), however, comment that the prediction would result in much higher (and potentially unachievable) increases in pile capacity in the long term (after around five years) compared to the semi-logarithmic function.

2.7.3 Hyperbolic Function (Tan *et al.*, 2004)

Tan *et al.* (2004) examined the case histories compiled by Axelsson (2000) and proposed an alternative approach using a hyperbolic function as follow:

$$\frac{Q}{Q_u} = \left[0.2 + 0.8\left(\frac{\frac{t}{T_{50}}}{1 + \frac{t}{T_{50}}}\right)\right] \tag{2-6}$$

where Q is pile capacity measured at time t, Q_u is the 'ultimate' pile capacity that 100% of set-up has been realised, and T_{50} is the time required for 50% of the set-up to realise.

The procedure requires T_{50} to be estimated by trial-and-error and was assessed to vary from less than one day to as large as 10 days in order to match the case histories. For $T_{50} = 2$ days as in the given example, the expression yields much higher capacity gain in

the short term (between 2 days to 2 months) but lower rises in pile capacity in the long term (after about 200 days) compared to both the semi-logarithmic and power-law functions.

The empirical relationships above give some general idea on how certain researchers currently envisage the rate of gain of shaft capacity with time. One important point of debate is whether or not the set-up process continues indefinitely, as the equations imply, and how the expected trend varies with some important variables (e.g. installation method, pile type and diameter, sand type and state). Besides the relationships described above, other mathematical models which are employed to depict time-dependent phenomena (e.g. Seber and Wild, 2003) are worthwhile exploring. On the other hand, it should be borne in mind that over-emphasising the accuracy of mathematical representation at this point has no practical value given the dearth of reliable observations and substantial uncertainties in the existing databases.

2.8 INFLUENCE OF INSTALLATION METHOD

The fact that there are many reported examples of set-up for driven piles in sand but none for bored piles leads to a hypothesis that pile set-up is strongly related to installation disturbance. Although jacked piles, as for driven piles, are categorised as displacement piles, experimental evidence suggests that their behaviour in sand is different.

In contrast to percussion driving, the jacked-in method presses the piles into the ground by the static reaction force provided by the dead weight of a jacking rig, which is noise and vibration-free, and usually in a far less number of loading-unloading cycles. White *et al.* (2002) measured noises and ground vibrations created by different methods of piling at a site and show that a press-in pile driver (an improved system that involves a compact machine that utilises the resistance from previously installed piles as the reaction) leads to a reduction of between 10 and 50 times in the level of ground vibrations (Figure 2.38).

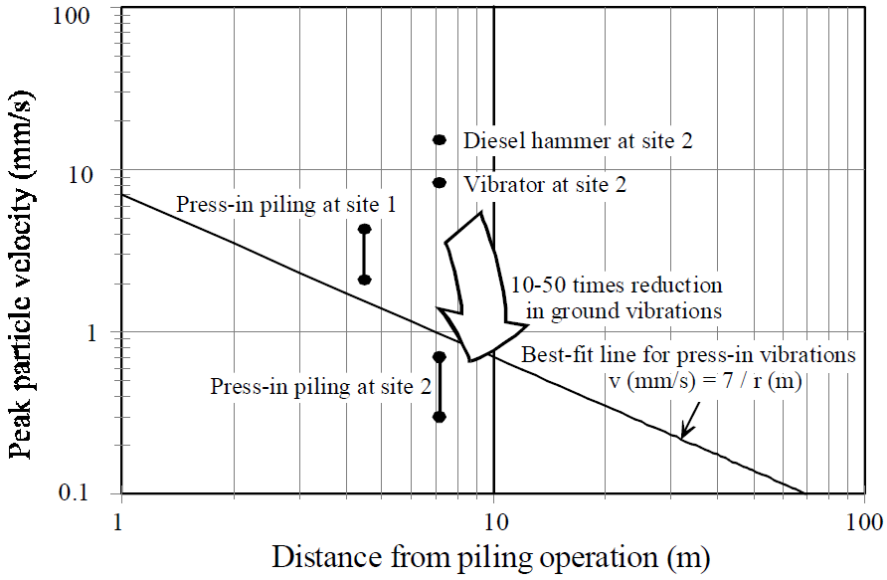

Figure 2.38. Comparison of ground vibrations created by different methods of piling (White *et al.*, 2002)

Differences in set-up between these two installation methods is important to ascertain if the observations and findings (of pile set-up) on driven piles could be directly applied to jacked piles since jacked-in technology is gaining popularity nowadays especially in urban areas. Besides, the jacked-in method is commonly employed in physical modelling (for better consistency and to prevent damage to the instrumentation) to investigate the behaviour of driven piles. In this Section, differing behaviours of jacked and driven piles as observed from laboratory and field experiments are reviewed, and indications of the apparent set-up shown by the jacked piles are highlighted.

2.8.1 Laboratory Experiments

Foray *et al.* (1989) investigated the effects of the pile installation method on pile bearing capacity in sand using a calibration chamber. An instrumented model pile of 55 mm diameter was installed by monotonic jacking and driving in separate cases into a dense sand sample (D_r = 0.8) which was pressurised to two different vertical stresses of 400 kPa and 800 kPa. Results of static load tests showed that the jacked piles mobilised slightly higher tip resistance, but significantly less (only about half) shaft resistance than the driven piles.

Experimental pile test programmes under 1-*g* conditions were performed by Al-Mhaidib and Edil (1998) and Alawneh *et al.* (1999) to study the uplift resistance of piles in sand. Different diameters of model piles (ranging from 41 mm to 178 mm) were installed by means of static jacking (in staged increments at a constant rate) or impact driving (hammer free falling from constant height) to target embedment before pull-out tests were conducted. Al-Mhaidib and Edil (1998) showed that the uplift capacities of jacked piles were larger than those of driven piles particularly in dense sand due to significantly higher disturbance caused by pile driving process. Interestingly, the results obtained by Alawneh *et al.* (1999) indicated the opposite trend.

De Nicola and Randolph (1997) and Paik and Salgado (2004) investigated the plugging behaviour of open-ended pipe piles using a geotechnical centrifuge and calibration chamber, respectively. The piles were driven or jacked monotonically into dense sand specimens and then loaded statically. Higher shaft capacities were consistently recorded for the jacked piles as compared to the identical driven piles. The tendency was explained as a result of better soil plugging that was formed during jacked installation, and thus greater radial soil displacement that increase the horizontal stresses acting on the pile shaft.

In a centrifuge programme, Lehane and White (2005) examined the influence of the pile installation method on the behaviour of pile shaft friction in sand. Three installation modes (i.e. monotonic, jacked and pseudo-dynamic) were modelled using different jacking procedures. The results of tension tests show that the ultimate shaft friction that can develop on the pile with pseudo-dynamic installation is greater than for monotonic and jacked installation. In addition, earth pressure measurements on the pile shafts revealed that, while stationary radial stress for the monotonically jacked piles were higher than those of jacked and pseudo-dynamic piles (due to less effect of friction fatigue), changes in radial stress during shearing were smaller.

The literature allows no consensus to be established regarding the difference between shaft frictions developed on jacked and driven piles installed in laboratory experiments. Model pile tests are recognised to be hampered by many modelling constraints such as particle size effects, inappropriate installation methods and procedures (e.g. monotonic

jacking), unrealistic ambient stresses (e.g. 1-*g* experiments), sample ageing effects (e.g. testing performed at differing periods) and many other limitations.

2.8.2 Field Experiments

An extensive pile test programme was conducted by the Japanese BCP Committee (1971) to investigate the influence of pile installation methods in sand. A 200 mm diameter closed-ended steel pipe pile, which was instrumented with a load cell assembly at the tip and six pairs of earth pressure cells mounted diametrically along the shaft, was employed repeatedly in the study. The pile was either buried, jacked or driven to an embedment that ranged from 4 m to 11 m into a thick deposit of medium to dense diluvial sand that was overlain by 4 m of loose sandy backfill; the ground water table was at about 9 m depth.

A series of loading cycles of approximately 100 mm penetration were repeated until a total settlement of 5 to 9 pile diameters was reached. Despite little difference between the jacked and driven piles being observed from the overall results of multiple re-tests (as reported by the committee), the first load cycle shows that the tip resistance of the driven pile (6C) was slightly larger than that of the jacked pile (1C), while its average shaft friction was considerably smaller (Figure 2.39).

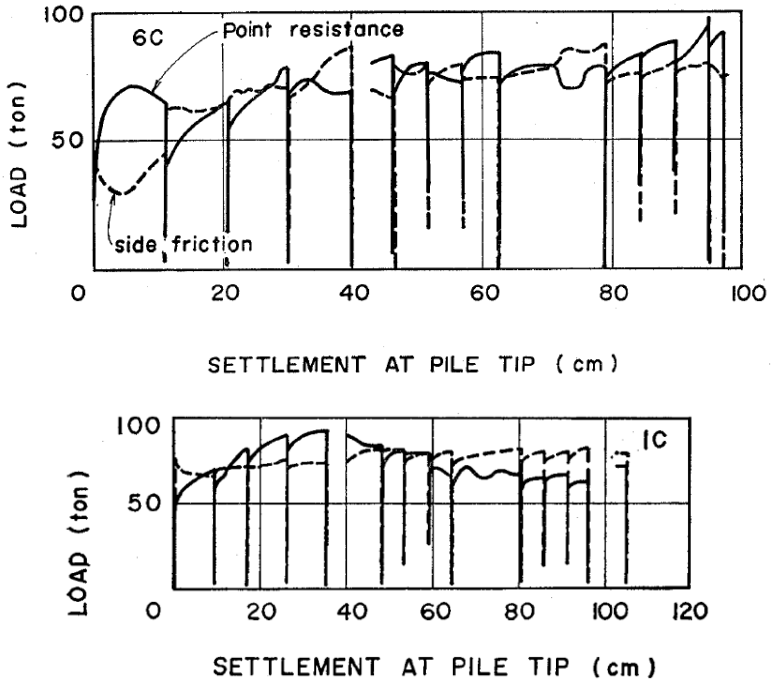

Figure 2.39. Load-settlement curves for driven (6C) and jacked (1C) piles (BCP_Committee, 1971)

Yang *et al.* (2006b) collated test data of 14 instrumented H-piles (5 jacked and 9 driven) to investigate the differences in capacity and deformation of jacked and driven piles in sandy soil. Jacked piles were terminated based on different 'pre-creeping' criteria (shown to have marked impact on its subsequent load bearing behaviour), whereas driven piles were terminated by the final-set criterion evaluated from Hiley formula. The maximum pile capacity used for data interpretation was derived from modified Davisson method or maximum capacity of the loading system, which may not necessarily be the failure load. No consideration was given to the effects of residual stresses locked in the piles after installation in the analysis.

The results of static compression load tests show that the shaft resistances of jacked piles were generally larger than that of driven piles but their base resistances (in terms of the percentage of total load at pile head) were comparatively smaller. This difference can be observed from the axial stress distribution recorded by two comparable piles installed by jacked and driven methods (Figure 2.40).

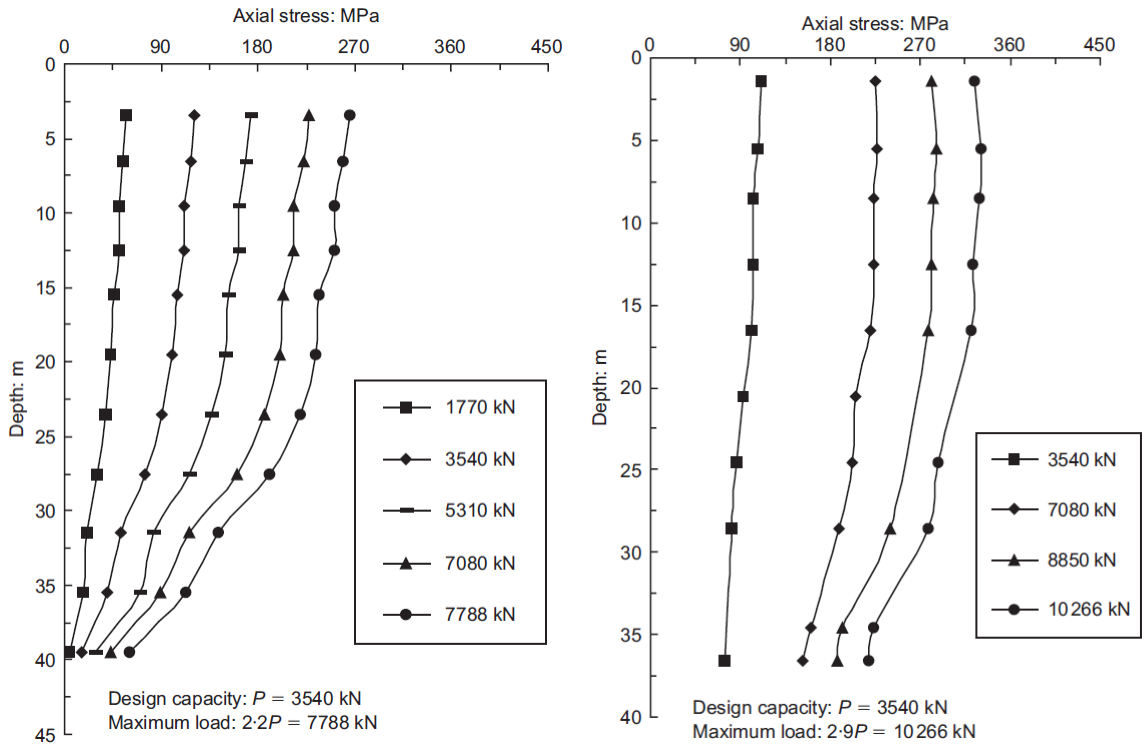

Figure 2.40. Typical axial stress distribution for: (a) jacked piles (PJ1); (b) driven piles (PD2) (Yang *et al.*, 2006b)

Another field study was reported by Zhang and Wang (2009) and this involved two instrumented H-piles (RJP-1 and 1B1-4) installed using different pile installation methods into typical sandy materials in Hong Kong. A reference pile, 1B1-4, was installed completely by driving to a final depth of 55.6 m, and statically load tested three days later. Pile RJP-1 was installed by jacking to a depth of 34.8 m and subjected to a maintained static load test after seven days. Thirty-two days later, the installation of RJP-1 was continued by driving to a final penetration depth of 55.7 m and load tested again seven days later. The driving process was monitored using a pile driving analyser (PDA) at several critical stages. Test results show that:

- The residual unit shaft resistance in the jacked pile (RJP-1, L = 34.8 m) was much larger than that of the driven pile (1B1-4) at corresponding depths after installation (Figure 2.41).

- The load-settlement response of the jacked pile was much stiffer than that of the driven pile. This is in keeping with the larger ultimate unit shaft resistance measured on the jacked pile.

- Remarkable changes of the load transfer behaviour were observed when the previously jacked RJP-1 switched to driving installation at 34.8 m depth (Figure 2.42). It can be seen that 12 blows of driving significantly reduced the shaft resistance at the upper portion of the pile, and continue driving (as shown by blow 45) destroyed the shaft resistance of the entire pile shaft created by pile jacking and behaved akin to a driven pile. The transformation from a jacked to a driven pile behaviour is believed to result from the effects of greater friction fatigue for increasing loading-unloading cycles and the influence of vibrational disturbance from dynamic impact.

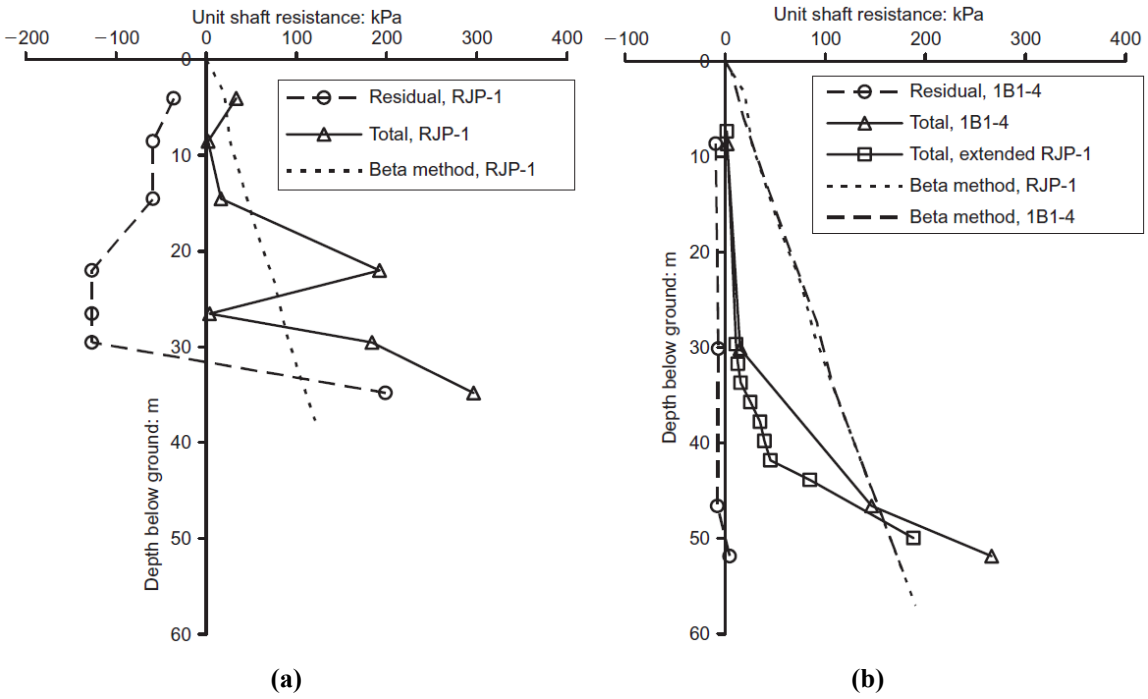

Figure 2.41. Unit shaft resistance at failure load: (a) jacked pile RJP-1 (L = 34.8 m); (b) driven pile 1B1-4 (L = 55.6 m) and extended RJP-1 (L = 55.7 m) (Zhang and Wang, 2009)

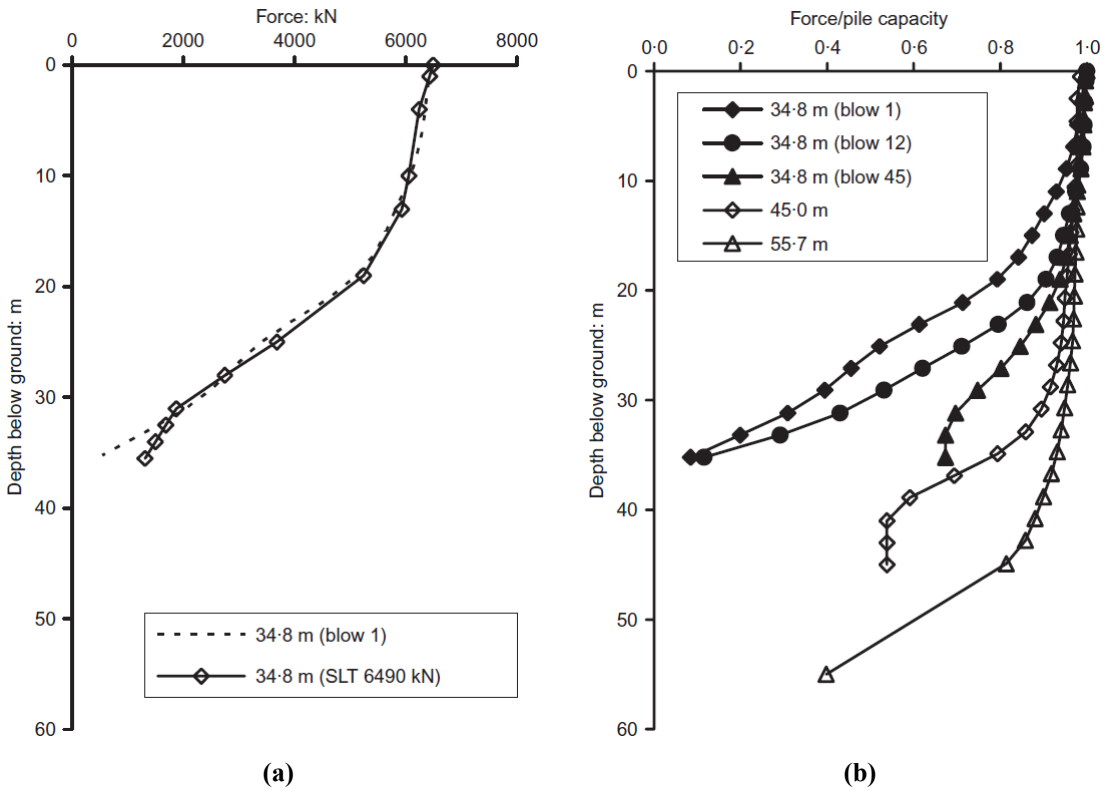

Figure 2.42. Changes of load transfer behaviour during driving of RJP-1: (a) comparison with static load test; (b) normalised load-depth relationships (Zhang and Wang, 2009)

2.8.3 Apparent Set-up of Jacked Piles

Since the jacked-in technology is relatively new to the piling Industry, the available literature is far less comprehensive than the coverage of driven piles. The two articles discussed in this section involve piles that were jacked into residual soils (alluvium and completely decomposed granite (CDG)) in Hong Kong and in the surrounding region, where clay-silt-sand mixtures predominate but the soils are generally classified as granular (Lumb, 1962, 1965).

Yang *et al.* (2006a) presented the results of full-scale field tests on two instrumented steel H-piles (PJ1 and PJ2) jacked into dense sandy soils at two reclaimed sites in Hong Kong. PJ1 (305 × 305 × 223 kg/m) was jacked to an embedded length of 40.9 m, with ground conditions comprising a 13 m thick deposit of alluvium overlying weathered granite strata at Site 1. PJ2 (305 × 305 × 180 kg/m) was installed at Site 2 to a shallower depth of 25.8 m in a soil profile consisting almost entirely of completely decomposed granite. The water levels were at 2.8 m and 3.6 m below ground surface for Site 1 and Site 2, respectively. The piles were load tested statically in stages according to the procedures outlined in the Hong Kong Code of Practice for Foundations (BD, 2004). The observed pile ageing effects are:

- For PJ1, a static load test was performed 4 days after installation. The pile was loaded to its working load and released (stage 1), then reloaded to twice the working load and maintained for 72 hours (stage 2). The measured axial stresses over the 3-day load-holding period indicated that neither the changes in shaft nor tip resistance was significant (Figure 2.43).

- PJ2 was load tested 2 days after installation. A second load test was performed 34 days after the first test to two times its working load to further investigate the time effects on jacked piles. The results showed a small gain in shaft friction over the lower part of the pile shaft (13%) and some increases in the end bearing (25%) compared to the first load test; the overall set-up remained insignificant (Figure 2.44).

Zhang *et al.* (2006) collated 9 field tests of H-piles (mostly of size 305 × 305 × 180 kg/m of grade 55C) from Hong Kong and 142 cases of precast square or circular concrete piles (range from 250 – 500 mm in width or diameter and 10 – 25 m in length) from Guangdong Province in China that indicated some changes of pile capacity after installation. Static load tests of the H-piles performed 6 – 17 days after installation showed a capacity gain of 6 – 33% as compared to the respective final jacking forces. While some data showing an increase of pile capacity with time, others (including the results of five centrifuge model tests in dry CDG) indicated the opposite trend. They suggested that the ratio of the ultimate pile capacity (P_{ult}) to the final jacking force (P_J) appears to be a function of pile slenderness ratio (Figure 2.45).

The authors argue that, for long piles, the pile capacity is dominated by shaft resistance and this increases with time ($P_{ult}/P_J > 1$) due to the dissipation of pore water pressure and other set-up effects. For short piles, the pile capacity is influenced to a greater extent by its tip resistance. The static capacity defined by Davisson's failure criterion usually involves a smaller base resistance than that mobilised during pile jacking at a constant rate of penetration, which results in a P_{ult}/P_J ratio of less than 1. It is worthwhile noting that the time scale of the ratio of pile capacity considered in Figure 2.45 is comparable to those databases of pile set-up assessed using the DLT (comparing BOR to that of EOID). The latter shows a significantly higher capacity gain after end of driving for driven piles as discussed in preceding sections.

It is seen that the fundamental difference between jacked and driven piles has not been fully understood especially the state of the sand adjacent to the pile shaft and how this evolves and affects the short, medium and long-term shaft capacities. This thesis addresses some of these issues to various extents, which aims to provide further insights on the phenomenon of pile set-up and the related scale effects.

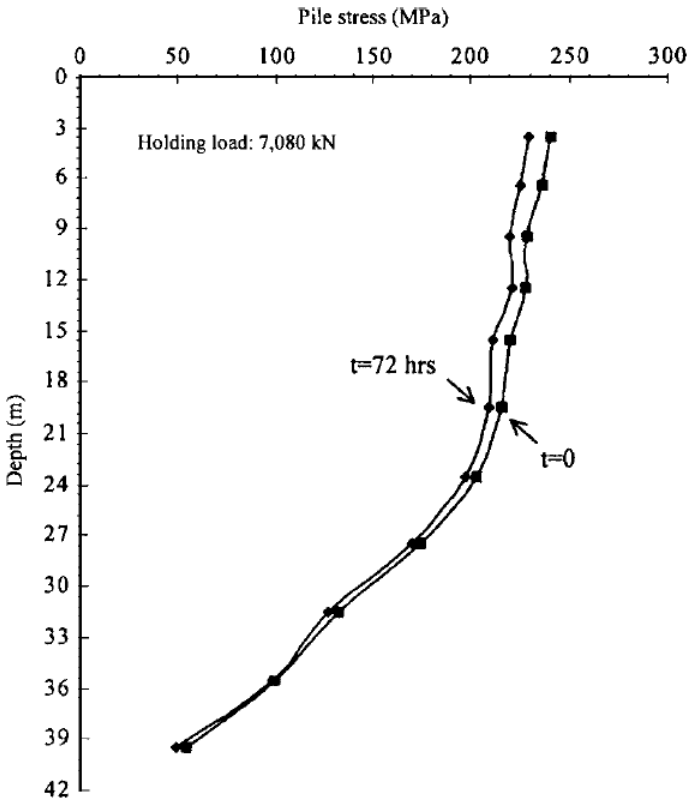

Figure 2.43. Creep-related changes of load distribution in PJ1 (Yang *et al.*, 2006a)

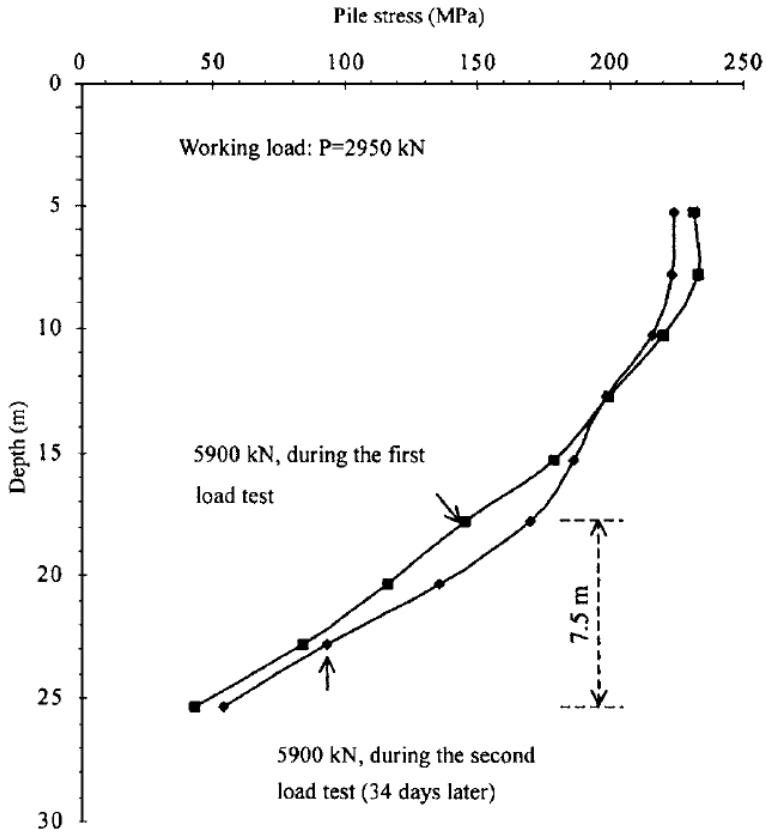

Figure 2.44. Time-related changes of load distribution in PJ2 (Yang *et al.*, 2006a)

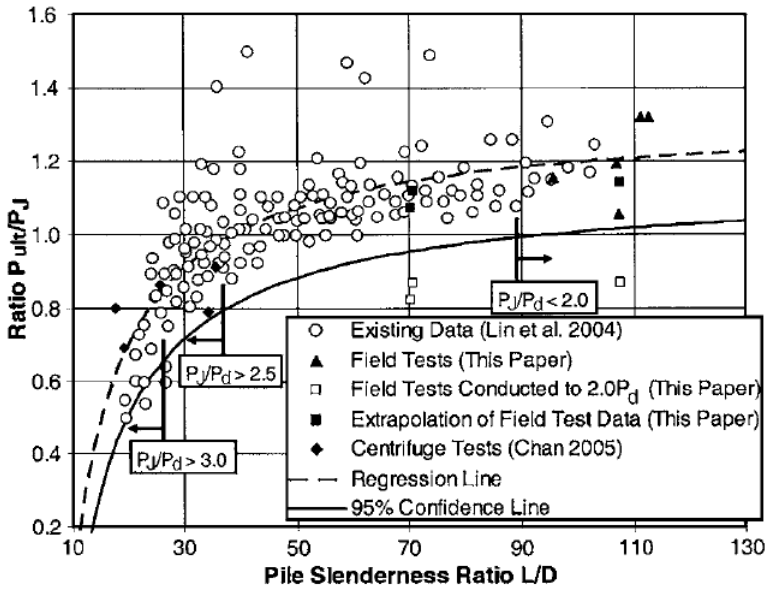

Figure 2.45. The ratio of pile capacity to final jacking force against pile slenderness ratio (Zhang *et al.*, 2006)

CHAPTER 3. CHAMBER TESTS AND RESULTS

3.1 INTRODUCTION

Investigation using full-scale test piles is often perceived by practice as being more convincing than small scale physical modelling. It is, however, rather expensive, time consuming and not generally suitable for parametric studies. As an alternative, model piles may be used to simulate the behaviour of full-scale piles under a controlled environment in the laboratory. Several attempts were made to model the phenomenon of pile set-up using small-scale physical models but the investigations were hampered by numerous restrictions.

This chapter describes an improved small-scale model pile test programme designed to investigate the ageing effects of pile shaft friction in sand. Challenges, considerations and limitations of the programme are discussed before presenting the experimental setup adopted and procedures employed in the study. Results show that the phenomenon of pile set-up is successfully modelled and that load-displacement characteristics are in keeping with those observed in centrifuge tests. Although the ageing effects observed in this laboratory-scale physical model may not be directly applicable to field scale piles, comparative studies involving various influential parameters provide qualitative indications of the relative influence of a variety of parameters.

3.2 CHALLENGES AND CONSIDERATIONS

3.2.1 Real Time

The actual time itself following displacement pile installation controls creep and creep-induced microscopic changes between sand particles under constant effective stress (Chow *et al.*, 1998; Bowman and Soga, 2005). Previous studies concluded that, while physical modelling using centrifuge testing facilities have allowed significant advances to be made, the fact that the creep time scaling factor in sand remains as unity means that it has been generally uneconomic to study pile set-up effects in a centrifuge (Garnier *et al.*, 2007).

3.2.2 Stress Similitude

Previous studies of model piles in sand have been performed at 1-*g* condition (e.g. Robinsky and Morrison, 1964; Meyerhof and Ranjan, 1972; Alawneh *et al.*, 1999), using pressure chamber (e.g. Nauroy and LeTirant, 1985; Yasufuku and Hyde, 1995; Chin and Poulos, 1996) and in a centrifuge (e.g. De Nicola and Randolph, 1999; Klotz and Coop, 2001; Lehane and White, 2005). Although physical model tested under normal gravity condition is more efficient and most commonly employed, excessive dilation in small scale 1-*g* tests can distort the extrapolation made to full-scale behaviour (Mikasa and Takada, 1973; Sedran *et al.*, 2001). With the impracticability of centrifuge facility, stress similitude becomes a great challenge in the physical modelling exercise. The next best option is to employ a pressure chamber. Modelling can be performed by reconstituting the same sandy material at the same density as that at in-situ and specifying appropriate stress conditions. It is noted that stress gradient similitude is not achieved in a pressure chamber test.

3.2.3 Sample Ageing vs. Pile Set-up

An increase in sand stiffness and strength over time at constant effective stress following disturbance (i.e. sand ageing) has been observed in ground reclamation and densification works and is revealed by increases in cone penetration end resistance (q_c) and shear wave velocity (V_s) (e.g. Mitchell and Solymar, 1984; Schmertmann, 1987; Charlie *et al.*, 1993; Ng *et al.*, 1998). Pile set-up in sand is another form of the sand ageing phenomenon that is believed to be caused by pile installation disturbance. Experimental studies of displacement piles in sand require a model sand bed to be prepared prior to any installation and testing works. The freshly deposited and pressurised sample by itself would age (e.g. Joshi *et al.*, 1995; Howie *et al.*, 2002; Wang and Tsui, 2009) which may interfere with the interpreted pile set-up effect. Therefore, it is important to characterise the sample ageing effect specifically for the experimental setup employed and identify an appropriate testing schedule so that this undesired side effect can be mitigated.

3.2.4 Consistency and Efficiency

Pressure chambers (often known as calibration chambers) have been widely employed to establish interpretation methods and engineering correlations for cone penetrometers and other in-situ testing tools. With all due measures taken to keep the sample consistent (so that the experiments are repeatable and thus comparable), the variation among chambers can sometimes be high, complicating interpretation. The conventional setup of accommodating only one inclusion for tool insertion (at the centre of chamber) can be very time consuming and expensive. One way to increase efficiency and sample consistency is by having more than one testing point in a chamber (i.e. as one would have in centrifuge testing).

3.2.5 Boundary and Interaction Effects

There are four boundary condition options available (i.e. BC1 to BC4 as shown in Figure 3.1) with BC1 and BC3 being the most commonly employed for pressure chambers (Parkin and Lunne, 1982; Salgado *et al.*, 1998; Jamiolkowski *et al.*, 2001). BC3 is preferred because the setup is simpler and the zero horizontal strain resembles the in situ condition. The difficulty of a flexible wall chamber to maintain zero radial displacement in BC2 and BC3 (Salgado *et al.*, 1998) would not be an issue if a rigid wall chamber is employed. Besides, the difference in stress state to that in field due to vertical stress that is applied from the base of chamber as in conventional chamber setup illustrated in Figure 3.2 (Wesley, 2002) can be improved by having the loading piston from top with a rigid base and smooth side walls.

Bolton *et al.* (1999) show that there are no significant boundary effects with rigid wall chambers if the closest distance from the penetration point to the nearest wall boundary is 10 times the cone diameter (i.e. 10D). The interaction effect between points is expected to be less severe than the wall boundary constraint and therefore adopting a minimum spacing between test piles of 10D is considered acceptable. It is worth noting that there is no universal agreement on the cut-off line for an ideally zero boundary and interaction effect within a practical modelling constraint. Nevertheless, the main concern of the intended experiment here would be the similarity of the boundary conditions among the test piles, accepting reasonably small interference from the chamber wall.

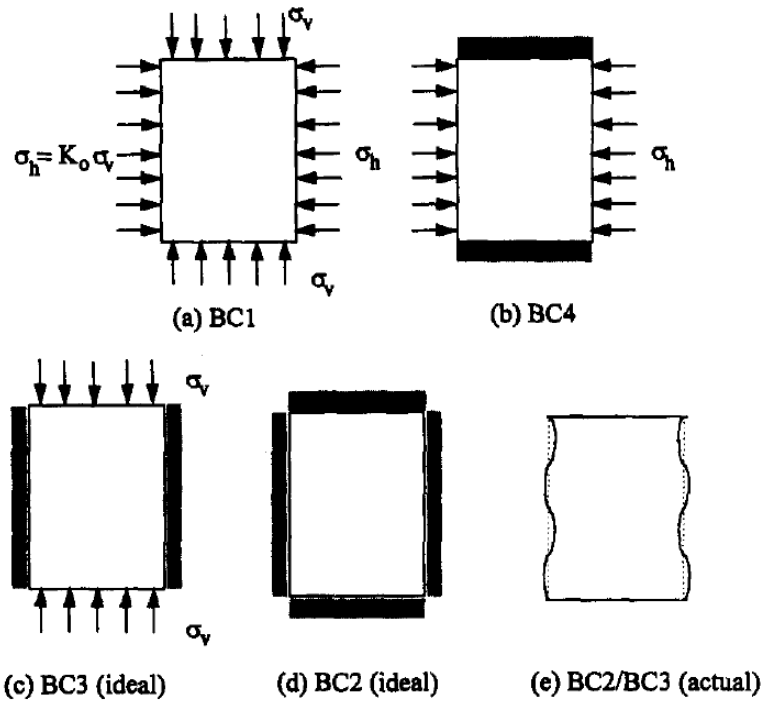

Figure 3.1. Types of boundary conditions in calibration chamber (Salgado *et al.*, 1998)

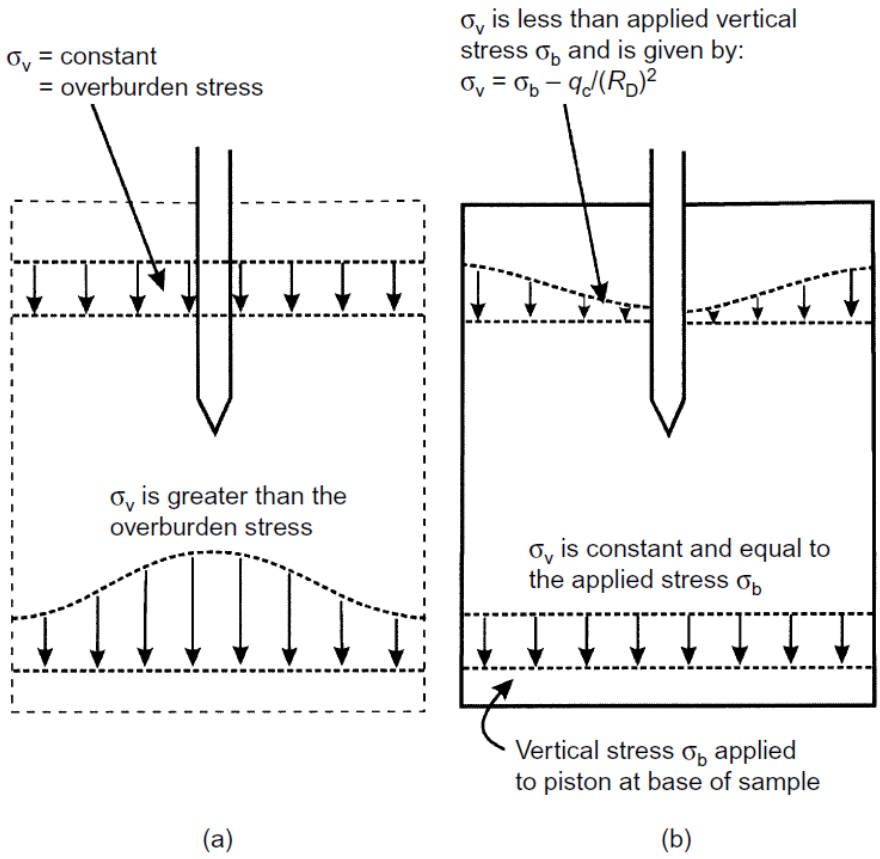

Figure 3.2. Difference in stress states in (a) field and (b) conventional calibration chamber (Wesley, 2002)

3.2.6 Particle Size Effects

By using a modelling-of-models approach (varying pile diameters and particle sizes) in the centrifuge, Foray *et al.* (1998) concluded that scale effects are insignificant if the diameter of a model pile is not less than 200 times the mean particle size (D_{50}). In contrast, Bolton *et al.* (1999) demonstrated in the centrifuge cone penetration tests that the normalised q_c values were identical for cases in which the cone diameter was larger than about $20D_{50}$. Despite different findings obtained, research has generally shown that scale effects, mainly due to particle size, can be significant in physical model in sands.

One feasible way to minimise this adverse effect is by employing very fine sand or silica flour in the model (e.g. De Nicola and Randolph, 1999). Smaller particles are, however, less vulnerable to crushing (Bolton and Lau, 1988) and have different grain shape and roughness that may affect the shear band thickness (Desrues and Viggiani, 2004). It is noteworthy also that natural sand deposits are seldom as uniform as commercial clean sands and usually comprise some small amount of fines that may influence their engineering behaviour.

3.2.7 Pile Installation Methods

In driven pile research, installation is usually performed by pushing the model piles monotonically into the soil sample to mimic the pile driving procedure (e.g. Robinsky and Morrison, 1964; Coop *et al.*, 2005). Recent investigations conducted by Lehane and White (2005) showed that different installation procedures employed (to mimic monotonic, jacked and pseudo-dynamic installations) have a significant influence on the radial effective stress developed on the pile shaft and thus its frictional resistance. The results of tension load tests revealed that the pile installed by monotonic jacking has much lower capacity and reaches its peak stress at a relatively small displacement compared to others. The pressure cells on the pile shaft indicated that the monotonically jacked pile had higher stationary radial stresses following installation (due to a lower degree of friction fatigue) but the changes in radial effective stress during shearing (due to constrained dilation of the contracted interface layer) were smaller.

3.2.8 Pile Load Tests

Chow *et al.* (1998) collated a number of well-documented case histories regarding the gain in pile shaft resistance with time for displacement piles in sand. The very high degree of scatter was mainly attributed to the differences in the definition of initial capacity (mostly derived from end of initial driving (EOID) measurement) and to the absence of a distinction made between static and dynamic load test results. In order to avoid short-term effects due to pore pressure dissipation following pile installation, load tests should be conducted at least 12 hours after driving as suggested by Tavenas and Audy (1972) and Åstedt *et al.* (1992), amongst others. Given differences between first-time test and re-test capacities (e.g. Axelsson, 2000; Jardine *et al.*, 2006), it is also desirable that any study of set-up effects should only consider 'first-time' or 'virgin' capacities.

3.3 TEST SETUP AND PROCEDURES

3.3.1 Soil Properties

The soil used in the pressure chamber tests presented in this chapter was collected from The University of Western Australia (UWA) test bed site at Shenton Park, located about 5 km from the city centre. The sand is predominantly siliceous with mild traces of carbonates; these carbonates have the potential to provide very weak cementation and bonding between particle grains. The sand is sub-angular to sub-rounded, uniformly graded with a mean particle size (D_{50}) of 0.42 mm and coefficient of uniformity of about 2. Maximum and minimum void ratios (e_{max} and e_{min}) were recorded as 0.79 and 0.44 respectively. Further details of the Shenton Park test site and its soil properties are provided in Chapter 4.

3.3.2 Equipment

A cylindrical steel chamber with an inner diameter of 395 mm, 400 mm height and 5 mm thickness was used to house the sand samples. The base plate was watertight sealed with a small opening left to allow saturation. The top plate was 40 mm thick with circular openings that allowed insertion of the model piles. The size of the openings could be modified to maintain a consistently small gap of approximately 1 mm when different diameters of piles were tested. The sample was subjected to vertical stresses

using a reaction frame (comprising rectangular hollow sections bolted to the laboratory strong floor) and a hydraulic jack placed at the centre of a top plate that jacked against the cross beam of the frame. A load cell was placed in line with the jack to ensure the required pressure was achieved and maintained at all times. This system, involving a near-rigid lateral wall with constant vertical stress, is classified as a BC3 chamber test.

An actuator, which is normally employed in beam centrifuge experiments, was used to perform jacked pile installation and tension load tests. It has two degrees of freedom, a capacity of 6.5 kN and can move in the vertical direction at a maximum rate of 3 mm/s. The actuator is controlled by an advanced multiple-axis actuator control system (PACS) associated with a data acquisition system (DigiDAQ) that had been developed in-house. A miniature load cell was attached to the model pile head to record forces required for both compression and tension loads. Cone penetration tests (CPT) were performed using a 7 mm diameter cone penetrometer to characterise the soil profile as well as to investigate the effects of sample ageing. The model piles were made from mild steel rods (or stainless steel tubes for the buried piles), available in three different sizes of 6 mm, 8 mm and 10 mm diameters with an embedded length of 300 mm. The surface of piles was either sandblasted to a centre line average roughness (R_{cla}) of about 2.5 μm to form an intermediate interface or bonded with sand grains ranged from 0.3 mm to 0.425 mm to create a fully rough interface as characterised by Lings and Dietz (2005). Figure 3.3 shows some pictures of the setup and equipment used in the experiment.

3.3.3 Sample Preparation

The sand was first oven-dried, sieved to remove impurities and particles larger than 1.18 mm and deposited by air-pluviation using an automated sand rainer. This method of deposition produces relatively homogeneous reconstituted sand samples with the desired relative density; the soil fabric created is expected to resemble that of natural wind-blown deposits, such as those at the Shenton Park site (Rad and Tumay, 1987). Dense samples were achieved by setting the shutter opening of the hopper at 2 mm while keeping the fall height constant at approximately 120 mm. The areal uniformity was monitored by setting four control points at the edge of each quadrant during the pluviation process and the final surface was levelled using a vacuum device. The

samples created were about 360 mm in height with an average relative density (D_r) of 75% and corresponding dry unit weight of approximately 17 kN/m^3.

Figure 3.3. Setup of the experiment and the equipment used: (a) setup of experiment; (b) cone penetrometer; (c) model piles ; (d) roughness-meter

The sample was then saturated by allowing water to permeate through the opening at the base plate. The water pressure head driving the flow was kept low (below 5 kPa) and a layer of geofabric laid at the bottom ensured flow was induced over the full base area.

Following saturation (which typically took about 1 hour), vertical stress was applied gradually in 10 increments with each increment maintained for about 5 minutes until a final pressure of 200 kPa (or 20 kPa in the test that investigated the effects of low stress level) was attained. Sample were then left to age under this constant effective stress for 7 days (before model piles were installed), and maintained at a constant vertical stress for the remainder of the experiment. For tests on buried piles, the hollow model piles were positioned on the stands that were fixed to the base plate before sand pluviation, saturation and pressurisation were performed. A few selected pictures are shown in Figure 3.4 to illustrate the sample preparation.

3.3.4 Sample Ageing

An investigation of sample ageing was performed using a 7 mm diameter cone penetrometer installed at 1 minute, 1 day, 7 days and 28 days after the final pressure has been applied to the top of the sample. The corresponding CPT net q_c data normalised by effective vertical stress σ'_v ($Q_n = (q_c - \sigma_v)/\sigma'_v$) plotted against normalised depth ($Z = z/D_c$) are presented in Figure 3.5. The measured Q_n profiles are typical of those measured in a sand of constant relative density in a pressure chamber (e.g. Houlsby and Hitchman, 1988; Lunne *et al.*, 1997). The cone resistance gradually developed during initial penetration up to approximately 8 to 10D_c, at which penetration a plateau was achieved and maintained until the end of probing at approximately mid-height of the sample (this was a limitation of the experiment arising due to the length of the penetrometer employed). An increase in cone tip resistance with time is clearly in evidence and is most significant between the 1-minute and 1-day results.

Mesri *et al.* (1990) proposed the following empirical expression for the estimation of the increase in cone resistance with time:

$$\frac{q_c}{q_{cR}} = \left(\frac{t}{t_R}\right)^{C_D C_\alpha / C_c} \tag{3-1}$$

where q_{cR} is a reference cone resistance at a reference time t_R (at the end of primary consolidation); q_c is cone resistance measured at time t ($t > t_R$); C_D reflects any densification or disturbance induced (e.g. by vibration and blasting); C_α represents the secondary compression index or creep coefficient; and C_c is the compression index.

Figure 3.4. Stages of sample preparation: (a) sand deposition using automatic sand rainer; (b) vacuum device; (c) a levelled surface; (d) saturation; (e) pressurisation

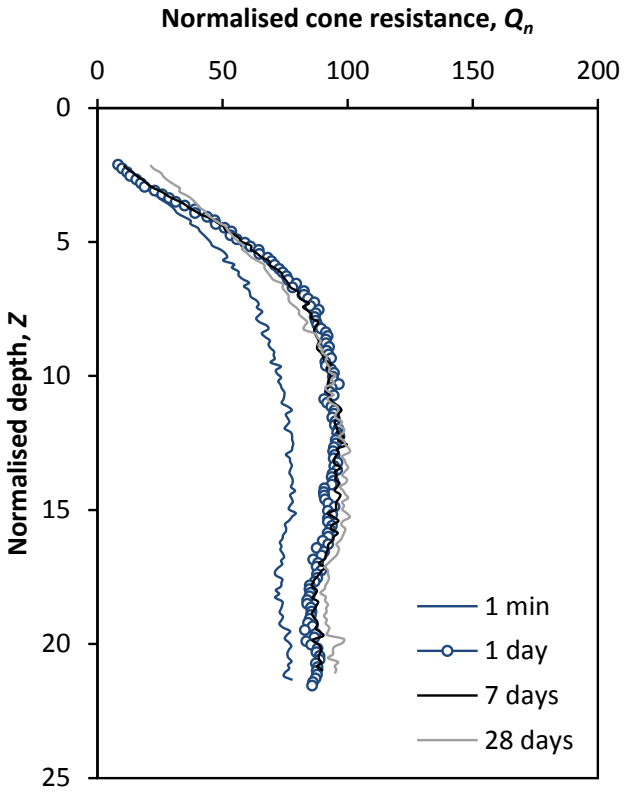

Figure 3.5. Normalised cone tip resistance at different points of time

Figure 3.6 shows the average of normalised cone tip resistances (below $10D_c$) against normalised time plotted on a logarithmic scale; both axes were normalised by their respective initial readings at 1 minute. By adopting C_D of 1.0 and C_α/C_c of 0.0225 (average for a wide range of clean granular soils which varied from 0.015 to 0.03; see Mesri *et al.* (1990)), Equation (3-1) can be seen on Figure 3.6 to fit the observed CPT data reasonably well.

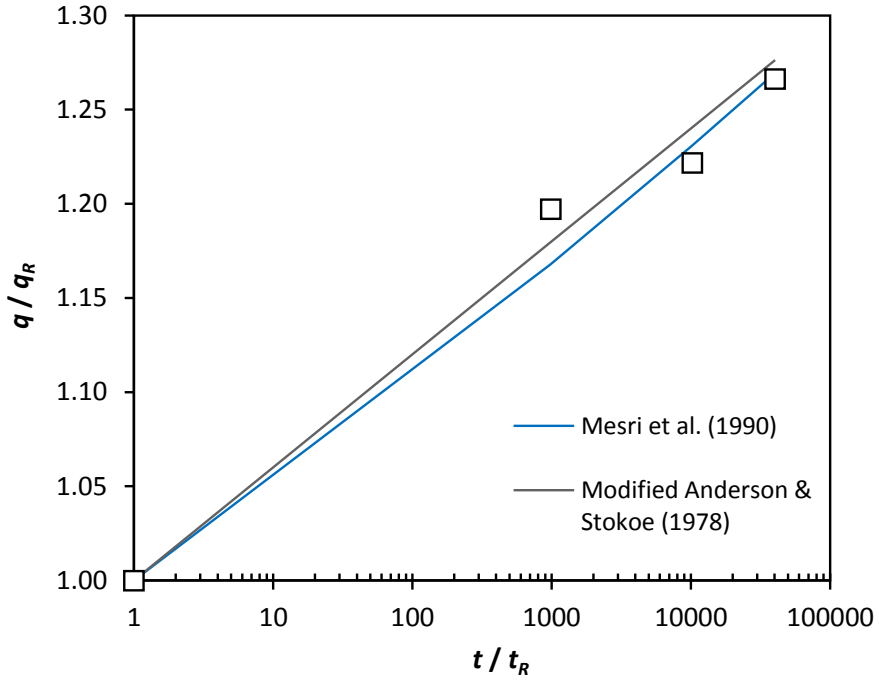

Figure 3.6. Changes of average normalised cone tip resistance with time

The gain in cone tip resistance with time can also be expressed using a simple logarithmic function; similar to that proposed by Anderson and Stokoe (1978) who quantified the ageing effects based on small strain shear modulus (G_o):

$$\frac{q_c}{q_{cR}} = 1 + N_{qc} \log\left(\frac{t}{t_R}\right) \tag{3-2}$$

where N_{qc} is the normalised change in q_c per log cycle of time. The least squares regression line can be approximated very well by assuming N_{qc} of 0.06 using Equation (3-2) as included in Figure 3.6. This 6% (for every log cycle of time) of sample ageing effects was the basis used to determine the working schedule for this experimental study. Considering various constraints, the model piles were installed after 7 days (~10000 minutes) of sample ageing, which means the gain in q_c over the investigated pile set-up period of 1 month would be less than 5%.

3.3.5 Pile Installation and Testing

Three different pile installation methods were considered in this study. Most of the model piles were installed by impact driving, which was achieved by controlled tapping action with a hand-held hammer with a specified number of impacts (average 400 blows for a total penetration of 300 mm) and guided by a wooden block to maintain verticality; this method mimicked the driven pile installation process. Some model piles were jacked monotonically into the sand samples using an actuator at a rate of 1 mm/s. However, 2 – 3 pushes were required for these 'monotonic' tests due to the limited travel length of the actuator. Six of the model piles (i.e. for one chamber test) were pre-installed or buried to examine ageing effects in the absence of effects of pile installation disturbance.

A total of six model piles were inserted into each sample in a hexagonal layout and maintained, as discussed above, at a minimum distance between piles and between a pile and the wall boundary equal to 10*D* (Bolton *et al.* (1999). The minimum distance between a pile tip and the rigid bottom boundary was 7.5*D*. The model piles were then load tested at a constant rate of 0.01 mm/s to their ultimate tension capacity or to a minimum displacement of 1*D*. Typical profiles of installation resistances, which are recorded as the numbers of hammer blows per every 40 mm penetration (for driven piles) and as the jacking forces measured by a load cell attached at the pile head (for jacked piles), are presented in Figure 3.7. It is noted that some boundary and scale effects of this small-scale experiment are inevitable but the relative response among the test piles of similar boundary conditions in the chambers is what is required.

The 1-day capacity was adopted as the reference benchmark capacity to assess any potential increase in pile shaft friction. All load tests were performed on 'fresh' model piles tested for the first time to avoid unnecessary complications in interpretation (except for a few re-tests to demonstrate their different behaviour). Figure 3.8 shows some pictures related to the experimental setup for pile installation and load testing.

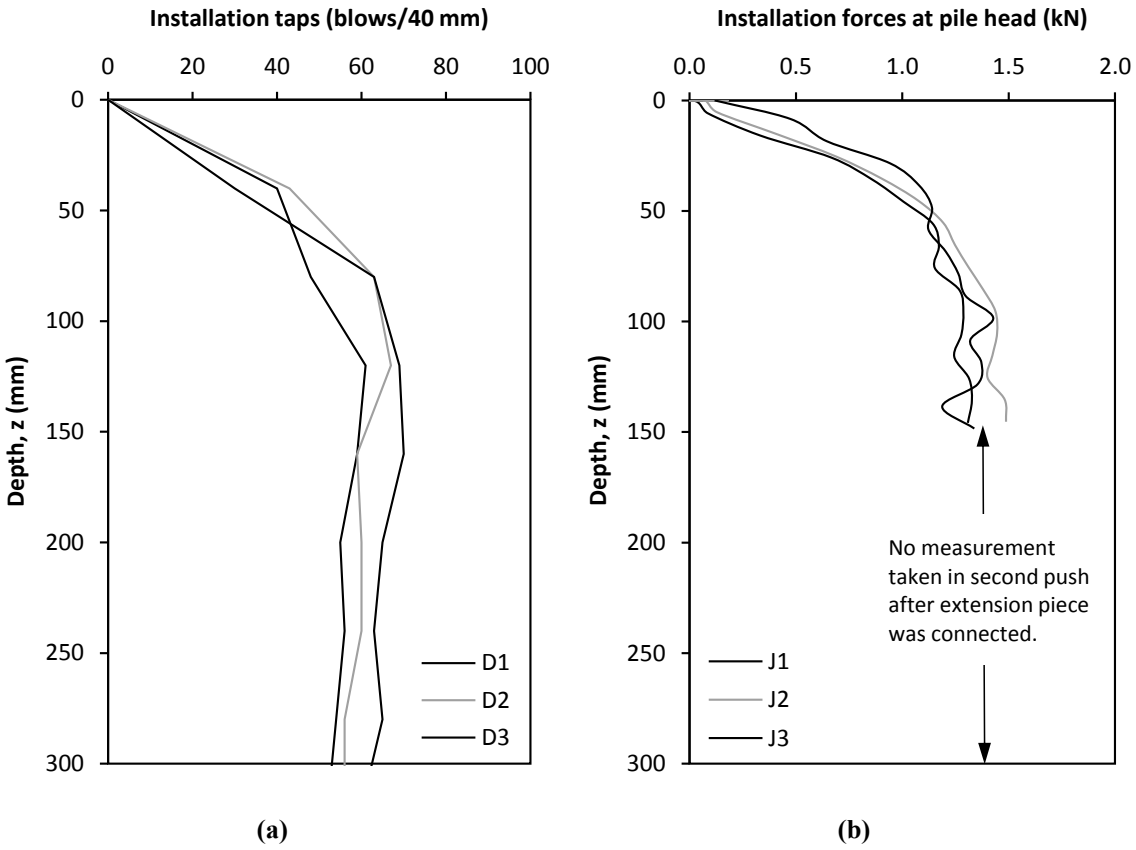

Figure 3.7. Installation resistance for C4: (a) driven; (b) jacked

3.3.6 Comparison with Previous Studies

The experimental setup and testing procedures employed in this study are summarised in Table 3.1. Previous laboratory-scale investigations on pile set-up in sand, which were reviewed in Chapter 2, are also attached for comparison. It is seen that there is a dearth of laboratory-scale model test on pile set-up due to various challenges as highlighted in Section 3.2; previous studies were constrained by various limitations (e.g. involved interpretation of re-tested piles and piles not loaded to failure). This set-up study is unambiguous in that it comprises an aged model sand bed with a set of 'virgin' pile shaft resistances determined from static tension load tests conducted to failure at various ageing periods.

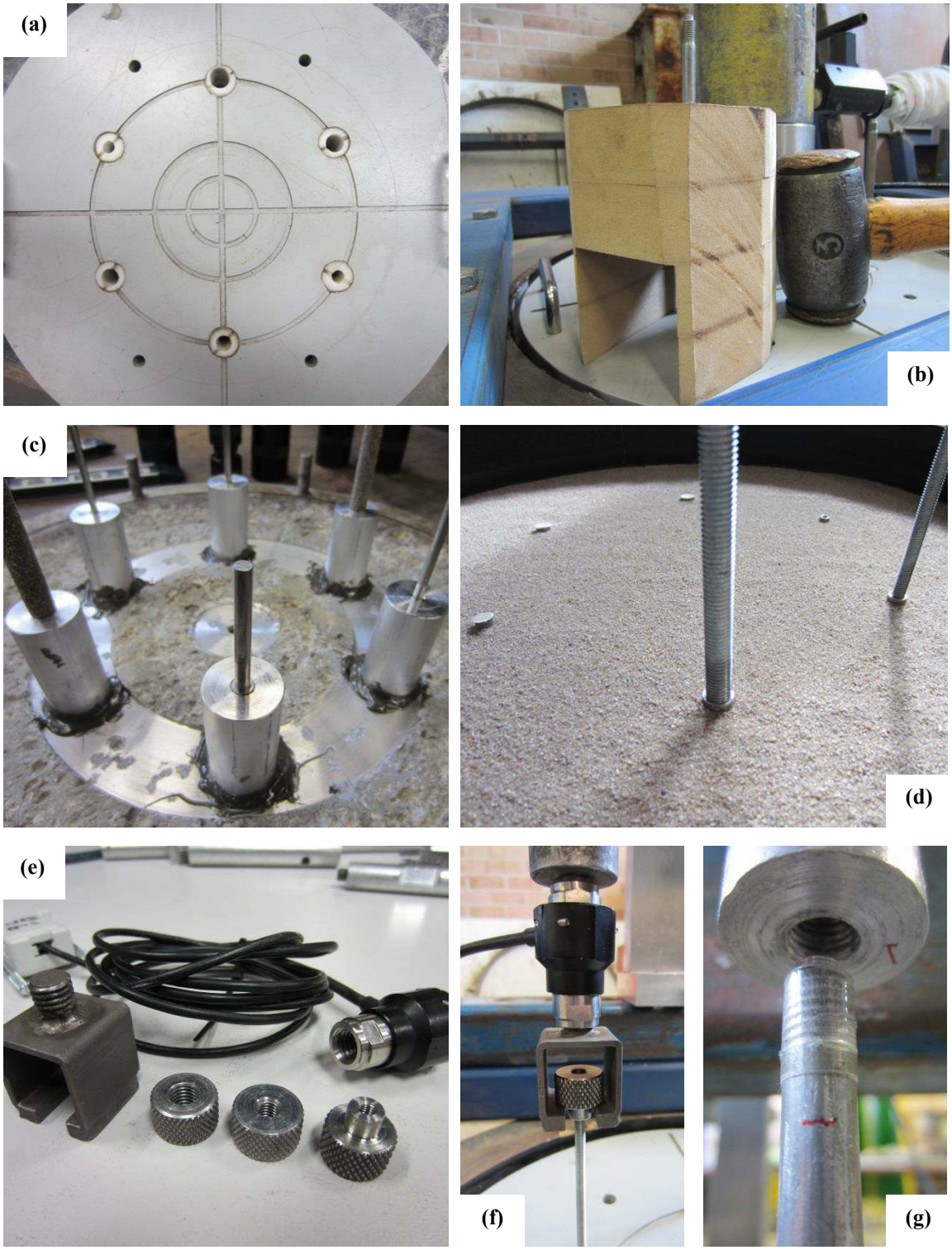

Figure 3.8. Details of pile installation and testing: (a) pile layout; (b) hammer and guide block for impact driving; (c) base stand to position buried piles; (d) connection at buried pile head; (e) load cell and connectors; (f) tension load test; (g) modified pile head for jacking

Table 3.1. Comparison of experimental setup and testing procedures for pile set-up study

Aspects	Bullock (1999)	Axelsson (2000)	White and Zhao (2006)	Present study
Model pile	L = 254 mm D = 9.52 mm L/D = 26.7 -	L = 970 mm D = 28 mm L/D = 34.6 R_{cla} = 9 – 13 μm	L = 200 mm D = 10 mm L/D = 20 Smooth	L = 300 mm D = 6 – 11 mm L/D = 27 – 50 Intermediate, Rough
Sand type	Silica sand D_{50} = 0.46 mm C_u = 1.7	Silica sand D_{50} = 0.65 mm C_u = 4.7	Carbonate sand D_{50} = 0.28 mm C_u = 2.1	Silica sand D_{50} = 0.42 mm C_u = 2.0
Sample preparation & saturation	Dry pluviation, shaking table D_r = 40, 60, 80% Dry	Compaction (≈ 13 layers) D_r = 63 – 73% Saturated	Dry pluviation D_r = 75% Saturated, fluctuated	Dry pluviation D_r = 75% Saturated
Testing facility & stress condition	Centrifuge (50-g)	Pressure chamber OD = 385 mm σ'_h = 0 – 30 kPa	1-g	Pressure chamber OD = 393 mm σ'_v = 20, 200 kPa
Sample ageing period	-	1 day	-	7 days
Pile layout & boundary/ interaction effects	- -	1 (central) s_w = 6D	14, 17 s_p = 15D; s_w = 20D	6 (hexagonal) s_p = 10D; s_w = 10D
Pile installation method	Driven N_{cyc} = 306 – 521	Driven N_{cyc} = 138 – 247	Mono-jacked N_{cyc} = 1	Driven, mono-jacked, buried N_{cyc} = 0 – 400
Pile set-up period	t_{max} = 6 hrs t_R = 15 min	t_{max} = 23 days t_R = 1 hr	t_{max} = 96 days t_R = 1 hr, 1 day	t_{max} = 30 days t_R = 1 day
Pile load test	Tension Re-test s = 4 – 7 mm (s/D = 42 – 74%)	Tension Re-test s = 1.4 mm (s/D = 5%)	Compression Re-test s = 1 mm (s/D = 10%)	Tension Virgin s > 8 mm (s/D > 100%)

3.4 RESULTS AND DISCUSSION

3.4.1 Test Programme

A total of 36 model piles installed in six separate chambers were employed to investigate the ageing effects of pile shaft friction and some related issues. The objective and general details of each chamber test are first explained before the results of tension load tests are presented. In general, all experiments followed the procedure described in Section 3.3 (unless stated otherwise). A typical chamber contained sand that was air-pluviated to a dense state (an initial relative density of about 75%) and subjected to a vertical pressure of 200 kPa throughout the experiment.

Table 3.2 lists the configuration of each chamber and pile, which includes the vertical pressure applied to the chamber, the pile diameter, length and surface roughness, and the installation method and equivalent cycles. The results of each tension load test and its corresponding displacement at failure for different ageing periods are summarised in Table 3.3. It is noted that different failure criteria are adopted for model piles installed by driven, jacked and buried methods and those at low pressure due to contrasting load-displacement behaviours. The average ultimate shaft shear stress (τ_{avg}) instead of total pile shaft capacity (Q_s) is presented so that piles of different diameter may be compared. The results of CPTs performed was presented as $q_{c\text{-}avg}$ in Table 3.3, which was computed from the average of q_c readings from below a depth of 80 mm (where q_c was effectively constant).

For ease of identification, a notation system is introduced to highlight the basic features of the pile test. It explains the chamber number, installation method, pile size, interface roughness and pile age in a systematic way as shown in Figure 3.9.

Table 3.2. Details of experimental setup and installation record

Test	Pressure	Installation		Pile		Interface
	(kPa)	Method	Cycle	*D* (mm)	*L*/*D*	Roughness
C4-DMi-3	200	Driven	399	8	37.5	Intermediate
C4-DMi-7	200	Driven	436	8	37.5	Intermediate
C4-DMi-28	200	Driven	455	8	37.5	Intermediate
C4-JMi-3	200	Jacked	2	8	37.5	Intermediate
C4-JMi-7	200	Jacked	2	8	37.5	Intermediate
C4-JMi-28	200	Jacked	2	8	37.5	Intermediate
C5-DLi-1	200	Driven	422	10	30	Intermediate
C5-DLi-7	200	Driven	428	10	30	Intermediate
C5-DLi-28	200	Driven	431	10	30	Intermediate
C5-DSi-1	200	Driven	422	6	50	Intermediate
C5-DSi-7	200	Driven	435	6	50	Intermediate
C5-DSi-28	200	Driven	432	6	50	Intermediate
C6-DMi-0.1	200	Driven	454	8	37.5	Intermediate
C6-DMi-1	200	Driven	443	8	37.5	Intermediate
C6-DMi-3	200	Driven	441	8	37.5	Intermediate
C6-DMi-7	200	Driven	452	8	37.5	Intermediate
C6-DMi-15	200	Driven	459	8	37.5	Intermediate
C6-DMi-30	200	Driven	445	8	37.5	Intermediate
C7-DSi-2	200	Driven	411	6	50	Intermediate
C7-DMi-2	200	Driven	414	8	37.5	Intermediate
C7-DLi-2	200	Driven	423	10	30	Intermediate
C7-DSr-2	200	Driven	426	7	42.9	Rough
C7-DMr-2	200	Driven	421	9	33.3	Rough
C7-DLr-2	200	Driven	413	11	27.3	Rough
C8-BSr-7	200	Buried	NA	8	38.0	Rough
C8-BMr-7	200	Buried	NA	10	30.3	Rough
C8-BLr-7	200	Buried	NA	11	27.0	Rough
C8-BSr-28	200	Buried	NA	8	38.0	Rough
C8-BMr-28	200	Buried	NA	10	30.3	Rough
C8-BLr-28	200	Buried	NA	11	27.0	Rough
C9-DMr-1	20	Driven	428	9	32.5	Rough
C9-DMr-7	20	Driven	426	9	33.0	Rough
C9-DMr-28	20	Driven	436	9	32.6	Rough
C9-JMr-1	20	Jacked	3	9	32.7	Rough
C9-JMr-7	20	Jacked	3	9	33.3	Rough
C9-JMr-28	20	Jacked	3	9	32.1	Rough

Table 3.3. Results of tension load test and CPT

Test	Age (day)	τ_{avg} (kPa)	Displacement	$q_{c\text{-}avg}$ (MPa)
C4-DMi-3	3.1	274.3	at 8 mm	39.2
C4-DMi-7	7.0	248.9	at 8 mm	
C4-DMi-28	27.9	320.0	at 8 mm	
C4-JMi-3	2.9	98.9	avg 3 - 8 mm	
C4-JMi-7	7.0	93.6	avg 3 - 8 mm	
C4-JMi-28	27.7	132.2	avg 3 - 8 mm	
C5-DLi-1	1.0	213.4	at 10 mm	32.5
C5-DLi-7	7.0	198.0	at 10 mm	
C5-DLi-28	28.0	289.9	at 10 mm	
C5-DSi-1	1.0	139.8	at 10 mm	
C5-DSi-7	6.9	-	at 10 mm	
C5-DSi-28	27.8	155.5	at 10 mm	
C6-DMi-0.1	0.1	208.0	at 10 mm	35.9
C6-DMi-1	0.9	235.8	at 10 mm	
C6-DMi-3	2.9	230.2	at 10 mm	
C6-DMi-7	7.1	235.6	at 10 mm	
C6-DMi-15	14.9	265.6	at 10 mm	
C6-DMi-30	30.0	277.6	at 10 mm	
C7-DSi-2	2.0	133.9	at 10 mm	25.7
C7-DMi-2	2.0	160.6	at 10 mm	
C7-DLi-2	2.1	150.0	at 10 mm	
C7-DSr-2	2.0	170.9	at 10 mm	
C7-DMr-2	2.1	214.0	at 10 mm	
C7-DLr-2	2.1	239.9	at 10 mm	
C8-BSr-7	6.8	200.0	at 1.5 mm	25.1
C8-BMr-7	6.9	179.8	at 1.5 mm	
C8-BLr-7	6.9	183.3	at 1.5 mm	
C8-BSr-28	27.9	-	at 1.5 mm	
C8-BMr-28	27.9	191.9	at 1.5 mm	
C8-BLr-28	27.9	194.0	at 1.5 mm	
C9-DMr-1	0.9	77.9	avg 3 - 8 mm	9.4
C9-DMr-7	6.9	69.3	avg 3 - 8 mm	
C9-DMr-28	28.0	62.6	avg 3 - 8 mm	
C9-JMr-1	0.8	41.8	avg 3 - 8 mm	
C9-JMr-7	6.8	34.2	avg 3 - 8 mm	
C9-JMr-28	27.8	32.2	avg 3 - 8 mm	

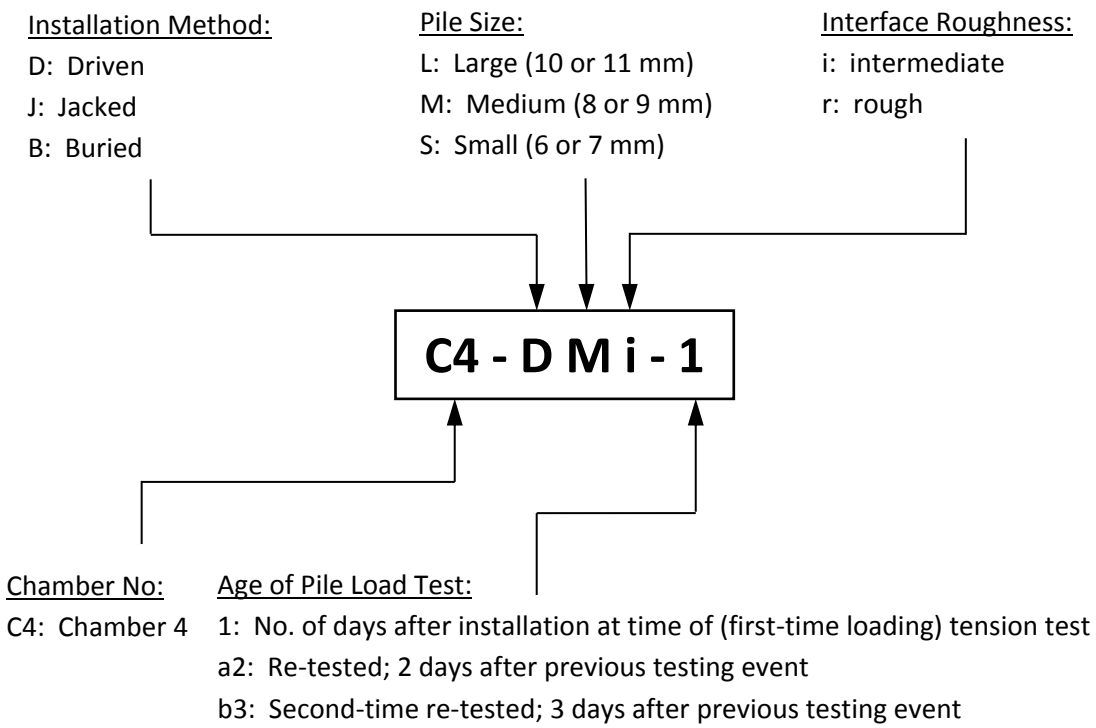

Figure 3.9. Notation used for model pile

C1 to C3 are trials involved in determining an effective test setup and configuration, which are not reported here. In C4, three model piles were installed by impact driving and tested at 3 days (initially planned at 1 day but was delayed due to malfunction of miniature load cell), 7 days and 28 days after installation to examine the ageing effect on pile shaft friction. Another three piles with the same specification were installed by monotonic jacking at 1 mm/s using an actuator (ideally in a single push but was forced to do it in 2 cycles allowed for the connection at mid-depth due to limited travel length of the actuator). Monotonic jacked installation (an idealised installation method to model displacement pile with the lowest level of friction degradation) was chosen to contrast with the ageing response of typical driven piles since pile set-up is claimed to be closely related to installation disturbance.

C5 was established to investigate if pile set-up is also a function of pile diameter. The understanding of the diameter effect is very important for any future extrapolation that allows prediction of set-up effect for field-scale piles. Two different diameters of pile, i.e. 6 mm and 10 mm, in a set of three for each size were driven and tested at 1 day, 7

days and 28 days after installation. The experiment also aims to investigate if the observations from literature (e.g. Lebêgue, 1964; Foray *et al.*, 1998; Lehane *et al.*, 2005a) that showed an inverse dependency of average shaft resistance with diameter on buried piles can be applied to displacement piles. The result for C5-DSi-7 was discarded because the pile was disturbed during installation. This was because the wooden guide could not be lifted up after installation as it was blocked by the lock nut attached to the hydraulic jack cylinder.

Based on the observation from C4 and C5 that showed some delay in the set-up process, C6 was built with a closer time interval between tests to further investigate the evolution of pile set-up. Six model piles were driven and tested at 1 hour, 1 day, 3 days, 7 days, 15 days and 30 days after installation to demonstrate a clearer time-dependent relationship. This experiment is also motivated by the results of extensive triaxial creep tests reported by Bowman and Soga (2005), which interpret the set-up phenomenon as due to kinematically constrained dilatant creep, preceding by a contractile stage.

Results from C5 indicated a variation of average shaft friction with diameter that differs with that reported in the literature. To further investigate this observation (which was considered to be potentially due effects of different installation methods), another chamber test (i.e. C7), which included three different sizes of piles, was performed. Given the strong influence of surface roughness on the interface shearing behaviour (e.g. Frost and DeJong, 2005; Lings and Dietz, 2005), two different pile interfaces were made (low-intermediate roughness and fully rough) for examination.

In order to verify the hypothesis that pile set-up is caused by installation disturbance (since no set-up has been reported on bored piles), the chamber was modified to accommodate pre-installed piles. C8 included six buried piles, each with a rough interface (two for each diameter), which were tested at 7 days and 28 days after pressurisation. It is noted that the smallest piles C8-BSr-7 and C8-BSr-28 failed prematurely due to slippage on the bushes and were therefore not loaded to the full tension capacity. Although C8-BSr-7 yielded, it showed a higher shaft resistance than larger diameter piles and allowed for reasonable extrapolation of the experimental observations.

No set-up effects appear to have been reported in the upper few metres of sand deposits. This may imply either that the surrounding stresses (as a function of depth) play an important role in the set-up process or that the ageing effects are more predominant near the pile tip. C9 was therefore subjected to very low vertical pressure of 20 kPa (in contrast to the standard stress of 200 kPa employed in other chambers) to investigate this effect. Six model piles of the same diameter with rough interfaces were installed by impact driving and monotonic jacking methods and subsequently load tested at 1 day, 7 days and 28 days after installation.

Although the model sand beds were prepared strictly according to the procedure described before, there were some relatively modest deviations in the average q_c values, as indicated in Table 3.3; these could be attributed to difficulty in pressurisation, effects of numerous pile installations and differing installation methods involved in each chamber. The CPTs were performed after all testings have been completed.

More importantly, the sample uniformity as shown by the consistent profiles of penetration resistance from both CPTs and pile head load measurements allows for confident comparisons to be made between results for different test piles within a chamber. The largest variation of CPT q_c profiles within a given chamber was noticed in C6 and is presented in Figure 3.10. Therefore, the interpretation in the following focuses mainly on a comparison between the test piles within each chamber and the trends (rather than the absolute values) between the chambers. The results of tension load tests for C4 to C9 are shown in Figure 3.11 to Figure 3.16.

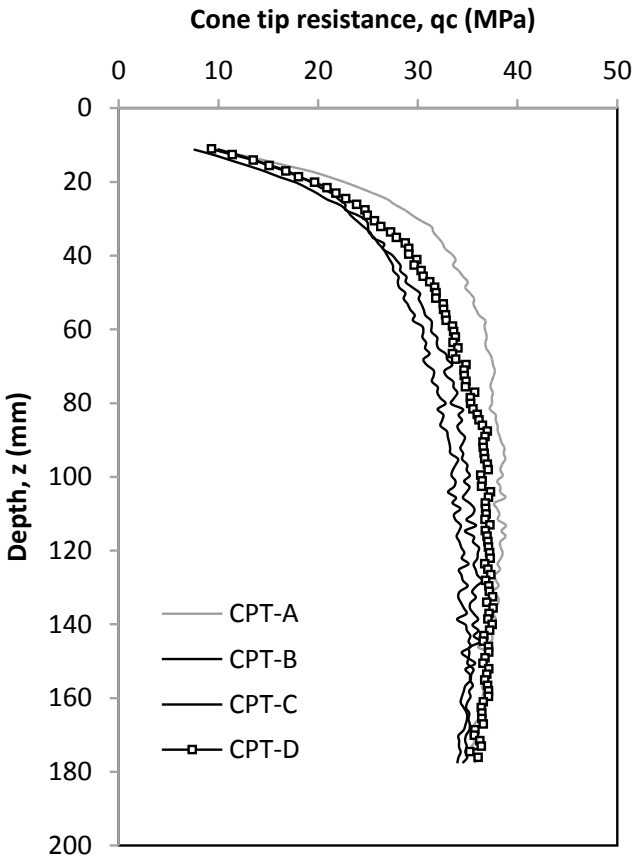

Figure 3.10. Variation of CPT q_c profiles for C6

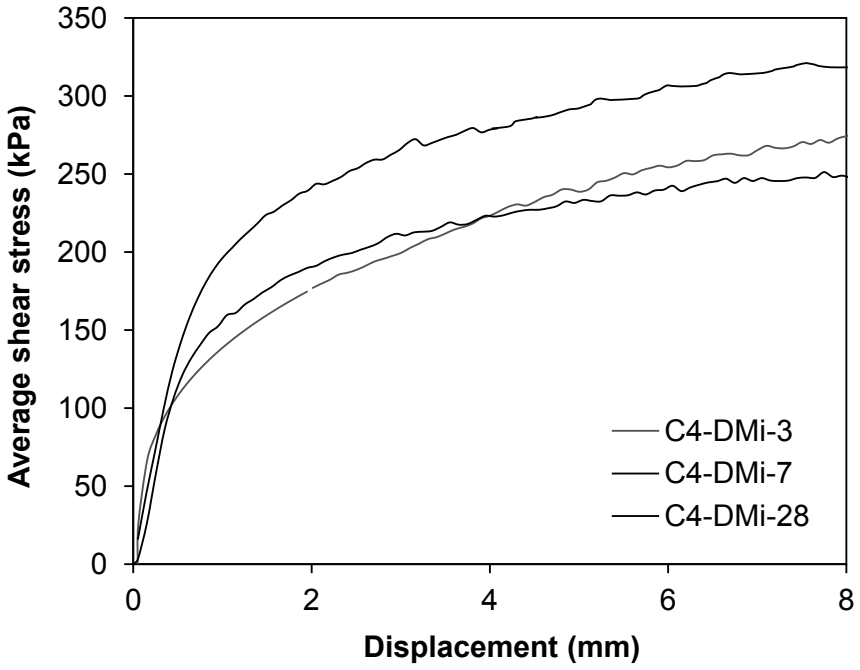

(a)

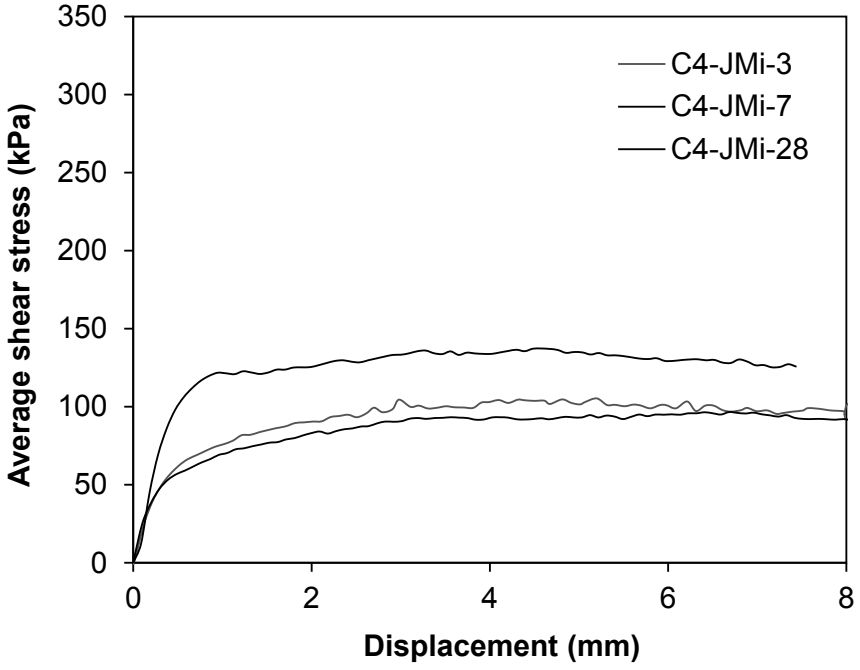

(b)

Figure 3.11. Results of tension load tests for C4: (a) Driven; (b) Jacked

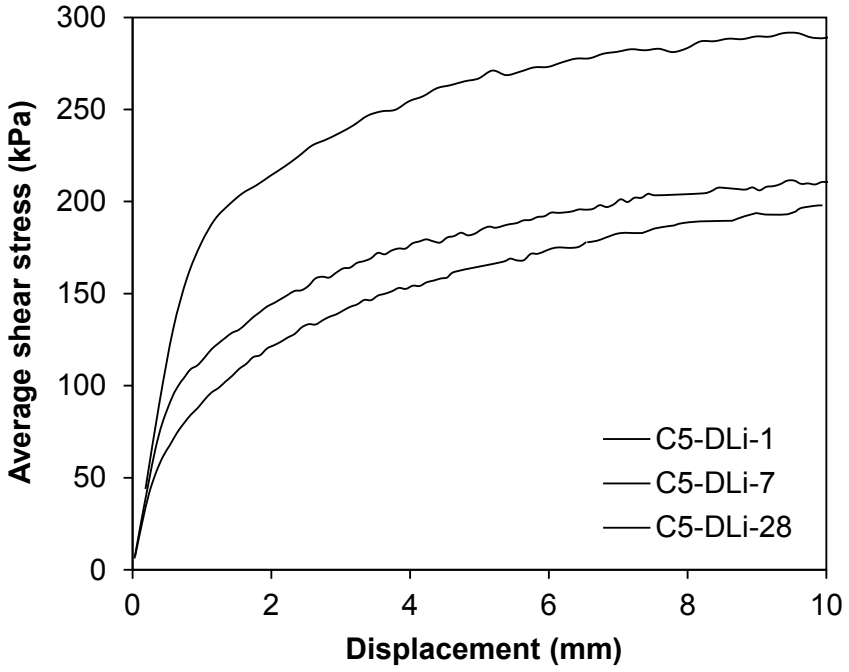

(a)

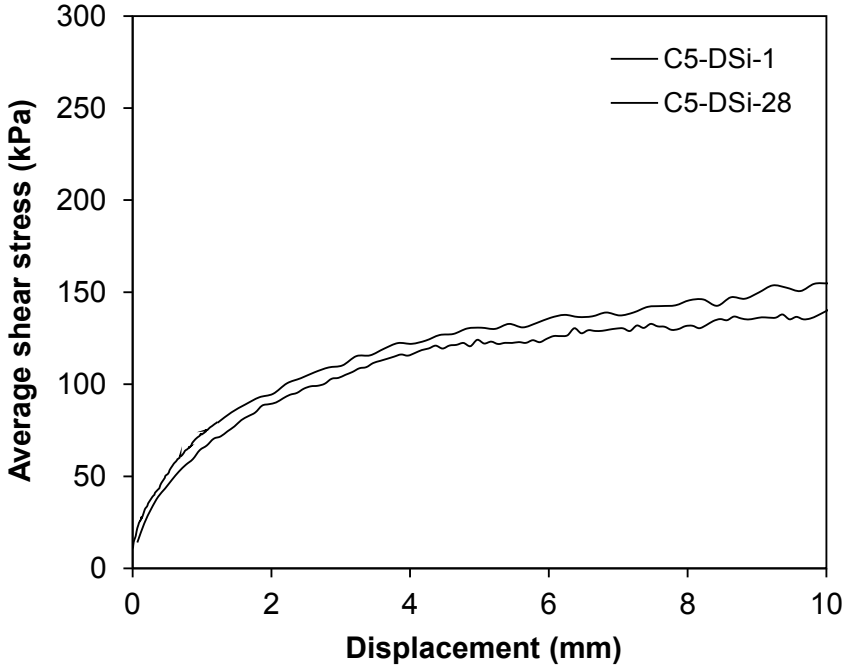

(b)

Figure 3.12. Results of tension load tests for C5: (a) Large diameter; (b) Small diameter

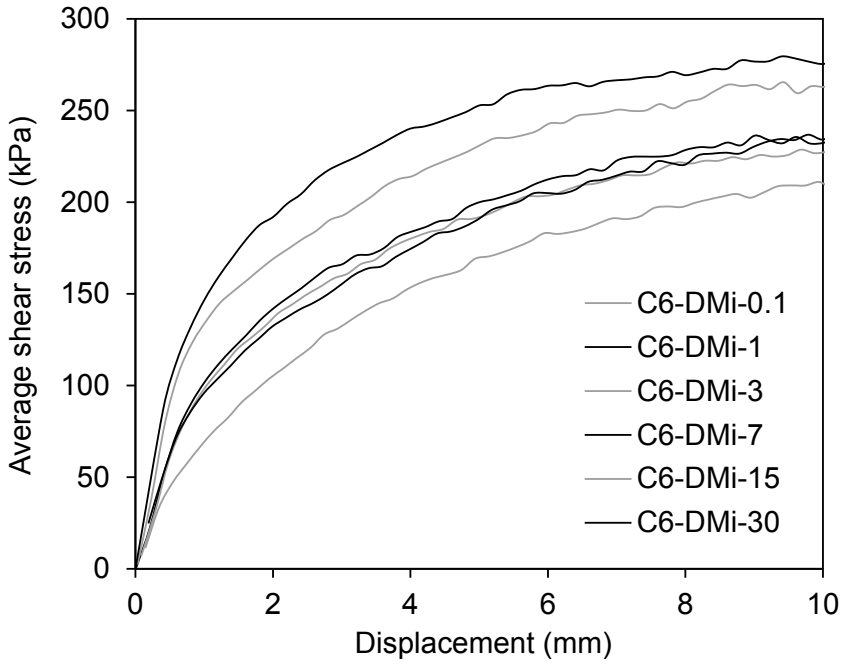

Figure 3.13. Results of tension load tests for C6

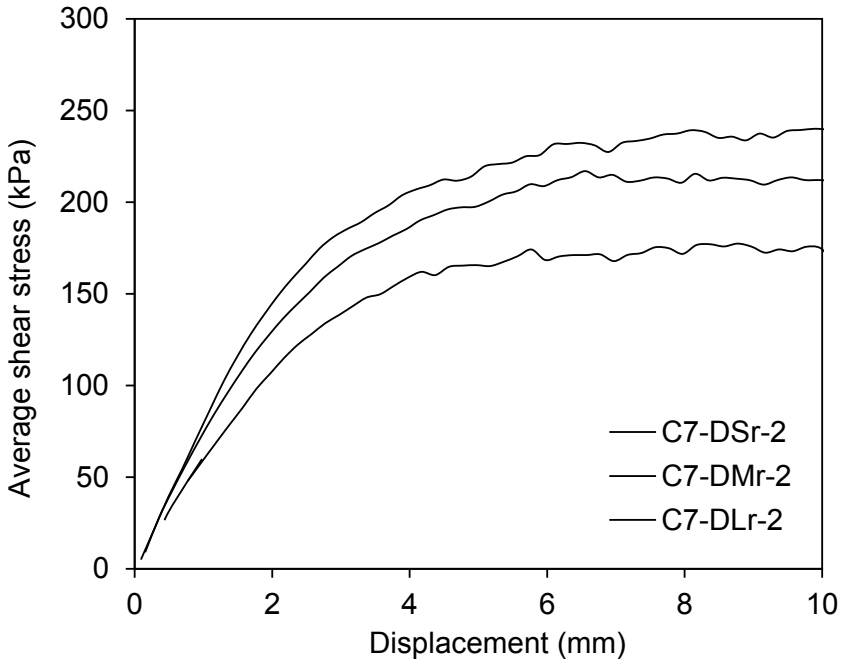

(a)

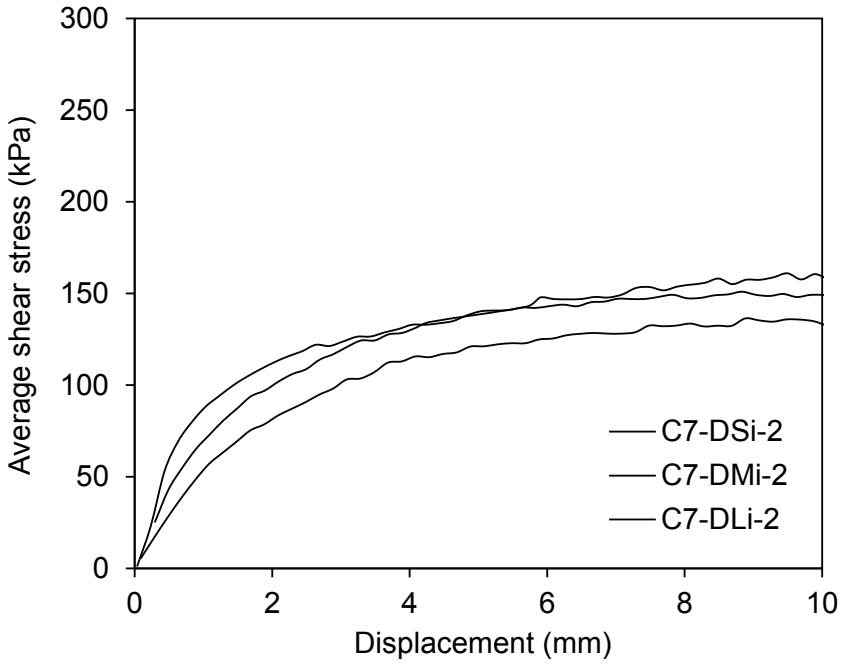

(b)

Figure 3.14. Results of tension load tests for C7: (a) Rough interface; (b) Intermediate interface

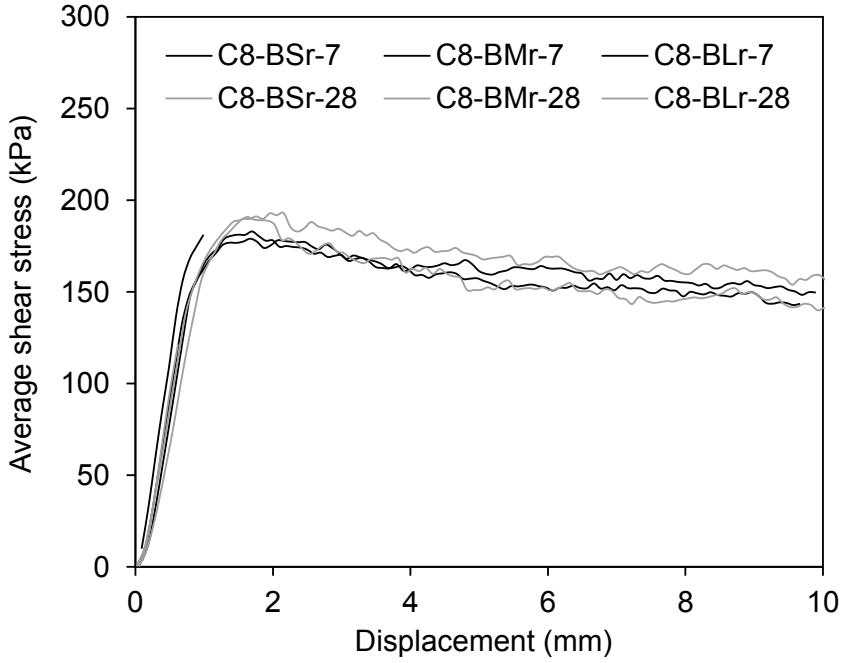

Figure 3.15. Results of tension load tests on buried piles (C8)

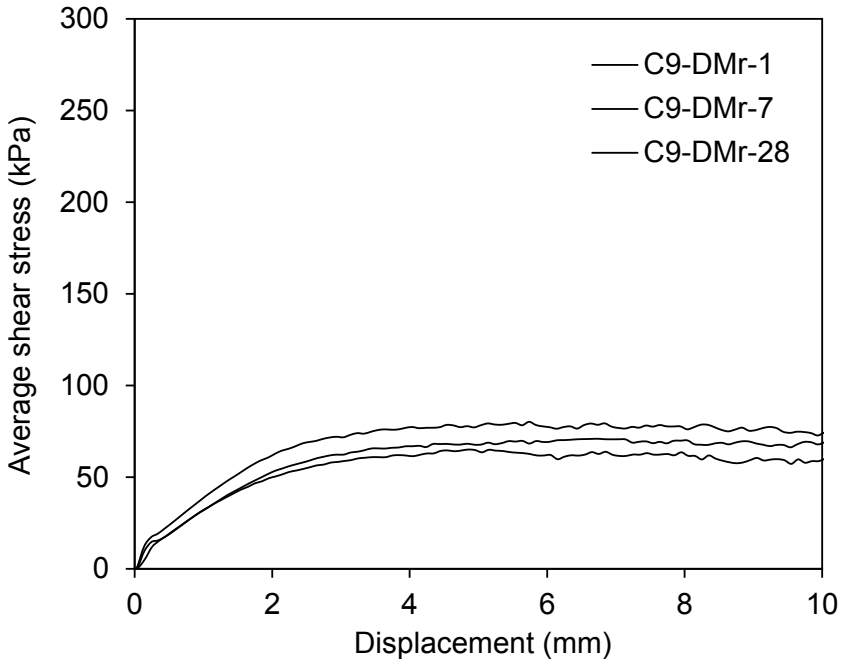

(a)

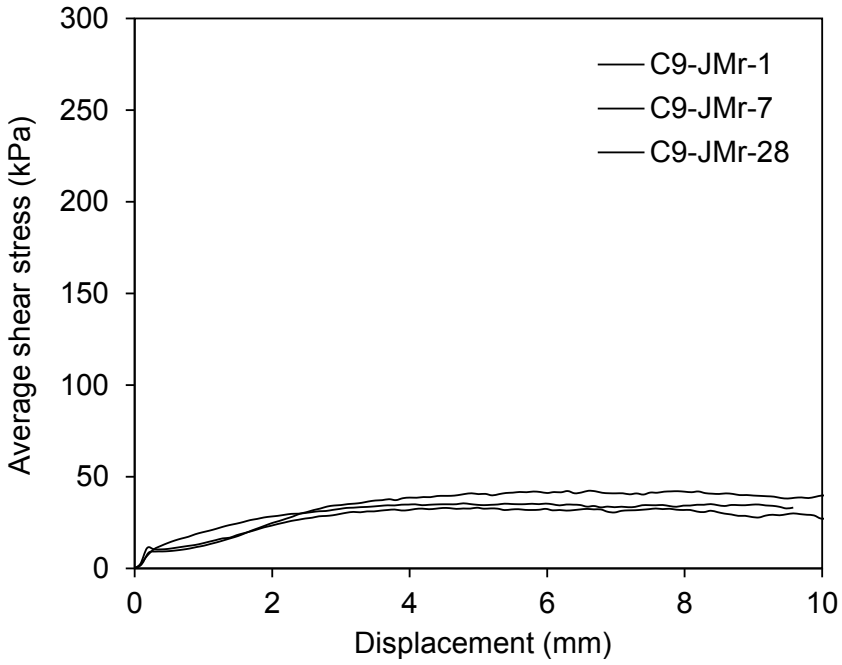

(b)

Figure 3.16. Results of tension load tests for C9: (a) Driven; (b) Jacked

3.4.2 Effects of Pile Set-up

The changes with time of pile shaft resistance observed in C4 and C5 are presented in Figure 3.17 and Figure 3.18 respectively. In C4, increases in pile shaft resistance over time are clearly observed for model piles installed by both installation methods. Pile shaft capacities for the 3-day and 7-day tests are comparable while the capacities recorded in the 28-day tests were at least 20% higher for both driven and jacked piles. A similar trend is observed in C5 for both sizes of model piles but showed different degrees of set-up to that seen in C4. Again, the 7-day capacity is comparable to the initial capacity measured at 1 day (the 7-day is slightly lower in fact) in contrast to the pile shaft capacity measured after 1 month.

Potential delay in pile set-up as observed in C4 and C5 is confirmed in C6 which involved closer testing intervals with first-time tests performed at 1 hour, 1 day, 3 days, 7 days, 15 days and 30 days after installation. As shown in Figure 3.19, the pile shaft capacity at 1 hour after installation is apparently lower than the rest; the 1-day, 3-day and 7-day capacities appear to be very close to each other, and the 15-day and 30-day measurements indicate a pronounced increase in pile shaft resistance. The time-dependent relationship suggests a multi-stage ageing response after pile installation with a delay during the initial period.

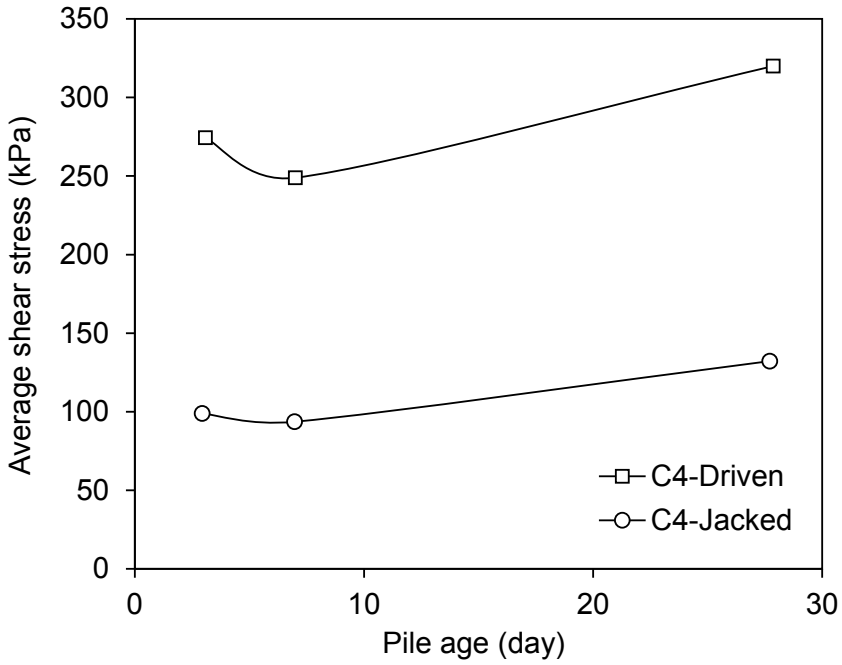

Figure 3.17. Changes of pile shaft resistance with time in C4

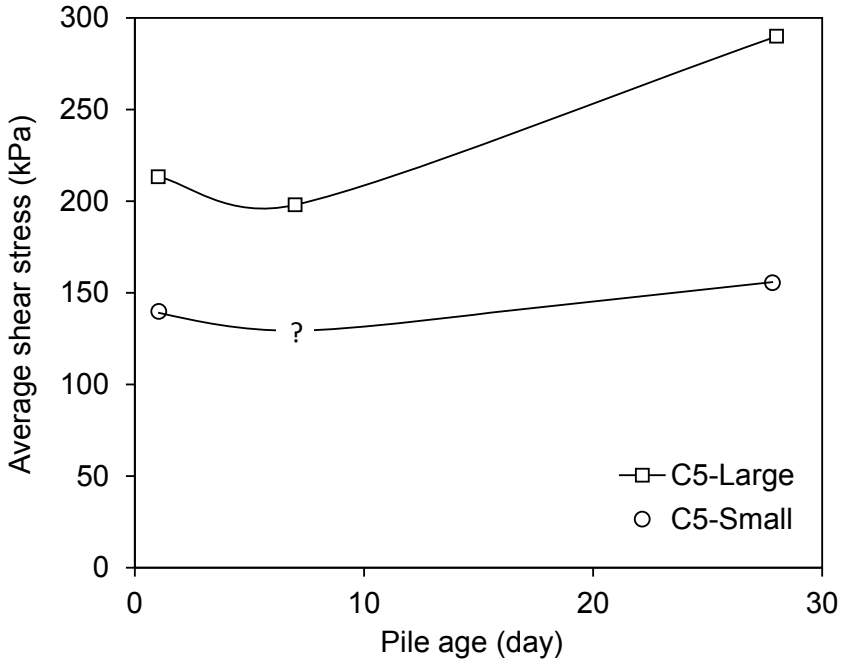

Figure 3.18. Changes of pile shaft resistance with time in C5

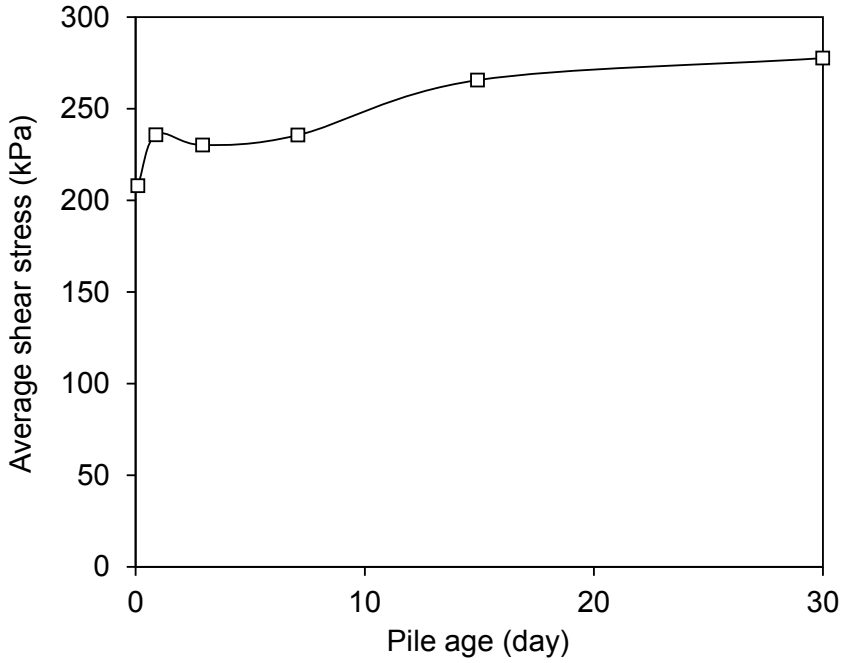

(a)

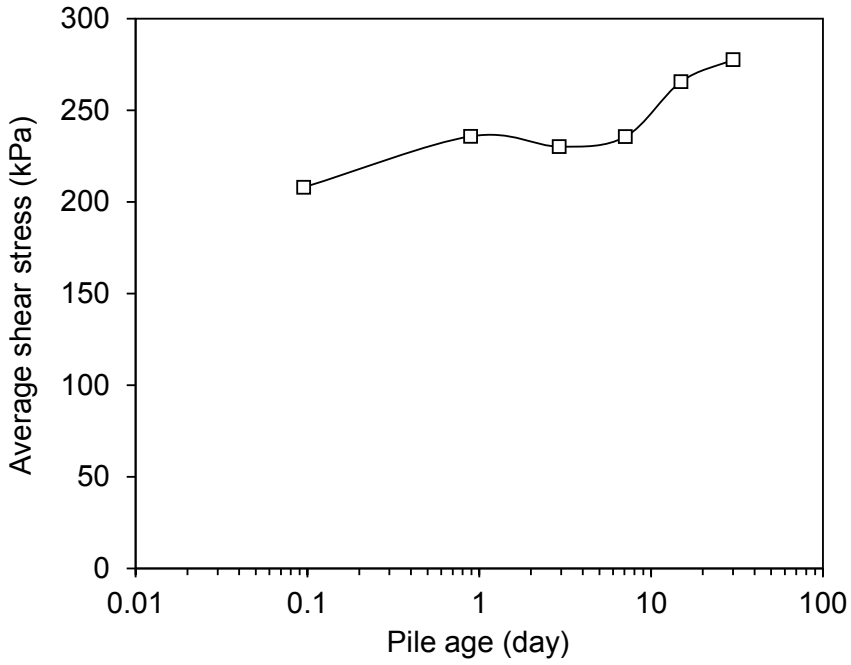

(b)

Figure 3.19. Changes of pile shaft resistance with time on C6: (a) normal scale; (b) semi-logarithmic scale

Similar delays in ageing have been observed in triaxial extension creep tests reported by Bowman and Soga (2005) who explained the phenomenon of pile set-up as the gradual accumulation of dilative capability that surmounts the initial contraction that occurs under a relatively low mean stress following the specific loading-unloading path induced by pile installation. For general sand ageing behaviour, Bowman and Soga (2003) investigated the microstructural change of dense sand during one-dimensional creep and demonstrated that the evenly spaced particles would align to be perpendicular to the load direction upon loading, which over time, rotated in space and clustered together. They suggest that the creep process begins in frictional slippage of weakly loaded particles, which allows the strongly loaded column of particles to buckle via particle rolling forming a self-supporting strong force network structure.

More recently, Karimpour and Lade (2010) performed drained triaxial compression tests at high pressure to study the behaviour of creep and stress relaxation in sand and indicated a unique relationship with the degree of particle breakage . They proposed that the root of time effects in sand is attributed to the particle crushing through a phenomenon known as static fatigue (or delayed fracturing). Michalowski and Nadukuru (2012) compared this time-delayed process to the delayed increase in penetration resistance observed after dynamic compaction of sands (e.g. Mitchell and Solymar, 1984; Schmertmann, 1987) and argued that the subsequent grain convergence leads to an increase in contact stiffness or an increase in elastic modulus of sand at the macroscopic scale, rather than an increase in strength.

3.4.3 Effects of Pile Installation Method

The influence of pile installation methods (driven vs monotonic jacked) was investigated in C4 (under high pressure of 200 kPa) and in C9 (under low pressure of 20 kPa). The results of tension load tests, as presented in Figure 3.11 and Figure 3.16, showed a clear and consistent trend of larger pile shaft capacity for driven piles than for monotonically jacked piles. This is in keeping with observations from centrifuge experiment reported by White and Lehane (2004) and Lehane and White (2005). Measurements of their earth pressure cells along centrifuge model pile shafts revealed that the pseudo-dynamic installation procedure (involving a series of downward jacking increments of 2 mm followed by extraction of 1.5 mm at 0.2 mm/s), in contrast to the

monotonic jacking procedure, leads to a lower stationary radial stress due to higher degrees of friction fatigue. However, the more densified interface zone tends to indicate a larger increase in radial stress during subsequent shearing under constrained dilation.

Differences in the density and fabric induced at the interface zone consequently affect the set-up behaviour of the pile shaft friction as indicated in Figure 3.17. Notwithstanding the lower percentage of capacity gain observed for the driven pile (due to its higher reference shaft resistance), its magnitude and growth rate appears to be more than 50% higher than that of the monotonically jacked pile. The observation suggests that piles that experience greater friction degradation during installation tend to show greater set-up over time. The same conjecture has been made by Bowman and Soga (2005) who model the level of disturbance using a faster loading rate in triaxial test.

Besides exhibiting higher shaft resistance, a larger displacement is required to mobilise the ultimate shear stress following more severe cyclic disturbance caused by impact driving. These displacements are about the same order as those typically required to mobilise full friction for full-scale piles. In this study, all model piles were load-tested to full ultimate conditions, which exceeded 8 mm pile head displacement for driven piles, in contrast to average of only 3 to 4 mm for the monotonically jacked piles (Table 3.3).

Figure 3.20 presents the changes of *buried* pile shaft resistance with time observed in C8. The pile shaft capacities measured after one month are barely larger than those tested after a week. These minor changes of capacities over time are not significant in comparison to what was indicated by the displacement piles. A comparison with the results of C4, C5 and C6, all of which involve displacement piles, confirms that pile set-up is caused by the disturbance during pile installation. It explains why set-up has not been reported for bored piles (similar in terms of absence in installation disturbance) and serves to validate the relevance of the experimental design and procedures employed in this study.

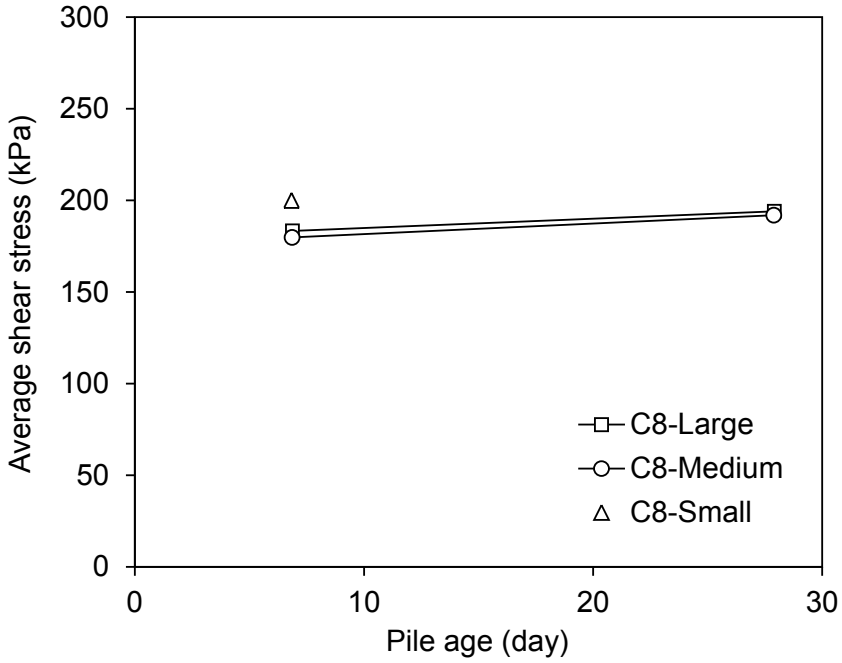

Figure 3.20. Changes of pile shaft resistance with time on C8

In contrast to driven piles, which show a ductile load-displacement response (e.g. Figure 3.12 and Figure 3.13), buried piles indicate a brittle response during tension load tests as shown in Figure 3.15. A clear peak average shear stress is noticeable and achieved within a relatively small shear displacement of approximately 1.5 mm.

3.4.4 Effects of Tension Re-test

In C4, a few driven model piles were re-tested to examine differences in behaviour with that of the first-time loaded pile. Figure 3.21 compares load-displacement curves of aged piles with comparable set-up periods. It is observed that the ultimate shaft resistances of the re-tested piles are smaller but stiffer and reach ultimate conditions at lower displacements than the 'fresh' piles tested for the first time. This behaviour is consistent with many field observations that involve static tension re-tests such as those reported by Jardine *et al.* (2006) and Schneider (2007), amongst others. It should be noted that the previous shearing direction influences its subsequent load-displacement behaviour. The trend of pure tension re-tests (T-T) described here therefore differs from that of a tension re-test that is preceded by a compression load test (C-T).

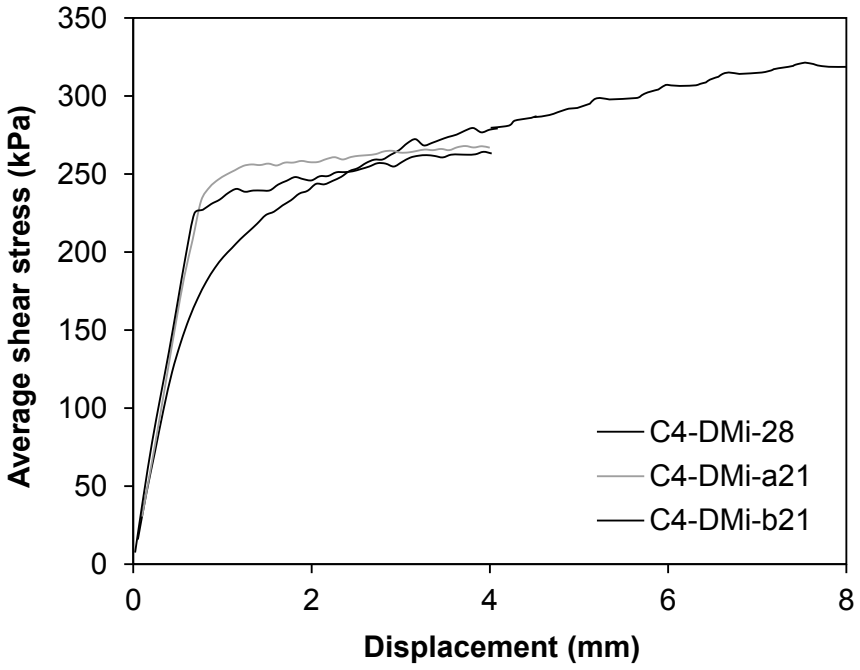

Figure 3.21. Comparison of the results of first-time tension load tests and the subsequent re-tests

3.4.5 Effects of Pile Diameter

As discussed in Chapter 2, literature on scale and diameter effects, although largely limited to buried/bored piles, suggests an inverse dependency of average ultimate shaft shear stress with pile diameter. The results of C8, which involve buried model piles of three different sizes, are plotted against pile diameter in Figure 3.22. While C8 shows a weak relationship that agrees with literature, the average shear stresses on driven piles, which were examined in C5 and C7 and presented in Figure 3.23, appear to increase with increasing pile diameter. The load-displacement curves measured in C5 and C7 are presented in Figure 3.12 and Figure 3.14, respectively. A further review of the literature on displacement piles in sand (e.g. Al-Mhaidib and Edil, 1998; Alawneh *et al.*, 1999) indicates some experimental inconsistencies related to the diameter effect, which require further examination.

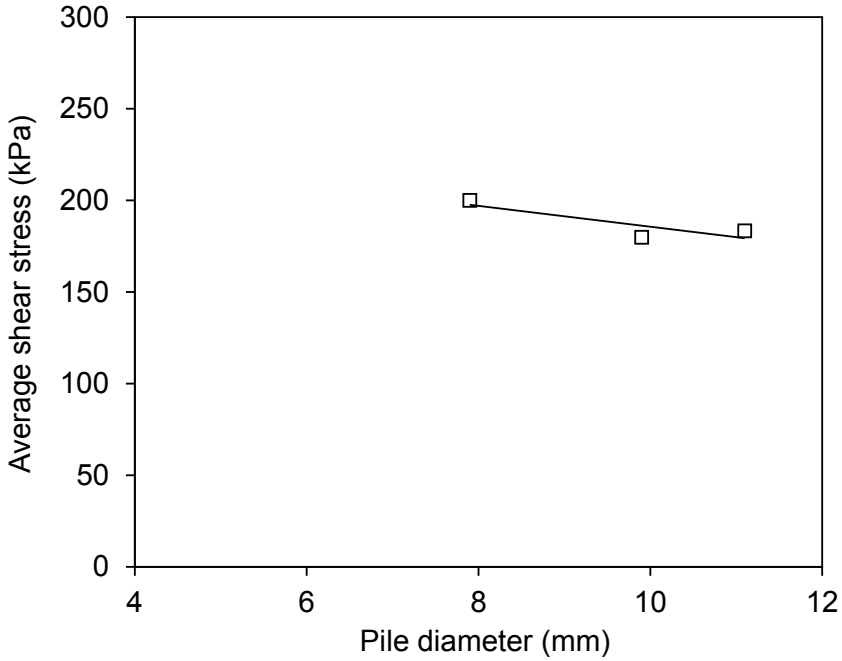

Figure 3.22. Variation of average shear stress with pile diameter on C8

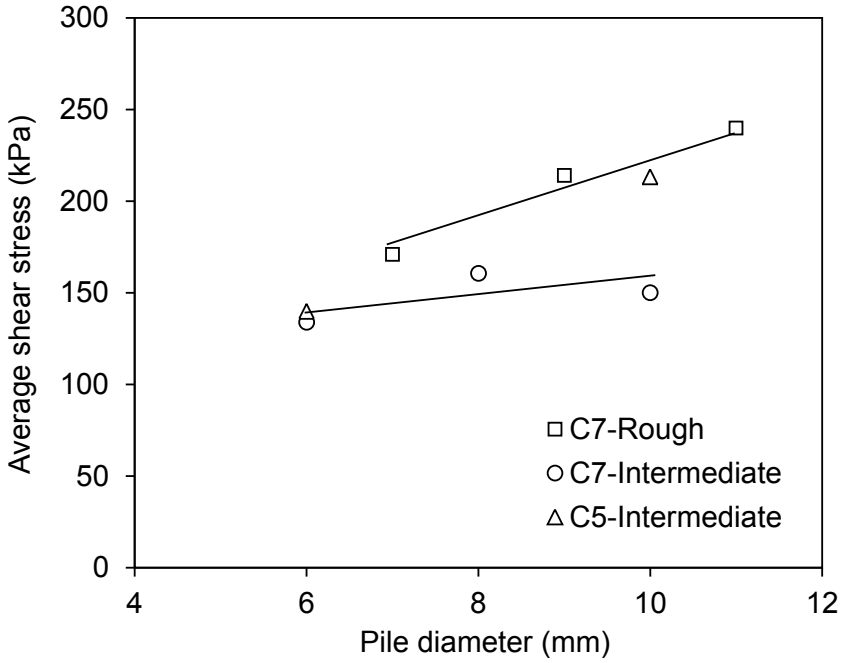

Figure 3.23. Variation of average shear stress with pile diameter on C5 and C7

The small chamber size and the symmetrical layout required to maintain a close identical boundary condition among test piles prohibited testing of any larger pile diameter. The range of pile diameters employed in this study was small and therefore a strong conclusion regarding diameter effects cannot be drawn. Of particular relevance to the effects of diameter seen on Figure 3.23 were the experiments reported by Lehane and White (2005). These revealed a significant distortion of radial effective stress acting on the small-scale model pile shaft in the centrifuge experiment as compared to those observed in field, in spite of comparable pile length and CPT q_c in both prototype and field scales. The observation prompts a more in-depth study of scale effects for driven piles in sand; this study is presented in Chapter 7.

In terms of pile set-up, different degrees of capacity increase were observed for three sizes of model driven piles in C4, C5 and C6 in a consistent pattern, which is shown in Figure 3.17 to Figure 3.19 and summarised in Table 3.3. The magnitude of capacity gain for 10 mm diameter piles in C5 is higher (41.0%) than that observed for 8 mm diameter piles in C4 and C6 (18.7% - 22.3%) while the 6 mm diameter piles in C5 showed the smallest change (11.2%). The percentage shown is for *indicative* purpose, which was calculated by considering the initial reference capacity as the average of pile shaft resistances measured from 1 day to 7 days after driving, before a marked set-up appeared.

The observation appears to agree with the argument of Bowman and Soga (2005) that the installation of larger piles disturbs the soil to a greater extent, thus showing a greater recovery of stiffness. The experimental results do *not* support the view that greater set-up may be expected for smaller diameter piles due to stronger dilation induced shear capacity (as predicted by cavity expansion theory). The significant set-up indicated by the first-time load tests on (relatively large) 457 mm diameter driven piles in dense sand reported by Jardine *et al.* (2006) also supports the argument that set up effects do not necessarily reduce with an increase in pile diameter.

It is worthwhile recalling the stress history associated with pile installation (e.g. White, 2005). Before cyclic shearing along the pile shaft comes into play, the soil has first been subjected to an immense disturbance during penetration around pile tip (i.e. compression when the tip approaches, then a change of principal stress direction to

extension as the soil flows to the shoulder). The process of giving way for pile insertion (either by impact driving or hydraulic jacking) inevitably destroys many of the contacts between particles and force networks or structured fabric that have been built over ages (Bowman & Soga, 2003) – with this disturbance extending to a relatively large influence zone, which is a function of pile diameter. The subsequent stress equilibration between the undisturbed far-field, the disturbed zone and the shear zone would all contribute to the ageing effect of pile shaft friction.

3.4.6 Effects of Stress Level

Figure 3.16 presents the results of tension load tests in the form of load-displacement curves for C9. As expected, under the very low vertical pressure of 20 kPa, the CPT q_c and pile shaft resistances are much lower than those measured in all the other chamber tests (with σ_v = 200 kPa). It was seen that, as in the high pressure tests (C4), monotonically jacked piles have a lower pile shaft resistance than the corresponding driven piles. However, unlike C4, both the jacked and driven piles at the low stress level mobilise ultimate shaft resistance at a similar pile head displacement of about 3 – 4 mm; discrepancies of failure mechanisms and stiffness response due to the differences in stress level for modelling in sand were reported by Mikasa and Takada (1973) and Ozkahriman and Wartman (2007).

The effect of pile set-up observed in C9 is presented in Figure 3.24. Instead of capacity gains seen in C4, C5 and C6 as discussed in Section 3.4.2, the pile shaft friction appeared to decrease slightly with time for model piles installed by both installation methods under low stress level. The absence of a set-up effect in this experiment may reflect the contribution of surrounding stresses in stimulating the stress equilibration process following installation disturbance. An absence of a set-up was also observed in 1-*g* model tests using stainless steel piles that were monotonically jacked into saturated carbonate sand (White and Zhao (2006).

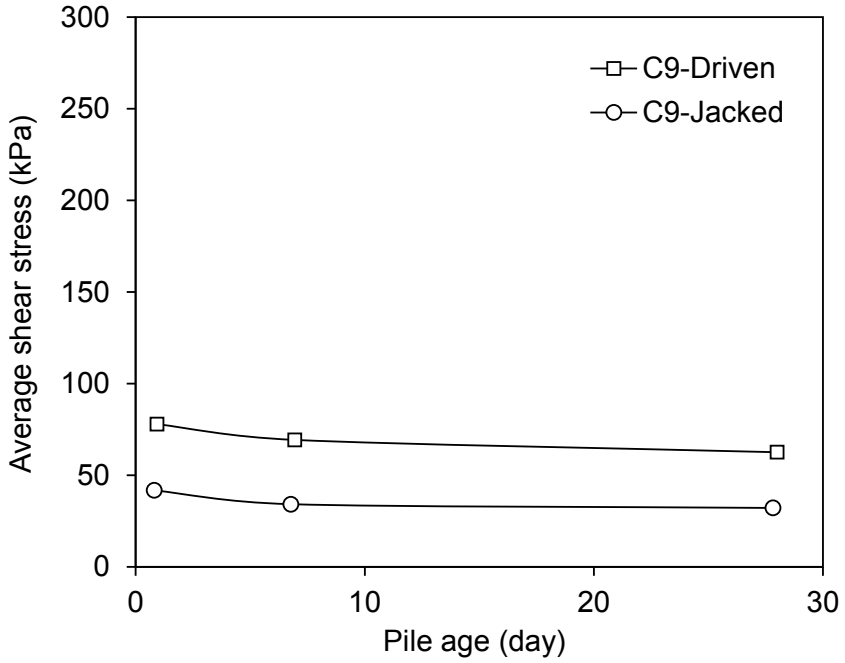

Figure 3.24. Changes of pile shaft resistance with time on C9

3.4.7 Other Observations

In all cases, there was little or no corrosion (for piles with rough surface coated with sand particles) observed on the model piles after extraction upon testing completed; the only corrosion noticed was very close to the top of the sample (where oxygen was present). This indicates that the increase in pile shaft resistance in this study cannot be attributed to the corrosive effects.

Besides, it is noticed that the shaft resistances for rough piles are greater than those of relatively smooth piles by about 20% as indicated in Figure 3.23. This may be related to the higher interface friction angle for the rough interface that tends to trigger a larger shear zone during installation and load testing. The extremely rough interface employed in this study is mainly to provide a contrast to the commonly employed intermediate roughness on model steel piles, which may be a little less the actual roughness of Industrial piles.

It is also noted that the average shaft shear stresses of these model-scale piles are generally higher than that observed in field (implied by CPT alpha methods and many

reported case histories) but appear to be smaller than that predicted by some recent CPT-based pile design methods (e.g. ICP-05 and UWA-05); the scale effects are assessed in Chapter 7.

CHAPTER 4. FIELD TESTS AND RESULTS

4.1 INTRODUCTION

Time-dependent increases in the shaft capacity of displacement piles in sand have been documented for decades but the phenomenon remains poorly understood and not incorporated in any pile design method. Several mechanisms have been hypothesised but no consensus was reached due to a dearth of reliable experimental evidence. A less ambiguous field test programme (GOPAL project) was reported by Jardine *et al.* (2006) but the full-scale pipe piles employed were un-instrumented prohibiting further exploration of the governing mechanisms.

This chapter reports on a series of field test programmes that employed three different sizes of model piles, each equipped with a surface stress transducer (SST), to investigate the ageing behaviour of displacement piles in sand. The effects of pile ageing were assessed from the changes of average pile shaft capacity with time obtained from static tension load tests (global set-up) and the variation of shaft stresses with time measured by the SSTs (local set-up). Short-term effects (within a day after installation) were also examined to give further insights on the phenomenon.

4.2 SITE DESCRIPTION

Three sand sites of differing mineralogy and groundwater regimes were investigated in this study, characteristics of which are described as follows:

4.2.1 Shenton Park (SP)

The majority of the field experiments were conducted at the University of Western Australia (UWA) test bed site at Shenton Park, located off Underwood Avenue, which is about 5 km from Perth city centre. The site is owned by UWA and was selected because of its availability and convenience. In addition, the site has been investigated extensively using a wide variety of in situ and laboratory tests (e.g. Lehane *et al.*, 2004; Schneider *et al.*, 2008a) and used for various field experiments including driven piles (Schneider, 2007), bored piles (Lehane, 2008), footings (Lehane *et al.*, 2008) and retaining walls (Li and Lehane, 2010).

A brief geological background of the test site is presented here, which was referred to the studies of Playford *et al.* (1976) and Davidson (1995). Figure 4.1 shows the geomorphology of the Perth region. The Shenton Park test site is situated on the Coastal Belt of the Swan Coastal Plain in a geomorphologic region known as the Perth Basin. The Swan Coastal Plain is bound by the Gingin and Darling Fault Scarps to the east and by the coastline to the west, and extends parallel to the coast to Geraldton in the North and Bunbury in the South. The scarps represent the eastern boundary of Tertiary and Quaternary marine erosion, at which the Swan Coastal Plain can be divided into a series of distinct landforms that are roughly parallel to the coast. Shenton Park is within the region of Spearwood Dune System, which consists of slightly calcareous aeolian sand and is a remnant from leaching of the underlying Pleistocene Tamala Limestone.

Tamala Limestone consists of a creamy-white to yellow, or light-grey calcareous aeolianite, which contains various proportions of quartz sand, shell fragments and minor clayey lenses. The quartz sand is predominantly medium grained, moderately sorted and sub-angular to rounded in shape. Its upper surface is exposed and leached to great extent that the upper part of the unit comprises unconsolidated sand with a very light cementation and bonding between particle grains. A generalised surface geology of the Perth region is presented in Figure 4.2.

Disturbed samples were collected from trial pit (also for the purpose of chamber tests as reported in Chapter 3) and using hand auger at about 2 m depth for classification tests. The sand is siliceous with traces of carbonates (< 5%), sub-angular to sub-rounded, uniformly graded with a mean particle size (D_{50}) of 0.42 mm and coefficient of uniformity (C_u) of about 2.5. Maximum and minimum void ratios (e_{max} and e_{min}) were recorded as 0.79 and 0.44 respectively. Figure 4.3 shows the mean particle size distribution of the sand; this distribution displayed minimal variation spatially or with depth at the site.

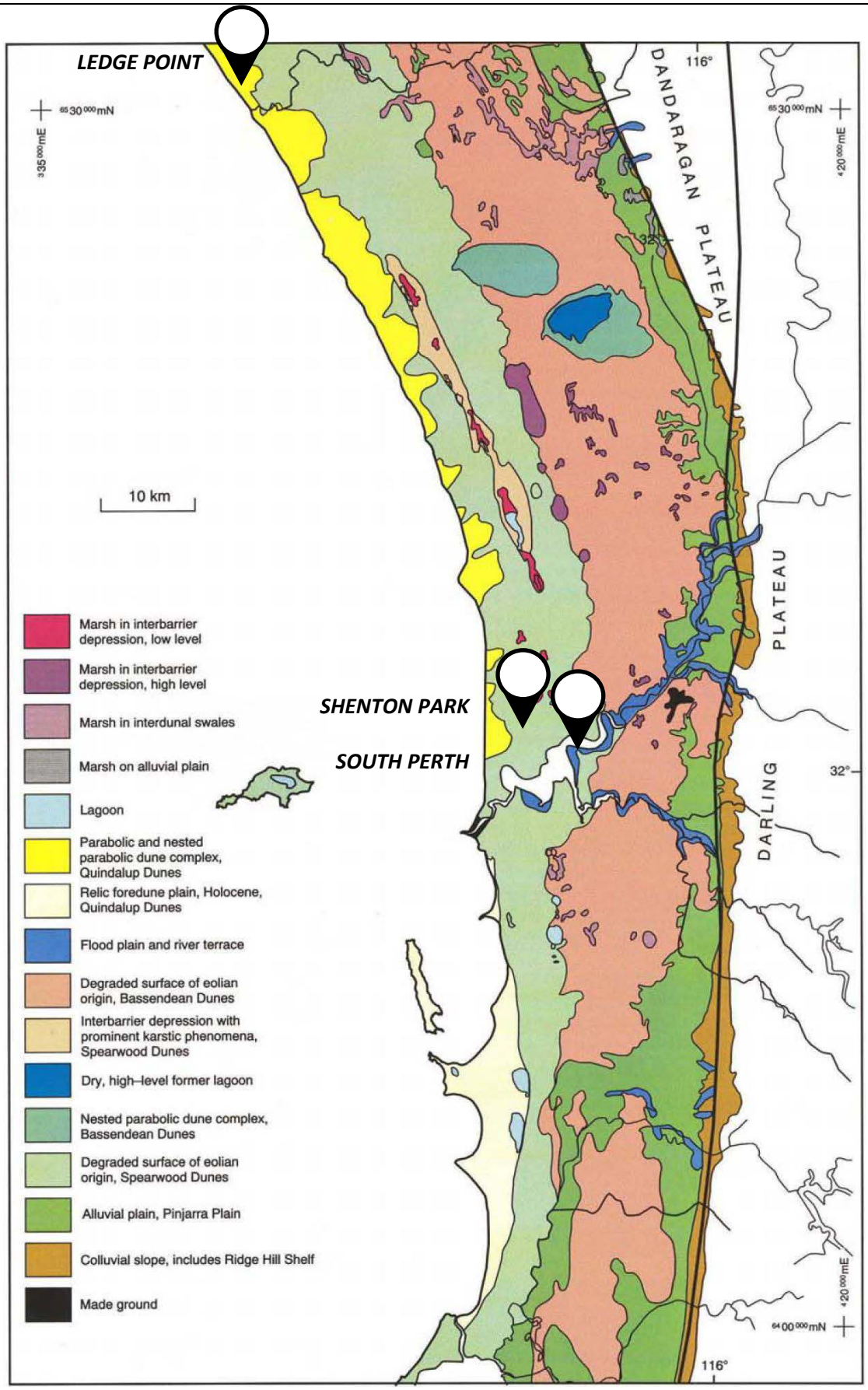

Figure 4.1. Geomorphology of the Perth region (Davidson, 1995)

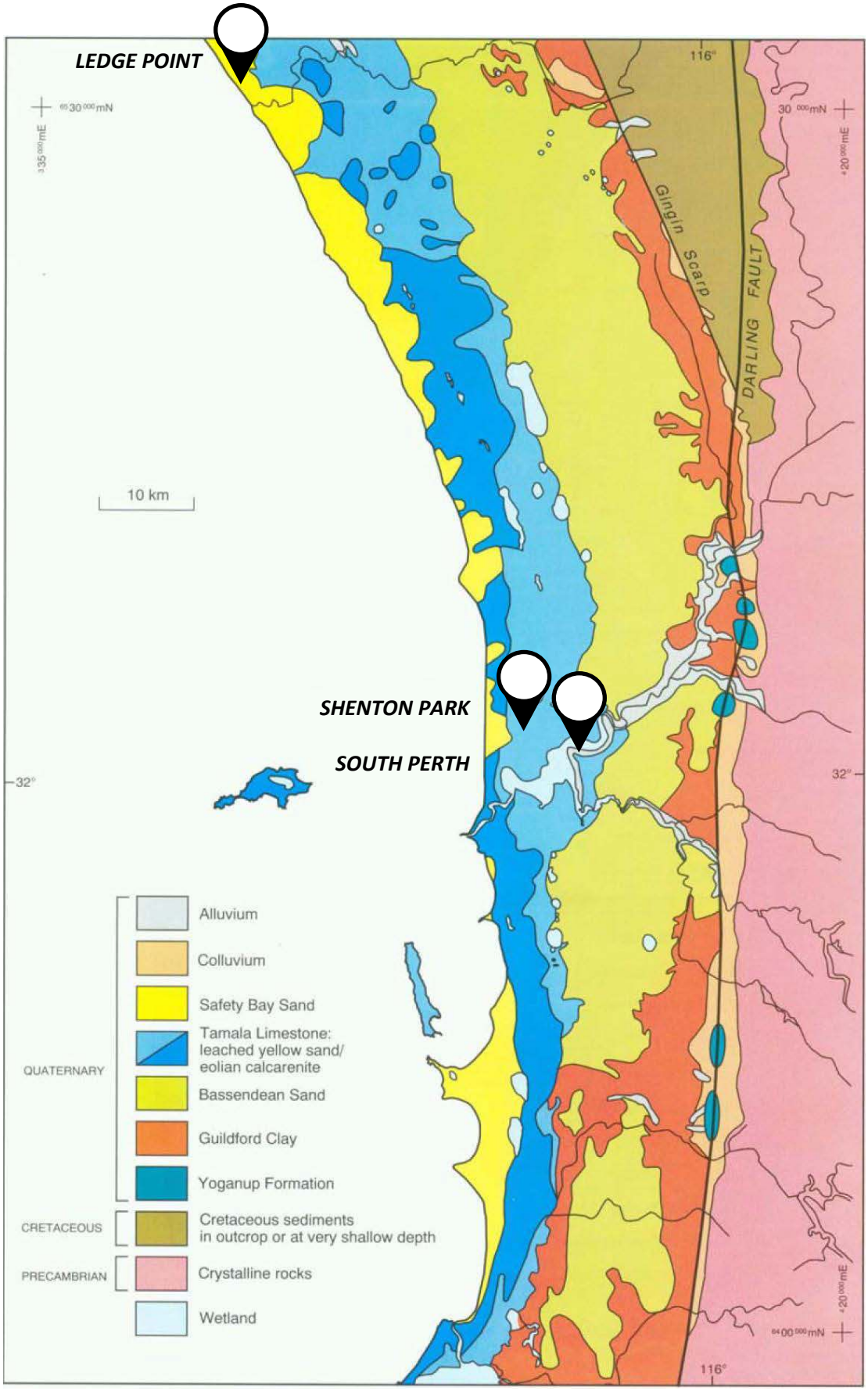

Figure 4.2. Generalised surface geology of the Perth region (Davidson, 1995)

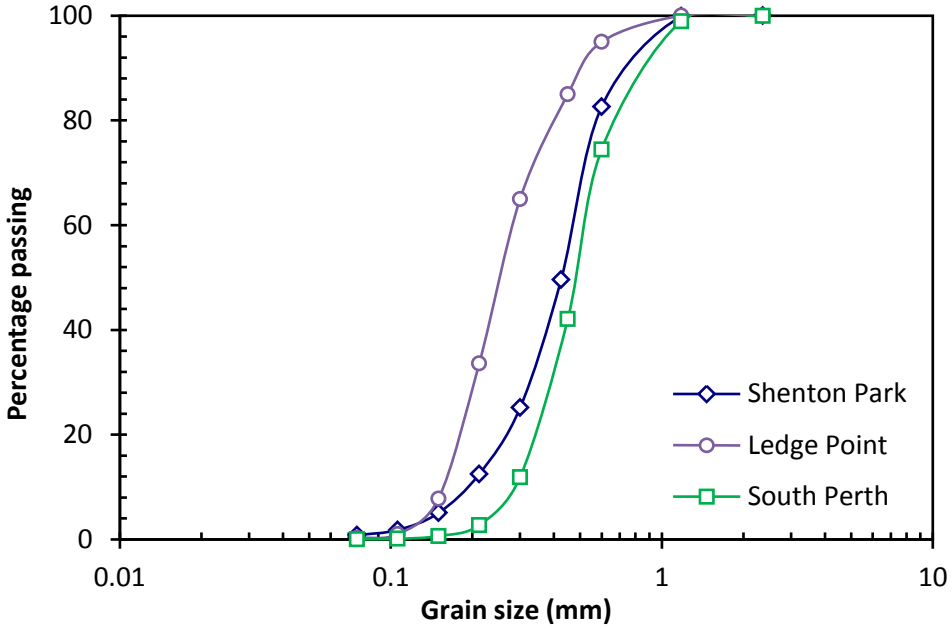

Figure 4.3. Grading curves for the test sands

The sand is identical to that found at an adjacent test location, about 500 m away, which has been investigated extensively by a previous PhD candidate at UWA (Schneider, 2007); it is therefore reasonable to expect that it exhibits similar characteristics and mechanical behaviour. A triaxial test performed by Schneider on a sand reconstituted to a void ratio of 0.6 ($\approx D_r$ of 0.58) after isotropic consolidation to a mean effective stress of 100 kPa indicated peak and constant volume friction angles of 38^o and 32^o, respectively.

A total of twenty standard and seismic cone penetration tests (CPTs and SCPTs) and two seismic dilatometer tests (SDMTs) were performed at various stages of the overall research programme. Figure 4.4 shows the layout of the in situ tests, which provide a good coverage of the entire test area, particularly in close vicinity to the test piles (to be discussed later). In general, there is a denser crust in the upper 1.5 – 2 m overlying a sand layer with a relatively uniform CPT end resistance to a depth of about 6 m. Limestone pinnacles below 6 m lead to erratic variations in the lower level of the sand stratum. The water table was at about 15 m depth within the limestone as reported by Lehane *et al.* (2004).

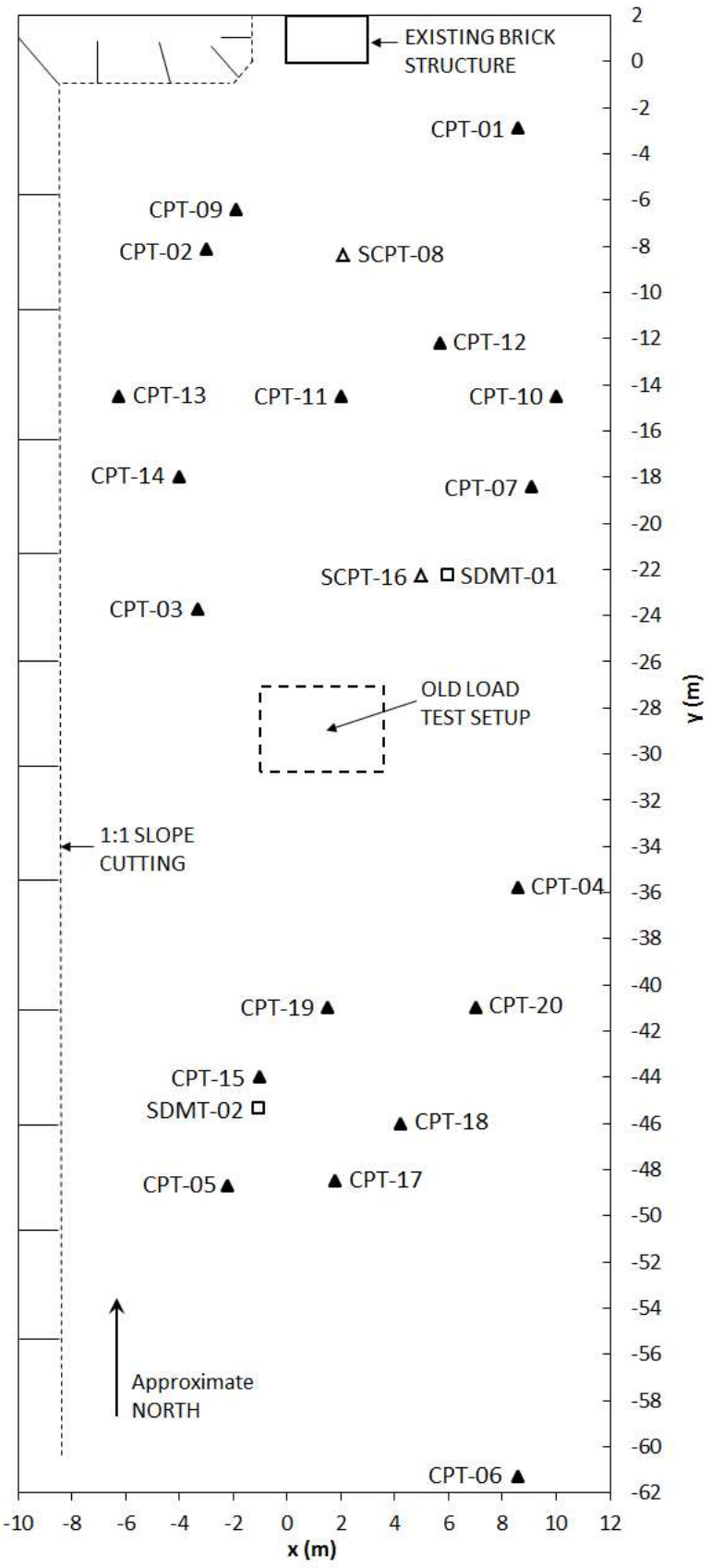

Figure 4.4. Layout of in situ tests at Shenton Park

The standard electric cone penetrometer with a diameter of 35.7 mm was employed in the site investigation. Figure 4.5 shows the CPT q_c profiles and the expected variation over the test site. It is seen that the uniform stratum ideal for an experimental study lie between 1.5 m and 5.5 m depth, with the horizontal coefficient of variations (CoV) in q_c of about 20%. The average q_c values increase with depth from 3.5 MPa at 2 m to approximately 6.5 MPa at 5 m depth, which corresponds to an average in-situ relative density (D_r) of about 45% (i.e. medium dense) estimated using the empirical correlation proposed by Jamiolkowski *et al.* (2001). The correlation was derived from a large number of calibration chamber test data and has been corrected for size and boundary effects.

$$D_r = \left[0.268 \cdot \ln\left(\frac{q_t/p_a}{\sqrt{\sigma'_{vo}/p_a}}\right) - 0.675\right] \times 100\% \tag{4-1}$$

where q_t is the total cone tip resistance ($\approx q_c$ in sand), σ'_{vo} is the effective overburden pressure, p_a is the atmospheric pressure (taken as 100 kPa) and the calculated D_r is in %.

The cone end resistance (q_c) and sleeve friction (f_s) measured from the CPT provide a useful guide to the mechanical characteristics (strength and stiffness) of the soil, which has been used for soil profiling and estimation of numerous geotechnical parameters. Soil type can be estimated from the Soil Behaviour Type (SBT) chart proposed by Robertson (1990) or using the simplified Soil Behaviour Type index (I_c) calculated based on the dimensionless normalised cone parameters (Q_{tn} and F_r) assuming a stress exponent (n) of 1.0 using the following expressions (Robertson and Wride, 1998):

$$I_c = [(3.47 - \log Q_{tn})^2 + (\log F_r + 1.22)^2]^{0.5} \tag{4-2}$$

$$Q_{tn} = \left(\frac{q_t - \sigma_{vo}}{p_a}\right) \cdot \left(\frac{p_a}{\sigma'_{vo}}\right)^n \tag{4-3}$$

$$F_r = \left(\frac{f_s}{q_t - \sigma_{vo}}\right) \times 100\% \tag{4-4}$$

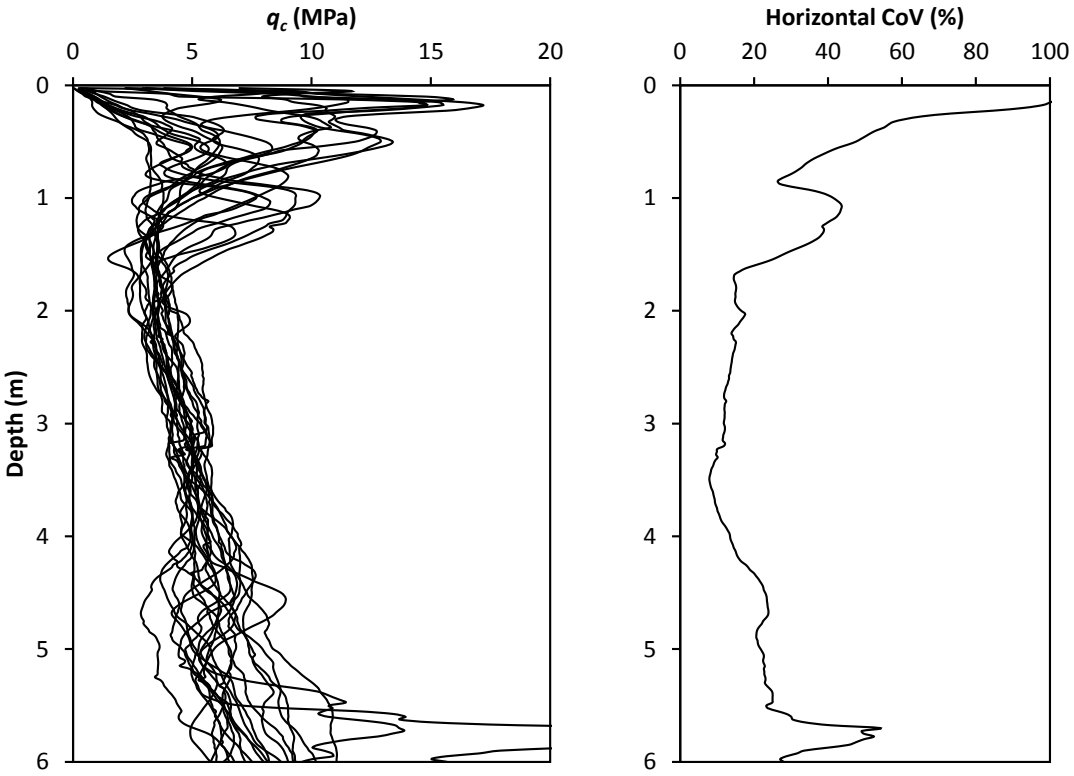

Figure 4.5. CPT q_c profiles and variation at Shenton Park

More recently, Robertson (2009) suggested that the term Q_{tn} used in SBT charts and SBT index should be calculated using a stress exponent n that varies with soil type via I_c using an iterative procedure described by Zhang *et al.* (2002). At Shenton Park, I_c for the stratum between 2 m and 5 m depth is 1.92 in average, with standard deviation of 0.06. It falls under zone 6 ($1.31 < I_c < 2.05$) of the soil behaviour type, which is described as clean sand to silty sand. It is noteworthy that the particle size distribution analyses did not reveal the presence of any significant quantity of silt.

The flat plate dilatometer test (Marchetti, 1980; Marchetti *et al.*, 2001) is another popular in situ test that was conducted at the test site. The device comprises a stainless steel blade with a flat circular steel membrane mounted flush on one side, which can be pneumatically expanded via a control unit. The blade is pushed into the ground using a CPT truck and paused at every 20 cm penetration interval to perform the test. Readings were recorded, and after correction, provide two pressure measurements: (*i*) the lift-off pressure (p_o) when the membrane is flushed with the blade; and (*ii*) the expansion

pressure (p_1) when the membrane is expanded to 1.1 mm. Three DMT 'intermediate' parameters, known as the material index (I_D), the horizontal stress index (K_D) and the dilatometer modulus (E_D), can then be derived for further interpretation:

$$I_D = \frac{(p_1 - p_0)}{(p_0 - u_0)} \tag{4-5}$$

$$K_D = \frac{(p_0 - u_o)}{\sigma'_{vo}} \tag{4-6}$$

$$E_D = 34.7(p_1 - p_0) \tag{4-7}$$

The results of DMTs are presented in Figure 4.6. It is seen that the I_D, which is a parameter reflecting the mechanical behaviour of the soil, is on average 2.13 with a standard deviation of 0.19 for the stratum between 2 m and 5 m depth. The soil is classified as a slightly silty sand ($1.8 < I_D < 3.3$) based on classification procedure proposed by Marchetti (1980) which concurs with that inferred from the I_c index. The K_D profile is indicative of the stress history and is usually similar in shape to the K_0 and OCR profile. At Shenton Park, the value of K_D reduces strongly with depth and reaches a steady value of between about 3 and 4 below 3 m. This trend for K_D matches the profile of K_0 inferred by Lehane (2008) from the lift-off pressures measured in self-boring pressuremeter tests at an adjacent site in Shenton Park. The K_0 values at this site reduced from 1.25 at 0.5 m depth to 0.5 at depths greater than 3.5 m, which are consistent with OCR values induced by the previous removal of 5 m sand at the site. The E_D stiffnesses plotted on Figure 4.6 are usually transformed into other forms of moduli depending on the application; e.g. see Marchetti (1980).

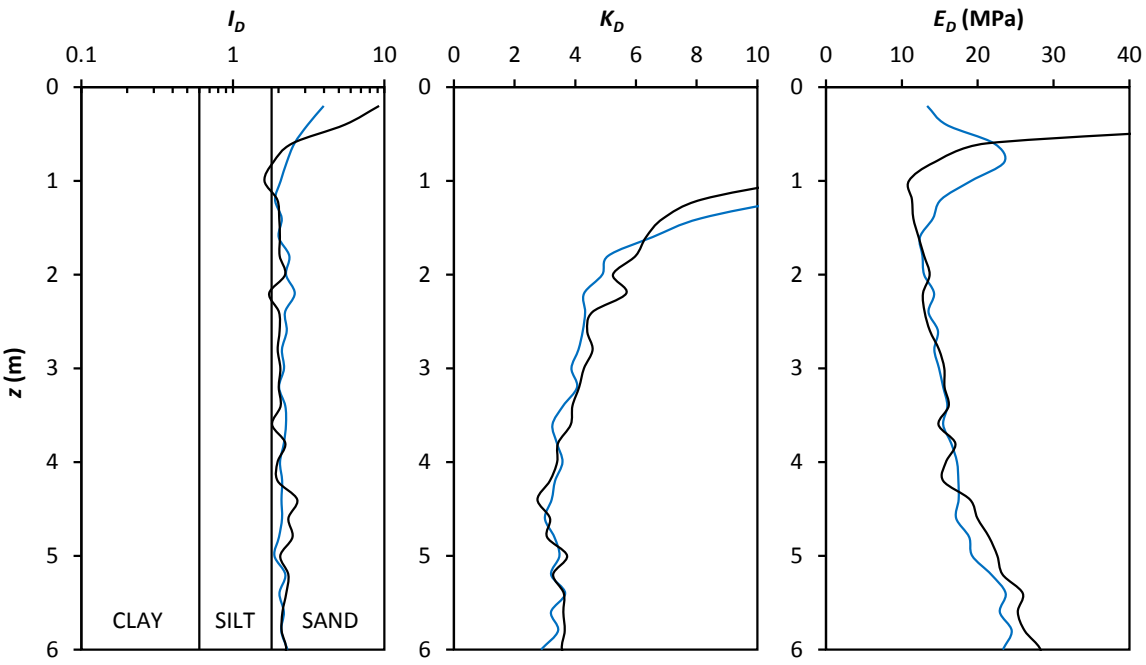

Figure 4.6. Results of DMTs at Shenton Park

The two DMTs and two of the CPTs performed at Shenton Park were equipped with a seismic module for measuring the shear wave velocity (V_s). The cone employed for these tests had a single geophone and allows calculation of a pseudo-interval downhole V_s (Robertson *et al.*, 1986). A more reliable V_s was measured in the seismic dilatometer tests as these incorporated two geophones (0.5 m apart) and hence provided a true-interval downhole measurement. Tests were performed at 0.5 m interval from 1 m depth onwards with a surface shear wave generated using an autoseis unit (except for SCPT-08 at 1 m interval which was imparted manually using a sledge hammer).

From V_s, the small strain shear modulus (G_o) may be determined using the theory of elasticity as follow:

$$G_o = \rho \cdot V_s^2 \tag{4-8}$$

where ρ is the total soil density assumed as 1680 kg/m^3 for this test site. Figure 4.7 shows the results of G_o over the depths of interest. It is noticed that the measurements from SDMT-01 and SDMT-02 utilising double geophones are generally more consistent and lead to slightly higher G_o values than those recorded in SCPT-16; G_o values inferred

from SCPT-08 are more variable presumably because an automated hammer was not employed to generate the shear wave.

Previous research shows that there is a relationship between the ratio of G_o/q_c and normalised cone tip resistance, which has been used as an indicator for stress history, ageing and cementation of sand (e.g. Baldi *et al.*, 1989; Rix and Stokoe, 1991; Fahey *et al.*, 2003). Normalised moduli are often represented in the following format:

$$\frac{G_o}{q_c} = K_G \left[\frac{(q_c/p_a)}{(\sigma'_{vo}/p_a)^{0.5}}\right]^{-n} = K_G \cdot {q_{c1N}}^{-n} \tag{4-9}$$

where K_G and n are the curve-fitting parameters. The exponent n is commonly taken as 0.67 or 0.75. Eslaamizaad and Robertson (1997) showed an increasing cementation and/or ageing of sands with increasing K_G value, and proposed a lower bound and an upper bound values of K_G for the unaged and uncemented sands of 110 and 280 respectively, when n = 0.67. Using the same framework, Schnaid *et al.* (2004) showed that the residual soils, which are known to exhibit bonding and relic structures, lie above the boundary of uncemented sands, and an upper bound K_G value of 800 is proposed for the cemented sands.

Schneider (2007) expanded the database by incorporating a wide variety of sand deposits and showed that by using n = 0.75, the K_G values could range from 110 for sands that have been liquefied historically to 1100 for the cemented sands and residual soils with a transition at K_G of approximately 330. For Shenton Park, a site specific correlation was proposed by Schneider (2007) with n = 0.75 and K_G of 500 indicating some level of cementation or structuring. Figure 4.8 shows the G_o/q_c ratio for the four sets of seismic data measured at the present test site. It is evident that the mean K_G value is similar to that observed by Schneider (2007).

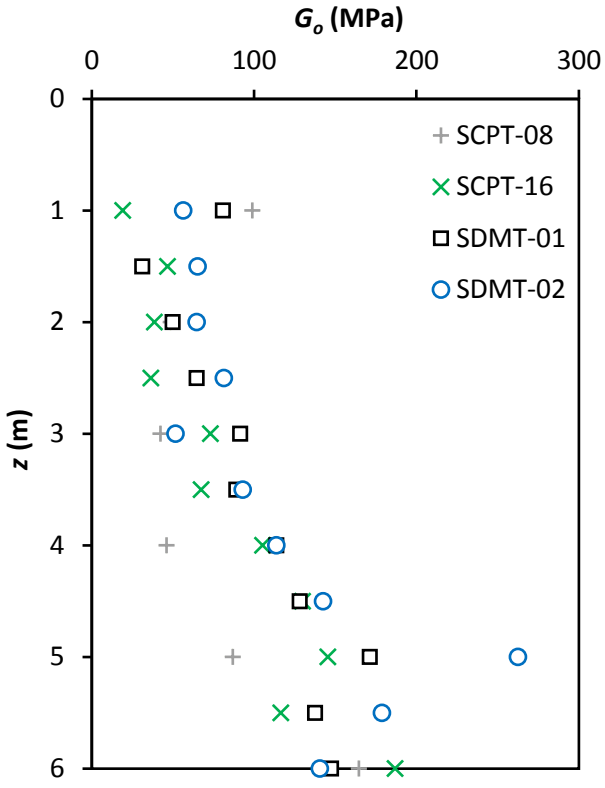

Figure 4.7. Measured *Go* from SCPTs and SDMTs at Shenton Park

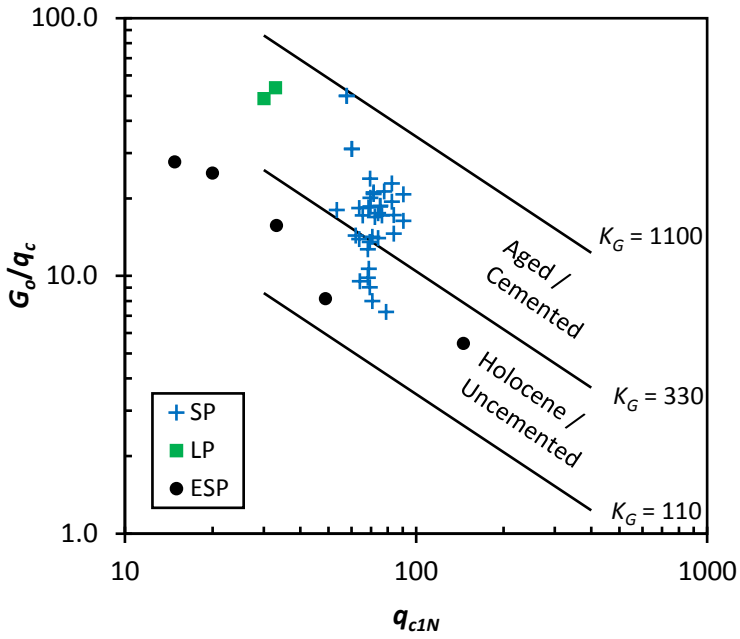

Figure 4.8. Ratios of G_o/q_c for stratum between 2 m and 6 m depth at the test sites

Another important feature of the Shenton Park sands is that they maintain a low level of saturation that varies slightly seasonally. Such slight variations may affect the in situ test parameters such as q_c and G_o values due to suction effects. Lehane *et al.* (2004) demonstrated that, in a treed area, the values of q_c, f_s and G_o at the end of dry season are higher (up to a factor of 2 at a depth of 3 to 4 m) than those parameters at the end of wet season, whereas no seasonal effect was observed in an open area where the effects of water extraction by trees were absent. At the test area employed for this study, no tree was present and hence no seasonal effect on the in-situ parameters was expected.

4.2.2 Ledge Point (LP)

This test site is adjacent to Ledge Point village situated about 100 km north of Perth along the coast of the Indian Ocean (Figure 4.1 and Figure 4.2). The site composes of calcareous sand dunes as part of the Quindalup dune system with a calcium carbonate content of 90%. The sand is uniformly graded with D_{50} of 0.25 mm, C_u of about 2 and e_{max} and e_{min} of 1.21 and 0.90 respectively (Sharma, 2004). Figure 4.3 contrasts the grain size distribution of the sand from Ledge Point with other test sites. The in situ water content varied between 5 and 8%, equivalent to a degree of saturation (S_r) of 10 – 20%. Figure 4.9 shows the results of a CPT conducted close to the pile test locations. The average CPT q_c values in the upper 3 m range between 2 and 3.4 MPa with an estimated in situ D_r of 40 ± 10% (using correlation proposed by Jamiolkowski *et al.* (1985) for highly compressible sands). These reflect a higher variability on site and that the sands are of irregular particles with an open structure as observed from microscopy images. The results of other in situ tests such as SCPTs, DMTs and SBPMTs were reported by Lehane *et al.* (2012). As shown in Figure 4.8, the G_o for this un-cemented calcareous sand is significantly higher than those of siliceous sands at a comparable stress level and density.

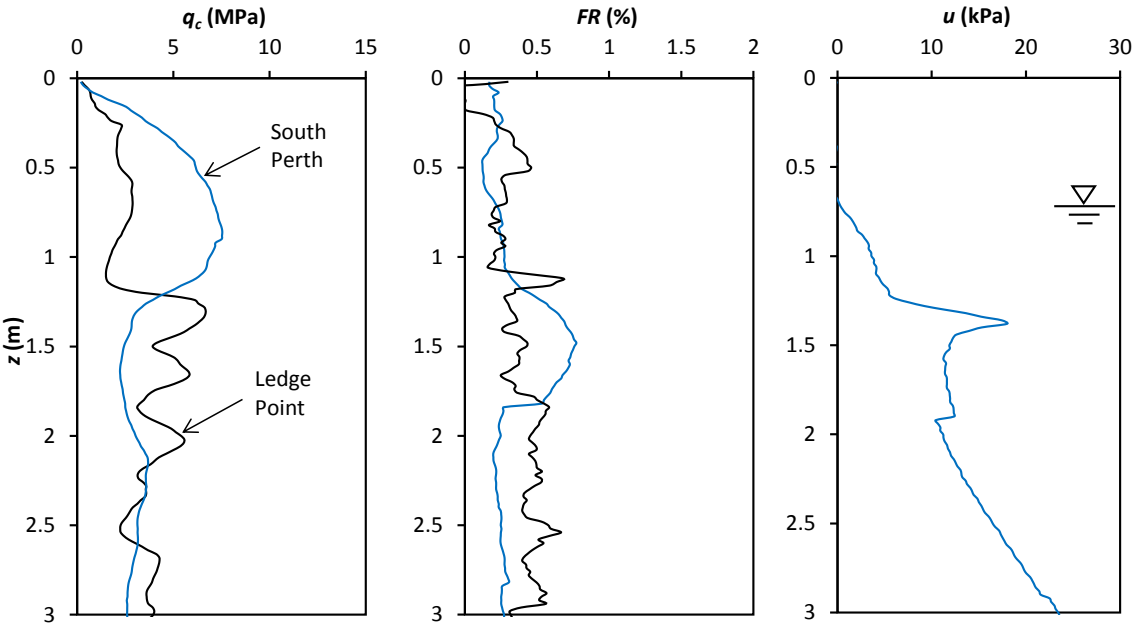

Figure 4.9. Typical results of CPT at Ledge Point and South Perth

4.2.3 South Perth Esplanade (ESP)

The South Perth site is a residential re-development area located close to the Swan River in the centre of Perth as indicated in Figure 4.1 and Figure 4.2. The site comprises a well compacted sand fill in the upper 1.5 m and is underlain by alluvial silica sand. Groundwater was encountered at about 1 m below ground level and fluctuated by 0.5 m due to tidal effects. The results of a piezocone penetration test (CPTu) located nearest to the test piles are presented in Figure 4.9. Except for a denser crust in the upper 1 to 1.5 m, the underlying sand layer relevant to the embedment of test piles (≈ 4 m) has an average CPT q_c resistance of 2.8 MPa. This corresponds to a D_r value of about 36% (i.e. in a loose to medium dense condition) estimated using the empirical correlation proposed by Jamiolkowski *et al.* (2001). Classification tests on samples recovered from the site indicated D_{50} and C_u values of 0.49 mm and 1.9 respectively, which are almost identical to those found at Shenton Park (Figure 4.3). Figure 4.8 compares the different characteristic of the sand at South Perth Esplanade in contrast to the other two sand sites.

4.3 THE INSTRUMENTED PILES

4.3.1 Surface Stress Transducers

Experimental investigations of pile shaft friction in sand generally use strain gauges or load cells to measure the axial pile load distribution, from which the distribution of local shaft friction can be calculated. A more complete understanding of the mechanisms controlling the shaft friction could be obtained if the lateral stresses acting on the pile shaft are also measured. Attempts have been made by mounting commercially available earth pressure sensors onto pile shafts, but such instrumentation generally suffers from various inaccuracies and has a poor reliability when subjected to (harsh) pile driving and when required to measure long-term effects such as pile set-up (Axelsson, 2000). Common errors associated with earth pressured cells were discussed by Dunnicliff (1993), amongst others.

One instrument which has been shown to have a high performance level is a specially designed device, referred to as a surface stress transducer, developed at Imperial College in collaboration with Cambridge Insitu. It allows for a designated surface roughness on the loading platen to be specified in order to capture the desired shearing mechanism and measures both the radial stress and shear stress acting on the pile shaft simultaneously. This superior instrument is the key component in the Imperial College Pile (ICP), which has been used with considerable success in various ground conditions around Europe (Bond, 1989; Lehane, 1992; Chow, 1997). Full design details of the SST are provided by Bond *et al.* (1991a). An exploded view of the instrument and its 'dogbone' Cambridge earth pressure cell are shown in Figure 4.10.

As highlighted in Chapter 1, the main objective of this thesis is to investigate the time-dependent behaviour of pile shaft friction and its diameter dependency so that the findings could be extrapolated to predict the field pile performance. Therefore, with the available research funding from the Australian Research Council (ARC) discovery grant, two new SSTs in the diameters of 65 mm and 135 mm were ordered from Cambridge Insitu, in concert with a 100 mm diameter SST borrowed from Imperial College London (ICL) to perform the investigation. The new SSTs share the same design as the original 100 mm diameter SST but were scaled accordingly (both the shear web and radial pillar) to achieve the same level of compliance to minimise cell action

effects. It is noted that model pile with a single SST will not provide a stress distribution along the pile shaft, but is sufficient to allow identification of the component that contributes to pile set-up and the related scale effects.

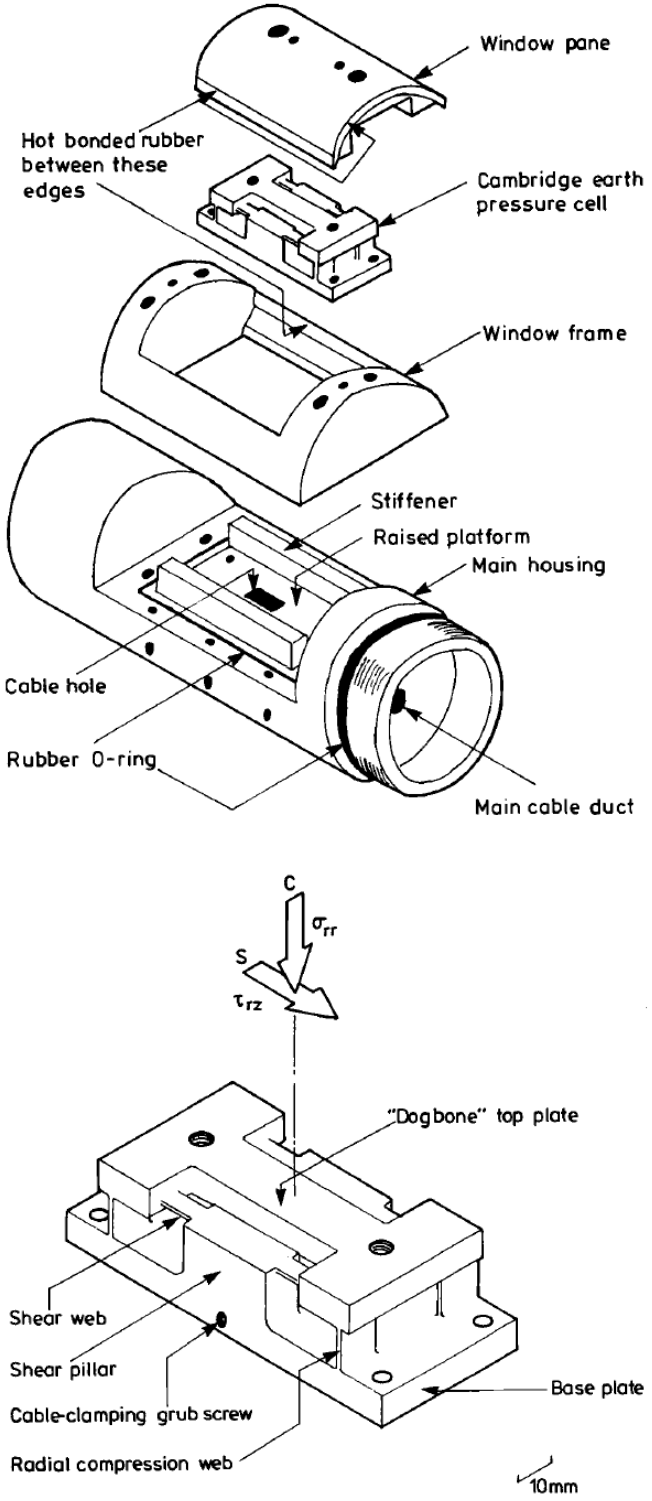

Figure 4.10. The surface stress transducer (Bond *et al.*, 1991a)

Calibrations were performed to allow for cross sensitivities associated with application of (*i*) negative and positive shear stress on the output from the radial stress gauges, (*ii*) radial stress on the output from the shear stress gauges, and (*iii*) axial compression and tension loads on the signals from the radial and shear stress gauges. In addition, a thermocouple housed within the SST allowed correction for temperature effects. Despite allowance for all of these effects and the fact that instrument zero readings before and after calibration were virtually identical (i.e. negligible zero drift), slight hysteretic responses of the gauges during axial loading and unloading were such that it was believed that resolutions of radial and shear stresses were not better than 2 and 1 kPa, respectively. Details of calibration and performance of the instruments are reported in Appendix A.

4.3.2 Pile Axial Load Cells

The SST calibration exercise showed that the smallest instrument (i.e. 65 mm diameter SST) is rather sensitive to axial loading. In order to improve the accuracy of the radial and shear outputs, two axial load cells were fabricated and assembled close to the SST to achieve a better axial load correction, as well as providing a measure of the shear stress between the two axial load cell locations. The design of the pile axial load cell is similar to that employed in the ICP (Bond *et al.*, 1991a), which was gauged at a thinned-wall section and covered with a protective sleeve. Calibration was performed against a Baldwin loading machine to the design capacity of 200 kN and showed a linear response. The outputs from the radial and shear circuits of the 100 and 135 mm diameter SSTs were much less sensitive to the axial load and could be corrected satisfactorily based on an estimated value.

4.3.3 Pile Assembly

The modular model piles comprise steel pipes, typically 0.5 m in length, a flat end cap and a top piece; all components were threaded and allowed for pile assembly during the installation sequence. The pile diameters employed were the same as the SSTs i.e. outer diameters (D) of 65 mm, 100 mm and 135 mm. Each pile is instrumented with a SST, which is fixed at about 0.7 m above the pile tip. This position is approximately 10 times the pile diameter ($10D$) above pile tip for the 65 mm diameter pile, which can be considered as a largely stable zone relatively free from major end effects (Campanella

and Robertson 1981). The height above pile tip of the SST for the 100 mm and 135 mm diameter piles is about 7*D* and 5*D*, respectively. The piles were installed to an average embedment length of about 3 m; this corresponds to a range of pile slenderness ratios (*L*/*D*) comparable to typical prototype piles.

4.3.4 Data Acquisition

A SST provides four channels of electronic data: Radial 1, Radial 2, Shear and Temperature. The strain gauges with typical output of 5 mV are amplified by 1000 times and configured to output up to ± 5 V in a 16-bit data acquisition system. The two radial stress channels are designed to monitor the normal compressive forces acting on the top and bottom of the Cambridge earth pressure cell, respectively. These channels are logged independently but an average value is taken to be representative of the radial force acting on the window pane. The shear channel is designed to respond to the shear forces acting along the window pane. When in the vertical position, positive shear readings correspond to an upward movement of the window pane relative to the instrument (e.g. shear stresses during pile penetration are considered positive). The temperature channel is utilised to correct for any temperature induced zero shifts in the other channels.

The data were acquired using an advanced data acquisition system called DigiDAQ that was developed in-house at UWA. The system can accommodate for a continuous data streaming at 100 Hz × 8 channels × 16 bit up to a total of 8 boxes of input (i.e. 64 channels) and data recording at high speed up to 1 MHz × 8 channels simultaneously (128,000 × 8 channel data per capture). In this study, two of the standard data logger boxes were sufficient and the data were logged at 0.1 seconds intervals during pile jacking and at intervals of about 2 minutes for long term monitoring.

4.4 TEST PROGRAMME AND PROCEDURES

4.4.1 Programme

A total of eighteen closed-ended piles, comprising three different diameters of 65, 100 and 135 mm, were jacked into three sand sites of different mineralogy and groundwater regimes. Table 4.1 summarises the basic details of the test piles. It is important to note that despite the majority of the experiments were conducted at the UWA test bed site in Shenton Park due to its availability and convenience, observations from the experiments at Ledge Point and South Perth Esplanade are equally important. At Shenton Park, the location of the test piles with traces of the in situ tests is indicated in Figure 4.11.

4.4.2 Installation

A CPT truck provided the reaction to install the model piles in a series of either 100 mm or 250 mm long jacking strokes at an average jacking speed of about 6 ± 2 mm/s. It should be mentioned that the standard penetration rate of 20 mm/s programmed in the CPT truck could not be easily altered and therefore pile installation was performed in the manual mode that resulted in some slight variations in penetration velocity. The piles were fully unloaded after each jacking stroke and left for a brief pause period of between 1 and 5 minutes before jacking recommenced; this incremental installation procedure attempted to mimic the pile driving procedure.

The total pile installation resistance was measured using another load cell, which was usually placed between the pile head piece and the loading platen from CPT truck. In most cases, this load cell was only employed over the last few increments of jacking in order to maintain the verticality of the model pile since it was not fixed to the pile. Figure 4.12 shows some pictures taken during pile installation and its preparation work.

Table 4.1. Basic details of the test piles

Site	Pile	*D* (mm)	*L* (m)	*L/D*	N_{cyc}	$q_{c\text{-}avg}$ (MPa)	Ref CPT
SP	100_spa^	101.5	3.72	37	15	5.0	SCPT-8 & CPT-9
	100_spb^	101.5	3.75	37	15	5.0	SCPT-8 & CPT-9
	65_spa	65.0	3.14	48	31	3.5	CPT-10 & 11
	65_spb#	65.0	3.20	49	32	3.5	CPT-10 & 11
	65_spc@	65.0	3.20	49	32	3.5	CPT-10 & 11
	135_spa	134.6	3.16	23	32	3.6	CPT-11, 13 & 14
	135_spb	134.6	3.16	23	32	3.6	CPT-11, 13 & 14
	65_spd	65.0	3.10	48	31	4.9	CPT-3 & SCPT-16
	100_spd	101.5	3.10	31	31	4.9	CPT-3 & SCPT-16
	135_spd	134.6	3.10	23	31	4.9	CPT-3 & SCPT-16
	65_spe+	65.0	3.49	54	35	5.3	CPT-15 & 17 to 20
	65_spf+	65.0	3.57	55	36	5.3	CPT-15 & 17 to 20
	135_spe+	134.6	2.73	20	27	5.1	CPT-15 & 17 to 20
	135_spf+	134.6	2.77	21	28	5.2	CPT-15 & 17 to 20
LP	100_lpA^	101.5	2.90	29	12	2.4	SCPT-1
	100_lpB^	101.5	2.90	29	12	3.3	CPT-2
ESP	65_espA*	65.0	3.80	59	38	3.6	CPTu-1
	65_espB*	65.0	4.00	62	40	3.5	CPTu-1

Note:

SP denotes Shenton Park, LP denotes Ledge Point and ESP denotes South Perth Esplanade.

^ The piles were installed using a longer jacking stroke of 250 mm in contrast to 100 mm for others.

The pile was not unloaded after each jacking stroke except at two occasions during extension of the pile casing.

@ The pile was installed following previous 1-month test without sandblasting, which has a rougher surface due to sand-bonding.

+ A hole was pre-bored to a depth of about 2 m from ground surface before installation to isolate the denser crust layer which showed greater variability.

* The pile was installed using a faster rate of about 15 mm/s compared to others of typically 6 ± 2 mm/s.

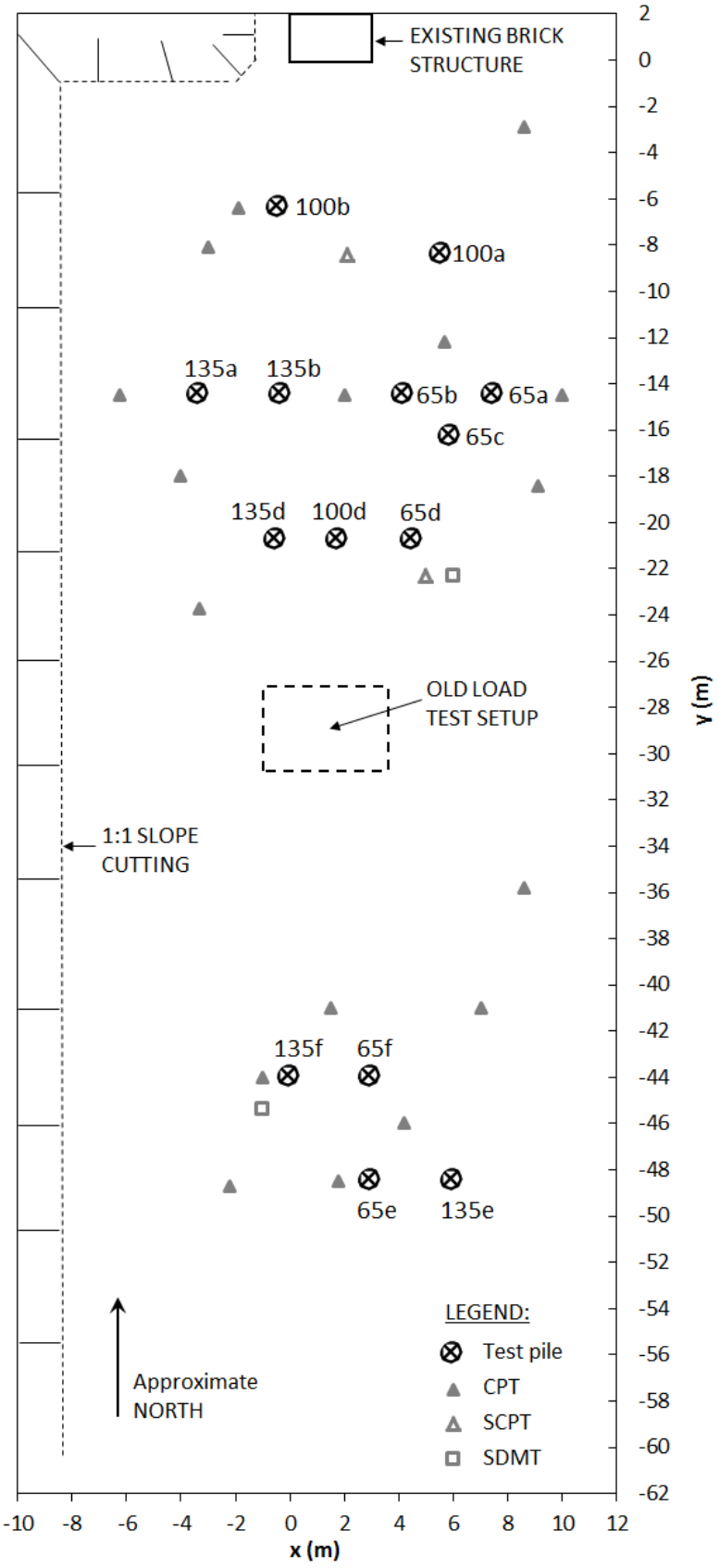

Figure 4.11. Layout of test piles at Shenton Park

Figure 4.12. Pile installation: (a) CPT truck provides the reaction and jacking facilities; (b) pile head connection for efficient incremental jacking procedures; (c) preboring in phase 4 testings

4.4.3 Equilibration

After pile installations were completed, logging of the SSTs continued at a lower frequency until the load tests were performed. This is an important piece of record since there has been a conjecture suggesting that the dominant mechanism of pile set-up in sand is the result of increases in the radial effective stress acting on pile shafts through relaxation creep following the collapse of circumferential arching effects (hoop stress) established around the pile shafts during installation (e.g. Åstedt *et al.*, 1992; Chow *et al.*, 1998).

At Shenton Park, power supply was not an issue since the logging equipment could be connected to a nearby permanent structure. Although there were some interruptions to the power supply during monitoring periods, frequent tracking of the progress (thus rectification whenever necessary) allowed the overall trend of the equilibration process over a long monitoring period to be captured satisfactorily. It should be mentioned that even with the well-designed SST and relative gentle installation procedures (compared to impact driving), erroneous outputs were occasionally recorded in this long-term data logging.

4.4.4 Load Testing

In this study, all model piles were statically load tested in tension to failure to derive the ultimate pile shaft capacity. The pile set-up was assessed by comparing the reference initial capacity measured one day after installation with the capacity measured on other piles which were load tested after longer equalisation periods. It is important to note that this programme only comprised first-time static tension load tests and thus the data are free from the various uncertainties associated with re-tests discussed in Chapter 2.

Tension tests were performed utilising the simple setup shown in Figure 4.13. A temporary structure comprising hollow steel beams was erected around the pile in a pyramidal arrangement to direct the reaction loads from the test to the ground away from the zone where it would influence the pile with minimal structural deflections. A high tensile strength threaded rod (varying in size depending on the expected pile shaft capacity) was connected to the top piece of the model pile at one end, passed through an opening on the uppermost beam, hydraulic jack cylinder, hollow load cell and lastly

locked with a stud at the top end. The uplift force was applied by expanding the hydraulic jack in a series of small increments (typically 5 – 10% of the maximum expected load) with each load maintained for a set of holding period of approximately 5 minutes, until failure occurred. Pile head displacements were measured by a LVDT mounted on a reference beam that was founded on separate supports either side of the load test setup.

4.5 RESULTS AND DISCUSSION

4.5.1 Installation

Figure 4.14(a) shows a profile of penetration resistances recorded by a load cell placed at the pile head of a 135 mm diameter model pile (135_spa) during installation. In Figure 4.14(b), the profiles of penetration resistances from two pile axial load cells, which were equipped in the 65 mm diameter model pile (65_spe) during phase 4 of the testing programme, are presented. The corresponding average q_c profiles are included in the plots to mirror the resemblance of both (and hence supports a CPT-based pile design approach). The axial load measurements together with an estimated pile end resistance ($\approx q_c$ from adjacent CPT data; averaged based on recommendations of Eslami and Fellenius (1997)) allow a rough estimate of the shear stress distribution along the pile shaft to be derived.

As indicated in Figure 4.14(b), the residual forces that developed along the pile shaft, where the load cells were located, are observed to increase with penetration depth (Holloway *et al.*, 1978). The measured values were cross-checked with those estimation derived from empirical equations proposed by Briaud and Tucker (1984) and Alawneh and Husein Malkawi (2000). The residual forces at the SST level for the 65 mm diameter model piles (65_spe and 65_spf) are approximately 3 kN. A slightly higher value is expected for the larger model piles but it is relatively insignificant in the axial load correction due to its low sensitivity, as noted earlier.

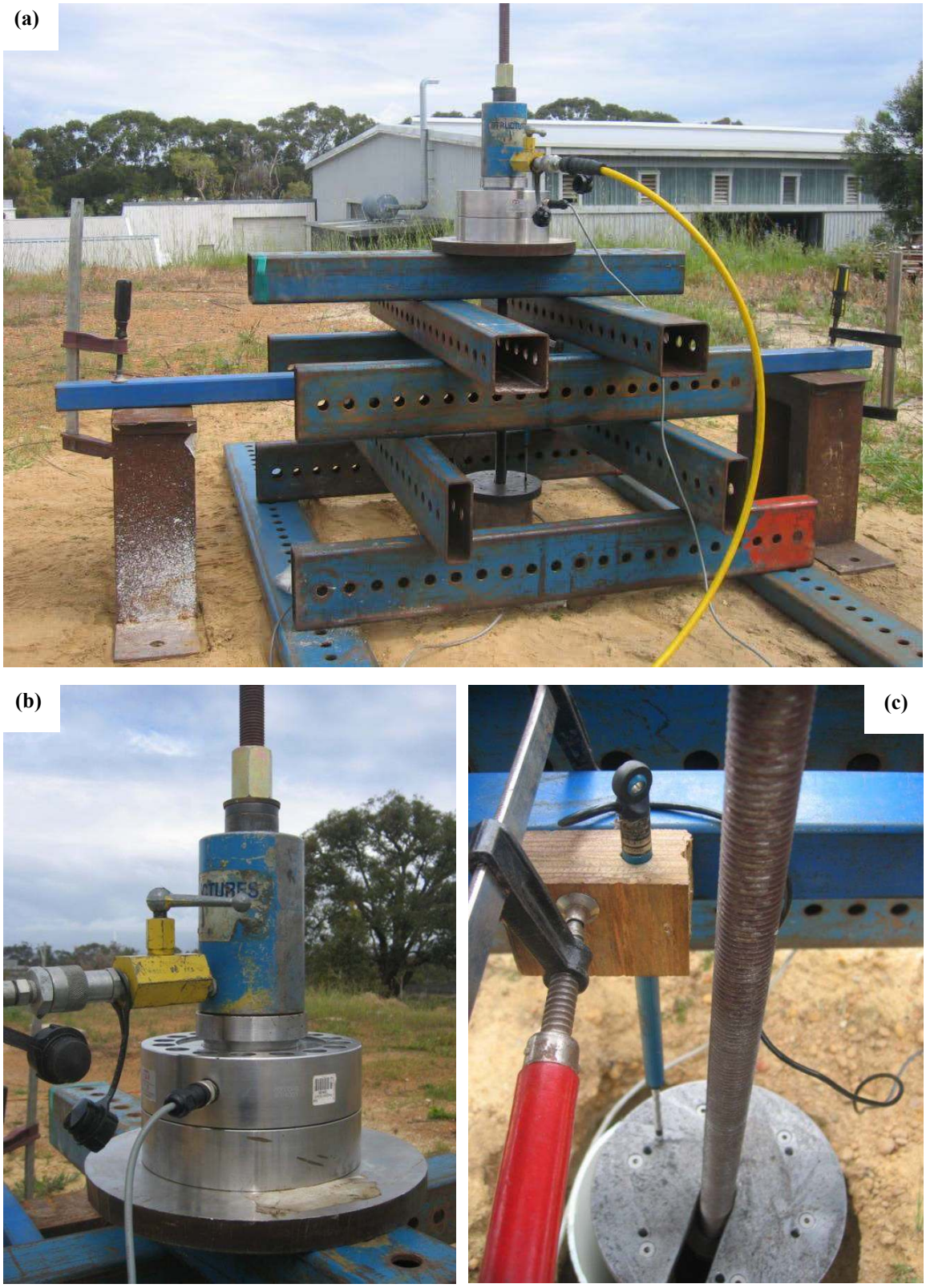

Figure 4.13. Tension load test: (a) overall test setup; (b) piston of the jack cylinder protruded during testing; (c) measurement of pile head displacement using LVDT

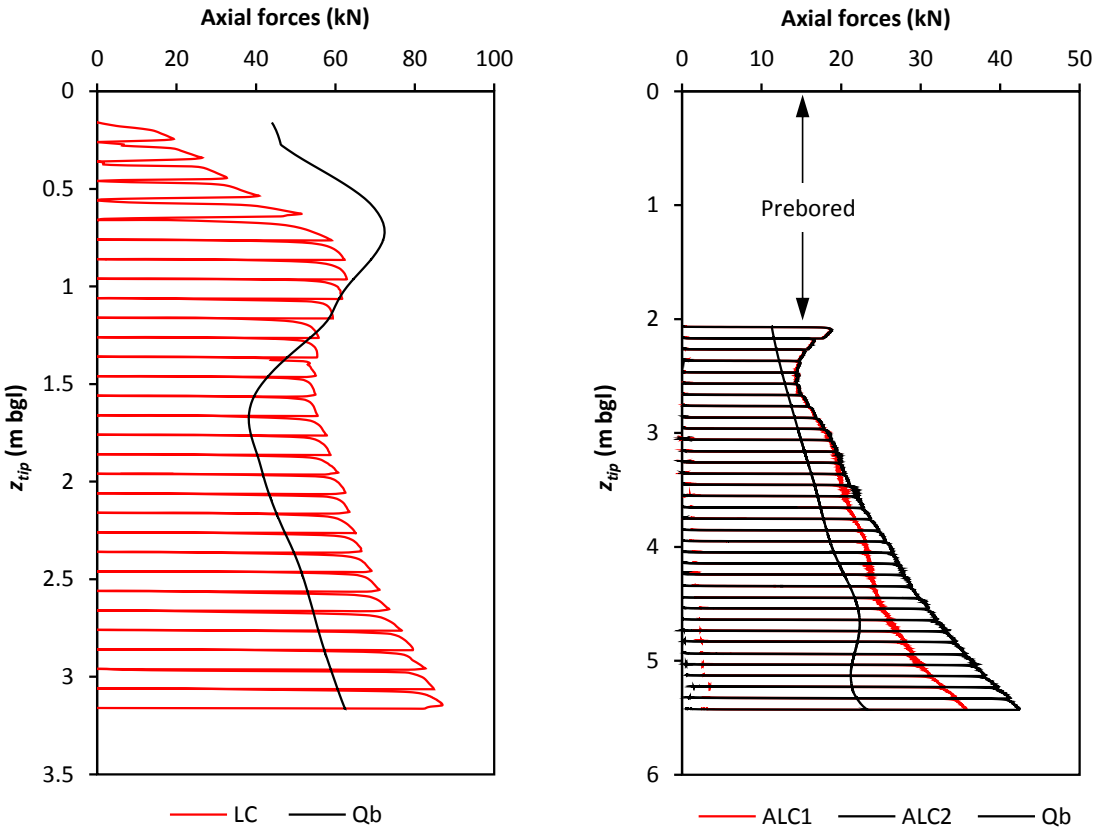

Note:
LC is the measurements from the separate load cell placed at the pile head;
ALC1 and ALC2 are measurements from pile axial load cells that were fixed at 1.3 m and 2.5 m above pile tip, respectively;
Qb is the estimated pile end resistance inferred from adjacent CPT data.

Figure 4.14. Typical profiles of penetration resistances during installation: (a) 135_spa; (b) 65_spe

Typical profiles of the measured radial and shear stresses acting on the pile shaft during the installation, as represented by a 135 mm diameter model pile (135_spa) at Shenton Park, are presented in Figure 4.15. The traces shown in Figure 4.15(a) correspond to the measured radial total stresses (equal to radial effective stresses since $u = 0$) while the piles were moving and when the piles were stationary in between the jacking stages. The profile of stationary radial stress can be seen to correlate very well to the adjacent CPT q_c profile as presented in Figure 4.15(c), which is the basis for CPT-based pile design methods (e.g. Jardine *et al.*, 2005; Lehane *et al.*, 2005b). The shear stresses as shown in Figure 4.15(b) are similarly well reflective of the radial stresses, which is

consistent with the Coulomb failure criterion, with shear stress being a function of radial stresses acting on the pile.

The interpretation of local shaft stresses in the following focusses on data recorded below 2 m depth because of the uniformity of the subsurface stratigraphy (as illustrated in Figure 4.5) and the availability of the pile head load measurements for axial correction of the SSTs. The last jacking increment in particular is of primary interest because it represents the local 'initial' condition following installation, which is used to assess the changes of localised behaviour during subsequent equilibration and load testing stages.

Figure 4.16 shows the variations of shear stress with radial effective stress for a typical loading stage of a 100 mm diameter model pile (100_spa) at Shenton Park. It is observed that after a small reduction in radial stress as the penetration takes place, continued shearing results in an increment of radial stress accompanying an increment of shear stress. This behaviour reflects the effects of constrained dilation during interface shearing, similar to those observed during load tests in previous ICP experiments (e.g. Lehane *et al.*, 1993). The stresses remain at a critical state condition during continued large displacement shearing (i.e. constant radial and shear stresses when the maximum shear stress is attained) until the pile is unloaded. Brittleness response was observed during pile installation at Ledge Point and South Perth Esplanade, which is examined later in Chapter 5. The interface friction angle ($\delta_f = \tan^{-1}[\tau_{rz}/\sigma'_r]$) between the sand and the window pane of the SST ranges from 25^o to 30^o subject to sand mineralogy and grading, which is consistent with that expected from the existing empirical correlations. The unloading process (indicated by the dotted line) brings the stress path back to the stress condition at rest, which consists of a slightly lower stationary radial stress with a small value of negative shear.

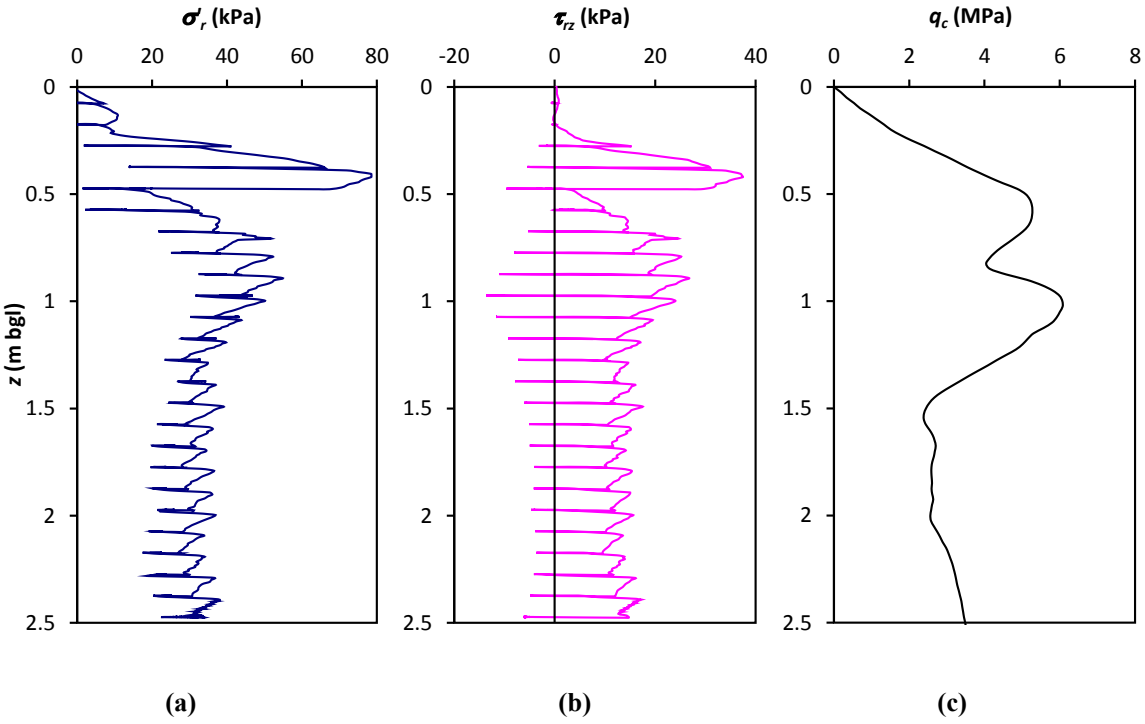

Figure 4.15. Typical profiles of SST measurements during pile installation

The stationary radial effective stresses (σ'_{rs}) recorded during the last 5 jacking strokes for all the test piles were normalised with their corresponding q_c measurements and compared with previous observations at other sand sites in Europe. As indicated in Figure 4.17, the normalised stresses (σ'_{rs}/q_c) for the three pile diameters employed at Shenton Park show a tendency to reduce with increasing h/D. These stresses are, however, well below the average values recorded for 100 mm diameter piles in medium dense sand at Labenne (Lehane, 1992) and dense sand at Dunkirk (Chow, 1997). Nevertheless, the data from South Perth are in keeping with the results obtained at Labenne and Dunkirk. The lower normalised radial stresses at Shenton Park are believed to be associated with light cementation and/or suction (see Figure 4.8), which enhanced the arching effects following pile insertion. It is interesting to note that the normalised stationary radial stresses at Ledge Point (calcareous sand) are much lower than those recorded at other test sites of predominantly siliceous sand.

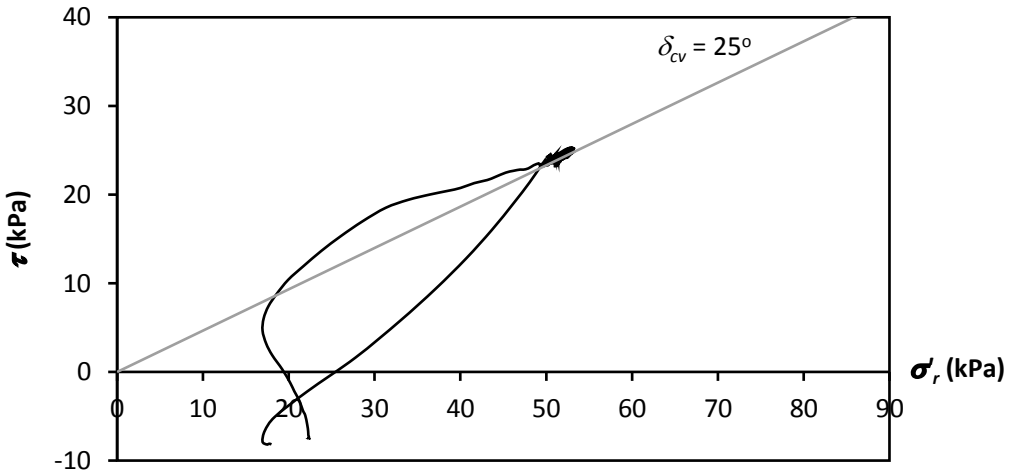

Figure 4.16. Typical stress path during an installation push

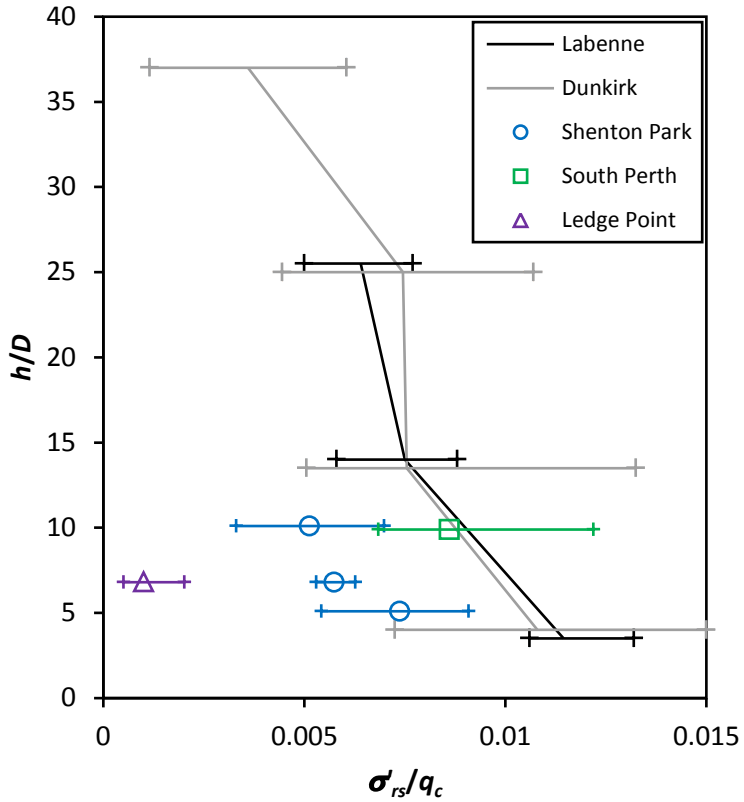

Figure 4.17. Variation of σ'_{rs}/q_c with h/D

4.5.2 Equilibration

Data logging was normally discontinued shortly after installation to proceed with other works and then resumed at the end of the day for long-term monitoring. On one occasion, the SST response of a 135 mm pile (135_spa at Shenton Park) was logged for up to about 2 hours following the last installation push without interruption. The results, which are presented in Figure 4.18(a), show that the σ'_{rs} increases with time immediately after installation (and did so following each installation push) and keeps increasing for some time after installation is completed. Subsequent monitoring overnight (Figure 4.18(b)) shows that the rate of increase of σ'_{rs} had reduced to about zero during this monitoring period. Plotting both results in a semi-logarithmic time scale, as in Figure 4.18(c), reveals that the changes of σ'_{rs} during equilibration period do not vary directly with the logarithm of time even though this form is commonly used to represent pile set-up in sand (e.g. Skov and Denver, 1988). It is noteworthy that the increases are in keeping with the observations of Lehane (1992) and Chow (1997), who found average increases in radial effective stress of 12% and 20% at Labenne and Dunkirk respectively over the monitoring periods of 15 hours.

The observations summarised on Figure 4.18 are supported by a longer period of monitoring records up to a maximum of 72 days at Shenton Park as shown in Figure 4.19. In this figure, the σ'_{rs} is normalised by its corresponding reference value measured at 1 day (σ'_{ro}) to contrast the variation of σ'_{rs} over time. Signals from 100_spb, 65_spb, 65_spc and 135_spb in the earlier phases of the programme were logged sporadically during the 1-month ageing period (Figure 4.19(a)). The several gaps of record in Figure 4.19(b) are due to temporary power cuts. Records from 100_spd were discarded due to continuous drifting of the radial stress signals. The presented radial stresses of 65_spd were based on a single radial channel output (R1) because the signal from R2 was lost one day after its installation. In spite of numerous difficulties faced during the long-term logging, it can be seen that the increases of stationary radial stress are small (with some cases even showing slight reduction) and generally not exceeding 10%. Similar trends were observed at Ledge Point and South Perth Esplanade.

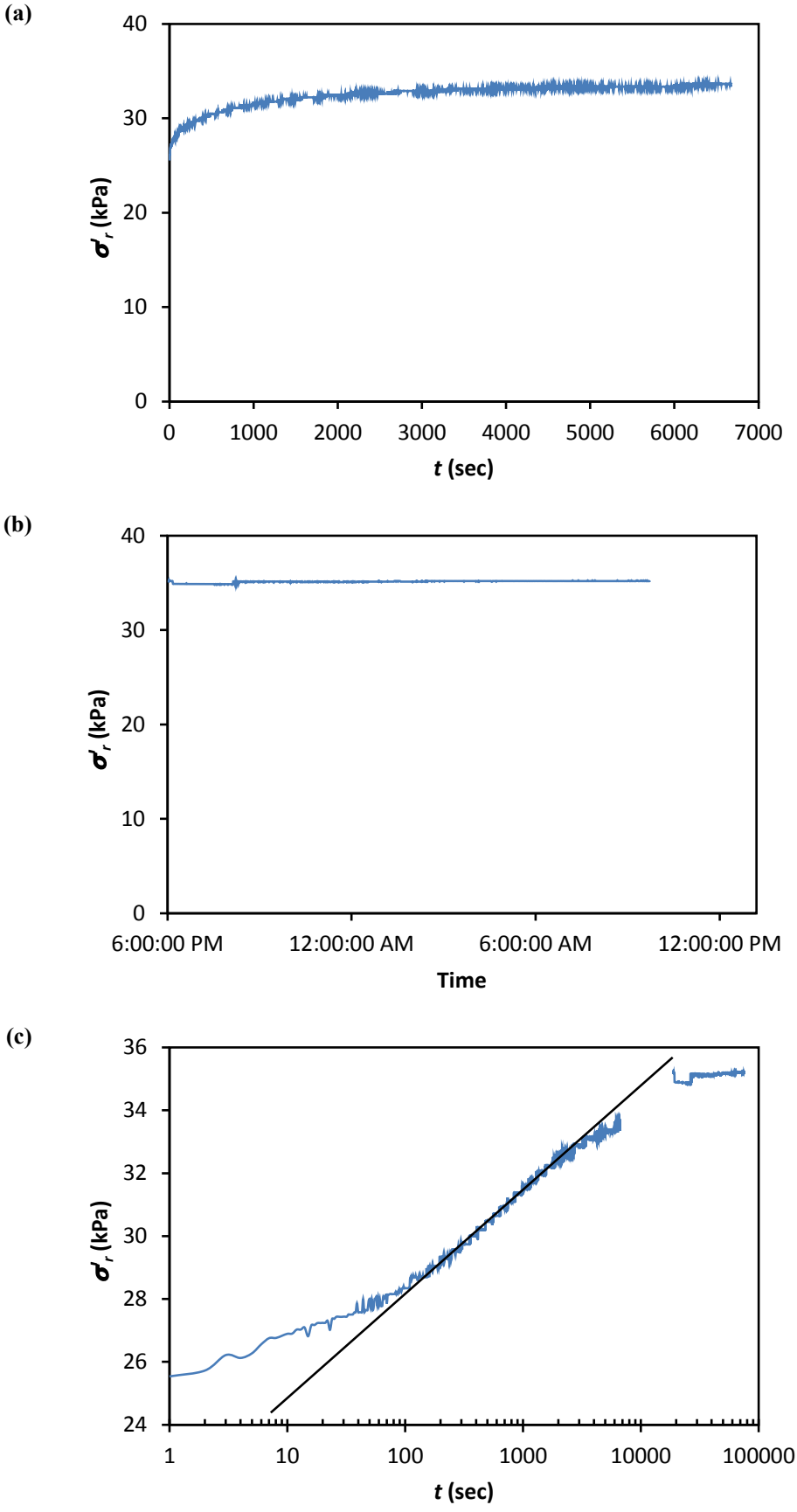

Figure 4.18. Typical changes of σ'_{rs} over 1 day of ageing period

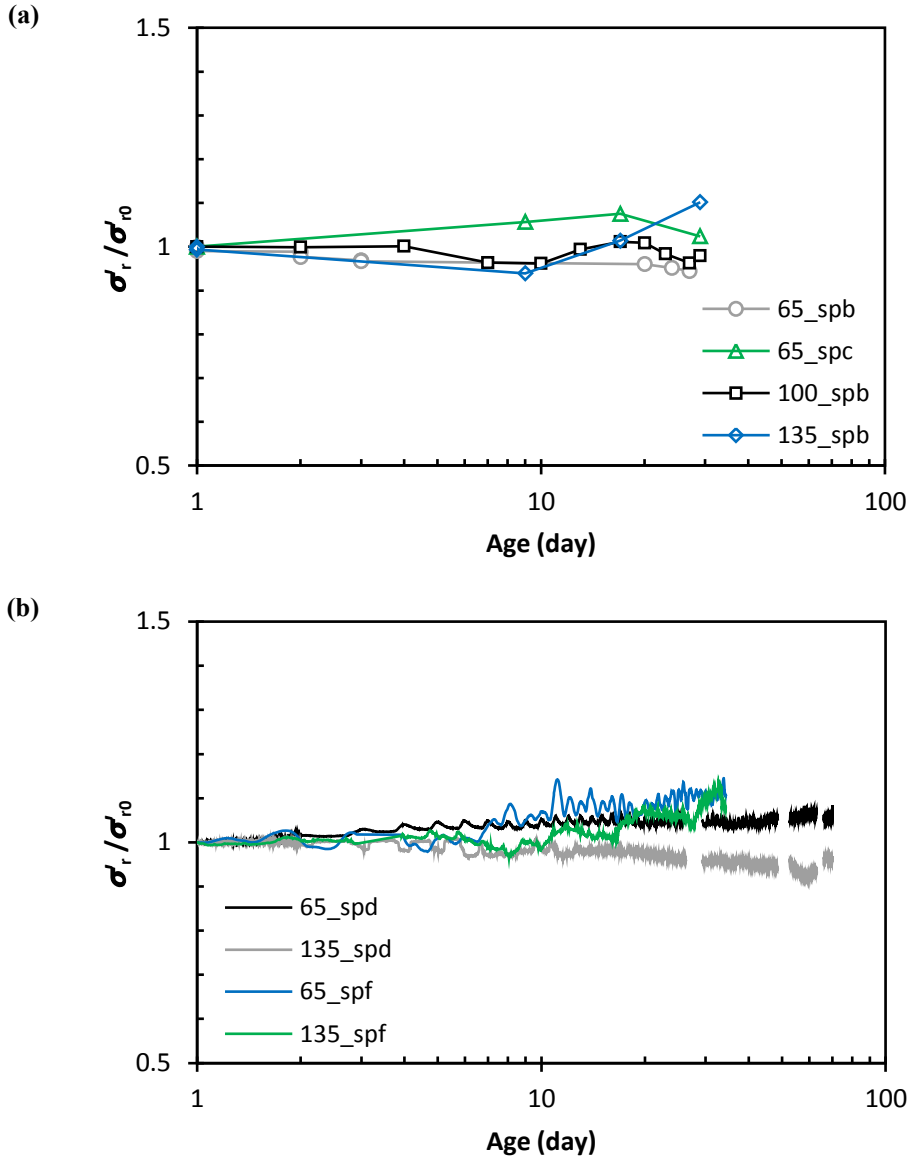

Figure 4.19. Changes of σ'_{rs} over long-term of ageing period at Shenton Park

These changes of stationary radial effective stress are very small compared to the 100% increase in radial stress of driven piles reported by Ng *et al.* (1988) and Axelsson (2000). It is worth noting that Axelsson later conducted a second series of tests at the same site and found only slight increases in the stationary radial effective stress. Axelsson acknowledges that his proposed trend involved uncertainty due to limitations of the commercial earth pressure cells employed in the experiments.

4.5.3 Load Testing

The results of tension load tests are summarised in Table 4.2. The pile shaft capacities are derived from the measured pile head loads and presented in terms of average pile shaft resistances (τ_{avg}) so that the model piles of different diameters and lengths may be compared. The results are grouped (and further categorised in series for those at Shenton Park) based on their diameters and test conditions to contrast the effects of pile set-up (to be discussed in next section).

Figure 4.20 presents the load-displacement curves of all the tension load tests at Shenton Park, which were loaded incrementally to their ultimate failure. A soft (ductile) overall response is in keeping with expectations, with mobilisation of full ultimate resistance requiring a pile head displacement of approximately 20 mm in all cases. It is noteworthy, however, that the initial stiffness of the piles is very stiff and significantly higher than what is normally observed in tension tests on piles in sand (e.g. typically one third of the capacity is mobilised at a pile head movement of only 1 mm). This trend may reflect either very light cementation and/or suction within the sand at Shenton Park (as suggested by the relatively high G_0/q_c ratio discussed in Section 4.2.1). Apart for the pile 65_spa, which employed a lightweight hand pump, all tension tests were performed using an electric pump at constant flow rates. The softening response at failure as observed in some of the test results (65_spa, 65_spe and 135_spe) was attributed to poor control of the pumps. Load-displacement curves at Ledge Point and South Perth Esplanade are presented in Figure 4.21 and Figure 4.22 respectively.

A typical stress path (from 100_spa) during a first time tension load test is shown in Figure 4.23. A similar stress trajectory to that occurred during an installation jacking stroke (see Figure 4.16) was observed but with shear stress increment heading towards the negative direction due to the uplifting action in the tension test. At the ultimate state, the interface friction angle is similar to that mobilised in compression (installation) loading. After the tension load was released, some downward movement occurred and the stress path followed the unloading path indicated by the dotted line on the figure. A residual positive friction was usually observed following the tension tests.

Table 4.2. Results of tension load tests

Site	Pile	Series	Age (day)	τ_{avg} (kPa)	τ_{avg}/τ_o
SP	100_spa	100-I	1	45.5	1.00
	100_spb		29	47.9	1.05
	100_spd		72	47.9	1.05
	65_spa	65-I	1	46.0	1.00
	65_spb		27	43.3	0.94
	65_spc*		29	49.8	1.08
	65_spd		70	55.7	1.21
	135_spa[#]	135-I	1	37.1	1.00
	135_spb		29	38.9	1.05
	135_spd		71	43.1	1.16
	65_spe[+]	65-II	1	51.7	1.00
	65_spf[+]		38	53.3	1.03
	135_spe[+]	135-II	1	43.1	1.00
	135_spf[+]		41	42.6	0.99
LP	100_lpA	-	1	5.8	1.00
	100_lpB		32	11.5	1.98
ESP	65_espA	-	1	16.0	1.00
	65_espB		9	20.1	1.26

Note:

SP denotes Shenton Park, LP denotes Ledge Point and ESP denotes South Perth Esplanade.

τ_o is the reference initial capacity taken from the tension load test that was performed on the next day after installation.

* The pile was installed following previous 1-month test without sandblasting (and has a rougher surface due to sand-bonding/welding).

[#] The result was extrapolated because the load cell capacity has been exceeded during the test.

[+] A hole was pre-bored to a depth of about 2 m from ground surface before installation to isolate the denser crust layer which showed greater variability.

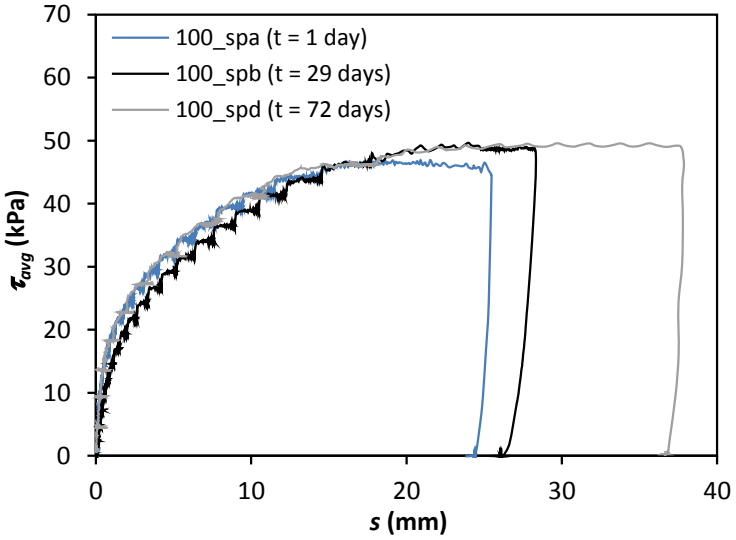
100_spa (t = 1 day)
100_spb (t = 29 days)
100_spd (t = 72 days)
τavg (kPa)
s (mm)
0
10
20
30
40
50
60
70

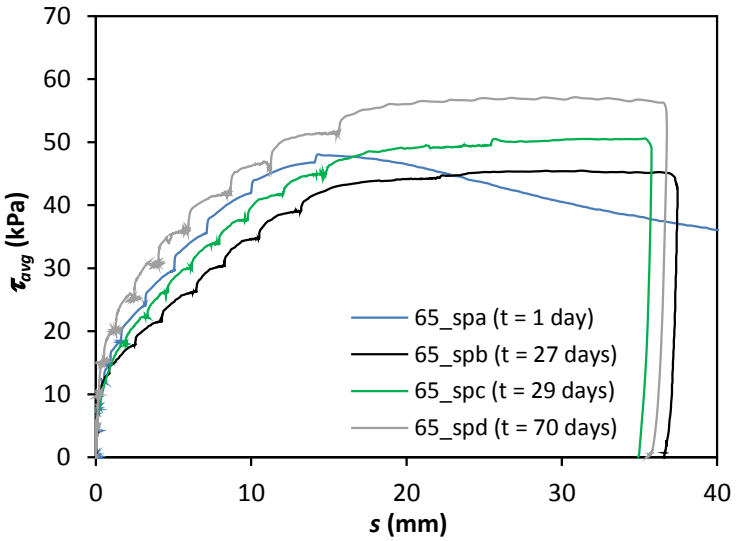
65_spa (t = 1 day)
65_spb (t = 27 days)
65_spc (t = 29 days)
65_spd (t = 70 days)
τavg (kPa)
s (mm)
0
10
20
30
40
50
60
70

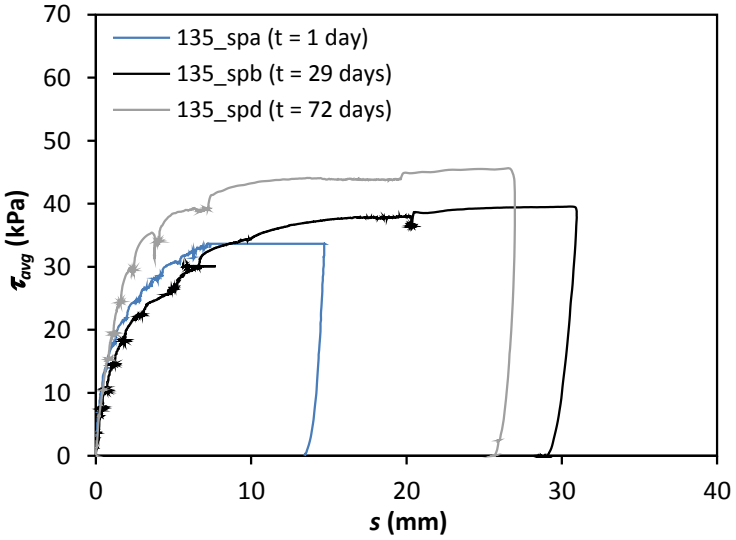
135_spa (t = 1 day)
135_spb (t = 29 days)
135_spd (t = 72 days)
τavg (kPa)
s (mm)
0
10
20
30
40
50
60
70

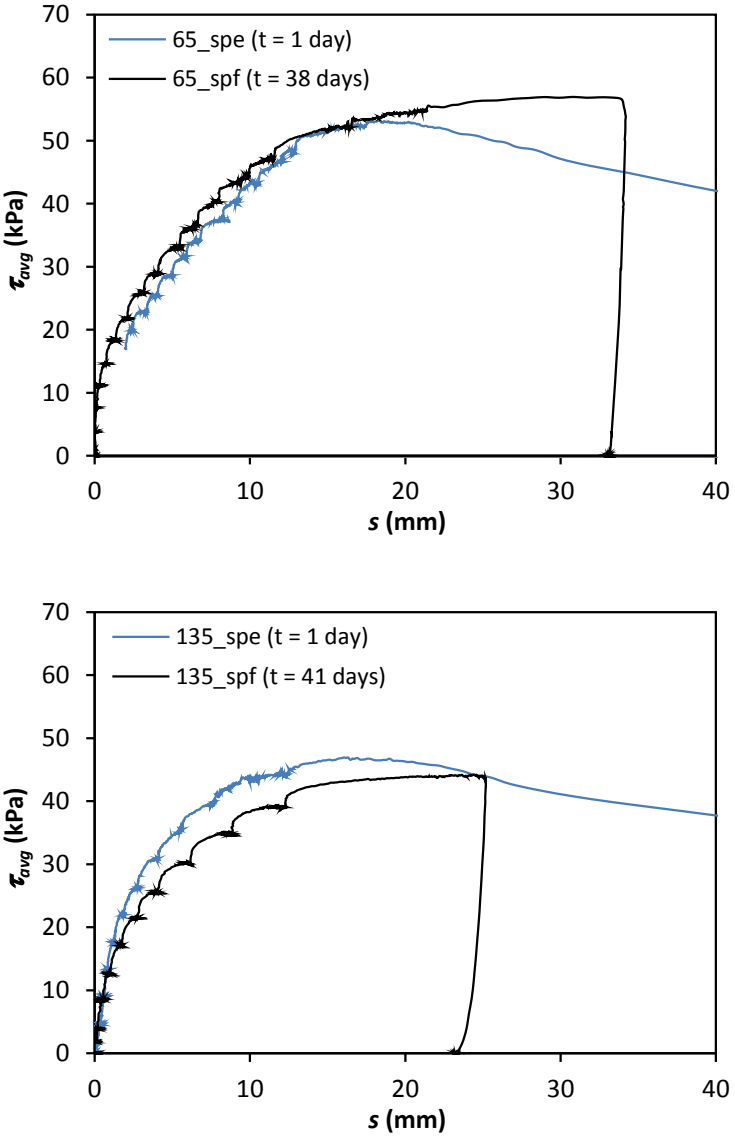

Figure 4.20. Pile head load-displacement responses (in series) at Shenton Park

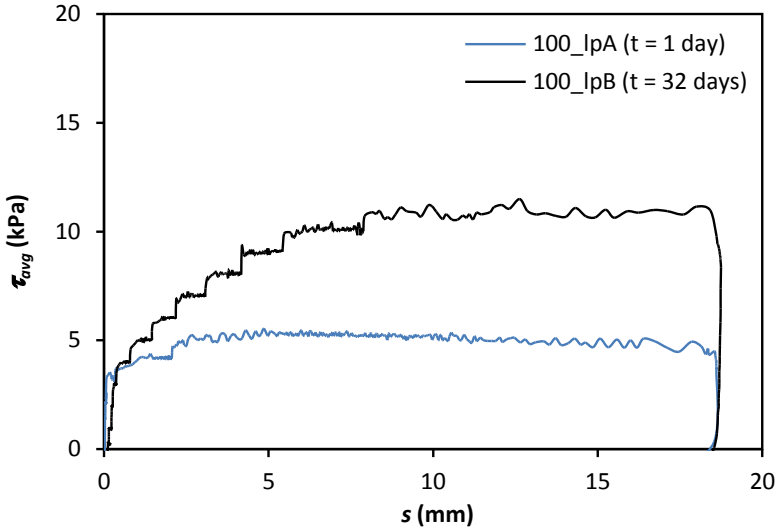

Figure 4.21. Pile head load-displacement curves at Ledge Point

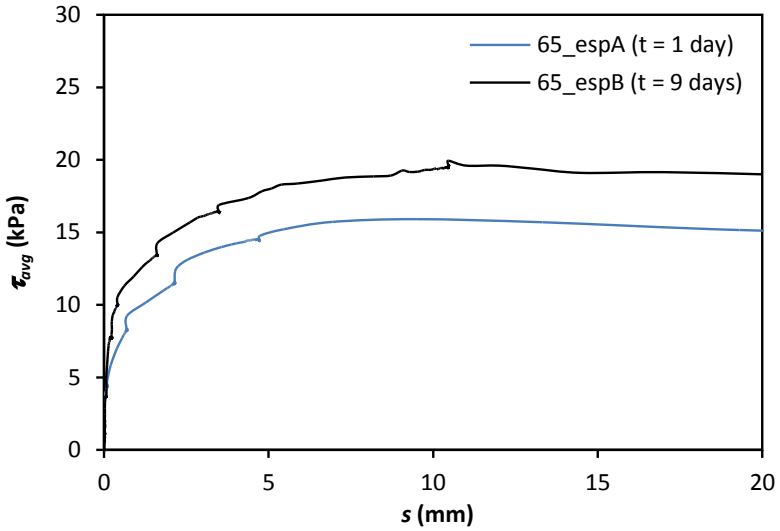

Figure 4.22. Pile head load-displacement curves at South Perth Esplanade

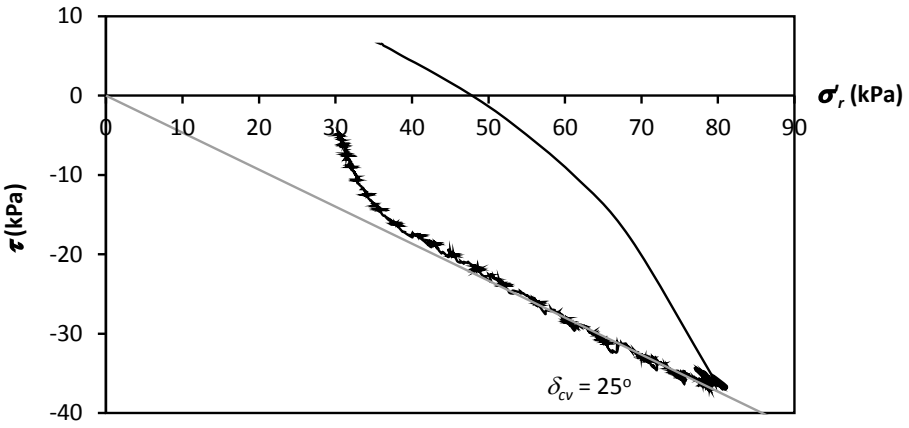

Figure 4.23. Typical stress path during a tension load test

4.5.4 Pile Set-up

The effects of global set-up are summarised in Table 4.2. The interpretation is based on average pile shaft capacities assessed from the measured pile head loads in tension load tests. Pile shaft capacity at 1 day after installation is taken as the reference initial capacity and any increase in capacity above the initial value is defined as set-up. Surprisingly, the magnitude of set-up at Shenton Park was barely noticeable as indicated by the load-displacement curves in Figure 4.20. The minor change with time of approximately 5% seen in most cases was insignificant and could be simply attributed to the inherent spatial variability among test locations or some seasonal variations between testing periods. It is important to note that this programme only comprised first-time static tension load tests, and thus is free from various uncertainties associated with characterising set-up behaviour as highlighted in Chapter 2.

For the assessment of local set-up, stress paths of the comparable pairs of fresh (1-day) and aged piles categorised in the same group are compared (Table 4.2). As shown in Figure 4.24 for the SST measurements at Shenton Park, it is interesting to observe that the largest diameter model pile has mobilised a higher local shear stress after 1 month (due to a major increase in $\Delta\sigma'_{rd}$), while no increment was noticed on the SSTs of the 65 mm and 100 mm diameter model piles. It is most likely that the observed local set-up for the 135 mm diameter piles is due to the fact that these SSTs were located at a lower number of pile diameters above the pile tip; a greater tendency of set-up over the

high stress regime near the pile tip was reported by Chow *et al.* (1998) and Kolk *et al.* (2005b), amongst others. Nevertheless, this effect is clearly localised as seen by the similarity between the (global) aged and 1-day shaft capacities discussed in Section 4.5.4 earlier.

In some cases, a relatively lower increase in radial effective stress at shearing ($\Delta\sigma'_{rd}$) is observed in the tension load test of the aged pile leading to a lower ultimate shear stress (τ_f). The response could be due to the effects of sand welding exhibited on to the (molybdenum) steel casings but not on the (relatively inert) stainless steel SST window pane. As a consequence, higher shear stresses would have been developed over the sand-welded steel casings than on the SST. Frost and DeJong (2005) demonstrated the significant influence of the surface roughness on the interface response of a multi-friction sleeve penetrometer. This welding phenomenon is such the local measurements plotted on Figure 4.24 are not totally representative of the entire shaft response.

On the contrary, relatively higher set-up was observed at the other two sand sites. At South Perth, the average pile shaft resistance at the ageing period of 9 days is about 30% higher than the initial reference resistance measured at 1 day after installation as indicated by the variation of pile head loads in Figure 4.22. Examination of the local measurements from SSTs indicated a trend consistent with the overall global behaviour. As indicated in Figure 4.25, the greater local shear stress of the aged pile was attributed predominantly to an increased radial stress change during shearing in concert with some minor increases of the stationary radial stress over the ageing period.

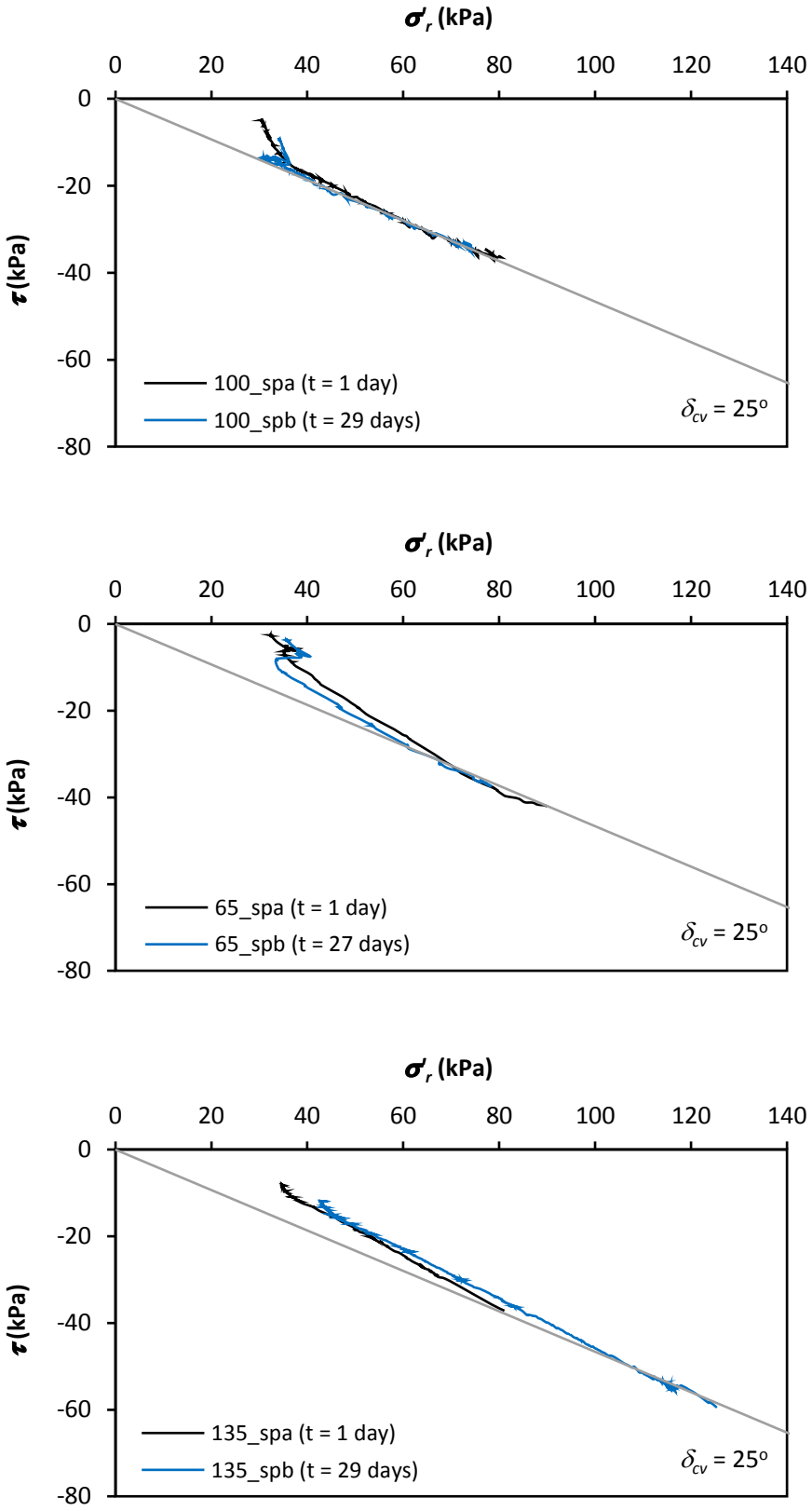
σ'r (kPa)
0
20
40
60
80
100
120
140
τ (kPa)
0
-20
-40
-60
-80
100_spa (t = 1 day)
100_spb (t = 29 days)
δcv = 25°
σ'r (kPa)
65_spa (t = 1 day)
65_spb (t = 27 days)
δcv = 25°
σ'r (kPa)
135_spa (t = 1 day)
135_spb (t = 29 days)
δcv = 25°

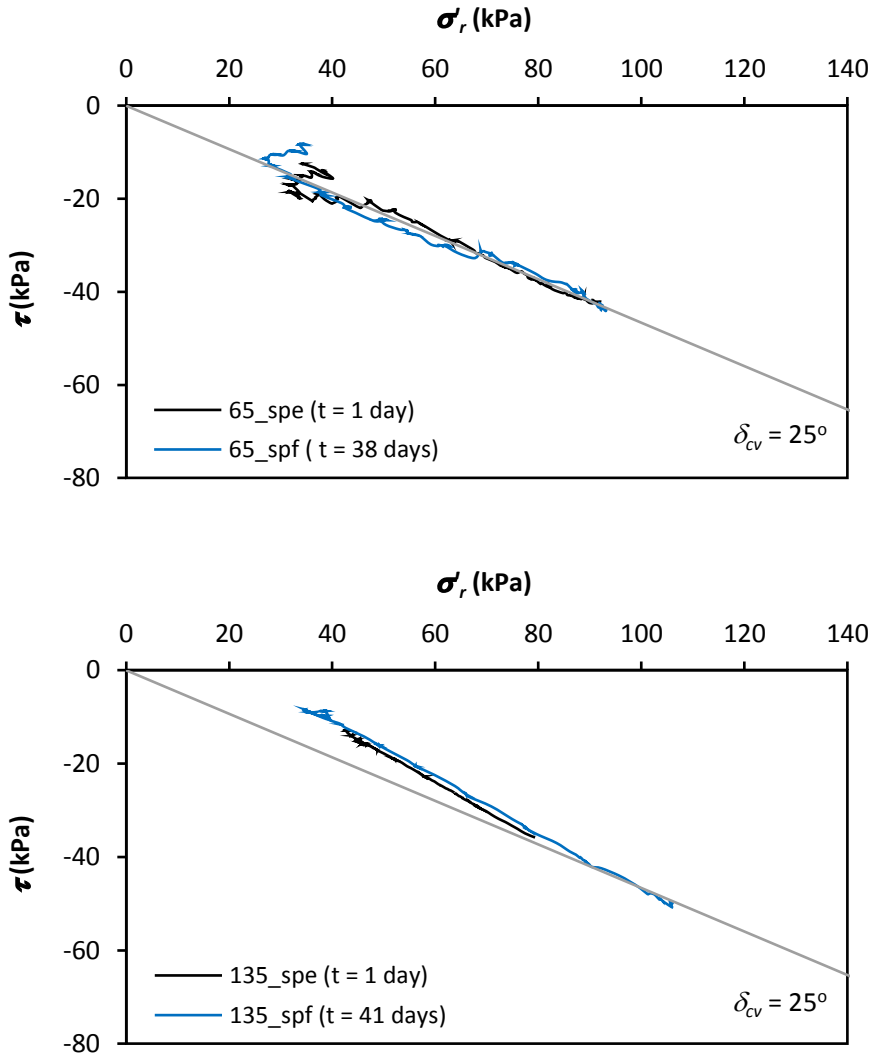

Figure 4.24. Stress paths of fresh and aged piles during tension load tests at Shenton Park

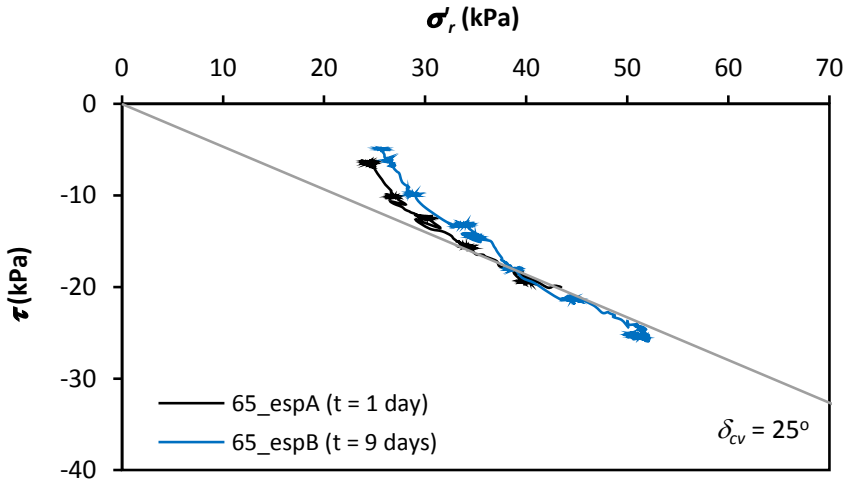

Figure 4.25. Stress paths of fresh and aged piles during tension load tests at South Perth

At South Perth, where piles were installed in a water-bearing stratum, signs of corrosion were observed when the aged pile was extracted 9 days after installation. The rust had started to develop on the pile shaft at around 1.5 m depth, where alternating wet and dry cycles occurred due to tidal effects, while no physical changes were noticed on the remainder of the pile shaft. A similar observation was reported by Chow *et al.* (1998) but to a much more severe extent after 5 years of embedment. The corrosion and sand bonding, however, has been discounted as the principal cause of pile set-up in sand since it is not consistent with the changes of shear stress distribution along the pile shaft that were measured over time (Chow *et al.*, 1998).

One plausible reason to explain the different set-up behaviour between South Perth and Shenton Park is the influence of environmental cyclic loading from tidal fluctuations. Jardine *et al.* (2006) concluded from a full-scale pile test programme that, while high-level cycling inflicts damage, low-level one-way cycling accelerates the beneficial ageing processes on piles in sand. A similar observation was reported from the model tests at 1-*g* (White and Zhao, 2006) and using a calibration chamber (Tsuha *et al.*, 2012). The tidal fluctuation of 0.5 m is likely to be minor in a full-scale pile but is relatively influential in the 3.8 m long model piles employed in this study; equivalent to a variation of about 6% of the ultimate pile shaft capacity at 1 day. It is important to note that the environmental factors such as the existence of groundwater and tidal fluctuations are not believed to be the root cause of the pile set-up phenomenon, but could enhance or accelerate the processes.

In addition, the difference could have been contrasted by the unusual characteristics of Shenton Park sand. The potential light cementation and/or suction effects described earlier may have hindered a complete soil flow mechanism during penetration (thus a smaller σ'_{rs}/q_c; see Figure 4.17) and affected the subsequent particle re-arrangement and stress equilibration process. Therefore, it is suggested that the observations at Shenton Park should not be deemed as a benchmark but rather an individual case of equivalent importance as the South Perth. On the whole, the nominal set-up observed at Shenton Park and South Perth is in keeping with previous investigation of jacked piles reported by Yang *et al.* (2006a) and Zhang *et al.* (2006), while in sharp contrast to significant capacity gain suggested by many case histories of pile set-up in sand for driven piles (e.g. Tavenas and Audy, 1972; Jardine *et al.*, 2006; Gavin *et al.*, 2013).

Results of the investigation at Ledge Point have been reported by Lehane *et al.* (2012), paper of which is attached in Appendix B for reference. There are a few additional points to note when the results are reviewed in conjunction with the findings at Shenton Park and South Perth. For essentially the same installation method and procedures at all three test sites, the disturbance (e.g. particle damage, friction fatigue, etc.) exerted on the weak calcareous sands at Ledge Point is anticipated to be larger than that imposed on the strong siliceous sands at Shenton Park and South Perth Esplanade (Boulon and Foray, 1986; Kelly, 2001; Luzzani and Coop, 2002; White, 2002). Bowman and Soga (2005) show that following pile penetration, weak and angular particles that flow to the shaft of the pile take a longer time to respond, changing from 'continuous' contraction to subsequent 'net' dilation under the new stress conditions.

The characteristics described above can be related to the higher set-up observed at Ledge Point (see Figure 4.21). It is postulated that at silica sand sites (Shenton Park and South Perth), by the time the 1-day test was performed, the majority of the strength and stiffness recovery had occurred and therefore long-term set-up was rather small. At Ledge Point, however, the stress equilibration process was rather slow with only a small portion of strength and stiffness recovered at 1 day, and hence a more pronounced set-up was contrasted when the capacity was measured at 1 month as the recovery continued. It should be noted that the pile shaft resistance at Ledge Point (5 to 10 kPa), as derived from the pile head load and those revealed by the SST measurements, is much smaller than those recorded at Shenton Park (≈ 50 kPa) despite only slight differences in relative density. The 'significant' set-up when expressed as the ratio to the initial 1-day capacity is high, but is relatively small in real terms.

Another feature, which has been highlighted by Lehane *et al.* (2012), is the contribution of bonded or welded sand crust developed along the pile shaft after embedded in the unsaturated ground for a month. Failure was forced to take place along a sand-sand rather than a sand-steel interface and gave rise to a higher level of dilation. The changes over the majority of the pile shaft however were not reflected by the SST measurements. Examination shows that the sand welding which was found on the (molybdenum) steel casings was not developed on the (relatively inert) stainless steel SST window pane, and thus resulted in a higher shear stress developed over the sand-welded steel casings than on the SST. Nevertheless, this factor is unlikely to be the

primary contributor since similar sand welding was observed at Shenton Park but in the absence of set-up effects.

4.5.5 Short-term Set-up

In the absence of prominent set-up assessed with reference to the initial 1-day capacity (particularly at Shenton Park), a further examination was performed to investigate if a short-term change has been taken place. Figure 4.26 compares the SST measurements obtained during the last installation pushes with those recorded during tension load tests performed at 1 day after installation. From three typical cases which represent each diameter of model pile employed in this study, it is clearly seen that the stationary radial effective stresses (σ'_{rs}) increase only slightly following installation, whereas significant changes in the increases in radial effective stress during shearing ($\Delta\sigma'_{rd}$) are evident. Accordingly, the ultimate local shear stresses (τ_f) during tension load tests are much larger than those measured during the last installation pushes. Experimental trial confirms that these variations are not attributed to the difference in shearing direction.

Comparison of the average pile shaft resistances during last installation pushes ($\tau_{avg\text{-}install}$; assuming q_b equals to the averaged q_c around pile toe (Eslami and Fellenius, 1997)) with those derived from the tension load tests ($\tau_{avg\text{-}test}$) shows that set-up did occur over this initial period in keeping with the localised behaviour indicated by the SSTs. The short-term responses described above, together with the negligible set-up observed over the subsequent ageing period suggests that the major underlying mechanism of pile set-up in sand for the jacked piles is that of constrained dilation due to an increase in the shear stiffness of the surrounding soil following installation disturbance.

The upcoming Chapter 5 will further examine the shaft shear stresses measured by the SSTs during installation and explain the possible mechanisms of the brittleness behaviour observed in some cases. The results of static load tests from this field test programme, combined with another programme at the same site that involved driven steel pipe piles, will be investigated in Chapter 6 to seek further insight on the poorly understood pile ageing effects.

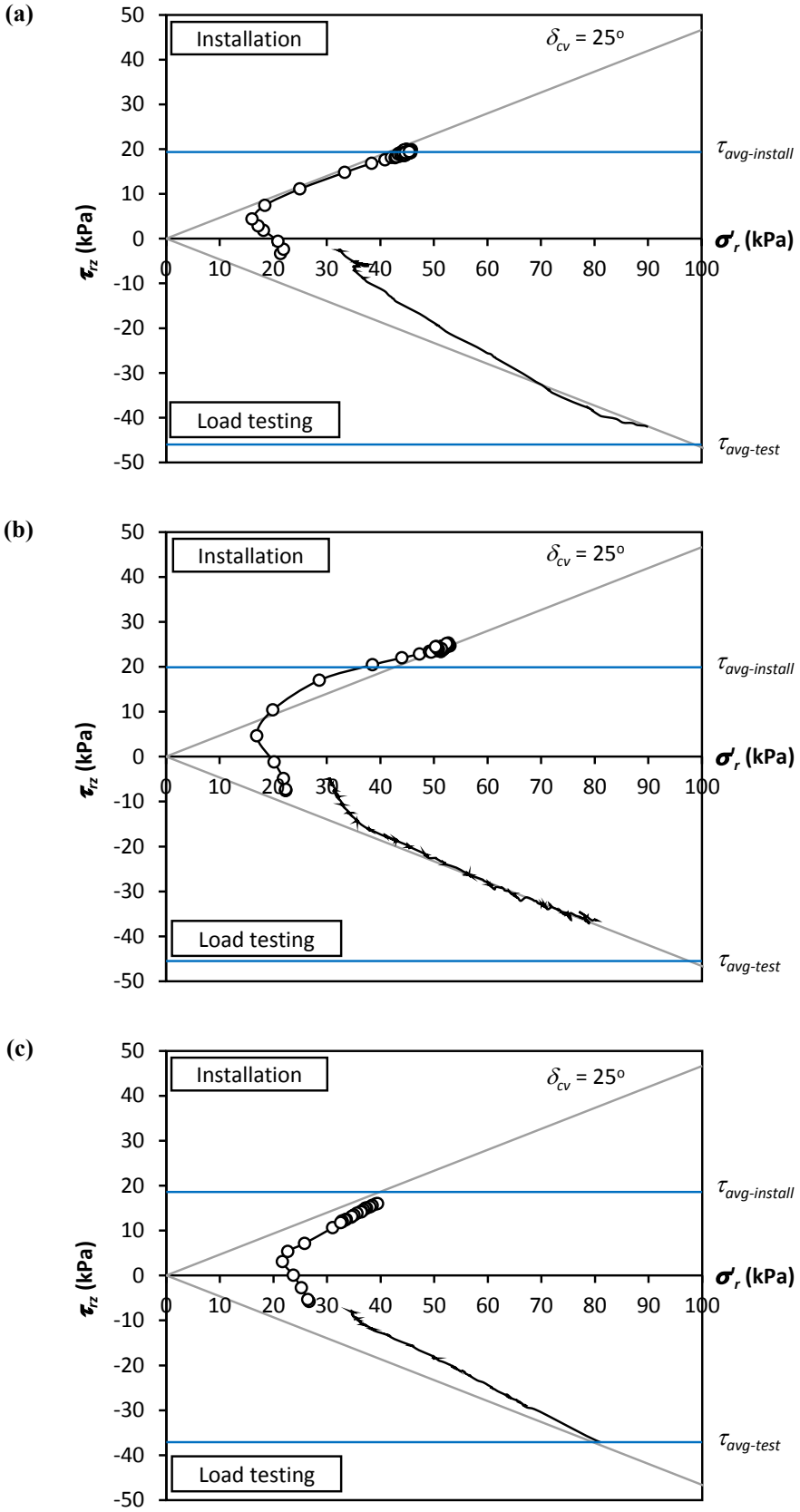

Figure 4.26. Comparison of the changes in pile shaft stresses between last installation push and subsequent tension load test after 1 day at Shenton Park: (a) 65_spa; (b) 100_spa; (c) 135_spa

CHAPTER 5. SHEARING AT THE SHAFTS OF PILES DURING PENETRATION IN SAND

5.1 INTRODUCTION

Better predictions for the shaft resistance of driven piles in sand can be achieved with an improved understanding of the mechanisms associated with large displacement and rapid shearing at the shaft-sand interface. Pile installation and dynamic load testing are important examples of rapid shearing deserving of further research.

Various laboratory interface tests have been employed to investigate the shearing behaviour along pile shafts based on observations reported from model and full-scale pile tests. However, the constraints and limitations on both field and laboratory setups have raised concerns on how well our current routine approaches reflect the actual behaviour at the pile shaft.

This chapter presents experimental findings obtained during installation of the instrumented model piles in a series of pile test programmes undertaken at several sand sites of different mineralogy and groundwater regimes. Three instances of brittleness of shaft shear stress observed during large displacement shearing are highlighted and these provide additional insights into mechanisms of interface shearing behaviour in sand at relatively fast shearing rates.

5.2 LABORATORY INTERFACE TEST DEVICES

5.2.1 Direct Shear Apparatus (DSA)

The most common interface shear test performed in routine practice is the direct shear apparatus (DSA). The test is identical to the soil-soil direct shear test except that the lower compartment of the shear box is replaced with a block of construction material of the required surface roughness. Studies have been performed covering a wide range of soils and interface materials using the DSA (e.g. Potyondy, 1961; Desai *et al.*, 1985; Al-Douri and Poulos, 1992; Jardine *et al.*, 1992).

Modifications to the direct shear apparatus have been suggested by Jewell (1989), Shibuya *et al.* (1997) and Lings and Dietz (2004) to address the non-uniform stress field

inherent in the classical setup. An improved apparatus was employed to further investigate the sand-steel interface behaviour at peak (Lings and Dietz, 2005) and post-peak (Dietz and Lings, 2006) conditions.

5.2.2 Simple Shear Apparatus (SSA)

Kishida and Uesugi (1987) highlighted the limitations of direct shear device and proposed a better alternative for interface test using a specially designed simple shear apparatus (SSA). The device consists of a stack of rectangular thin plates confining the sample that placed on top of a construction material of greater size. Performance of the apparatus can be referred to Uesugi and Kishida (1986a), Uesugi *et al.* (1988) and Uesugi *et al.* (1989).

Parametric studies conducted by Uesugi and Kishida (1986b), Frost *et al.* (2002), Lings and Dietz (2005), DeJong and Westgate (2009), amongst others, using either DSA or SSA, found that the major factors influencing the interface behaviour are the sand type and relative roughness (R_n) i.e. the ratio of the mean effective particle size (D_{50}) to a measure of the interface surface roughness (R_{cla}). The devices used, however, are limited to relatively small displacement for general applications.

5.2.3 Ring Shear Apparatus (RSA)

The ring shear apparatus (RSA), which allows for unlimited shear displacement and exhibits smaller end effects than the DSA, is claimed to model more realistically the large displacement interface behaviour relevant to a displacement pile. Jardine *et al.* (2005) recommend site-specific ring shear tests, which consider the appropriate stress level, interface material, pre-shearing history and roughness characteristics for the assessment of pile shaft friction.

Various types of RSA have been explored by Tika (1999), Kelly (2001), Corfdir *et al.* (2004) and Ho *et al.* (2011) to investigate a range of aspects related to the drained interface shearing resistance in sand. The results showed that particle damage together with a change in interface roughness following large displacement shearing have resulted in different ultimate interface friction angles from those derived using the DSA. However, neither the top nor bottom interface positions considered in the experiments

represent the actual vertical alignment of a pile shaft interface and thus the effects of fines migration. More importantly, the loss of soil through the gap of confining rings affects the accurate measurement of vertical deformation and density change during the course of an experiment (Lehane, 1992; Tika, 1999; Kelly, 2001).

5.2.4 Other Apparatus

Investigations of interface shear behaviour have been made by shearing a rod which is confined within a cylindrical sample of sand within a cylindrical cell; such tests have been performed with minor modifications to the common triaxial device (Coyle and Sulaiman, 1967; Jewell and Randolph, 1989; Reddy *et al.*, 1998). The setup does not seem to overcome problems exhibited by DSA and SSA.

An ideal laboratory interface shearing device is perhaps the ring torsion apparatus developed by Yoshimi and Kishida (1981) and a dual interface apparatus suggested by Paikowsky *et al.* (1995). These devices have not gained popularity as they are complicated and require advanced instrumentation (e.g. X-ray) and expertise to operate.

5.2.5 Constant Normal Stiffness (CNS) Condition

Conventional DSA, SSA and RSA interface tests are performed under constant normal load (CNL) condition; CNL tests are also referred to as constant stress tests. Boulon and Foray (1986) demonstrated that the pile shaft interface shearing mechanisms are intermediate between the constant normal load and constant volume conditions, and can be modelled approximately by imposing a spring with an appropriate stiffness normal to the interface (termed a constant normal stiffness (CNS) condition). Figure 5.1 presents some typical stress paths recorded by Boulon and Foray (1986) for siliceous and calcareous sands in loose and dense conditions sheared under CNS interface conditions.

The interface shearing behaviour using CNS-DSA was further investigated to cover various aspects including relative density, sand type, surface roughness, normal stress and normal stiffness on the monotonic, cyclic and post-cyclic responses (e.g. Tabucanon *et al.*, 1995; DeJong *et al.*, 2003; Porcino *et al.*, 2003; DeJong *et al.*, 2006; Mortara *et al.*, 2007; Mortara *et al.*, 2010). Besides DSA, the CNS condition has also been incorporated into the SSA (Evgin and Fakharian, 1996) and RSA (Kelly, 2001) devices.

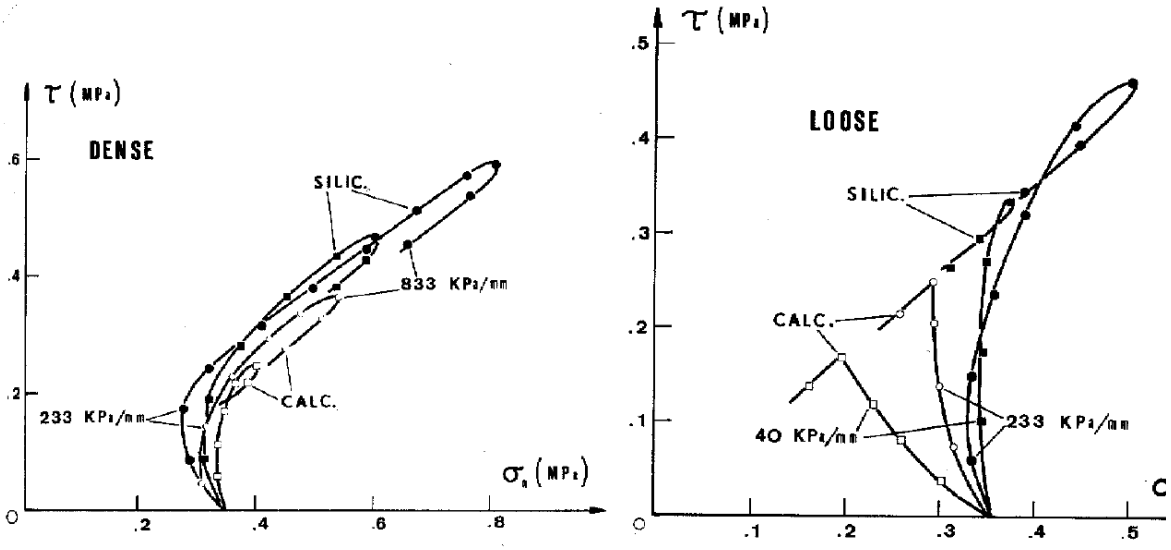

Figure 5.1. Behaviour of loose and dense sands in CNS interface shear tests (Boulon and Foray, 1986)

The CNS approach was explored by Airey *et al.* (1992), Fioravante (2002) and Lehane *et al.* (2005a) to model pile shaft friction in sand and proved to compare favourably with experimental observations. Lehane *et al.* (2005a) showed, however, that CNS tests will always only approximate the response at the pile shaft as the normal stiffness reduces as the cavity strain (dilation at the interface) increases.

5.3 PILE INSTALLATION RECORDS

5.3.1 Surface Stress Transducer (SST)

Monitoring of shaft stresses during the installation of an instrumented model pile is clearly the most desirable approach to improve understanding of shearing behaviour at a pile shaft. This approach captures the true pile penetration mechanism and soil flow, real boundary conditions, actual particle damage and fines migration and varying normal stiffness – none of which can be simulated completely satisfactorily in the laboratory. However, the scarcity of an accurate and highly repeatable earth pressure cell equipped on the pile shaft has been a major obstacle.

One notable exception is the instrument, referred to as a surface stress transducer (SST), developed at Imperial College in collaboration with Cambridge Insitu. It allows for a

designated surface roughness to be specified in order to capture the desired shearing mechanism and measures both radial stress and shear stress acting on the pile shaft simultaneously. The instrument is the key component in the Imperial College Pile (ICP), which has been used with considerable success in various ground conditions around Europe (Bond, 1989; Lehane, 1992; Chow, 1997). Full design details of the SST can be found in Bond *et al.* (1991b).

Previous experiments did not examine the detailed stress changes that occur during installation jacking. The pile test programmes discussed below employed two SSTs in the diameters of 65 mm and 135 mm fabricated by Cambridge Insitu for The University of Western Australia (UWA) and a 100 mm diameter SST borrowed from Imperial College London (ICL), equipped with an advanced data acquisition system that developed in-house at UWA. The DigiDAQ system can accommodate for a continuous data streaming at 100 Hz × 8 channels × 16 bit up to a total of 8 boxes of input (i.e. 64 channels) and data recording at high speed up to 1 MHz × 8 channels simultaneously (128,000 × 8 channel data per capture). This rate of data acquisition is considerable faster than that employed by the Imperial College research team (Bond, 1989; Lehane, 1992; Chow, 1997).

5.3.2 Pile Test Programmes

Full details of the pile test programmes are reported in Chapter 4. This section extracts some of the information that is relevant to fast jacking induced during pile installation. The model test piles are (reduced-scale) closed-ended steel piles with outer diameters (D) of 65 mm, 100 mm and 135 mm. Each pile is instrumented with a single unit of SST, which is fixed at about 0.7 m above the pile tip. The position is approximately 10 times the pile diameter (10D) above pile tip for the 65 mm diameter pile, which can be considered as a largely stable zone relatively free from major end effects (Campanella and Robertson, 1981). The heights above pile tip for the 100 mm and 135 mm diameter piles are about 7D and 5D, respectively. The piles were installed to an average embedment length of about 3 m, which resulted in a range of pile slenderness ratios (L/D) comparable to typical prototype piles.

A CPT truck provided the reaction to install the model piles in a series of either 100 mm or 250 mm long jacking strokes at an average jacking speed of about 6 ± 2 mm/s. A

faster rate of average 15 mm/s was employed for the test programme at Esplanade South Perth due to limited timeframe allowed to work within the commercial site. The piles were fully unloaded after each jacking stroke and left for a brief pause period of between 1 and 5 minutes before jacking recommenced; this incremental installation procedure attempted to mimic the pile driving procedure.

Three sand sites, namely Shenton Park (Site A), Esplanade South Perth (Site B) and Ledge Point (Site C) were explored in this study. Site A is a UWA test bed site, which is about 5 km from Perth city centre and comprises predominantly siliceous sand of the 'Spearwood' dune system. Site B is located adjacent to Swan River with groundwater table at about 1.5 m below existing grade and underlain by alluvial sand. Site C is adjacent to a small village, about 100 km north of Perth, and consists of uncemented calcareous sand with 90% calcium carbonate content. Further description of the test sites can be referred to Section 4.2.

Figure 5.2 compares the typical profiles of cone tip resistance (q_c) and corresponding in-situ relative densities (D_r) estimated from the empirical correlations proposed by Jamiolkowski *et al.* (2001), assuming medium compressibility for Sites A and B and high compressibility for Site C. It is seen that the sand stratum between 2 m and 2.5 m (where examination is focussed, as discussed later) has an average q_c value of about 3.5 MPa and average D_r values ranging from 30% to 45% (i.e. loose to medium dense). Despite having comparable sand states in the focus area, it is shown in the following that installation shaft shear stress records displayed different trends. The following representative cases are highlighted here:

- *Case I* : 65 mm vs 135 mm diameter piles (at Site A)
- *Case II* : Site A vs Site B (for 65 mm diameter piles)
- *Case III* : Site A vs Site C (for 100 mm diameter piles)

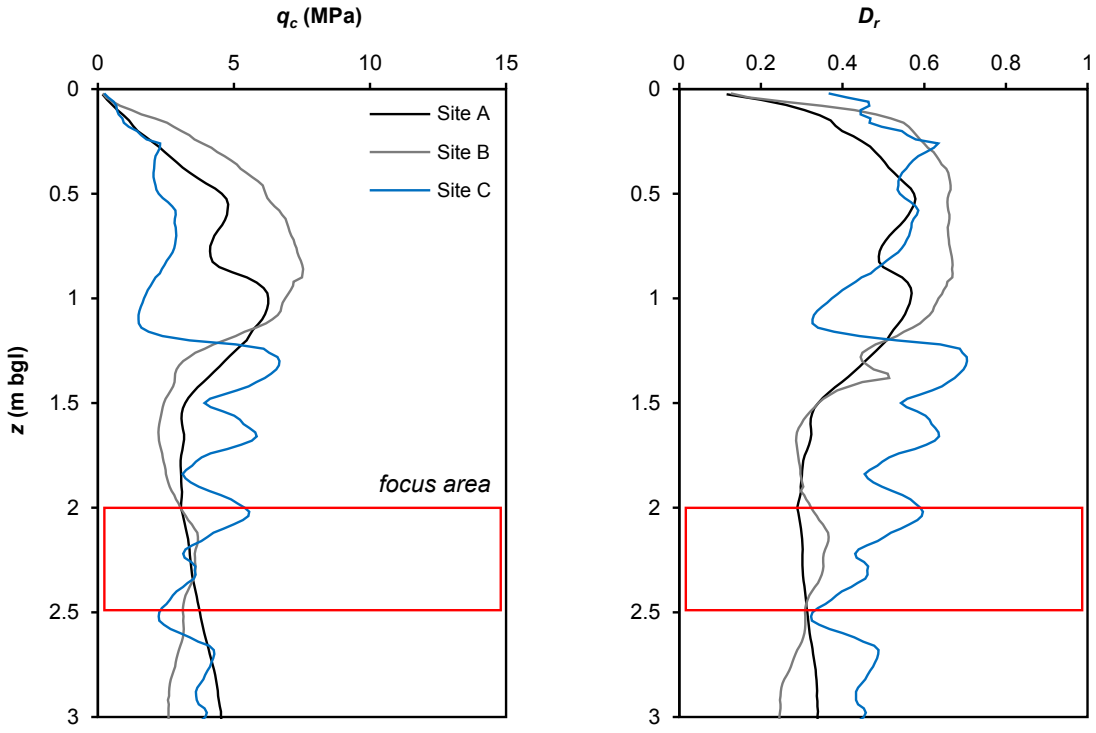

Figure 5.2. Comparison of CPT end resistance (q_c) and estimated relative density (D_r) using correlations by Jamiolkowski *et al.* (2001) for three investigated sand sites

5.3.3 Radial and Shear Stresses

Figure 5.3 to Figure 5.5 show the profiles of radial total stress and shear stress recorded by the SSTs during pile installation for the three cases, respectively. The segments from 2 to 2.5 m depth (or larger segments from 1.4 to 2.4 m for *Case III* that involved longer jacking strokes of 250 mm) were extracted for comparison in view of their similarities in respect to both D_r and stress level (see Figure 5.2). The traces shown correspond to the measured stresses while the piles were moving and when the piles were stationary in between the jacking stages. It is seen that the shaft stresses at Site A (except 135 mm diameter pile) remained about constant during shearing, whereas both radial and shear stresses at Sites B and C reduced as shearing continued. The reductions were recovered (to different degrees) during subsequent jacking strokes following shear reversal in the unloading-reloading processes.

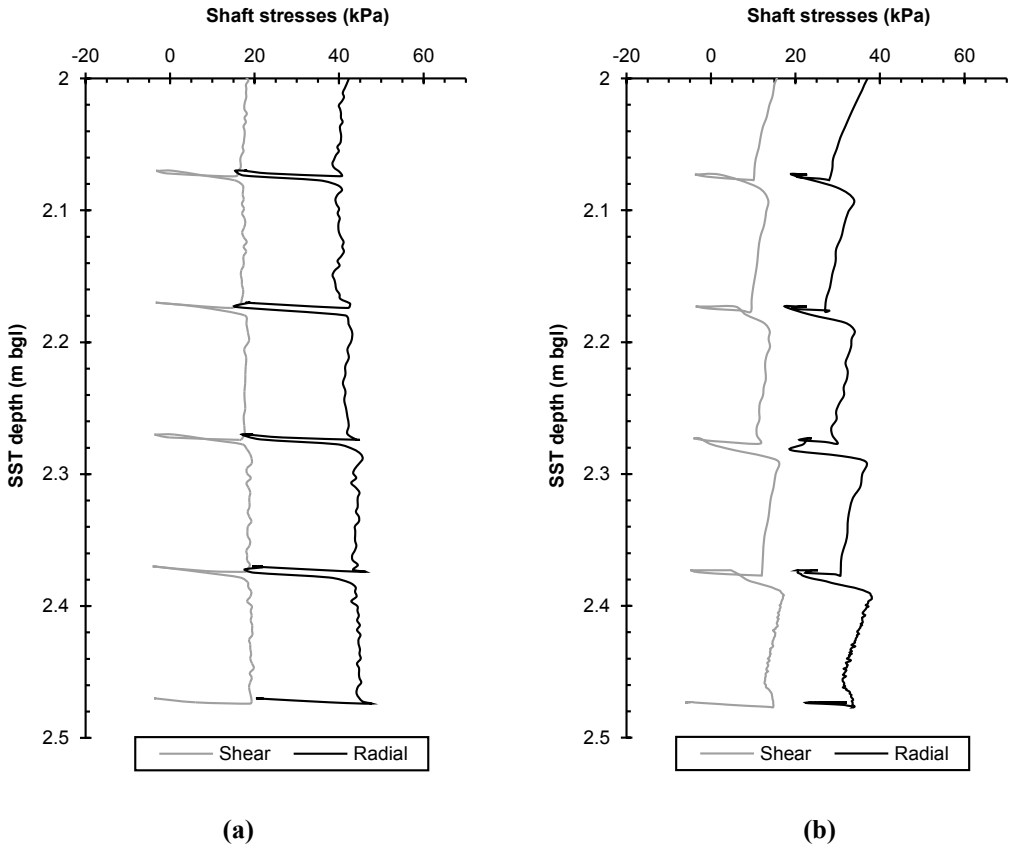

Figure 5.3. Profiles of radial total stress and shear stress during pile installation at Site A for (a) 65 mm diameter pile and (b) 135 mm diameter pile

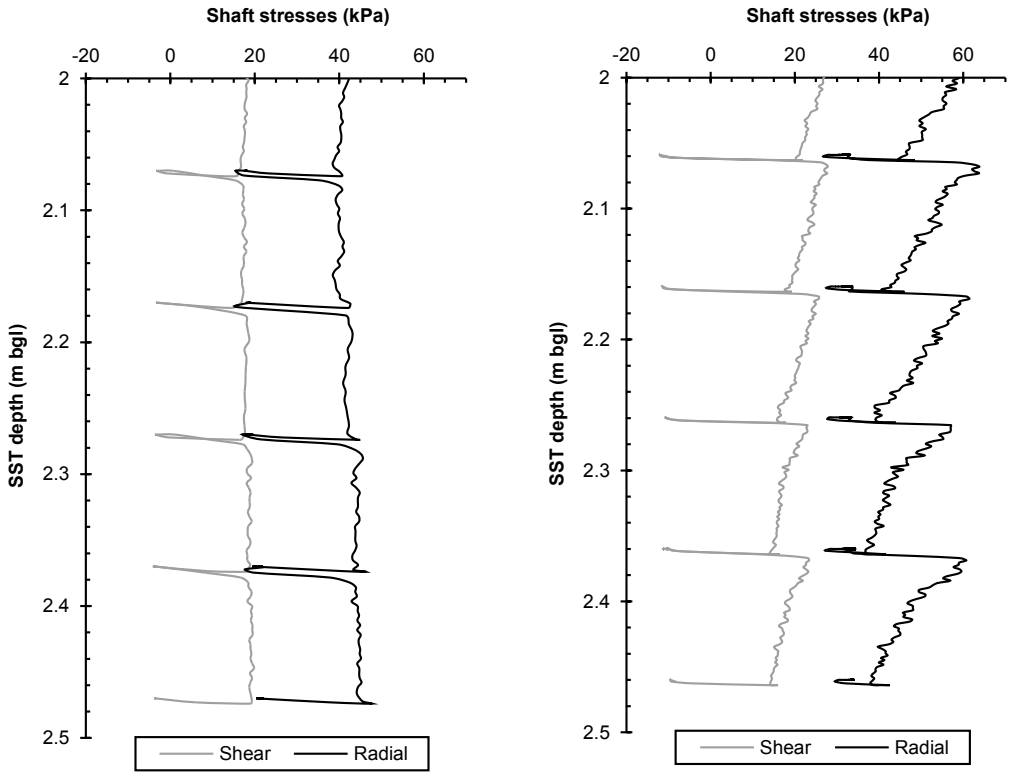

Figure 5.4. Profiles of radial total stress and shear stress during installation of 65 mm diameter model piles at (a) Site A and (b) Site B

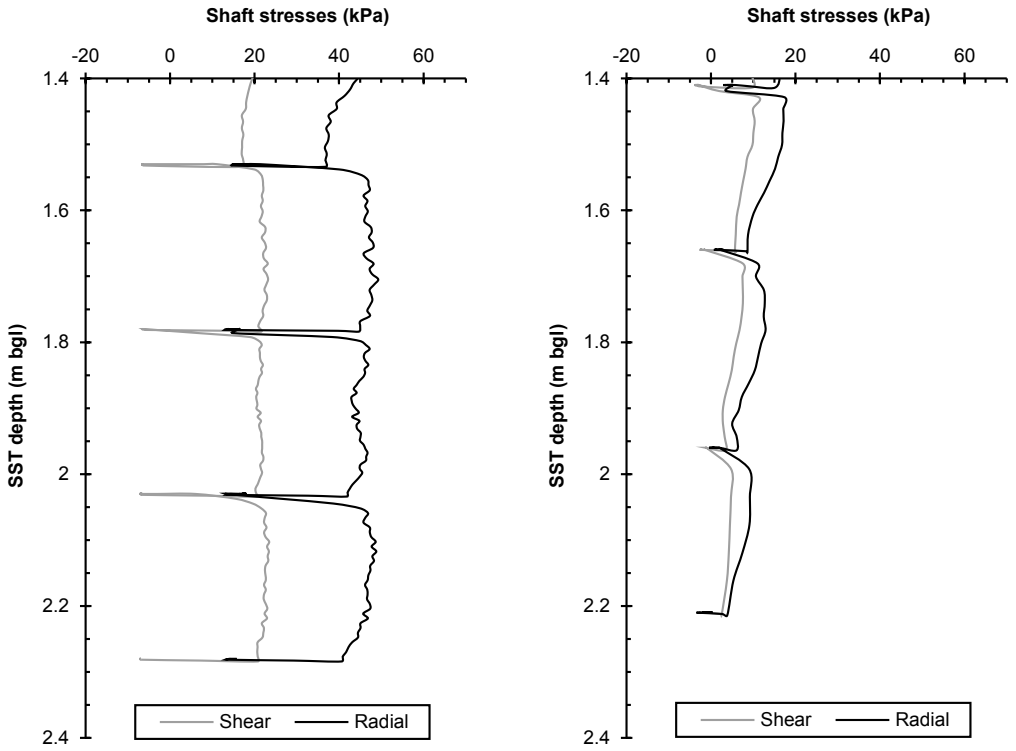

(a) **(b)**

Figure 5.5. Profiles of radial total stress and shear stress during installation of 100 mm diameter model piles at (a) Site A and (b) Site C

The variations of shear stress (τ) with radial total stress (σ_r) recorded for a typical loading stage at the three test sites are presented in Figure 5.6. The effective stress path at Site B was derived based on a hydrostatic pressure of about 10 kPa and an assumed negative excess pore pressures of 20 kPa generated at peak shear stress (at interface friction angle of 25^o as at Site A). At all sites, after a small reduction in σ_r, continued shearing results in an increment of radial stress accompanying an increment of shear stress. This behaviour reflects the effects of constrained dilation during interface shearing, such as those observed during load testings in previous ICP experiments (e.g. Lehane *et al.*, 1993) and that seen on Figure 5.1 in CNS interface shear tests. However, while the shaft stresses at Site A (except the 135 mm diameter pile) remained at critical state conditions during continued large displacement shearing (i.e. constant τ and σ'_r when the maximum shear stress is attained), both τ and σ'_r reduced considerably at Sites B and C after the peak values were reached. It is noteworthy that the interface friction angle ($\delta_f = \tan^{-1} [\tau / \sigma'_r]$) at both Sites A and B was approximately 25^o, whereas a higher δ_f of 30^o was recorded at Site C (the calcareous sand site), which is in agreement with that expected from laboratory interface shear tests.

5.3.4 Normalised Shear Stress

The measured local shear stresses normalised by their corresponding peak shear stresses (τ_{peak}) for a range of different (and typical) jacking stages are presented in Figure 5.7. It is evident that the shear stress for the 65 mm diameter pile at Site A increased to a certain plateau, which was then maintained as shearing continued. In contrast, at the same site, the shear stress for the 135 mm diameter pile reached its peak and decreased significantly with penetration. At Site B, apparent shear stress brittleness was observed during jacking into a water-bearing sand stratum. A similar trend to that seen at Site B was recorded when installing a 100 mm diameter model pile into a calcareous sand layer above water table at Site C. It should be noted that the shear displacements in Figure 5.7 (also in Figure 5.3 to Figure 5.5) are crude estimations in the absence of displacement measurements during penetration, which do not represent the initial curve stiffness accurately.

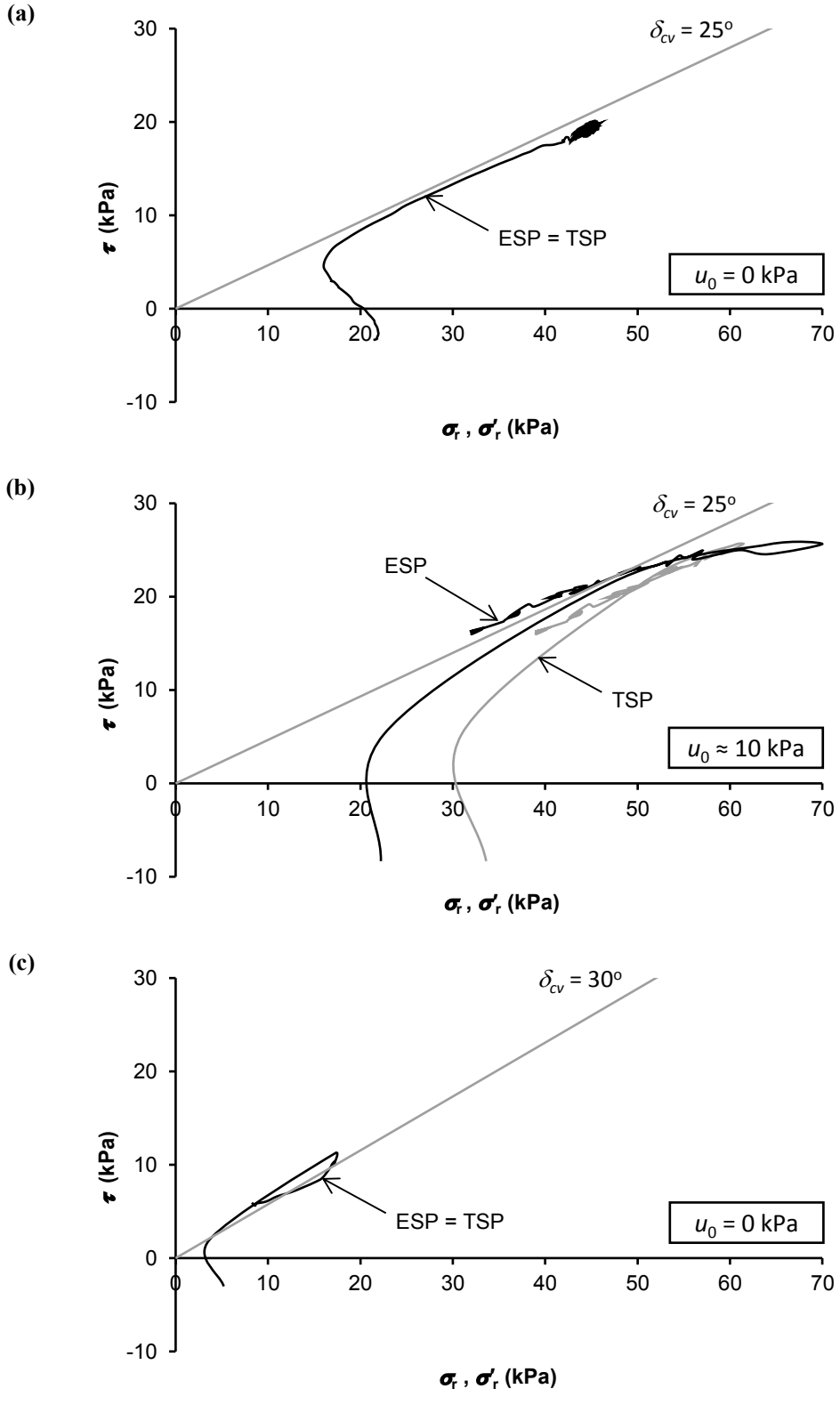

Figure 5.6. Stress paths for a typical shearing stage during pile installation at (a) Site A, (b) Site B and (c) Site C

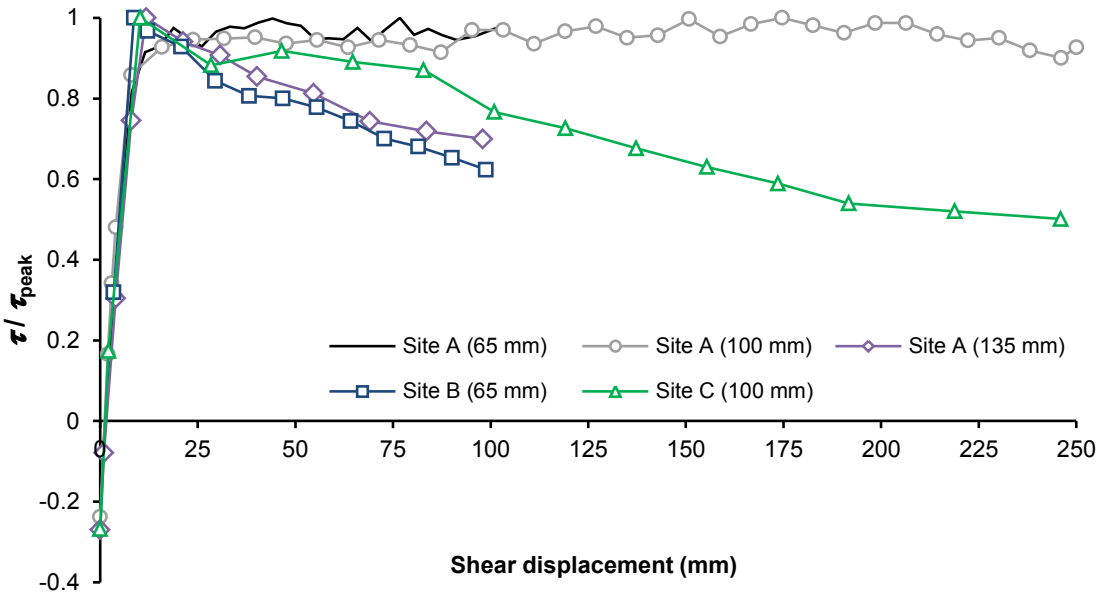

Figure 5.7. Typical profiles of normalised shear stress versus shear displacement during installation jacking

5.5 DISCUSSION

Besides the limitations of the laboratory interface tests apparatus mentioned earlier, interface shearing is usually considered drained or undrained and there has not been much research into the response of partially saturated sands or sands that are sheared under partially drained conditions during pile installation. In addition, there has been little reliable direct measurement of radial and shear stresses acting on the pile shaft reported in the past due to various constraints. Therefore, interpretation of this pioneering investigation on the shaft stresses during pile installation has to be made in light of various indirect evidence. The foregoing observations suggest that there may be more than one mechanism giving rise to the observed reduction in shear stress at large displacements, of which the most plausible explanation in each case is discussed below.

5.5.1 Pile End Effects

In *Case I*, the fact that the SST was located at about 5*D* above pile tip for the 135 mm diameter pile, in contrast to 10*D* for the 65 mm diameter pile, suggests an influence of soil flow relative to the pile tip during penetration. Campanella and Robertson (1981) varied the position of friction sleeve of a standard cone penetrometer and identified a highly sheared zone at a short distance to about 10 cone diameters behind the tip (Figure 5.8). A similar trend was observed by DeJong (2001) and Hebeler (2005) but with a smaller unstable zone and frictional difference. These observations cannot be deemed as a primary reference since a penetrometer is relatively smaller in diameter, with a cone shape at the tip, have a smooth interface and jacked monotonically throughout penetration.

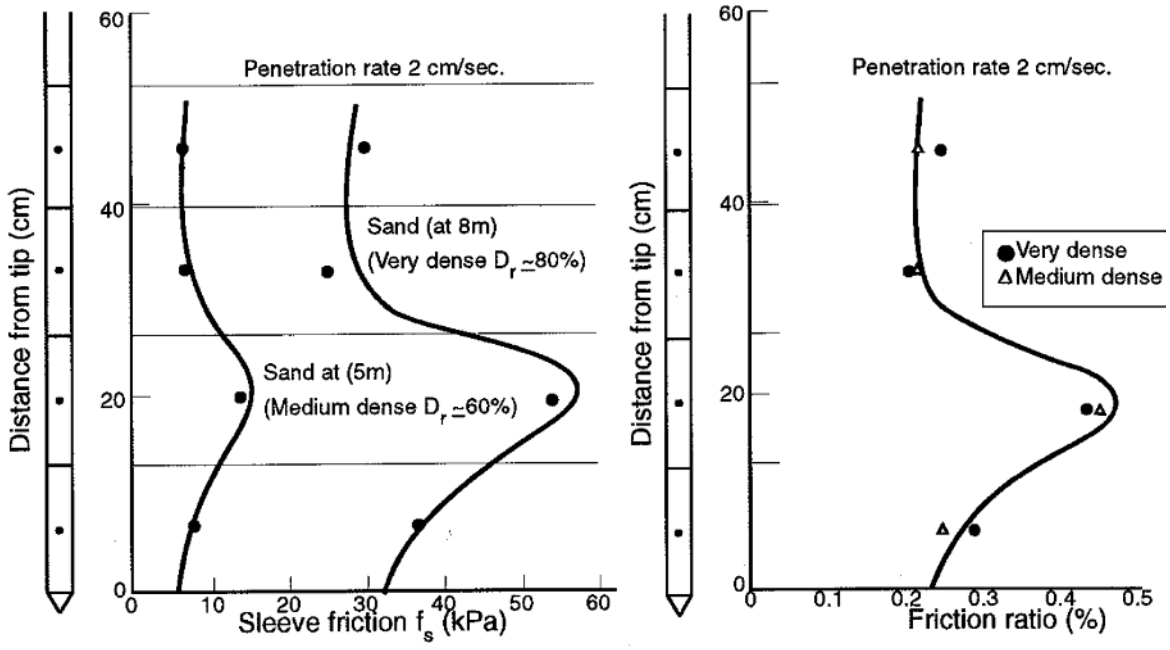

Figure 5.8. Sleeve friction and friction ratio along shaft during cone penetration in sand (Campanella and Robertson, 1981)

White (2002) investigated the penetration mechanism of a plain-strain model pile in sand using a novel image-based deformation measurement technique. Although the study of steady-state deformation during installation was mainly focussed below the pile tip, an experiment with additional PIV meshes above the tip clearly illustrated the displacement trajectories of soil flow over a certain influence zone that reflect a deep bearing capacity failure mechanism (Figure 5.9). It should be noted that the experiment differed from the field tests discussed here as it employed a plain-strain model and the smooth-surfaced model pile was monotonically jacked at a much lower rate of 1 mm/min.

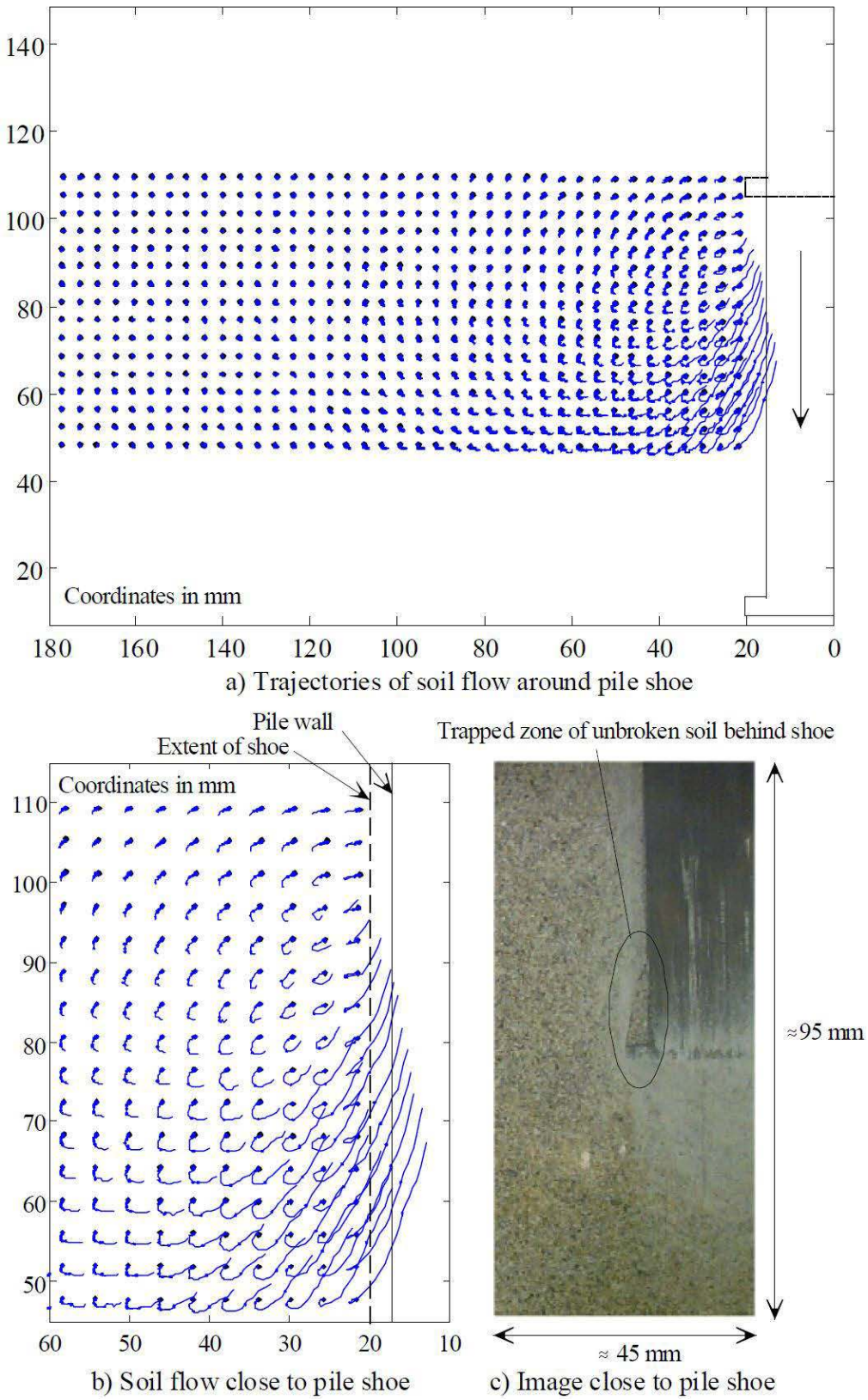

Figure 5.9. Trajectories of soil flow around pile shoe (White, 2002)

The influence of pile end during penetration is expected to extend beyond certain distance above pile tip, generally idealised as a failure surface shown in Figure 5.10 (e.g. Tomlinson and Woodward, 2007). In CPT-based pile design methods, various recommendations have been proposed to take into account this influence by averaging a wide range of q_c values up to eight pile diameters (Schmertmann, 1978; Fleming and Thorburn, 1983; Eslami and Fellenius, 1997; Xu and Lehane, 2008) above the pile tip (besides an influence zone below) in order to match the pile load test results, which imply its relevance.

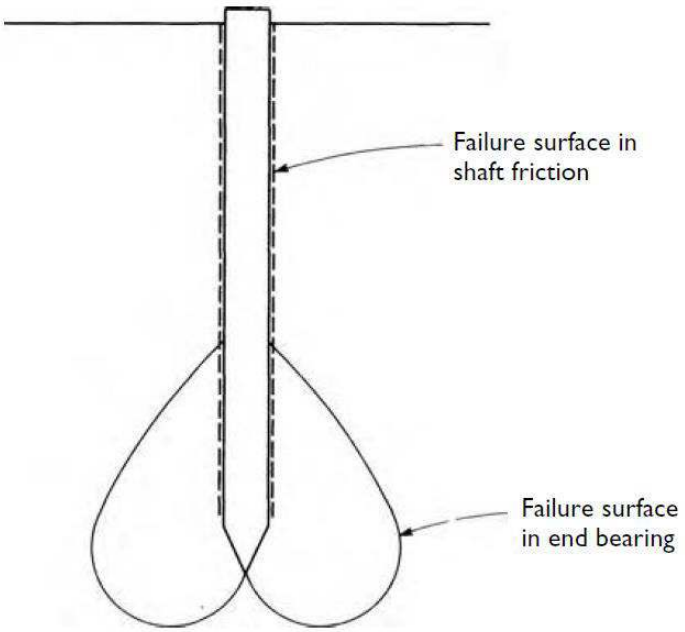

Figure 5.10. Failure surfaces for compression loading on piles (Tomlinson and Woodward, 2007)

Besides the relative position of SST for the 135 mm diameter pile that was closer to the pile tip, the pile end effects could have been aggravated by the slightly higher rate of penetration (about 50% faster) for the larger pile. The position and penetration rate, together with a potentially greater degree of disturbance for a larger diameter pile, have further implications for the assessments of diameter dependence of ageing effects for shaft friction. In line with other findings on pile set-up effects in this study, it is reasonable to assume that the stress equilibration process at the shaft commences at the pile shoulder, from the point at which the principal stress rotations are virtually completed. Details of the short-term pile ageing effects can be referred to Chapter 3.

5.5.2 Dissipation of Negative Pore Pressure

The same explanation discussed in preceding section is certainly not applicable to *Case II* given that the SST on the 65 mm diameter model piles was at the same location relative to the tip at both Sites A and B. At Site B, the higher penetration rate (4 times faster than at Site A) and its fully saturated conditions suggest that negative pore pressure could have been generated during the start of the jacking phase and that these then dissipated as shearing continued, resulting in lower effective stresses (Figure 5.6(b)). The tendency for shear stresses to stabilise towards the end of each jacking stage coupled with the recovery in shear stresses that can be developed during each subsequent jacking stage (as seen on Figure 5.4(b)) is consistent with the development of transient excess pore pressures.

White (2002), and others (mostly using laboratory interface tests), demonstrated that the fines produced by particle damage during shearing are mostly accumulated within the shear zone adjacent to shearing interface (Figure 5.11). This in turn would lower the permeability of the soil in the shear zone, thus allowing some excess pore pressure generation during shearing. Silva and Bolton (2005) performed centrifuge piezocone tests (PCPTs) in saturated silica flour sample and indicated an increasing negative excess pore pressure with penetration rate.

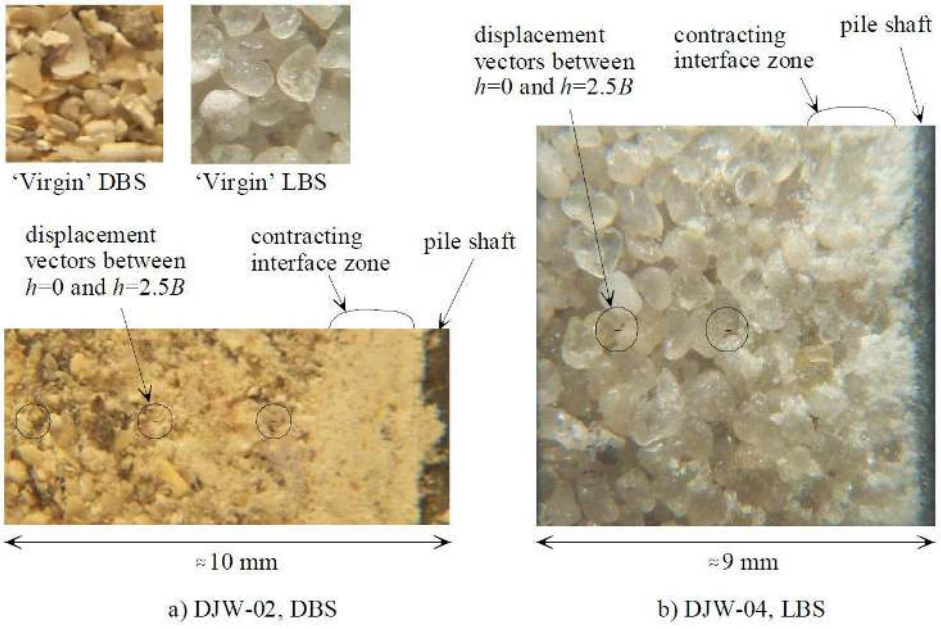

Figure 5.11. Particle damage at interface shearing zone for (a) Dog's Bay sand and (b) Leighton Buzzard sand (White, 2002)

The dilative response of the medium dense sand in this case can be appreciated by considering the low mean effective stress, which results in a negative value of state parameter, as emphasised by Wood (2007). Using the framework of state parameter, DeJong *et al.* (2012) illustrated various stress paths and volumetric responses when probing a cone penetrometer in an intermediate soils at various penetration rates thus causing differing drainage conditions. As indicated in Figure 5.12(b), an instantaneous undrained condition (U) created as penetration commences, which subsequently turns to partially drained (PD) and drained (D) conditions as shearing continued (due to dissipation of negative pore pressure and thus lower effective stresses) is relevant to the shaft response recorded in this study.

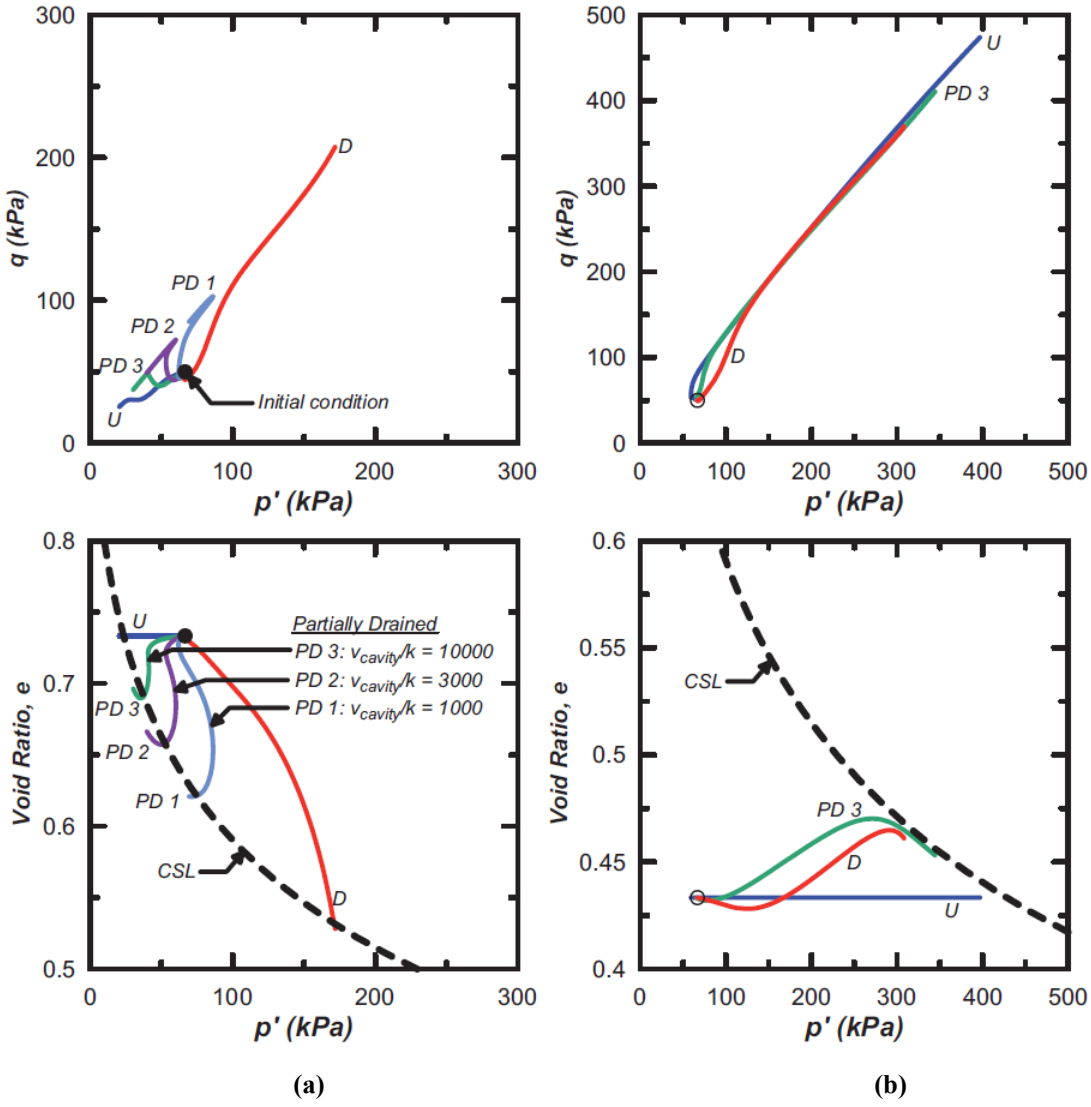

Figure 5.12. Stress paths and volumetric responses at the cavity wall for various drainage conditions in sand with state parameter of (a) 0.10 and (b) -0.20 (DeJong *et al.*, 2012)

5.5.3 Breakage of Weak Particles

In *Case III* that involves sand sites of different mineralogy, it is instructive to elaborate on other experimental evidence from previous research (e.g. Boulon and Foray, 1986; Coop and Lee, 1993; Tabucanon, 1997; Kelly, 2001; Luzzani and Coop, 2002; Sadrekarimi and Olson, 2010; Yang *et al.*, 2010):

- Particle rearrangement (e.g. sliding and rolling) and damage (e.g. crushing and abrasion) of sands during shearing influence its volumetric response when sheared.

- The damage caused by compression and shearing is much more severe than that under compression only (at an equivalent stress level), and is significantly aggravated by cyclic shearing.

- Particle damage due to shearing continues to very large strains and is influenced by interface roughness that tends to decline with shearing.

- Calcareous sand is weak, angular in shape and is much more susceptible to damage during shearing than siliceous sand.

The fundamental behaviour of (interface) shearing in sand as listed above points to the underlying mechanism that contributes to the post-peak reduction in shear stress at Site C, arose due to contraction following particle breakage as shearing continued. This permanent change of fabric is consistent with the progressive reduction in installation shear stresses shown in Figure 5.5(b) and Figure 5.6(c). A range of monotonic and cyclic CNL and CNS direct shear interface tests on Ledge Point sand showed a dilative response at a low initial stress level of 25 kPa and a post-dilative contraction arising from grain crushing (Lehane *et al.*, 2012). Further evidence of this effect is seen on Figure 5.13 (Kelly, 2001), which shows considerable brittleness of shear stresses in large-scale CNS ring shear tests on Barry's Beach calcareous sand but no brittleness on the Sydney silica sand when shearing against a rough interface.

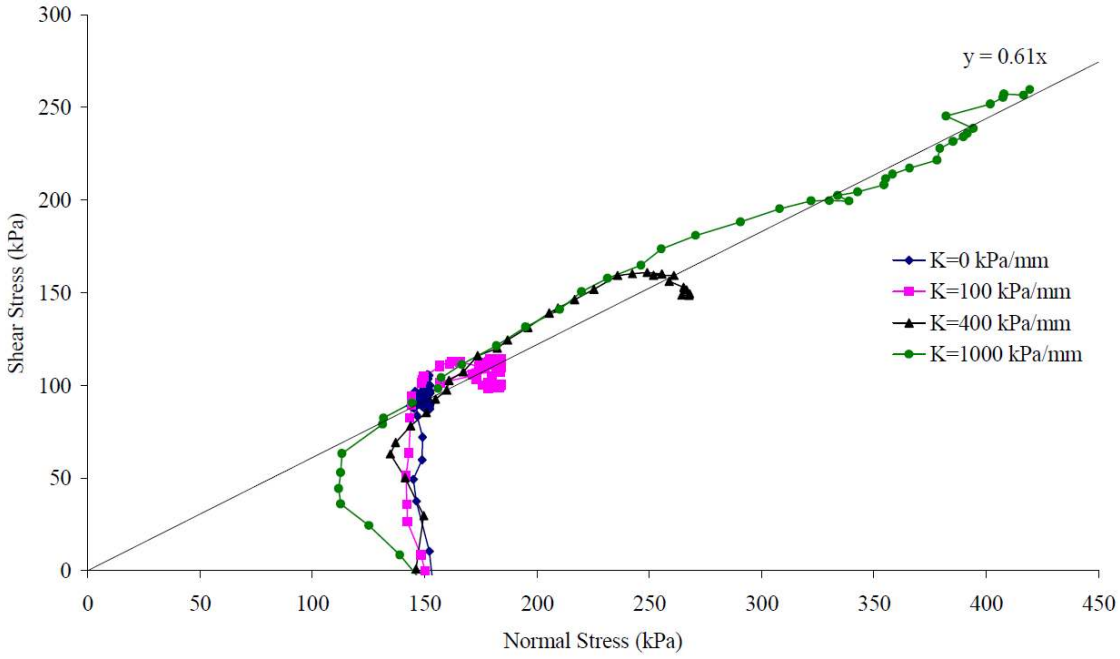

(a)

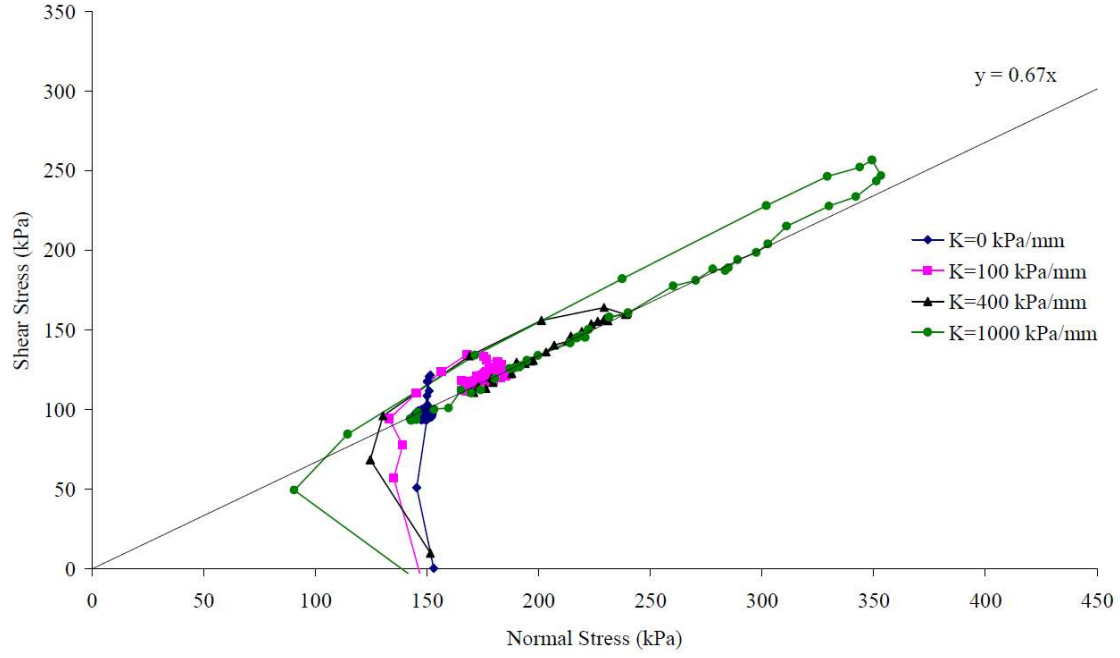

(b)

Figure 5.13. Effective stress paths from CNS ring shear tests shearing (a) Sydney silica sand and (b) Barry's Beach calcareous sand against rough interface (Kelly, 2001)

Except for particle breakage (in *Case III*) which was successfully simulated in laboratory interface tests, pile end effects and dissipation of negative pore pressure (as for *Case I* and *Case II*, respectively) can hardly be modelled using existing interface test devices summarised in Section 5.2. Although the interface friction angles for the cases with and without brittleness do not differ much, the complete shearing behaviour, especially under complex conditions (e.g. partially drained, partially saturated, cemented), requires further research. It is noteworthy that pile shaft friction is not only about the interface friction angle but also the associated changes in radial stresses that contribute to the shaft shear stresses (as implied by the Coulomb failure criterion). Failure to capture the reduction of shaft stresses during shearing can lead to higher than anticipated shaft capacity.

CHAPTER 6. STRENGTH AND STIFFNESS RECOVERY FOLLOWING INSTALLATION DISTURBANCE

6.1 INTRODUCTION

Increase in the shaft capacity of driven piles following installation is commonly known as 'set-up'. The observations, despite highly scattered, generally indicate an increasing trend for capacity gain with time. None of the pile design methods has considered this time effect explicitly and the existing set-up characterisation approach (Skov and Denver, 1988) offers little valuable information for further interpretation and comparison.

This chapter brings together the results from two different investigation programmes on time effects for displacement piles; both were performed at the same sand site but each used a different pile installation method. The investigation reveals a significant influence of installation disturbance on a pile's subsequent set-up behaviour. A new characterisation approach is proposed which considers the phenomenon of pile set-up as a recovery process following the disturbance induced by pile installation. The approach explains the contrasting set-up behaviour of the two pile test programmes considered here and is also validated further by reliable full-scale field test data.

6.2 INVESTIGATION AT UWA TEST BED SITE

Two major pile test programmes that aimed to investigate the effects of time on the capacity of displacement piles in sand were performed at the UWA test bed site in Shenton Park in West Perth. The first programme involved twelve un-instrumented open and closed-ended driven steel pipe piles. Piles were first installed in May 2005 and testing of these piles was continued over the subsequent year, as part of research by a previous PhD candidate at UWA (Schneider, 2007). The second programme, which is the primary experimental investigation of the present study (see Chapter 4 for details), employed closed-ended steel pipe piles with three different diameters were installed in a series of jacking stages and load tested in several phases between April 2008 and September 2011. The two test sites were 500 m apart, thus shared a very similar stratigraphy, mineralogy and stress history.

6.2.1 Programme 1: Driven Piles

Seven out of twelve tests on driven steel pipe piles described by Schneider (2007) are discussed here as they had comparable diameters (ranging from 88.9 mm to 114.3 mm) to the jacked piles installed as part of the current study. Five of the piles were open-ended (P03 and P12 being closed-ended) and were driven by dropping a 25 kg mass from a fall height of 0.5 m to final embedment lengths ranging from 2.5 m to 4 m. The plug height (in open-ended piles) and the number of blows were recorded at 100 mm intervals during installation. It is noted that the undersized hammer, and thus unusually large total number of blows (N_b) for the installation in medium dense sand, provides a rather extreme example of disturbance to the in-situ soil. Basic information and installation details of the model piles are summarised in Table 6.1.

Table 6.1. Installation details of driven piles

Pile	D_o (mm)	D_i (mm)	L (m)	End	IFR_{mean}	N_b	$q_{c\text{-}avg}$ (MPa)
P01	88.9	83.7	4	Open	0.65	1642	5.9
P03	88.9	78.9	4	Closed	0	4344	5.9
P04	88.9	78.9	4	Open	0.72	1840	5.9
P05	114.3	107.9	4	Open	0.80	1830	5.9
P06	88.9	82.5	4	Open	0.72	1486	5.9
P11	88.9	83.7	2.5	Open	0.54	305	2.7
P12	88.9	83.7	2.5	Closed	0	451	2.7

Note:

The IFR_{mean} was computed from the measured IFR profile averaged over the final 20 diameters of penetration.

The $q_{c\text{-}avg}$ for piles P01 to P06 (Series 1) and P07 to P12 (Series 2) refers to the average of CPT1 – 12 and CPT13 – 18, respectively, corresponds to their time of installation.

Table 6.2 presents the results of tension load tests performed on the driven piles at different ageing periods. Average pile shaft resistance (τ_{avg}) instead of total pile shaft capacity (Q_s) is presented here so that piles of different diameters and lengths may be compared. In general, results show a significant increase in pile shaft resistance with time in all cases. The closed-ended piles, which were subjected to larger number of installation blows, exhibit higher capacity gains with time relative to their initial capacity measured at about 4 days. The shaft capacity of one pile increases by more than a factor of 10 over the period of 1 year. This is a remarkable observation given that many engineers believe that set-up for driven piles in sand is not significant.

The major drawback of this dataset is that ageing was inferred from tension re-tests. Jardine *et al.* (2006) claim that the ageing observed in re-tests is not as high as in first-time tests because of a disruption to the ageing process in re-tests. Despite this trend, Tomlinson (1996) and Kolk *et al.* (2005b) have noted significant set-up of shaft friction from static re-tests. Therefore, while bearing in mind that a re-test is not an ideal case, the evidence of strong capacity gain from a straightforward experiment in this programme cannot be denied but demands careful consideration. It could be argued that the gain in capacity observed in these re-tests would have been even higher if all tests were first-time tension tests.

The data from the second re-test (T3) in test series 1 (P01 – P06) is excluded in the following analysis because large shearing displacement (>20 mm; except P03) in the preceding test (T2) seems to have disturbed the set-up behaviour as noticed from the unusual brittleness of its load-displacement curve (see Schneider (2007)). It is interesting to note that the capacity of T3 is generally slightly smaller than that of T2 given approximately the same time lapsed from previous testing event (in a similar sense to set-up period) but with disruption; see zigzag pattern on tension re-tests as suggested by Jardine *et al.* (2006). The relative influence on T4 is smaller since the time interval between T3 and T4 is longer.

Table 6.2. Load test results for driven piles

Pile [C/O]	Test	Age (day)	τ_{avg} [+] (kPa)	τ_{UWA} [#] (kPa)	τ_{ICP} [#] (kPa)
P01	T1	4	16	43.5	44.5
[O]	T2	70	44		
	T3*	140	43		
	T4*	376	53		
P03	T1	4	7	48.2	54.3
[C]	T2	69	31		
	T3	138	47		
	T4*	375	80		
P04	T1	3	23	43.6	45.7
[O]	T2	68	54		
	T3*	137	52		
	T4*	374	62		
P05	T1	3	20	37.1	38.0
[O]	T2	71	48		
	T3*	137	45		
	T4*	374	54		
P06	T1	3	26	43.0	44.9
[O]	T2	71	51		
	T3*	137	47		
	T4*	374	65		
P11	T1	5	17	34.6	33.5
[O]	T2	71	32		
	T3*	259	49		
P12	T1	5	7	37.4	40.6
[C]	T2	71	27		
	T3*	259	54		

Note:

'C' denotes closed-ended while 'O' denotes open-ended.

* The load-displacement curve shows brittle response (stiffer and with apparent peak) which is a typical sign of disruption from previous tension load test.

[+] The measured pile shaft resistance at failure was taken from its ultimate value mobilised at large displacement.

[#] The UWA and ICP capacities were computed with reference to the q_c profile from the average of CPT1 – 12.

The estimated pile shaft capacities from UWA-05 and ICP-05 methods are presented in Table 6.2; description of the UWA-05 and ICP-05 pile design methods is attached in Appendix C for reference. The two design methods give a very close prediction in all cases (with τ_{UWA} marginally smaller than τ_{ICP} consistently), which are higher than the initial capacity measured at about 4 days after installation. However, by the time the second test was performed after 2 months, significant set-up was recorded on all piles and most of the OEPs have reached a higher resistance than the medium-term capacities estimated from UWA-05 and ICP-05 methods. The CEP, although indicating a lower capacity than the OEP in second test (due to its lower initial capacity), continued to grow and exceed the OEP capacity when tested again after 1 year. The pile set-up behaviour will be discussed further in Section 6.3.

6.2.2 Programme 2: Jacked Piles

Full details of the second pile test programme have been reported in Chapter 4. This section extracts some basic information to enable comparisons be drawn with the driven pile programme described above. A total of fourteen closed-ended piles, comprising three different diameters of 65, 100 and 135 mm, were jacked into the sand bed at Shenton Park to an average embedment of about 3 m. A CPT truck provided the reaction to install the model piles in a series of 100 mm long jacking strokes (except 100_spa and 100_spb, which used 250 mm) at an average jacking speed of about 6 mm/s. The piles were fully unloaded after each jacking stroke and left for a brief pause period of between 1 and 5 minutes before jacking recommenced. The installation details of the jacked piles are summarised in Table 6.3.

Static tension load tests were performed at specific ageing periods of up to 72 days, as presented in Table 6.4. The interpretation presented here is based on the overall pile performance as assessed from the measured pile head load; localised pile shaft response measured by the SSTs are discussed in Chapter 4. It is important to note that this programme only comprised first-time static load tests and therefore is free from various uncertainties associated with characterising set-up behaviour from pile re-tests.

Table 6.3. Installation details of jacked piles

Pile	*D* (mm)	*L* (m)	*L/D*	N_{cyc}	$q_{c\text{-}avg}$ (MPa)	Ref CPT
100_spa*	101.5	3.72	37	15	5.0	SCPT-8 & CPT-9
100_spb*	101.5	3.75	37	15	5.0	SCPT-8 & CPT-9
100_spd	101.5	3.10	31	31	4.9	CPT-3 & SCPT-16
65_spa	65.0	3.14	48	31	3.5	CPT-10 & 11
65_spb	65.0	3.20	49	32	3.5	CPT-10 & 11
65_spc	65.0	3.20	49	32	3.5	CPT-10 & 11
65_spd	65.0	3.10	48	31	4.9	CPT-3 & SCPT-16
135_spa	134.6	3.16	23	32	3.6	CPT-11, 13 & 14
135_spb	134.6	3.16	23	32	3.6	CPT-11, 13 & 14
135_spd	134.6	3.10	23	31	4.9	CPT-3 & SCPT-16
65_spe^{+}	65.0	3.49	54	35	5.3	CPT-15 & 17 to 20
65_spf^{+}	65.0	3.57	55	36	5.3	CPT-15 & 17 to 20
135_spe^{+}	134.6	2.73	20	27	5.1	CPT-15 & 17 to 20
135_spf^{+}	134.6	2.77	21	28	5.2	CPT-15 & 17 to 20

Note:

* The piles were installed using a longer jacking stroke of 250 mm in contrast to 100 mm for others.

$^{+}$ A hole was pre-bored to a depth of about 2 m from ground surface before installation to isolate the stiff crust layer which showed greater variability.

In sharp contrast to the set-up observed in Programme 1, the magnitude of set-up observed in Programme 2 was barely noticeable. The minor change with time of approximately 5% seen in most cases was insignificant and could be simply attributed to the inherent spatial variability among test locations or some seasonal variations between testing periods. The review of the time-dependence of shaft friction of jacked piles (e.g. Yang *et al.*, 2006a; Zhang *et al.*, 2006) discussed in Chapter 2, though not directly relevant in this case, suggests that the much smaller capacity change with time observed in this experiment could have been pre-empted.

Table 6.4. Load test results for jacked piles

Pile	Series	Age (day)	τ_{avg} (kPa)	τ_{UWA} (kPa)	τ_{ICP} (kPa)
100_spa	100-I	1	45.5	45.1	42.7
100_spb		29	47.9	45.1	42.8
100_spd^		72	47.9	43.8	40.1
65_spa	65-I	1	46.0	46.2	49.5
65_spb		27	43.3	46.5	49.9
65_spc*		29	49.8	46.5	49.9
65_spd		70	55.7	52.5	53.8
135_spa	135-I	1	37.1	33.5	30.1
135_spb		29	38.9	33.5	30.1
135_spd		71	43.1	40.8	34.4
65_spe^{+}	65-II	1	51.7	70.5	78.1
65_spf^{+}		38	53.3	70.5	78.1
135_spe^{+}	135-II	1	43.1	50.0	46.6
135_spf^{+}		41	42.6	50.6	47.3

Note:

^ The pile test was conducted at different period of time with others in the same series, besides different in the length of jacking stroke during installation.

* The pile was installed following previous 1-month test without sandblasting, which has a rougher surface due to sand-welding.

$^{+}$ A hole was pre-bored to a depth of about 2 m from ground surface before installation to isolate the stiff crust layer which showed greater variability.

The UWA and ICP predictions for the jacked piles are provided in Table 6.4. It is evident that the UWA-05 method generally estimates a higher unit shaft capacity for the larger piles (100 and 135 mm diameters) compared to the ICP-05 method but gives a lower estimate for the smaller 65 mm diameter piles. Both methods overestimate the average unit shaft friction for small diameter piles to a larger degree (a small-scale effect implicit in the formulation will be examined in Chapter 7) and for piles with the pre-bore in series 65-II and 135-II. Overall, the UWA prediction compares better with the measured capacities at 1 day after installation than the ICP does in this case.

6.2.3 Inferences from a comparison of Programme 1 and 2

Bringing the test programmes 1 and 2 together assists with the inference of factors affecting set-up given their contrasting set-up characteristics in the same soil conditions. The suspected influence of suction and cementation on the set-up measured in the first programme cannot be dominant since the adjacent second programme recorded negligible change in the pile shaft capacity. Even for the first programme itself, test series 1 (P01 – P06) that was installed at the end of dry season does not differ much from the load test results of series 2 (P07 – P12) that was carried out within the wet season.

It is possible (although improbable) that suction pressures could have been sustained within the structured sand mass during pile (and CPT) jacking while these pressures would have been destroyed by severe dynamic impacts imposed during the pile driving process. However, the effects of possible light cementation or high suctions, as evident from the surface cracking around the piles during the 1-year tension re-tests, are expected to be minor. This is because a marked set-up was observed after a period of just 2 months (and within the same season) and this period is certainly not long enough to allow any significant suctions or cementation to develop.

Bowman and Soga (2005) claim that set-up effects are less significant at lower stress levels, for smaller diameter piles and in the absence of small cyclic perturbations such as imposed tidal fluctuations. The set-up observed for the driven piles and the lack of set-up shown by the jacked piles suggest that these effects do not have a controlling influence on whether set-up occurs or not. It is clear, however, that the pile installation technique (or more specifically the degree of disturbance induced by pile installation) is significant.

A comparison of the load test results from both testing programmes unveils an important message. The driven piles that were subjected to overly large number of hammer blows show a much smaller pile shaft resistance than the identical piles installed by jacking in the short and medium term. Nevertheless, this driven pile capacity increases substantially with time reaching a value larger than that of the jacked piles a few months later. The very strong set-up behaviour exhibited by the driven piles, which is commonly perceived as a capacity gain, should perhaps be interpreted as

a recovery process (as the major component) following its severe disturbance during installation. It is noteworthy that the programme of driven piling discussed here is a rather extreme example of disturbance (e.g. with over 1000 blows per metre installed) compared to the level of disturbance that might be imposed during a typical commercial piling contract in similar ground conditions. Based on these observations, the following sections examine an alternative framework to assist assessment of the potential set-up of shaft capacity.

6.3 CHARACTERISATION OF PILE SET-UP

Existing empirical relationships proposed to characterise the pile set-up were reviewed in Chapter 2. Being particular about the mathematical function to model the experimental observations has limited value at present given the lack of understanding of the underlying mechanisms as well as the dearth of quality data. The way in which the measured pile capacity is normalised to describe the time-dependent characteristic is however of importance and is worthy of discussion here. This discussion uses the results from the two pile test programmes at Shenton Park and a reliable dataset from a full-scale pile set-up study at Dunkirk, France.

6.3.1 Normalisation with Initial Capacity

Pile set-up is usually assessed by comparing the pile capacity measured at a time t after installation to that measured at a reference time, t_o. A minimum of 12 hours is commonly specified as the reference time to ensure complete dissipation of excess pore pressure generated in siltier sand deposits following pile driving. Ideally, a set of 'virgin' ultimate pile shaft resistances determined from static tension load tests at various ageing periods provide a 'true' measure of set-up. Other data sets, which comprise the majority of the existing database, remain as valuable qualitative indicators.

The most popular functional form describing set-up is the simple logarithmic time function proposed by Skov and Denver (1988), which will be employed here. The expression and corresponding set-up factor A are defined as:

$$\frac{Q_s}{Q_{so}} = 1 + A \log\left(\frac{t}{t_o}\right) \tag{6-1}$$

$$A = \frac{(Q_s/Q_{so}) - 1}{\log(t/t_o)} = \frac{(\tau_{avg}/\tau_o) - 1}{\log(t/t_o)} \quad (6\text{-}2)$$

where A is the gradient of the ratio of pile shaft capacity (Q_s) normalised with its initial capacity (Q_{so}) over a logarithmic time scale. Alternatively, the ratio in terms of average pile shaft resistance (τ_{avg}) is preferred if piles of different diameters and lengths are involved.

As presented in Table 6.5, all the driven piles at Shenton Park indicate a substantial increase in pile shaft capacity, with increases in capacity of up to 10 for closed ended piles (CEPs) and 3 for open-ended piles (OEPs) over an ageing period of about one year. The results correspond to average Skov and Denver's A values of 3.61 for CEPs and 0.93 for OEPs, taking the first tension tests (T1) performed around 4 days after installation as the reference initial readings (τ_o and t_o). On the other hand, as presented in Table 6.6, the jacked piles that exhibited negligible change in pile shaft capacity over time (with even some slight reduction in certain cases) indicate an average A value of merely 0.016.

The τ_o-normalised ratios are plotted against time to a logarithmic scale in Figure 6.1. While the plot indicates a clear dependence of set-up behaviour on the pile installation method and end condition, it is not possible to further extrapolate or generalise these observations. It is worth noting that Skov and Denver (1988) suggest an A factor of 0.2 with reference to an initial capacity measured at t_o of 0.5 days for pile set-up in sand; this value was determined for a case history in Hamburg, Germany involving driven 350 mm square prefabricated concrete piles with embedded lengths of about 21 m. From a larger database, albeit with a large scatter, Chow *et al.* (1998) and Axelsson (2000) derived average A values of 0.5 and 0.4 respectively.

Table 6.5. Characterisation of set-up for driven piles at Shenton Park

Pile	Test	Age (day)	τ_{avg}/τ_o*	A^+	τ_{avg}/τ_{UWA}	B	$\tau_{lim}{}^{\#}$ (kPa)	τ_{avg}/τ_{lim}
P01	T1	4	1.00	-	0.37	-	65.6	0.24
[O]	T2	70	2.75	1.41	1.01	0.52		0.67
	T4	376	3.31	1.17	1.22	0.43		0.81
P03	T1	4	1.00	-	0.15	-	76.7	0.09
[C]	T2	69	4.43	2.77	0.64	0.40		0.40
	T4	375	11.43	5.29	1.66	0.77		1.04
P04	T1	3	1.00	-	0.53	-	65.8	0.35
[O]	T2	68	2.35	0.99	1.24	0.52		0.82
	T4	374	2.70	0.81	1.42	0.43		0.94
P05	T1	3	1.00	-	0.54	-	56.0	0.36
[O]	T2	71	2.40	0.94	1.29	0.53		0.86
	T4	374	2.70	0.75	1.46	0.42		0.96
P06	T1	3	1.00	-	0.60	-	64.4	0.40
[O]	T2	71	1.96	0.70	1.19	0.42		0.79
	T4	374	2.50	0.72	1.51	0.43		1.01
P11	T1	5	1.00	-	0.49	-	50.0	0.34
[O]	T2	71	1.88	0.77	0.92	0.38		0.64
	T3	259	2.88	1.10	1.42	0.54		0.98
P12	T1	5	1.00	-	0.19	-	56.2	0.12
[C]	T2	71	3.86	2.48	0.72	0.46		0.48
	T3	259	7.71	3.92	1.44	0.73		0.96

Note:

'C' denotes closed-ended while 'O' denotes open-ended.

* The τ_o refer to the first tension load tests that were conducted 3 – 5 days after installation.

$^+$ The computed *A*-value is similar to that defined by Skov and Denver (1988) but referring to the initial readings taken at 3 – 5 days after installation.

$^{\#}$ The τ_{lim} is derived from UWA-05 method by assuming c = -0.1 to represent the upper limit of the pile shaft friction with minimum friction degradation.

Table 6.6. Characterisation of set-up for jacked piles at Shenton Park

Pile	Series	Age (day)	τ_{avg}/τ_o	A	τ_{avg}/τ_{UWA}	B	τ_{lim} [#] (kPa)	τ_{avg}/τ_{lim}
100_spa	100-I	1	1.00	-	1.01	-	62.8	0.72
100_spb		29	1.05	0.04	1.06	0.04	62.9	0.76
100_spd^		72	1.05	0.03	1.09	0.05	60.7	0.79
65_spa	65-I	1	1.00	-	1.00	-	58.9	0.78
65_spb		27	0.94	-0.04	0.93	-0.05	59.3	0.73
65_spc*		29	1.08	0.06	1.07	0.05	59.3	0.84
65_spd		70	1.21	0.11	1.06	0.04	70.5	0.79
135_spa	135-I	1	1.00	-	1.11	-	45.1	0.82
135_spb		29	1.05	0.03	1.16	0.04	45.1	0.86
135_spd		71	1.16	0.09	1.06	-0.03	56.7	0.76
65_spe[+]	65-II	1	1.00	-	0.73	-	89.4	0.58
65_spf[+]		38	1.03	0.02	0.76	0.01	89.5	0.60
135_spe[+]	135-II	1	1.00	-	0.86	-	64.0	0.67
135_spf[+]		41	0.99	-0.01	0.84	-0.01	64.9	0.66

Note:

^ The pile test was conducted at different period of time with others in the same series, besides different in the length of jacking stroke during installation.

* The pile was installed following previous 1-month test without sandblasting, which has a rougher surface due to sand-welding.

[+] A hole was pre-bored to a depth of about 2 m from ground surface before installation to isolate the stiff crust layer which showed greater variability.

[#] The τ_{lim} is derived from UWA-05 method by assuming c = -0.1 to represent the upper limit of the pile shaft friction with minimum friction degradation.

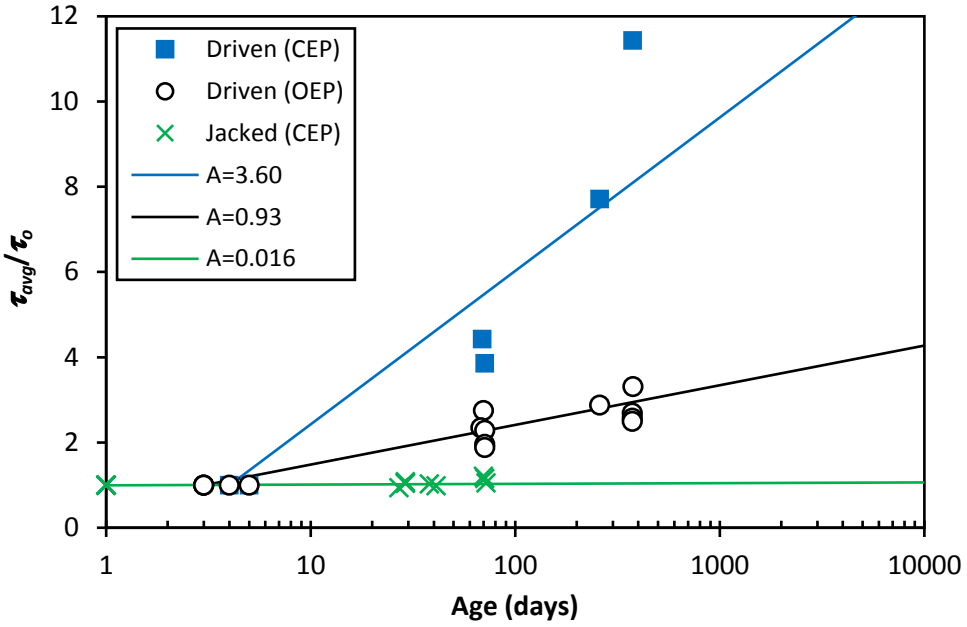

Figure 6.1. Changes of normalised average shaft resistance (against initial reading) with time

6.3.2 Normalisation with UWA-05 Capacity

A deficiency in the dataset described earlier is the inherent spatial variability in ground conditions in the vicinity of the test piles. In order to allow for the overall effects of local variations in ground conditions, Jardine *et al.* (2006) normalised the measured pile shaft friction with the estimated capacity based on ICP design method corresponding to the nearest CPT profile. In this study, a similar approach was followed but utilising the UWA design method in the normalisation exercise. The UWA method is preferred because it allows for different levels of friction fatigue for jacked and driven piles and the effect of plugging on the shaft resistance for open-ended piles is considered to be accounted for in a more direct manner. Nevertheless, both methods are expected to yield similar outcomes in this characterisation since their predictions do not differ much as discussed earlier.

The measured pile shaft resistances for the driven piles were normalised by their corresponding UWA predictions and presented in Table 6.5. Besides showing an increasing trend with time, the ratios illustrate that the medium-term capacity measured at about 4 days after driving is much lower than the value estimated from UWA-05

method; these ratios are as low as 0.17 and 0.51 for CEPs and OEPs respectively. The pile shaft capacity increases with time and approaches the UWA prediction after around 40 days for the OEP and 140 days for the CEP (estimated using the logarithmic and power-law functions that best match the available data statistically, with $r^2 > 0.9$). The capacity continues to increase and reaches a shaft resistance that is, on average, about 45% higher than the UWA medium-term prediction after about one year.

In contrast, the average of the ratios of the jacked piles (as presented in Table 6.6) at one day after installation is about 0.9, which is much higher than the corresponding ratio for the driven piles in both the short and medium term. The measured capacities do not change to any significant extent over the entire ageing period adopted of 72 days.

Figure 6.2 presents a semi-log plot against time for the normalised ratios discussed above. Besides showing on how the shaft friction of different types of piles varies with time, it is seen that the shaft capacity of the driven CEP does not attain a ratio that is much larger than that of the driven OEP and jacked CEP (in contrast to what may be inferred from Figure 6.1). The driven CEPs essentially recover from the very low initial capacity to attain a long-term capacity comparable to that of the driven OEPs and jacked CEPs. The normalisation by the UWA capacity on Figure 6.2 appears to have less scatter and to provide a more consistent pattern than the normalisation by the 3 – 5 days capacity seen on Figure 6.1.

Similar to the set-up factor *A* defined by Skov and Denver (1988), pile set-up could be characterised by the gradient of the semi-log plot shown in Figure 6.2. This gradient is referred to here as *B* and is defined as:

$$B = \frac{(Q_{s2}/Q_{UWA}) - (Q_{s1}/Q_{UWA})}{\log(t_2/t_1)} = \frac{\left(\tau_{avg2}/\tau_{UWA}\right) - \left(\tau_{avg1}/\tau_{UWA}\right)}{\log(t_2/t_1)} \qquad (6\text{-}3)$$

The *B* coefficients are provided in Table 6.5 and the average values for the driven piles vary from 0.59 for CEPs to 0.46 for OEPs. The coefficient of variation (CoV) of these values is approximately 0.02 in both cases, which is a considerable improvement on the corresponding CoV for the *A* coefficient of about 0.2. The values of *B* coefficient for jacked piles remain insignificant.

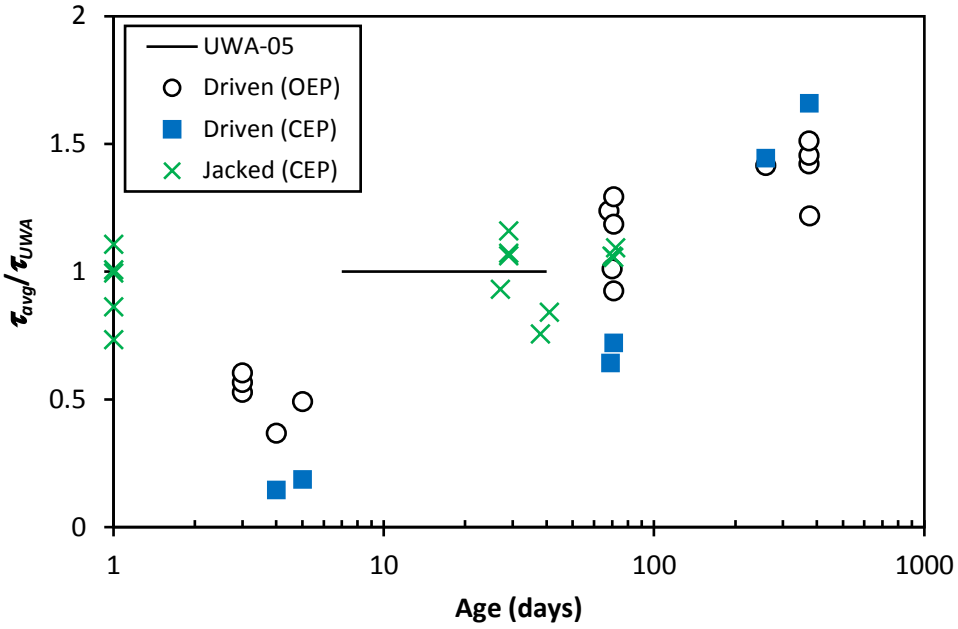

Figure 6.2. Changes of normalised average shaft resistance (against UWA capacity) with time

6.3.3 Set-up Factors *A* and *B*

The set-up factor *A* as discussed above has been widely used to quantify the pile set-up behaviour (e.g. Chow *et al.*, 1998; Axelsson, 2000). An average trend of $A = 0.5$, for instance, means a 50% increase per log cycle of time, or a doubling of the initial capacity at 1 day after an ageing period of 100 days. Great savings can be made if such a capacity gain can be justified and incorporated in pile design. The set-up data however are highly scattered for reasons referred to above and, as a consequence, effects of set-up are not implemented in routine design practice. This section further explores the relevance and robustness of set-up factors *A* and *B* for quantification of pile set-up.

Table 6.7 presents a simple example to illustrate shortcomings in the use of *A* as a means of quantifying pile set-up. The interpretation assumes that capacity varies with the logarithm of time and that capacities after ageing periods of 5, 50 and 500 days are identical for the two cases considered. The initial pile load test was conducted 12 hours after installation for Case I and Equation (6-2) gives a set-up *A* factor of 1.0; note that 12 hours is the minimum lapse time recommended by Tavenas and Audy (1972) and

Axelsson (2000) to ensure complete dissipation of excess pore pressure. Case II is identical to Case I except that its initial pile test was carried out 5 days after installation (which is not at all unusual for static load tests). Equation (6-2) now, however, indicates an A value of 0.5, despite pile capacities for both Cases I and II being identical.

Table 6.7. Example showing different characterisation of set-up factors *A* and *B*

Case	Pile	Age (day)	Q_s (kN)	Q_s/Q_{so}	A	Q_{UWA} (kN)	Q_s/Q_{UWA}	B
I	PT0*	0.5	200	1.00	-	500	0.40	-
	PT1	5	400	2.00	1.00	500	0.80	0.40
	PT2	50	600	3.00	1.00	500	1.20	0.40
	PT3	500	800	4.00	1.00	500	1.60	0.40
II	PT1*	5	400	1.00	-	500	0.80	-
	PT2	50	600	1.50	0.50	500	1.20	0.40
	PT3	500	800	2.00	0.50	500	1.60	0.40

Note:

* The initial pile test that is used to derive factor *A*.

In contrast, using the same approach, the set-up factor B, derived using Equation (6-3), is the same for Cases I and II. The results in Table 6.7 show that $B = 0.4$ regardless of when the initial pile test was conducted. It is evident that the value of A can be highly misleading as it depends critically on the reference test capacity (i.e. as measured at the reference time, t_o). Clearly values of A derived assuming the EOID dynamic capacity as the reference capacity will differ considerably from values deduced from static load tests.

6.3.4 Comparison with Full-scale Field Data

Despite the improved consistency seen by normalising the measured resistance with the capacity estimated from the UWA-05 method, a comparison of the results of a reliable full-scale pile set-up study, reported by Jardine *et al.* (2006), discloses the weakness of this approach. Figure 6.3 shows the data from the GOPAL project (Jardine *et al.*, 2006) together with those of driven CEPs and OEPs from Shenton Park, plotted on the same axes. The ratio of τ_{avg}/τ_{UWA} (equivalent to the Q_m/Q_{ICP}) for the 457 mm diameter open-

ended steel pipe pile tested 9 days after driving is close to unity and this ratio increases to approximately 2.3 after around eight months. This time relationship that conforms to intact ageing characteristic (IAC) as defined by Jardine *et al.* (2006) has changed their speculation on the performance of medium-term ICP prediction from around 50 days (Jardine and Chow, 1996) to 10 days.

Examination shows that the discrepancy between the Shenton Park and GOPAL project could be attributed to the assumed constant c parameter (c = -0.5 for driven piles) that was used to represent the different degrees of installation disturbance. As highlighted before, the unusually large number of blows incurred during installation of driven piles at Shenton Park is expected to cause excessive disturbance and low initial capacity. The GOPAL piles at Dunkirk were installed with about 125 blows/m in sand with $q_{c\text{-}avg}$ of about 20 MPa (R1 at Dunkirk); these piles may therefore be expected to have lower levels of friction fatigue to the OEPs at Shenton Park, which required an average of 458 blows/m in sand with $q_{c\text{-}avg} \approx 5.8$ MPa. If a higher c parameter is adopted for Shenton Park piles, which gives a lower medium-term τ_{UWA} prediction, the τ_{avg}/τ_{UWA} ratio will be higher and match the trend with time of the GOPAL data.

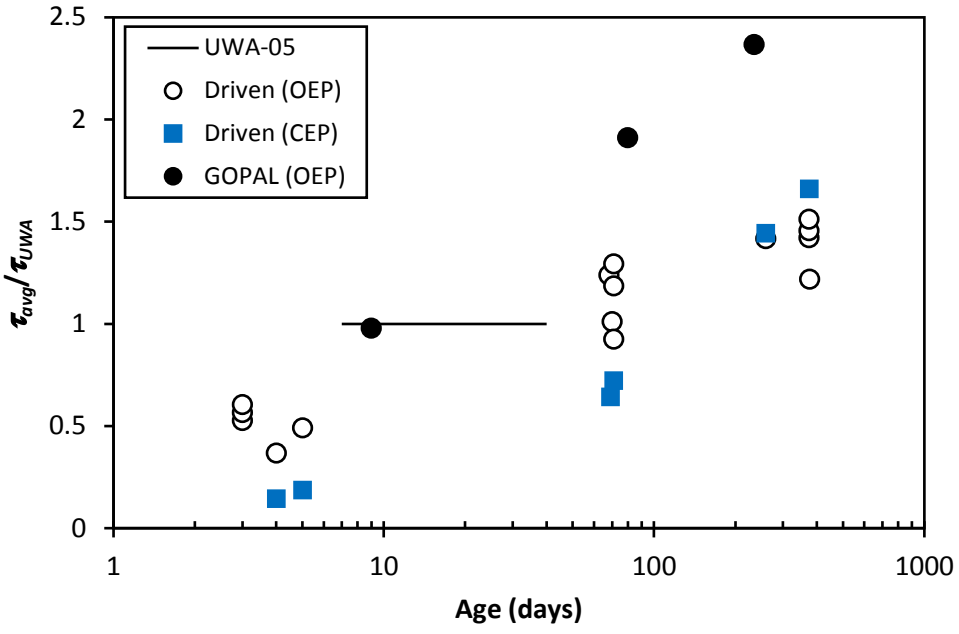

Figure 6.3. Comparison between interpreted set-up behaviour of driven piles at Shenton Park and Dunkirk (GOPAL project) after normalisation with UWA-05 capacity

6.3.5 Normalisation with UWA Limit Capacity

Based on the foregoing, it is proposed to normalise the measured pile shaft capacity by a projected upper limit of the shaft resistance estimated from UWA-05 method (τ_{lim}) corresponding to a minimum anticipated level of friction fatigue for a displacement pile (i.e. a pile jacked monotonically to its final embedment in a single push). This limit capacity can be derived using a friction fatigue parameter (c) of zero. However, it is noted that a small level of friction degradation has been exhibited by monotonically jacked piles in the plain-strain model pile experiments conducted in a surcharged calibration chamber (White and Bolton, 2004) and the small-scale model pile tests performed using centrifuge facility (White and Lehane, 2004), and therefore a c value of -0.1 is selected here to calculate τ_{lim}. The estimated τ_{lim} for driven and jacked piles at Shenton Park are presented in Table 6.5 and Table 6.6, respectively.

Conceptually, for jacked piles that experience less installation disturbance, their initial capacity should not be far off from the limit capacity and therefore the level of recovery is expected to be low. In contrast, driven piles that are subjected to more severe disturbance during installation would be expected to exhibit a lower initial capacity and hence a higher recovery rate to reach the limit capacity. CEPs, which require larger blow counts than OEPs for penetration would tend to have the lowest capacity after driving, but exhibit more marked recovery levels.

Figure 6.4 illustrates the changes of pile shaft resistance (after normalised with τ_{lim}) with time for all the driven CEPs and OEPs and jacked CEPs from Shenton Park, together with full-scale driven OEPs from GOPAL project. The semi-log plot is consistent with the expectations discussed above and clearly demonstrates the superiority of this approach. It is evident that:

- The phenomenon of pile set-up is now represented as a recovery process following pile installation disturbance.
- Distinctive trends among displacement piles subjected to various degrees of disturbance (as reflected from differing installation methods and pile end conditions) emerge from this representation.

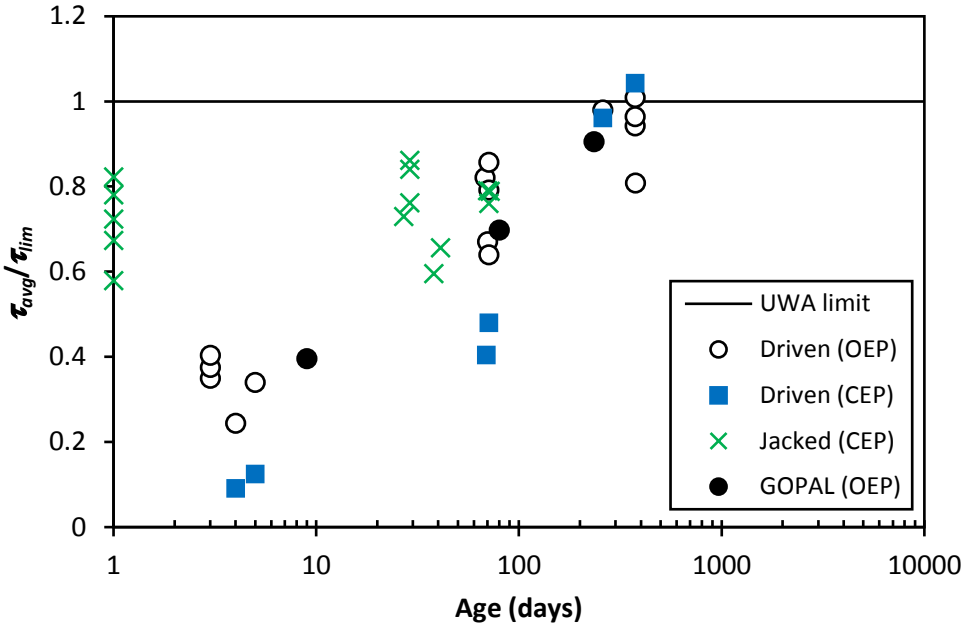

Figure 6.4. Changes of normalised average shaft resistance (against UWA limit capacity) with time

The plot shows that impact driving installation process can, for the case of very heavy driving, lead to a shaft capacity a little larger than the theoretical limit estimated here (τ_{lim}); no such tendency is observed on the jacked piles at the same site. The time-dependent change of pile shaft resistance indicates a lower rate of set-up or possibly a delay during the initial period (most obvious for the driven CEP here) when the sand particles rearrange themselves and redistribute the stresses following severe disturbance (Bowman and Soga, 2005; Jardine *et al.*, 2006).

6.3.6 Proposed Empirical Correlation

Based on the improved representation of pile set-up behaviour described above, a new empirical correlation is proposed here to predict this time-dependent relationship. For a ratio of τ_{avg}/τ_{lim} that ranges between zero (completely lost) and one (fully recovered), and increases in a decreasing rate with time, a monomolecular model that is commonly used to depict limited growth in nature is employed (Seber and Wild, 2003). The model is expressed as:

$$\frac{\tau_{avg}}{\tau_{lim}} = 1 - N_d \cdot e^{-kt} \quad (6\text{-}4)$$

where τ_{avg}/τ_{lim} (as the y-axis) is a new normalised ratio as discussed in preceding section, t (as the x-axis) is the pile age after installation in days, and k and N_d are the curve-fitting parameters. The k parameter controls the rate of recovery, whereas N_d is used to reflect the degree of disturbance imparted during installation (ranges from zero to one).

Three curves are plotted in Figure 6.5 to compare with the existing pile set-up data in the sequence of increasing disturbance: (*i*) jacked CEP at Shenton Park, (*ii*) driven OEP at Shenton Park and for GOPAL project, and (*iii*) driven CEP at Shenton Park. The curves assume a k value of 0.0085 and respective N_d values of 0.35, 0.65 and 0.95, which fit the data reasonably well. The model curves and data are also presented in an alternative form using semi-logarithmic scale in Figure 6.6. It is interesting to note that the proposed correlation incorporates a delay or a much smaller rate of set-up during the initial period, which is consistent with the experimental observations presented here and agrees with the trend of set-up recently hypothesised by Jardine *et al.* (2006).

After around one year, complete stress equilibrium under the new environment following installation disturbance (e.g. breakage, densification, stress distribution, etc.) is close to being reached and therefore little change in capacity is expected thereafter. Instead of assuming an endless capacity increase, either logarithmically (e.g. Chow *et al.*, 1997) or following power-law function (e.g. Mesri and Smadi, 2001) without a valid reason or experimental verification, the proposed empirical correlation limits the time-dependent changes of pile shaft resistance to a projected limiting capacity of a displacement pile based on UWA-05 method; this approach is clearly more readily applied in design.

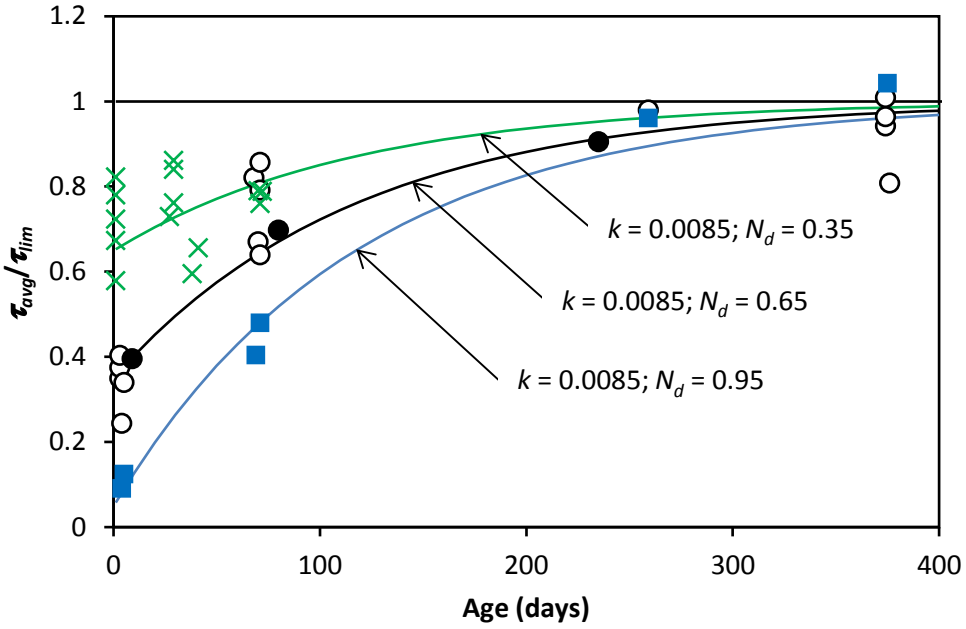

Figure 6.5. Proposed empirical correlation for pile set-up

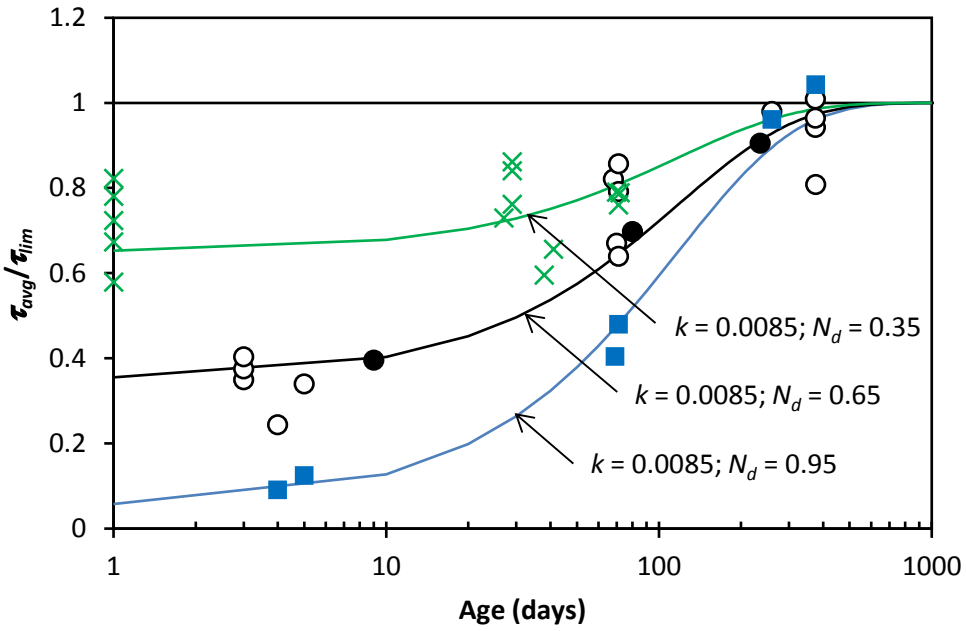

Figure 6.6. Proposed empirical correlation for pile set-up (semi-log)

CHAPTER 7. SCALE EFFECTS ON PILE SHAFT FRICTION AND THE UWA-05 METHOD

7.1 INTRODUCTION

The effects of scale on the shaft friction mobilised by small diameter model piles in sand have been acknowledged for decades. However, in spite of numerous studies, no satisfactory means of extrapolating the results from model piles to full-scale piles has been developed. Even for full-scale test piles, concern was raised recently as to whether their results were relevant to very large diameter offshore piles (Gavin *et al.*, 2011; Knudsen *et al.*, 2012).

This chapter presents an examination of scale effects for shaft friction of driven piles, employing the UWA-05 design method as the base calculation approach. A database comprising reliable pile tests that involve a wide range of pile scales was compiled for this examination. Preliminary assessments on the database showed an absence of any systematic effect of pile diameter on unit shaft friction, which appeared contrary with trends reported in the literature and implicit in recent CPT-based pile design methods. This finding prompted a further investigation here of the diameter dependency implied by UWA-05 method and a subsequent re-examination of the database of model and full scale pile tests to gain additional insights on the longstanding contentious issue of scale effects.

7.2 SCALE AND DIAMETER EFFECTS

This section reviews some current understanding on the diameter dependency of pile shaft friction in sand from both model tests and field experiments.

7.2.1 Model Tests

Experiments of model piles in sands performed at 1-*g*, such as those reported by Lebêgue (1964), Robinsky *et al.* (1964), Hettler (1982), Tejchman and Tejchman (1994), amongst others, confirm the existence of a scale effect for pile shaft friction. All of these tests indicate that smaller diameter piles have a higher unit shaft resistance

(τ_f), but this scale effect is less pronounced in loose sand and for piles with a relatively smooth interface.

Boulon and Foray (1986) attribute the significant scale effects in shaft friction of model piles to the localisation of deformation along the pile shaft, which results in higher dilative response in the small diameter piles. Using a cavity expansion analogy to deduce the increase in lateral stress ($\Delta\sigma'_{rd}$) with respect to a radial expansion (Δr) during shearing, the boundary condition at the pile-soil interface was idealised as:

$$k_n = \frac{\Delta\sigma'_{rd}}{\Delta r} = \frac{4G}{D} \tag{7-1}$$

where k_n is the equivalent normal stiffness and G is the equivalent shear modulus of the sand mass constraining the dilation.

The scale effects was explored by Foray (1991) and others at Grenoble using a calibration chamber by varying the lateral stiffness k_n to replicate the model and prototype conditions based on Equation (7-1). They showed that the scale effects become relatively smaller at higher stress levels (due to less dilative response of the sand at the interface) and are most significant for rough piles in dense sand. The observed scale factor was high and mainly attributed to the relatively large grain size (D_{50} = 0.7 mm) employed in the experiments.

Reddy *et al.* (1998) developed a soil-pile-slip test apparatus from a triaxial cell to study the load-displacement behaviour of tension piles. Three different diameters of model piles (D = 12.7 mm, 25.4 mm and 38.1 mm) were investigated under confining pressures of 70, 120 and 170 kPa. Again, the results showed an inverse relationship between ultimate average shear stress and pile diameter.

Using centrifuge facilities, Foray *et al.* (1998) examined the scale effects of pile shaft friction in conjunction with different mean grain sizes (D_{50} = 0.32 mm and 0.7 mm). Four different diameters (D = 16 mm, 27 mm, 35 mm and 55 mm) of instrumented piles with 'fully rough' interfaces (glued with sand grains) were buried in a very dense quartz sand specimen. The results of tension tests indicate that lower values of τ_f are mobilised by the larger diameter piles, but higher values of τ_f (for a given diameter) develop in the coarser sand (in keeping with their hypothesis). The scale factor is shown to relate

closely with the ratio of D/e (where e is the mean interface thickness, taken approximately as $10D_{50}$ (Desrues and Viggiani, 2004)) and the effect was observed to become negligible for D/e values greater than 20. A similar observation was reported by Garnier and König (1998).

Another series of centrifuge tests was performed by Fioravante (2002) to investigate the shaft friction mobilisation of non-displacement piles in sand. Three model piles of different roughness were tested in two silica sands. Based on the variation of normalised average shear resistance with D/D_{50}, he argues that the limit of $D/D_{50} > 200$ as proposed by Foray *et al.* (1998) and 100 by Garnier and König (1998) could be overestimated, and suggests a limiting ratio of 30 – 50.

Lehane *et al.* (2005a) further examined the scale effects on unit shaft friction of buried piles that can develop in dense sand. A series of tension tests was conducted on rough model piles with a range of diameters (D = 3mm, 5 mm, 10 mm and 18 mm) with constant length of 130 mm and tested under four centrifuge acceleration levels (g = 30, 50, 100 and 180) to mimic different initial stress levels. Besides a diameter dependency of τ_f that is readily observed, the shaft resistance is shown to be dominated by dilation and the $\Delta\sigma'_{rd}$ value, due to the much larger k_n value for model piles as implied by Equation (7-1). A practical approach, which incorporates the results of constant normal stiffness (CNS) interface tests coupled with non-linear cavity expansion stiffness, is proposed to predict the lateral stress changes that take place during loading of both model-scale and full-scale piles.

Despite this general agreement on the existence of scale effects, it is noteworthy that the model piles in the various studies were mostly pre-installed during sample preparation (or monotonically jacked into the sand specimen in a few 1-g tests). As a result, the stresses along the pile shaft, and thus its shearing behaviour, differ from those adjacent to driven piles due to the effects of pile installation. It is also understood that the soil displacement and cyclic shearing during installation of a driven pile is always accompanied by some particle breakage, which results in different interface conditions during subsequent loading.

Some limited studies have involved impact driven model piles in sand with differing diameters. Al-Mhaidib and Edil (1998) carried out a large-scale model test in a 3 m × 3

m × 3 m test pit to investigate the uplift behaviour of pile foundations. Smooth-surfaced steel piles of different diameters (D = 45, 89 and 178 mm) were installed by burial, jacking and driving into a saturated sand bed prepared in loose and dense states. The results of pull-out tests indicated no direct relationship between the average unit shaft friction and pile diameter.

Alawneh *et al.* (1999) conducted a total of 64 pull-out tests on 41 mm and 61 mm diameters model piles with intermediate and rough interfaces. The piles were installed by static jacking and impact driving into medium dense and dense dry sands contained in a rigid steel box (1.1 m × 1.1 m × 1.3 m). The observed diameter dependency on pile shaft resistance was not consistent. For piles with intermediate roughness, the average unit shaft resistance during uplift was higher for the larger diameter piles, whereas the average unit shaft resistance of larger fully rough piles was lower in dense sand but not in medium dense sand.

7.2.2 Field Tests

In contrast to model-scale experiments which are usually performed in a laboratory under controlled environment, field experiments are normally limited in numbers, much more costly and time-consuming, and complicated by inherent variability of local soil conditions. Therefore, it is common to gather the field test results from various sources of similar nature and characteristics, and assessed from a broader view using a statistical approach.

Indirect evidence can be inferred from existing pile design methods that are widely practiced in the industry. For example, the CPT alpha methods of De Cock *et al.* (2003) and Eslami and Fellenius (1997) do not suggest any variation of unit shaft resistance with diameter.

It is worth paying attention to a recent initiative to develop more rational CPT-based pile design methods for offshore driven piles in sand (Clausen *et al.*, 2005; Jardine *et al.*, 2005; Kolk *et al.*, 2005a; Lehane *et al.*, 2005b). Three of these methods (i.e. ICP-05, UWA-05 and Fugro-05) incorporate a diameter dependence of unit shaft friction. A large volume of well-documented pile load tests was collated for calibration purposes. By comparing the measured capacity (Q_m) with that calculated using the UWA-05

method (Q_c), Lehane *et al.* (2005d) showed that there is no apparent bias of Q_c/Q_m with pile length (L), diameter (D), aspect ratio (L/D) and average sand relative density (D_r).

7.3 PRELIMINARY ASSESSMENT

Previous investigations of scale and diameter effects on pile shaft friction, however, were constrained by a limited range of pile diameters employed (applicable only to each testing environment) and there have been few (if any) attempts that combined the results of pile load tests from model scale (e.g. 10 mm diameter pile) and full scale (e.g. 1 m diameter pile) together in a single database.

A database comprising four well-documented sources and covering a wide range of pile scales is established here for the assessment of scale and diameter effects. All the data involved impact driven piles in sand which were load-tested in tension and where CPT data were available.

7.3.1 Expanded Database

The first data set is extracted from the UWA database (Lehane *et al.*, 2005b; Schneider *et al.*, 2008b) of full-scale impact driven CEPs and OEPs that were statically tested in tension. In total, there are 12 CEP and 13 OEP available in the original database but 3 were excluded in this assessment to avoid complications due to significant ageing effects (ID 200: 200 days; ID 402: 69 days) and doubtful CPT data (ID 400; see Monzón (2006)). Table 7.1 presents some basic details of the 22 well-documented pile load tests, which are mainly on steel pipe piles (except for 3 concrete piles) that range from 280 mm to 1.22 m in diameter (average 0.55 m) and are 5.3 m to 47 m long (average 21.1 m). The piles were installed by impact driving into primarily siliceous sand deposits and load tested typically within a month of installation.

The second data set considered here is a pile test programme conducted by Schneider (2007). The programme involved 12 un-instrumented open and closed-ended steel pipe piles driven into medium dense siliceous sand deposits at a UWA test site in Perth. The reduced-scale model piles varied from 33.7 mm to 114.3 mm in diameter and 2.5 m to 4 m in length, which correspond to a wide range of slenderness ratio as summarised in Table 7.2. A series of tension re-tests was carried out with ageing periods of up to 1 year but only the first-time tested results that were conducted around 3 – 5 days after

installation are considered here. It should be noted, however, that an undersized hammer was employed, which resulted in much lower shaft resistance due to excessive disturbance as indicated by the extremely large number of installation blows (as elaborated more detail in Chapter 7).

The third set of data is a centrifuge pile test programme performed by Bruno (1999). The programme utilised 2 small-scaled model piles, with and without instrumentation, with a removable end cap that could be used to model both open and closed-ended pile conditions. The model piles were 9.5 mm in diameter (with an extra 1 mm thick epoxy coating for the instrumented piles) with maximum embedment length of approximately 200 mm. The piles were installed using a model pile driver in dense to very dense saturated silica flour samples and load-tested at several different embedment depths; all tests were performed at 100-*g* in the centrifuge. Results of the first static tension load tests at each test embedment (with $L/D > 10$) were selected and summarised in Table 7.3. It is noteworthy that all tests were performed shortly after reaching their final penetration depth and the capacities measured were lower than achieved with an equilibration period of 1 day.

The model pile tests conducted in a pressure chamber by the author as reported in Chapter 3 are also included here. The sand samples were collected from the UWA test site, deposited to a dense condition and pressurised to typically 200 kPa for 1 week (and maintained for the entire testing programme) before any installation and testing works. Different diameters of small-scale closed-ended model piles at intermediate and fully rough normalised roughness, which ranged from 6 mm to 11 mm with embedment length of 300 mm were investigated. The un-instrumented piles were installed by controlled tapping to certain specified number of blows using a hand-held hammer; piles with other installation methods are excluded here. Static tension load tests were performed between 1 and 30 days after installation. Table 7.4 shows the details of each load test considered in the assessment.

Table 7.1. Details of full-scale pile tests from UWA database

Site	Pile	D (m)	t_w (mm)	L (m)	End [C/O]	IFR_{avg}	Age (day)	τ_{avg} (kPa)	$q_{c\text{-}avg}$ (MPa)
Drammen	A	0.280	-	8.0	C	0	-	12.8	3.0
Drammen	D/A	0.280	-	16.0	C	0	-	17.7	3.4
Drammen	E	0.280	-	23.5	C	0	-	14.1	4.6
Hoogzand	II	0.356	-	6.8	C	0	-	158.6	24.0
Hsin Ta	TP5	0.609	-	34.3	C	0	28	40.1	5.1
Ogeechee River	H-16	0.457	-	15.0	C	0	1.5	71.5	11.3
Lock and Dam 26	3-2	0.305	-	11.0	C	0	35	51.2	15.0
Lock and Dam 26	3-5	0.356	-	11.1	C	0	27	49.1	15.1
Lock and Dam 26	3-8	0.406	-	11.1	C	0	28	63.6	15.1
I-880	2-T	0.610	-	10.7	C	0	16	97.5	15.1
I-880	2-W	0.610	-	12.3	C	0	20	135.9	17.7
SFOBB	E31R	0.610	12.7	13.3	O	0.83	25	52.6	7.5
Dunkirk	R1	0.457	13.5	19.3	O	0.78	9	52.3	20.3
EURIPIDES	Ia	0.763	35.6	30.5	O	0.99	7	41.0	12.5
EURIPIDES	Ib	0.763	35.6	38.7	O	0.97	2	105.1	22.8
EURIPIDES	Ic	0.763	35.6	47.0	O	0.96	11	122.0	28.8
EURIPIDES	II	0.763	35.6	46.7	O	0.95	7	98.3	29.5
Hoogzand	I	0.356	16.0	7.0	O	0.66	37	104.9	24.4
Hoogzand	III	0.356	16.0	5.3	O	0.77	19	89.4	18.5
Hound Point	pa	1.220	24.2	34.0	O	0.95	11	29.6	11.1
Hound Point	pb	1.220	24.2	41.0	O	0.95	4	23.8	11.4
I-880	2-P	0.610	19.1	12.3	O	0.82	28	85.0	16.7

Note:

'C' denotes closed-ended while 'O' denotes open-ended.

Pile ID 200 and 402 are excluded to avoid complication from significant ageing effect (tested after 200 and 69 days respectively).

Pile ID 400 is excluded due to doubtful CPT data (Monzón, 2006).

Table 7.2. Details of reduced-scale pile tests at Shenton Park (Schneider, 2007)

Pile	D (m)	t_w (mm)	L (m)	End [C/O]	IFR_{avg}	Age (day)	τ_{avg} (kPa)	$q_{c\text{-}avg}$ (MPa)
P01	0.0889	2.6	4	O	0.65	4	16.0	5.9
P02	0.0424	2.6	4	O	0.34	4	15.0	5.9
P03	0.0889	5.0	4	C	0	4	7.0	5.9
P04	0.0889	5.0	4	O	0.72	3	23.0	5.9
P05	0.1143	3.2	4	O	0.8	3	20.0	5.9
P06	0.0889	3.2	4	O	0.72	3	26.0	5.9
P08	0.0424	2.6	2.5	O	0.28	5	17.0	4.1
P09	0.0337	2.6	2.5	O	0.17	5	9.0	4.1
P10	0.0337	2.6	3.5	O	0.17	5	15.0	5.2
P11	0.0889	2.6	2.5	O	0.54	5	17.0	4.1
P12	0.0889	2.6	2.5	C	0	5	7.0	4.1

Note:

'C' denotes closed-ended while 'O' denotes open-ended.

The piles, particularly the larger diameter CEP, were subjected overly large number of blow count due to undersized hammer (25 kg).

Pile P07 which was installed using a much smaller hammer (10 kg) is excluded due to unnecessary disturbance (over-driving that caused lateral movement and 'gapping') (Schneider, 2007).

Much lower capacities were measured as compared to jacked pile at the same site and significant set-up was observed over time; see Chapter 4 for details.

Table 7.3. Details of small-scale centrifuge pile tests (Bruno, 1999)

Pile	D (m)	t_w (mm)	L (m)	End [C/O]	IFR_{avg}	τ_{avg} (kPa)	$q_{c\text{-}avg}$ (MPa)
A1-3	0.0095	0.55	0.1152	O	0.48	55.3	13.2
A1-4	0.0095	0.55	0.1572	O	0.62	57.2	17.0
A1-5	0.0095	0.55	0.1968	O	0.65	49.5	20.8
A2-3	0.0115	0.55	0.111	O	0.37	55.3	12.9
A2-4	0.0115	0.55	0.1529	O	0.40	54.9	16.6
A2-5	0.0115	0.55	0.1928	O	0.47	56.4	20.3
B1-3	0.0095	0.55	0.114	O	0.59	61.9	15.0
B1-4	0.0095	0.55	0.1561	O	0.62	86.1	19.9
B1-5	0.0095	0.55	0.1977	O	0.61	112.5	26.4
B2-3	0.0115	0.55	0.1107	O	0.15	39.0	14.6
B2-4	0.0115	0.55	0.1521	O	0.34	57.8	19.4
B2-5	0.0115	0.55	0.1924	O	0.34	85.6	25.4
E3-2	0.0115	0.55	0.1266	O	0.32	81.8	12.4
E3-3	0.0115	0.55	0.1855	O	0.43	71.9	15.7
E6-2	0.0095	0.55	0.1256	O	0.44	65.0	12.3
E6-3	0.0095	0.55	0.1875	O	0.66	67.9	15.8
F2-2	0.0115	0.55	0.1389	O	0.49	31.9	14.3
F5-2	0.0115	0.55	0.1383	O	0.41	51.3	18.7
G2-2	0.0115	-	0.1131	C	0	43.1	14.5
G2-3	0.0115	-	0.1886	C	0	56.4	21.7
G3-2	0.0095	-	0.114	C	0	49.7	14.6
G3-3	0.0095	-	0.1887	C	0	49.5	21.7
G4-2	0.0095	-	0.1147	C	0	46.8	17.3
G4-3	0.0095	-	0.1885	C	0	51.4	25.4
G6-2	0.0115	-	0.1149	C	0	46.2	17.3
G6-3	0.0115	-	0.1898	C	0	57.2	25.5
H3-2	0.0095	0.55	0.1375	O	0.74	56.9	18.1
H3-3	0.0095	0.55	0.1877	O	0.82	51.4	21.3

Note:

'C' denotes closed-ended while 'O' denotes open-ended.

Piles F2-3 and F5-3 are excluded after examined to be erroneous (much lower than the subsequent tests and at adjacent points).

Tension load tests were performed shortly after penetration to the targeted embedded depths.

Table 7.4. Details of small-scale pile tests in pressure chamber (Full details in Chapter 3)

Pile	D (m)	L (m)	End [C/O]	Age (day)	τ_{avg} (kPa)	$q_{c\text{-}avg}$ (MPa)
C4-DMi-3	0.008	0.3	C	3	274.3	39.2
C4-DMi-7	0.008	0.3	C	7	248.9	39.2
C4-DMi-28	0.008	0.3	C	28	320.0	39.2
C5-DLi-1	0.010	0.3	C	1	213.4	32.5
C5-DLi-7	0.010	0.3	C	7	198.0	32.5
C5-DLi-28	0.010	0.3	C	28	289.9	32.5
C5-DSi-1	0.006	0.3	C	1	139.8	32.5
C5-DSi-28	0.006	0.3	C	28	155.5	32.5
C6-DMi-1	0.008	0.3	C	1	235.8	35.9
C6-DMi-3	0.008	0.3	C	3	230.2	35.9
C6-DMi-7	0.008	0.3	C	7	235.6	35.9
C6-DMi-15	0.008	0.3	C	15	265.6	35.9
C6-DMi-30	0.008	0.3	C	30	277.6	35.9
C7-DSi-2	0.006	0.3	C	2	133.9	25.7
C7-DMi-2	0.008	0.3	C	2	160.6	25.7
C7-DLi-2	0.010	0.3	C	2	150.0	25.7
C7-DSr-2	0.007	0.3	C	2	170.9	25.7
C7-DMr-2	0.009	0.3	C	2	214.0	25.7
C7-DLr-2	0.011	0.3	C	2	239.9	25.7
C9-DMr-1	0.009	0.3	C	1	77.9	9.4
C9-DMr-7	0.009	0.3	C	7	69.3	9.4
C9-DMr-28	0.009	0.3	C	28	62.6	9.4

Note:

'C' denotes closed-ended.

Pile C5-DSi-7 is excluded due to severe disturbance during installation process; see Chapter 3 for details.

7.3.2 Direct Observation

In order to ensure a valid comparison among the results of pile shaft friction from various different sources of varying stiffness and boundary conditions, a proper normalisation procedure is essential. One convenient way is by normalising the average pile shaft resistance (τ_{avg}) by the average of CPT-q_c values along the pile shaft ($q_{c\text{-}avg}$), which can be easily extracted from the CPT data available for different scales of testings.

In addition, the normalisation resembles a familiar form of correlation between the local shaft friction (τ_f) and cone tip resistance (q_c) in the pile design methods that are generally known as CPT alpha methods (e.g. Eslami and Fellenius, 1997; De Cock *et al.*, 2003; Schneider *et al.*, 2008b). The proposed representation of the overall pile shaft resistance is expressed as:

$$\frac{\tau_{avg}}{q_{c-avg}} = \frac{1}{\alpha_s} \tag{7-2}$$

The $\tau_{avg}/q_{c\text{-}avg}$ values are plotted against pile diameter (D) and slenderness ratio (L/D), and presented in Figure 7.1 and Figure 7.2, respectively. It is seen that there is no clear diameter dependency of these values as suggested by the literature and recent CPT-based pile design methods (e.g. ICP-05 and UWA-05), despite diameters differing by more than two orders of magnitude.

The trends indicated in Figure 7.1 and Figure 7.2 prompted the following reassessment of the pile design methods and further examination of the database.

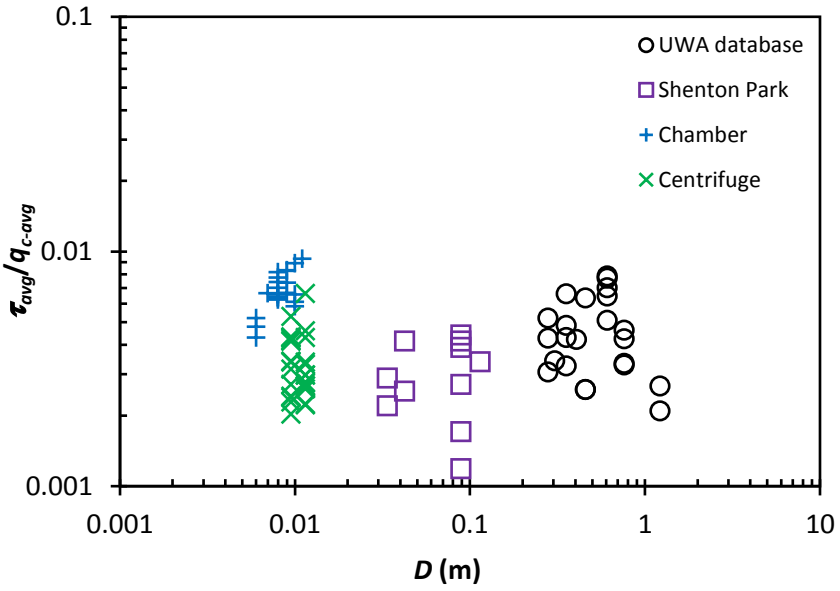

Figure 7.1. Variation of $\tau_{avg}/q_{c\text{-}avg}$ with D for wide range of data set (preliminary)

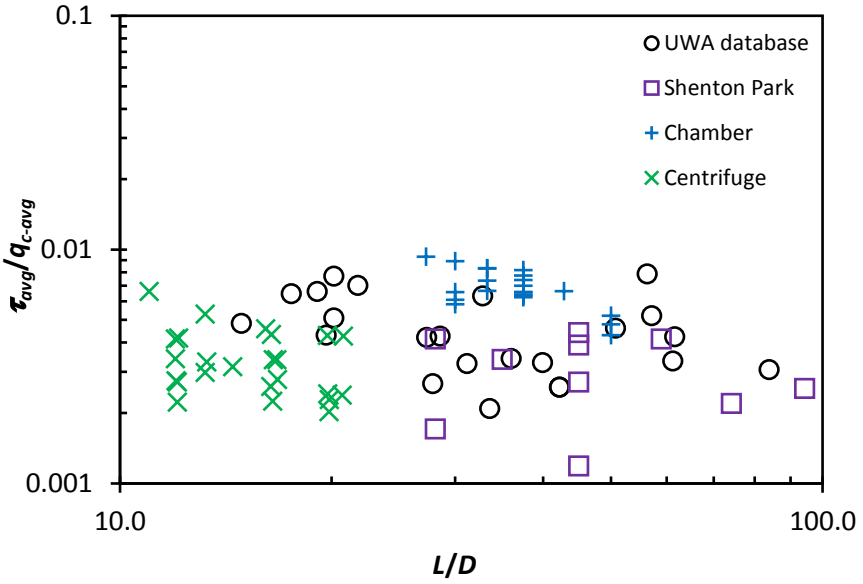

Figure 7.2. Variation of $\tau_{avg}/q_{c\text{-}avg}$ with L/D for wide range of data set (preliminary)

7.4 REPRESENTATION OF THE UWA-05 METHOD

Formulation of UWA-05 method (see Appendix C) involves two major components (stationary and dilation), which are compensatory with respect to pile diameter and that the relative magnitudes of these components also vary along the entire shaft length. As a result, the dominant component that governs the pile shaft resistance of small and large diameter piles is different. The relationship can be revealed by numerical integration (Appendix D) but it does not give a clear quantitative indication on how the stationary and dilation components compensate each other over a wide range of pile diameters. An improved understanding can be achieved by performing a well-defined parametric study.

Recent parametric studies performed by Gavin *et al.* (2011), Thomassen *et al.* (2012) and Knudsen *et al.* (2012) to predict the static capacity of driven monopiles for offshore wind farms using the existing CPT-based design methods, however, showed some confusing outcomes. Knudsen *et al.* (2012) inferred an unexpected continuous increase in τ_{avg} for UWA-05 and other methods when the pile diameter was varied from 0.5 m to 3 m. Gavin *et al.* (2011) showed that UWA-05 predicted a very low capacity for an open-ended pile compared to other methods and argued that the existing CPT methods are too conservative in the dense sand typically encountered in the offshore (North Sea) environment.

This section examines the scale and diameter effects of pile shaft friction implied by the UWA-05 method through a parametric study. The assessment covers not only the range of full-scale offshore piles but also the small-scale diameter piles that have not been explored before. In this study, a constant volume interface friction angle (δ_{cv}) of 27^o was assumed and the dilation of the interface layer during shearing (Δr) was taken as 0.02 mm (typical for lightly rusted steel piles in a medium sand). The operational shear stiffness (G) was estimated based on the empirical correlation with q_c and effective vertical stress (σ'_{vo}) proposed by Baldi *et al.* (1989).

7.4.1 Idealised Soil Profile and Pile Geometry

Two idealised soil profiles were generated to represent medium dense and dense conditions having the CPT q_c profiles of $q_c = 1.9\ z^{0.5}$ and $q_c = 6.6\ z^{0.5}$, respectively;

where z is the depth below ground level. Based on the correlation proposed by Jamiolkowski *et al.* (2001), these correspond to the uniform relative densities (D_r) of approximately 42% and 75% respectively assuming an effective unit weight (γ') of 10 kN/m^3. The assumed parameters and profiles are typical of the siliceous sand deposit commonly found worldwide.

A wide range of pile diameters (D) and corresponding practical range of pile lengths (L) was investigated in the study. The study comprised: (*i*) small-scale piles that are usually employed in the laboratory with diameters between 5 mm and 30 mm; (*ii*) reduced-scale piles such as the heavily instrumented ICP piles, which may range from 30 mm to 200 mm in diameter; and (*iii*) full-scale piles that usually range from 200 mm to 3 m in offshore applications.

In the first series of parametric studies, constant pile lengths of 300 mm, 3 m and 30 m were assumed for the small-scale, reduced-scale and full-scale piles, respectively. This corresponds to the slenderness ratios (L/D) that range from about 10 to 100. Another series of calculations was performed assuming constant slenderness ratios of 10, 30, 60 and 100 with the diameters varying accordingly. For assessment of the effect of the pile end condition, a thick walled pile (D/t_w = 30, where t_w is the wall thickness) was assumed in the analysis to represent the typical case of open-ended piles that are driven into very dense sand.

7.4.2 Tension Capacity of Closed-ended Pile at Constant *L*

Figure 7.3 shows the variation of average unit shaft resistance (τ_{avg}) with diameter for certain specified pile lengths in medium dense and dense sand; a common representation employed in the literature. It is evident that, except for the overall magnitude of τ_{avg} in medium dense sand (which is lower than that in the dense sands), both cases show a very similar trend with respect to pile diameter. τ_{avg} decreases with increasing D for the small-scale piles but increases with increasing D for the full-scale piles, with the transition taking place at around D = 200 mm and D = 90 mm in medium dense and dense sands, respectively. The changes are attributed to the varying relative influence of τ_s and τ_d at different diameters. The τ_d component is critical for small-scale piles but is also noted to be more influential in the looser sand condition.

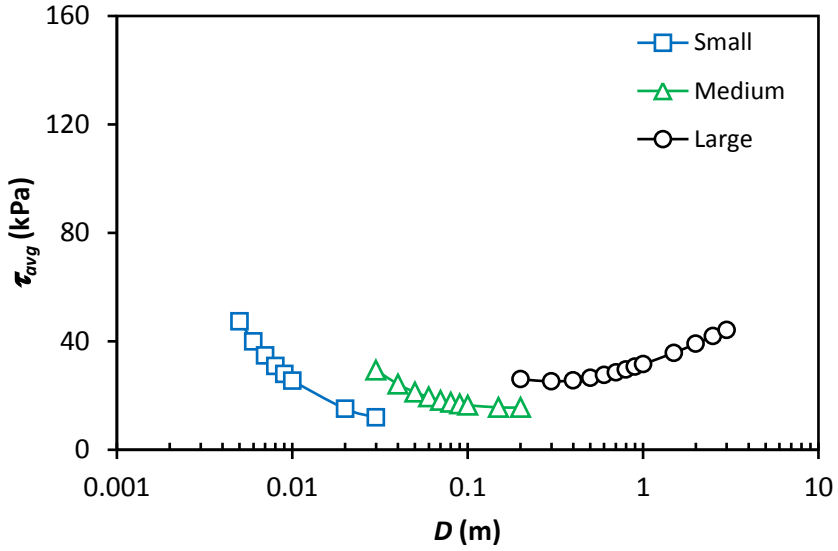

(a)

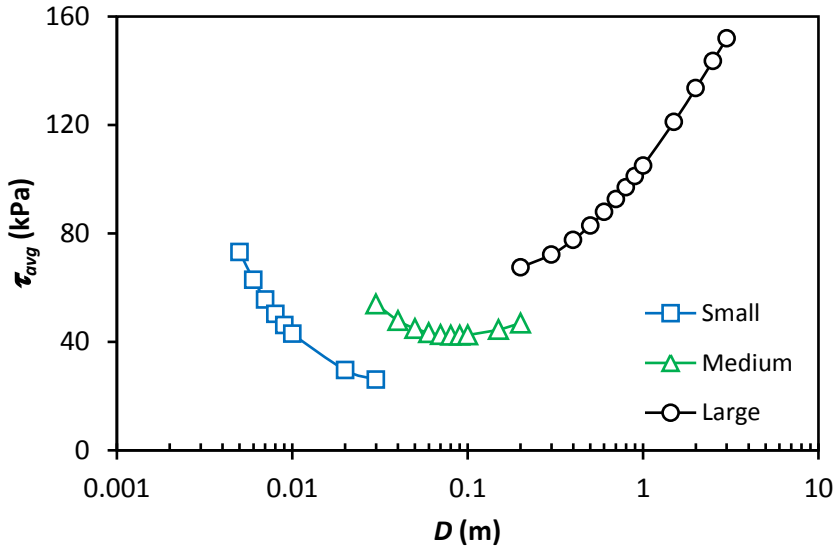

(b)

Figure 7.3. Variation of τ_{avg} with D at constant L: (a) medium dense sands; (b) dense sands

In view of the different q_c values (as a function of z or L) that were considered between the small-scaled, reduced-scale and full-scale piles, the τ_{avg} were normalised with each respective $q_{c\text{-}avg}$ and represented in Figure 7.4. Normalisation of the τ_{avg} transforms its diameter dependency relationship to a consistent but slightly different form. As indicated in the figure, UWA-05 method projects significantly higher $\tau_{avg}/q_{c\text{-}avg}$ values

for the small-scale piles, which are in some cases up to 10 times higher than the same ratios for the full-scale piles. Nevertheless, it is noteworthy that while higher τ_d is expected from the formulation (see cavity expansion analogy; e.g. Boulon and Foray (1986)) and observed in centrifuge experiments for buried piles (Lehane and White, 2005), the diameter effect in small-scale *driven* piles has not yet been validated (to be examined later).

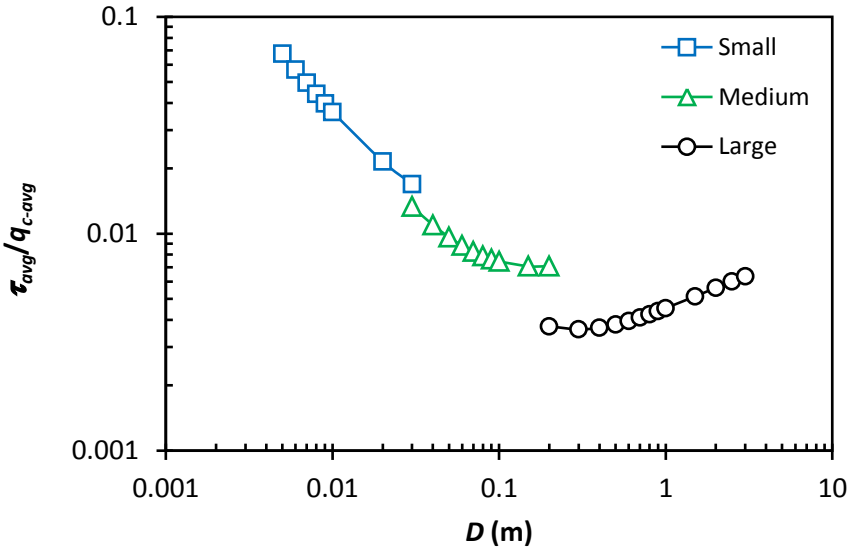

(a)

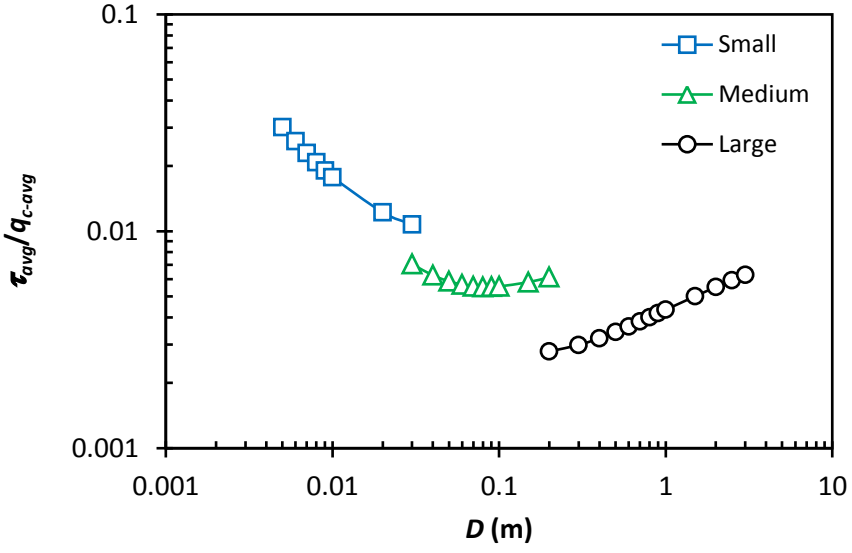

(b)

Figure 7.4. Variation of $\tau_{avg}/q_{c\text{-}avg}$ with D at constant L: (a) medium dense sands; (b) dense sands

Over the range of diameters of full scale piles, the $\tau_{avg}/q_{c\text{-}avg}$ ratios increase with D (similar to the variation of τ_{avg} with D discussed earlier) in spite of an overall trend that seems to suggest a diminishing trend of the reduction with diameter. The relationship is in keeping with the expectation from numerical integration for the case of constant L as presented in Appendix D. However, as the slenderness ratio tends to reduce with increasing diameter, the foregoing observation may have been compromised by the effects of slenderness ratio.

7.4.3 Tension Capacity of Closed-ended Pile at Constant *L*/*D*

A second series of calculations assuming constant L/D values of 10, 30, 60 and 100 was conducted to further explore the effect of diameter on pile shaft resistance. Typical results from the dense sand are presented here and in the following sections. As indicated in Figure 7.5, for full-scale piles at constant L/D, $\tau_{avg}/q_{c\text{-}avg}$ remains essentially constant as expected from the analytical integration of the UWA-05 formulation, described earlier. The slight decrease of $\tau_{avg}/q_{c\text{-}avg}$ with D is attributed to the minor dilation term on the full-scale piles. By superimposing the previous results (at constant L) on the same figure, it is interesting to note that the trend for an increase $\tau_{avg}/q_{c\text{-}avg}$ with D observed in the preceding section (and also noted by Knudsen *et al.* (2012) and others) is basically an interference of the L/D effect, which gradually reduces from $L/D = 100$ to $L/D = 10$ as D increases. This also implies that the UWA-05 method does not necessarily predict an increase in unit shaft resistance when extrapolated to full-scale offshore piles.

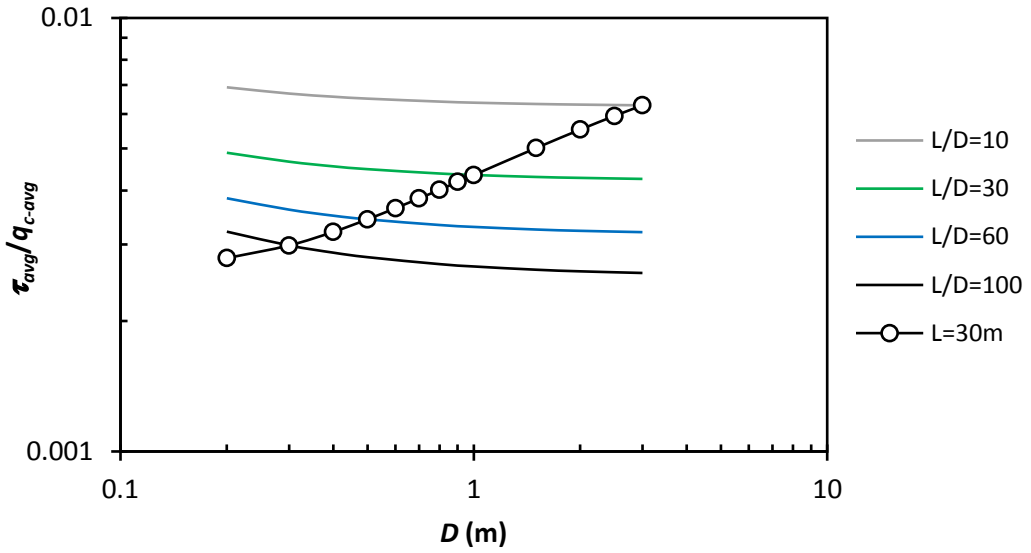

Figure 7.5. Comparison of $\tau_{avg}/q_{c\text{-}avg}$ with D between constant L and constant L/D

Figure 7.6 shows the variation of τ_{avg} and $\tau_{avg}/q_{c\text{-}avg}$ at constant L/D for pile diameters from 5 mm to 3 m diameter. It can be seen that at any single D, τ_{avg} at the larger L/D ratio tends to be higher because of the greater pile length and corresponding q_c (which increases with depth, z). However, after the τ_{avg} is normalised by the corresponding $q_{c\text{-}avg}$ values (for a consistent comparison), the $\tau_{avg}/q_{c\text{-}avg}$ ratio at the larger L/D ratio appears to be lower than those at smaller L/D. This relationship is sensible and in keeping with the concept of friction fatigue embodied in the formulation of the UWA-05 method.

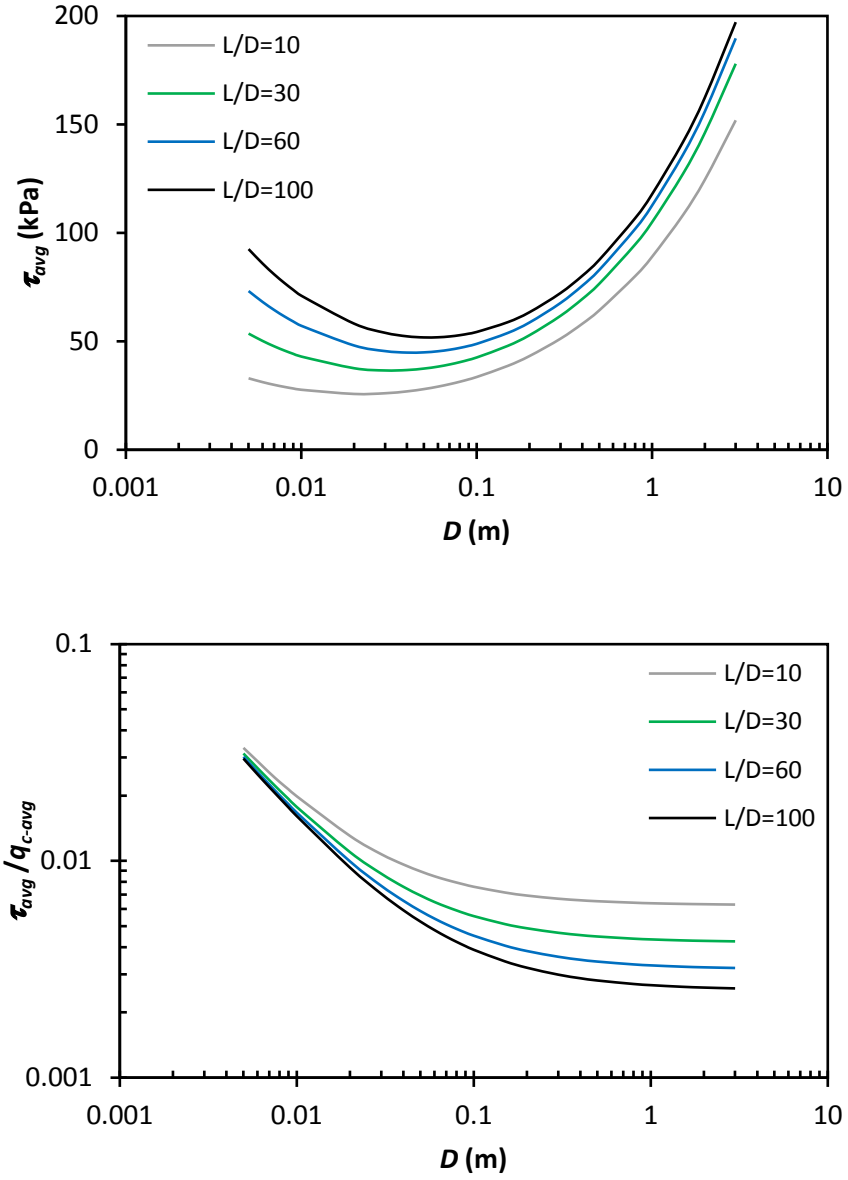

Figure 7.6. Variation of τ_{avg} and $\tau_{avg}/q_{c\text{-}avg}$ with D at constant L/D

The $\tau_{avg}/q_{c\text{-}avg}$ ratios are plotted against L/D for different D values in Figure 7.7. Again, the trend of decreasing $\tau_{avg}/q_{c\text{-}avg}$ with L/D agrees with the relationship incorporated in the formulation of UWA-05 method (see Appendix D). It is important to note that, as far as full-scale piles are concerned, the $\tau_{avg}/q_{c\text{-}avg}$ ratios fall within a narrow range of profile with respect to L/D. Model-scale piles, which are governed by the dilation term, show a much higher $\tau_{avg}/q_{c\text{-}avg}$ ratio and relatively smaller rate of reduction with L/D.

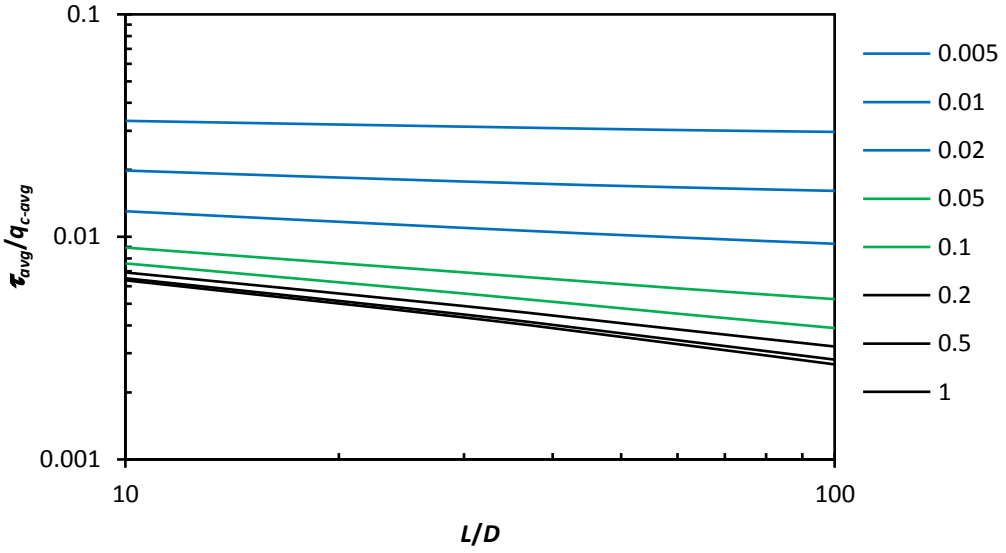

Figure 7.7. Variation of $\tau_{avg}/q_{c\text{-}avg}$ with L/D for different diameters (m)

7.4.4 Tension Capacity of Open-ended Pile at Constant L/D

Further to the findings of tension capacity of CEP at a constant L/D as presented in preceding section, another parametric study was performed to examine the influence of pile end condition on the diameter dependency. The assessment assumed a D/t_w of 30, which is representative of the typical open-ended piles employed for offshore structures. Results for other D/t_w ratios can easily be deduced. A higher D/t_w for the same diameter simply means a thinner wall that tends to displace less soil, remains unplugged and results in lower shaft resistance.

Figure 7.8 shows a comparison between CEPs and OEPs at the constant L/D of 10 and 100 to contrast their variation of $\tau_{avg}/q_{c\text{-}avg}$ with D. It can be seen that the predicted shaft resistance for OEPs is always lower than for CEPs because the generated radial effective stress is lower due to the smaller volume of soil being displaced during installation. The difference expands gradually as the diameter increases up to approximately 1.5 m, above which the UWA-05 method assumes full coring with an incremental filling ratio (IFR) of 1.0.

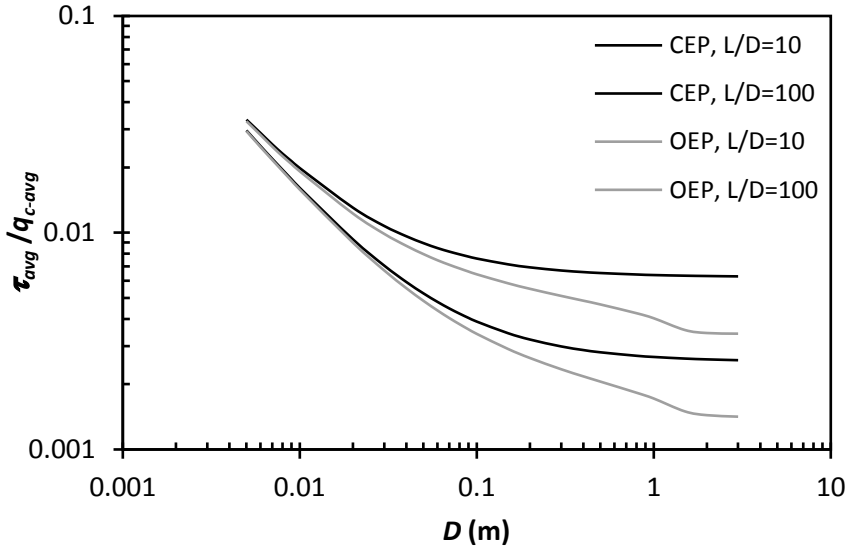

Figure 7.8. Comparison of $\tau_{avg}/q_{c\text{-}avg}$ with D at constant L/D between CEP and OEP

As for the CEP, the unit shaft resistance as predicted by the UWA-05 method remains almost unchanged when extrapolated to the full-scale offshore piles (D > 1.5 m) at a constant L/D. The variations of $\tau_{avg}/q_{c\text{-}avg}$ with D at the constant L/D, and with respect to L/D for the OEP are presented in Figure 7.9 and Figure 7.10, respectively.

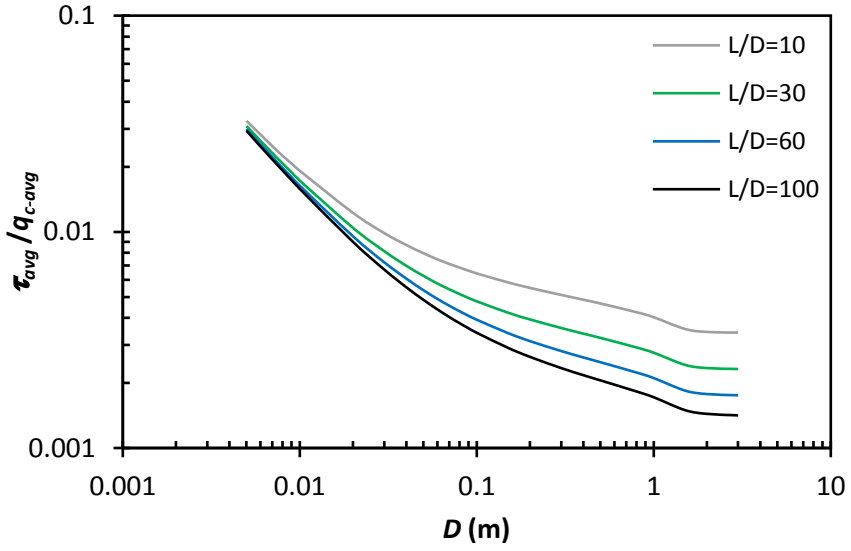

Figure 7.9. Variation of $\tau_{avg}/q_{c\text{-}avg}$ with D at constant L/D for different diameters of OEP

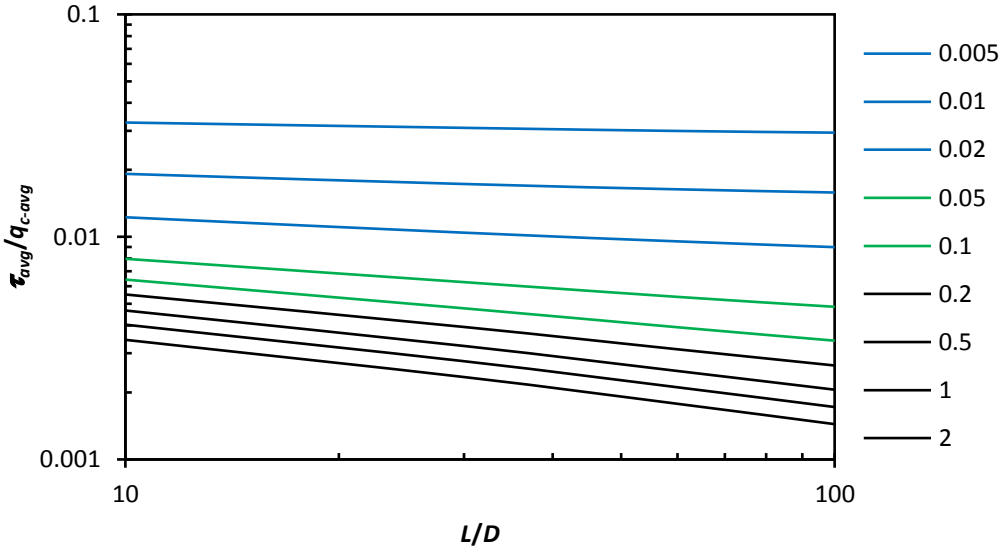

Figure 7.10. Variation of $\tau_{avg}/q_{c\text{-}avg}$ with L/D for OEP with different diameter (m)

7.5 VALIDATION OF THE PREDICTED SCALE EFFECTS

Following a better understanding of the diameter dependency implied by the UWA-05 method, existing direct and indirect experimental evidence are re-examined to investigate the performance of UWA-05 predictions and more importantly to provide additional insights on the scale and diameter effects. Comparisons are made between the UWA-05 predictions on dense sand and (*i*) the recommendation from existing CPT alpha methods, and (*ii*) the database presented in Section 7.3, which involved full-scale, reduced-scale and small-scale pile test results.

It is noteworthy that UWA-05 is not an exact solution but an empirical design method developed based primarily on available experimental observations. Except for the range of pile diameter covered within the UWA-05 database that has been calibrated, extrapolation to either very large offshore piles or laboratory-scale model piles demands careful and considerable judgment.

7.5.1 CPT Alpha Methods

Nine CPT alpha methods, which are reportedly applicable to displacement piles in sand, are considered in this assessment and are listed in Table 7.5. Priority is given to the closed-ended driven steel pipe piles that are most commonly employed in the offshore environment. Since the majority of pile load tests used to calibrate design methods are in compression, corrections are necessary to ensure comparability with the tensile capacity predicted using the UWA-05 method. The pile shaft resistance in tension is now acknowledged to be lower than that in compression for the reasons described by Lehane *et al.* (1993), De Nicola and Randolph (1993) and Jardine *et al.* (2005).

Table 7.5. Summary of CPT alpha methods for displacement piles in sand

Reference	α_s #	$\tau/q_c = 1/\alpha_s$	Q_{st}/Q_{sc}	$(\tau/q_c)_1$	$(\tau/q_c)_2$
Meyerhof (1956)	200	0.005	-	0.005	0.004
Schmertmann (1978)	83	0.012	0.67	0.008	0.008
De Ruiter and Beringen (1979)	300	0.0033	0.75	0.0025	0.0025
Bustamante and Gianeselli (1982)	200*	0.005	-	0.005	0.004
Eslami and Fellenius (1997)	250	0.004	1.0	0.004	0.004
De Cock *et al.* (2003) – Belgium	200*	0.005	-	0.005	0.004
De Cock *et al.* (2003) – The Netherlands	100	0.010	-	0.010	0.0075
De Cock *et al.* (2003) – Italy	250	0.004	-	0.004	0.003
De Cock *et al.* (2003) – France	300*	0.0033	-	0.0033	0.0025

Note:

The most appropriate values as for closed-ended steel pipe piles in dense sand ($q_c \geq 25$ MPa).

* A smaller value was recommended for precast concrete piles.

$(\tau/q_c)_1$ were computed without reduction of pile shaft capacity in tension, unless otherwise stated.

$(\tau/q_c)_2$ considered a reduction factor of 0.75 for those general recommendations without distinction of loading direction (compression or tension).

The τ/q_c ratios recommended by the respective methods (with and without consideration of the UWA-05 correction factor for tension capacity of 0.75) are summarised in Table 7.5 and presented in Figure 7.11(a) and (b). In the same figure, the range of UWA-05 predictions in dense sand for the piles with a diameter of 200 mm and 1 m (extracted from parametric study in the preceding section) are shown for comparison purpose. It is seen that except for the high values used in The Netherlands (De Cock *et al.*, 2003) and recommended by Schmertmann (1978), which are based on Dutch practice and observations from model-scale piles by Nottingham (1975), all other recommendations do not differ significantly from the UWA-05 predictions at typical L/D values adopted for most piling projects.

It is interesting to note that the lower α_s values assigned to lower q_c values (thus higher unit shaft friction) as for some of the CPT alpha methods is in agreement with the tendency of decreasing $\tau_{avg}/q_{c\text{-}avg}$ with L/D predicted by the UWA-05 method; q_c is generally lower where L or L/D is lower.

7.5.2 UWA Database on Full-scale Pile Tests in Tension

The full-scale pile tests in the UWA database (Table 7.1) is first re-examined with respect to a different approach adopted in this study (i.e. overall performance in terms of $\tau_{avg}/q_{c\text{-}avg}$). For detailed characterisation, besides distinguished by its end condition (i.e. CEP and OEP), the data were subdivided into 3 categories based on their slenderness ratio: (*i*) short: $L/D < 25$; (*ii*) medium: $25 < L/D < 75$; and (*iii*) long: $L/D > 75$. Figure 7.12 and Figure 7.13 show the $\tau_{avg}/q_{c\text{-}avg}$ ratios of full-scale test piles plotted against D and L/D, respectively. It can be seen that the OEP generally have lower shaft resistance than the CEP (for the comparable L/D) and $\tau_{avg}/q_{c\text{-}avg}$ for both the CEP and OEP decreases with increasing L/D; these trends are in good agreement with those observed earlier the UWA-05 method.

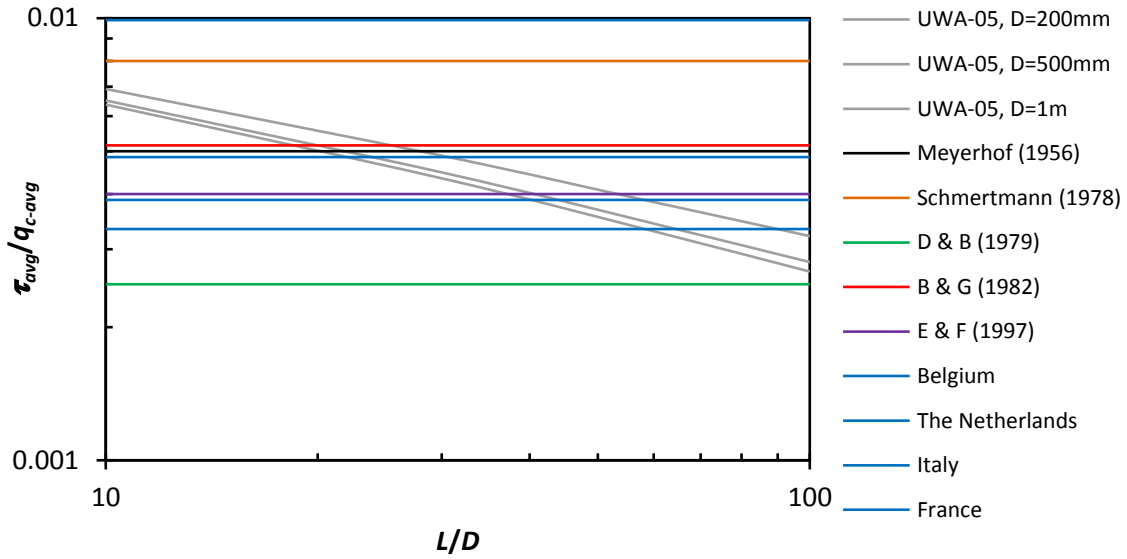

(a)

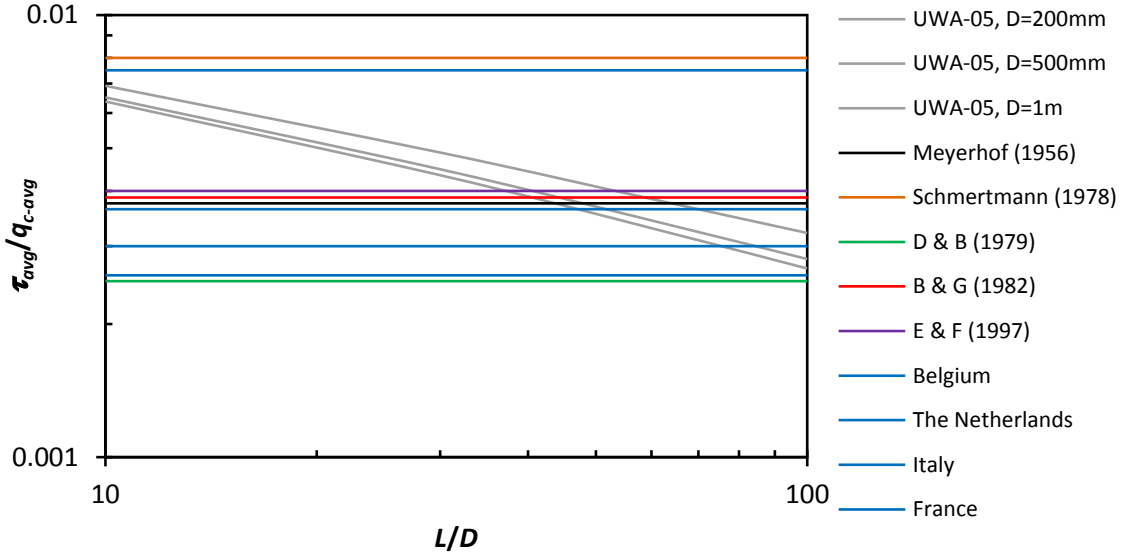

(b)

Figure 7.11. Comparison of τ/q_c with L/D between the recommendation of CPT alpha methods and prediction of UWA-05 method: (a) uncorrected; (b) corrected

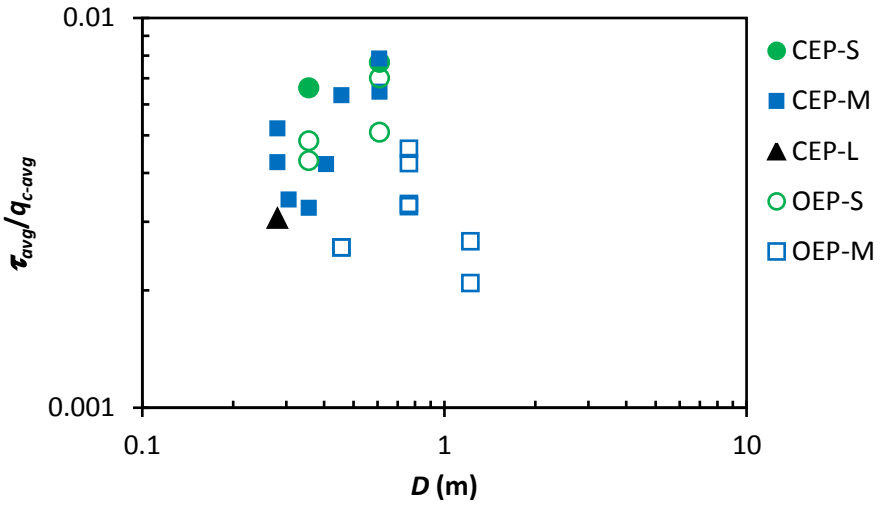

Figure 7.12. Variation of $\tau_{avg}/q_{c\text{-}avg}$ with D for full-scale piles

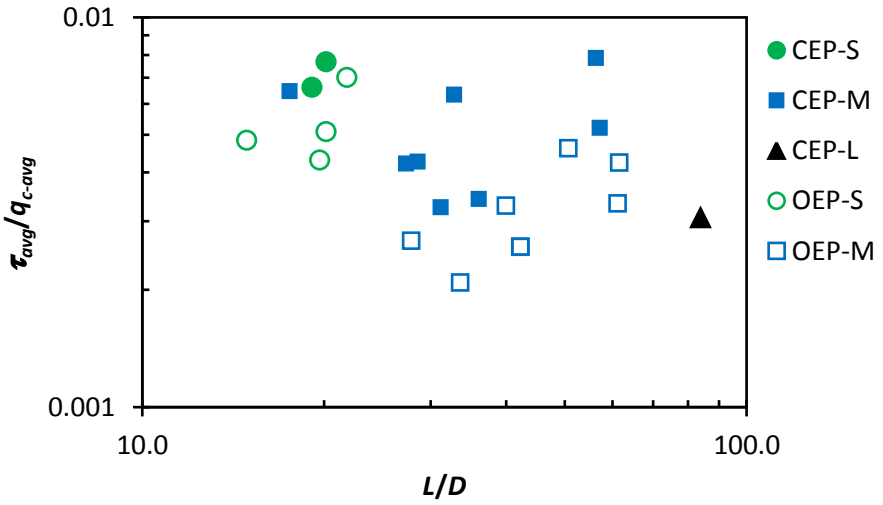

Figure 7.13. Variation of $\tau_{avg}/q_{c\text{-}avg}$ with L/D for full-scale piles

7.5.3 Expanded Database with Wide Range of Pile Scales

Further re-examination is performed on the expanded database (Table 7.1 to Table 7.4), which includes the results of static tensile load tests from a wide range of pile scales. The data are from different sources (see Section 7.3.1 for details) with variation of installation and testing procedures (most notably the equivalent impact force and pile age), which are crucial in a generalised interpretation.

Following improved understanding of ageing and installation effects on shaft resistance discussed in previous chapters, amendments deemed necessary for each data set are listed in the following:

- For those full-scale pile tests (from UWA-05 database) which were tested after 10 days following installation, an amendment was made by assuming the pile shaft resistance to exhibit a set-up factor B (Equation 6-16) of 0.48 in the first month. The factor was derived in accordance to the proposed empirical correlation that has been verified by the set-up behaviour of full-scale piles from GOPAL project (see Chapter 6); the pile R1 is also one of the data considered in the UWA database.

- The reduced-scale piles at Shenton Park, which were subjected to excessive disturbance during installation (see Chapter 6), were increased by a factor of 1.5 and 3 for OEP and CEP respectively to represent a reasonable range of pile shaft resistance under more typical driving conditions. The author's other pile test programme at the same site (Chapter 3), which employed a series of non-symmetrical incremental jacking procedures to mimic the pile driving process, provides an upper bound reference for this amendment.

- The small-scale centrifuge pile tests, which were tested shortly after installation, were increased by a factor of 2 to account for the short-term ageing effects. Insights were gained from observations of global and local changes of pile shaft resistance between the last installation push and that tested after 1 day following installation (see Chapter 3). Another centrifuge experiment (Lehane and White, 2005) that employed different jacking procedures to model the installation of driven piles, after amended, fall on the high side of the characterisation that serves as an upper bound reference.

The amended data are re-examined and presented in Figure 7.14 and Figure 7.15, where a more consistent pattern is observed from that evident on Figure 7.1 and Figure 7.2. Typical UWA-05 predictions in dense sand from the parametric study earlier are also included in the plots for comparison purposes. It is seen that the $\tau_{avg}/q_{c\text{-}avg}$ of all the test data vary with D and with L/D in a similar fashion to that predicted by UWA-05. The

$\tau_{avg}/q_{c\text{-}avg}$ ratios of the model scale piles are, however, over-predicted by UWA-05 by a factor of about 2.

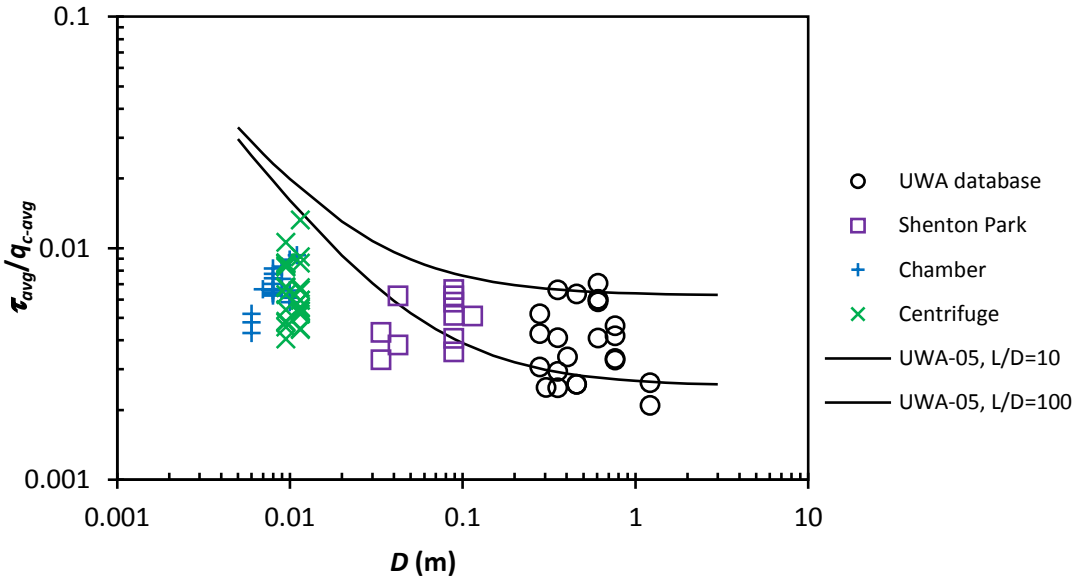

Figure 7.14. Variation of $\tau_{avg}/q_{c\text{-}avg}$ with D for full database of tension tests

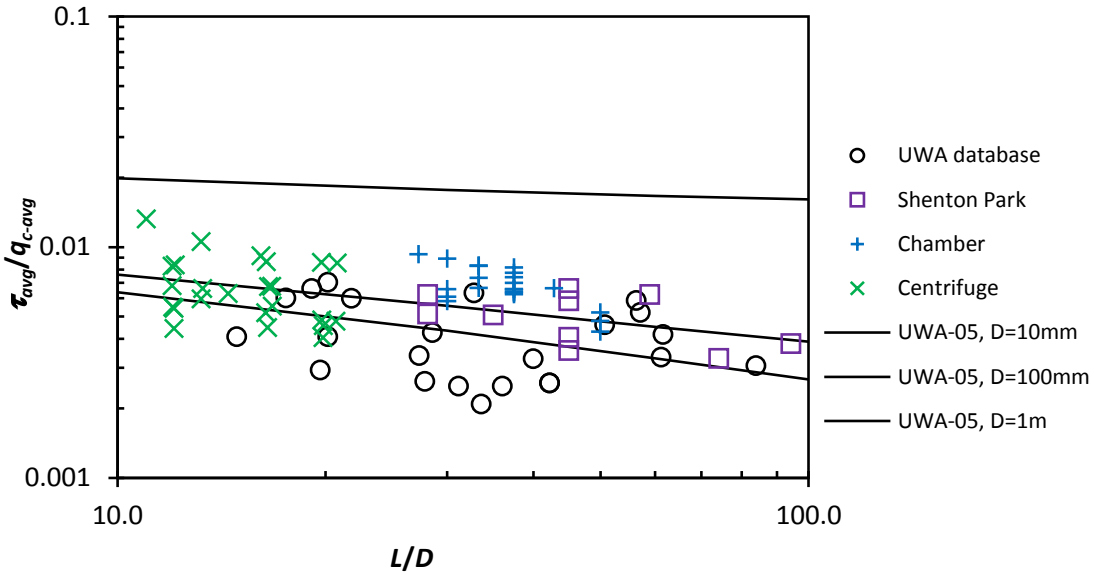

Figure 7.15. Variation of $\tau_{avg}/q_{c\text{-}avg}$ with L/D for full database of tension tests

The relationship between $\tau_{avg}/q_{c\text{-}avg}$ and L/D is further examined by categorising the data into either model or prototype scale, and according to their end conditions. Figure 7.16 and Figure 7.17 show the variation of $\tau_{avg}/q_{c\text{-}avg}$ with pile end condition at model scale and prototype scale, respectively. It is observed that while the difference between OEP and CEP is hardly discernible at the model scale, the $\tau_{avg}/q_{c\text{-}avg}$ ratios of OEPs are in general slightly lower than CEPs at prototype scale. This is in agreement with the UWA-05 prediction with respect to plugging effect in OEP as discussed in Section 7.4.4.

Figure 7.17 (in concert with Figure 7.8) show that the UWA-05 prediction for OEP in dense sand is reasonable and does not seem to be overly conservative as claimed by Gavin *et al.* (2011). It is noteworthy that Lehane *et al.* (2005d) have addressed this issue ever since the formulation of UWA-05 method and pointed out that design methods that do not include an appropriate soil displacement term (e.g. A_{rs}, see White *et al.* (2005)) will tend to over-predict the capacity of full-scale offshore piles.

The same data set are also divided based on their pile end condition, that is OEP and CEP, and plotted in Figure 7.18 and Figure 7.19 respectively to indicate the variation of $\tau_{avg}/q_{c\text{-}avg}$ with the pile scale. Regardless of the end condition, $\tau_{avg}/q_{c\text{-}avg}$ of model piles are clearly higher than that of the prototype piles as shown in both figures. The observation suggests that the scale effects as reported in the literatures do exist, but are over-predicted when extrapolated from the UWA-05 method. The high sensitivity of predictions to the interface properties, the sand type, the assumed G value and its distribution, amongst others, contribute to the discrepancy. Apparently, the complete mechanisms of small-scale model piles have not been fully captured in the UWA-05 method and required further research.

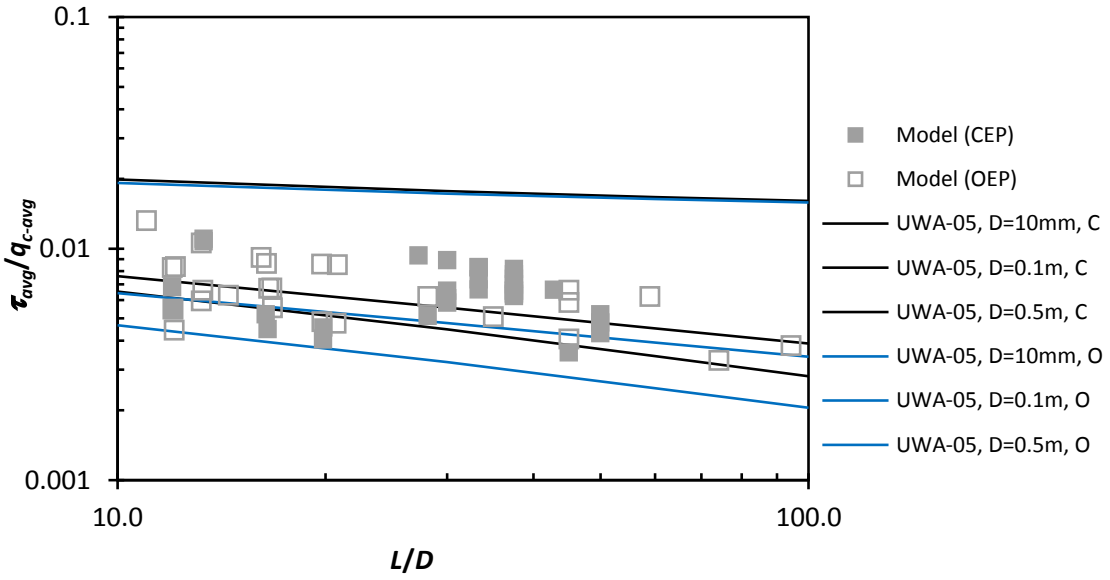

Figure 7.16. Variation of $\tau_{avg}/q_{c\text{-}avg}$ with L/D for all model-scale piles (D < 200 mm)

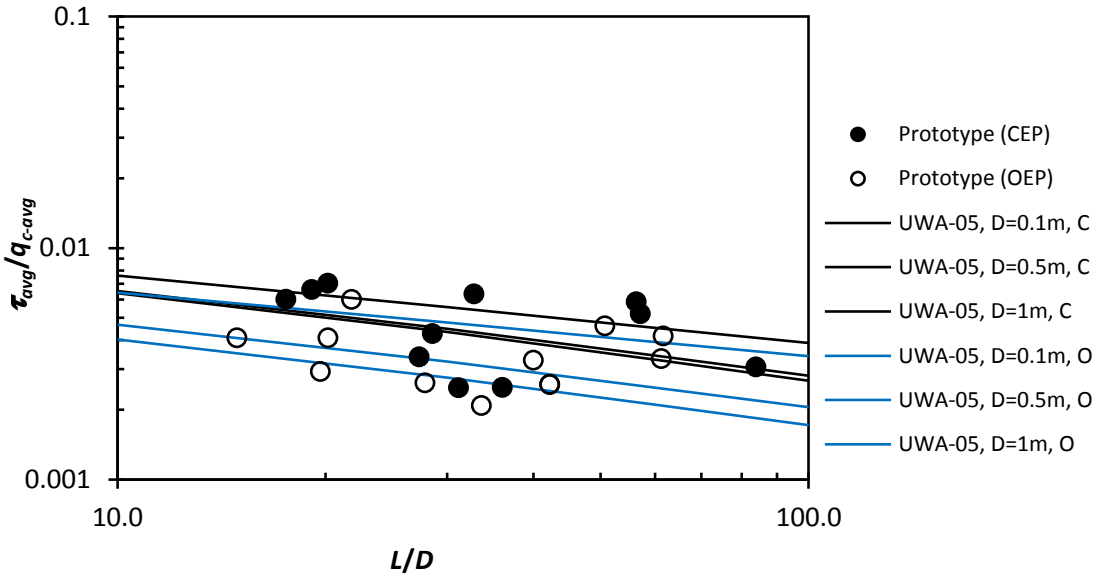

Figure 7.17. Variation of $\tau_{avg}/q_{c\text{-}avg}$ with L/D for all prototype-scale piles (D > 200 mm)

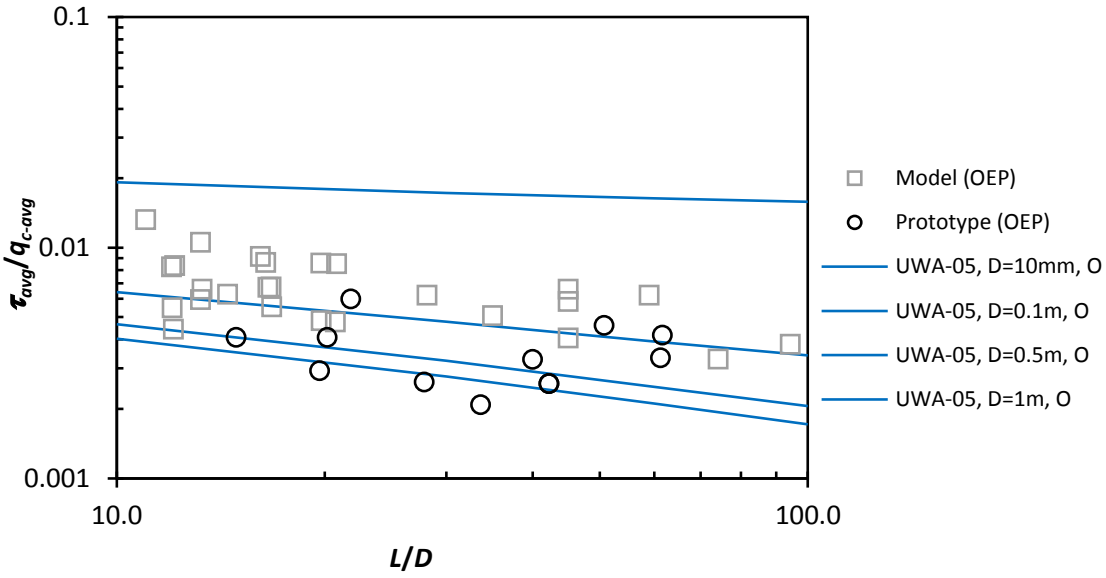

Figure 7.18. Variation of $\tau_{avg}/q_{c\text{-}avg}$ with L/D for all OEP

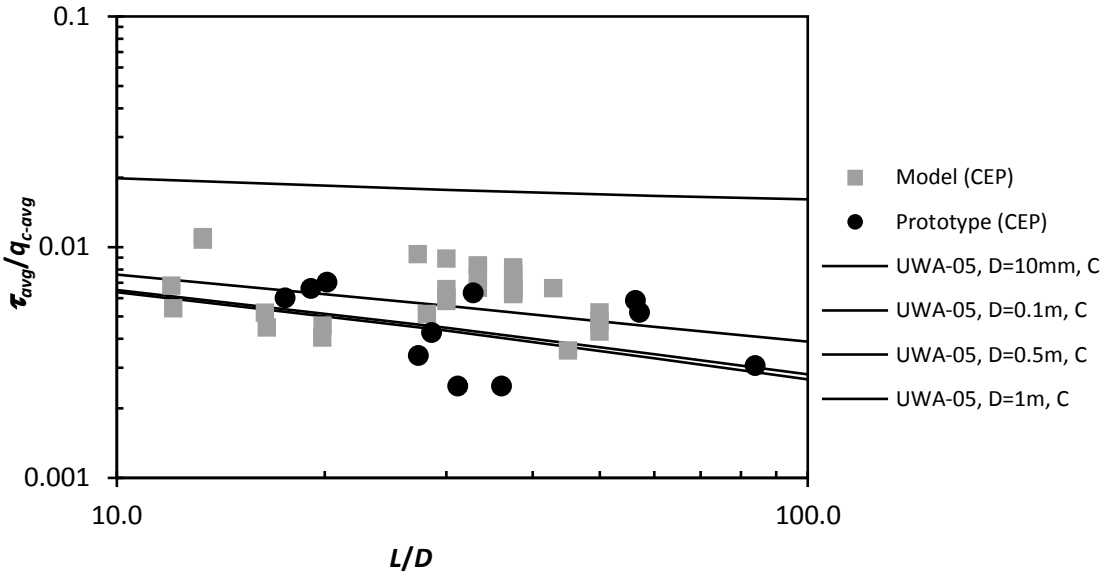

Figure 7.19. Variation of $\tau_{avg}/q_{c\text{-}avg}$ with L/D for all CEP

CHAPTER 8. CONCLUSIONS AND RECOMMENDATIONS

8.1 INTRODUCTION

This chapter summarises the main findings related to time and scale effects of pile shaft friction of displacement piles in sand using the writer's experimental investigations conducted in the field and in a pressure chamber in the laboratory. The results, combined with other well-documented case histories, after examination, yield further insights on these longstanding contentious phenomena. The conclusions on time and scale effects are presented in separate sections, and this is followed by suggestions for future research.

8.2 CONCLUSIONS

8.2.1 Time Effects

The majority of the case histories included in existing databases investigating pile set-up in sand were assessed from dynamic load tests and involved capacities determined from pile re-tests. A variety of factors contribute to uncertainties in quantifying the degree of set-up and in understanding the factors contributing to the phenomenon. While the observations are widely scattered, they do indicate a general tendency for an increase in shaft capacity with time, i.e. set-up. "True" set-up is ideally measured in a set of 'fresh' or 'virgin' (first-time loaded) static tension load tests conducted to full failure at various ageing periods. Little data of this nature have been published to date.

Conclusions from laboratory experiments

One component of this research project examined pile set-up in a small-scale model pile test programme conducted in a pressure chamber. Important improvements to previous laboratory studies of set-up include quantification of the separate (and potentially interfering) sample ageing effect, investigation of the influence of the installation method and examination of the impact of pile diameter and surface roughness. All tests measured virgin shaft capacities and involved testing to full ultimate conditions. The key findings of these experiments are as follows:

- The increases in pile shaft resistance with time revealed by the displacement piles (jacked and driven; low-intermediate and fully rough shaft surfaces) were not observed for buried piles tested under the same conditions. It may therefore be concluded that pile set-up is related to the disturbance caused by installation.

- The rate of set-up for driven piles is higher than that of monotonically jacked piles, suggesting that piles imparting greater disturbance to the sand during installation (e.g. friction degradation, vibration) show greater levels of set-up.

- The changes of pile shaft friction with time following installation does not follow a simple logarithmic time function. A delay during the initial period has been observed before significant increases in pile shaft friction were recorded.

- The ultimate shaft resistances of the re-tested piles, in particular the pure tension re-tests (T-T), are smaller but stiffer and reach ultimate conditions at lower displacements than the 'fresh' piles tested for the first time at a comparable set-up period.

- Greater set-up is observed for the larger diameter chamber pile despite the expectation of a reduction in the dilation component of shaft resistance as the pile diameter increases.

- Under very low vertical stress, representative of the sand deposits close to ground surface, the pile shaft friction appears to decrease slightly with time. This absence of positive set-up at very low stresses reflects the contribution of surrounding stresses in stimulating the stress equilibration process following installation disturbance.

- Little or no corrosion was observed on the model piles after their extraction indicating that corrosive effects are not the primary contributor to the increase in pile shaft resistance. Minor corrosion effects were observed close to the surface where there was greater exposure to oxygen.

Conclusions from field piles (incorporating SSTs)

The results of field experiments conducted for this research project have added significantly to the existing database of *reliable* case histories for pile set-up in sand. The measured evolution of the shaft stresses recorded by the SSTs during the pile test programme (including installation, equilibration and load testing stages) provides useful insights on the underlying mechanisms of pile ageing phenomenon. The key findings of these (jacked pile) experiments are as follows:

- Ageing of shaft friction for the jacked piles in the field experiments (assessed from the capacity change over time with reference to the initial 1-day capacity) is generally insignificant compared to that of the driven piles (as seen, for example, in the chamber tests and discussed later).

- The mechanisms controlling the time-dependent behaviour of pile shaft friction in sand (installed using same jacking procedures) are influenced by the mineralogy and ageing/cementation characteristics of the sand bed.

- The shaft capacity of a jacked pile tested one day of installation can be up to double of that recorded during the last installation push, i.e. there is very short-term set-up for the jacked piles.

- Continuous monitoring of the changes of stationary radial effective stresses (σ'_{rs}) measured by the SST from the last installation push until the next day indicates a gradual increase in σ'_{rs} over this (short-term) period. Subsequent monitoring of the σ'_{rs} up to a maximum of 72 days shows that the overall increases in σ'_{rs} are relatively small and occurred almost entirely within one day of installation.

- While σ'_{rs} increases are small, significant increases in radial effective stress during shearing ($\Delta\sigma'_{rd}$) within a day following installation disturbance are observed (average at 80% of total increment). The observation suggests that the major underlying mechanism of pile set-up in sand is that of constrained dilation due to an increase in the shear stiffness of the surrounding soil following installation disturbance.

- Very low gains in shaft friction were revealed by the SSTs on the 65 mm and 100 mm diameter piles after one day. However, the SST on the135 mm diameter pile showed greater set-up (increased by up to 50% after one month) possibly because it was located at a lower number of pile diameters above the pile tip – a zone with higher relative stress levels and with higher potential for set-up as observed in previous investigations (e.g. Chow *et al.*, 1998; Kolk *et al.*, 2005b).

- More significant capacity gain was observed in the calcareous sand at Ledge Point than at Shenton Park suggesting a slower (ageing) response of weak and angular particles in the stress equilibration process. While the majority of the strength and stiffness recovery was completed within a day at Shenton Park, only a small portion was recovered after 1 day at Ledge Point. A similar response was observed by Bowman and Soga (2005) in the triaxial creep experiments.

- Greater set up was exhibited by the jacked piles at South Perth than at Shenton Park suggesting an influence of environmental cyclic loading from tidal fluctuations at South Perth; this trend is consistent with the hypothesis proposed by Jardine *et al.* (2006) and others. Environmental factors such as the existence of groundwater and tidal fluctuations are not believed to be the root cause of the pile set-up phenomenon, but could enhance or accelerate the processes. The difference could have also been contrasted by the unusual characteristics of Shenton Park sand, which exhibits light cementation and/or suction effects that have hindered a complete soil flow mechanism during penetration.

- Signs of corrosion were observed when the aged pile at South Perth (in saturated sand site) was extracted 9 days after installation. The rust had started to develop on the pile shaft at around 1.5 m depth, where alternating wet and dry cycles occurred due to tidal effects, while no physical changes were noticed on the remainder of the pile shaft. The fact that set-up has been observed in different pile materials (e.g. concrete, steel, timber) and the inconsistency found by Chow *et al.* (1998) between the area of corrosion and the changes of shear stress

distribution measured over time suggests that corrosion is not the principal cause of pile set-up in sand.

- A noticeable bonding of sand particles (up to ≈ 5 mm thick) was found on much of the (molybdenum) steel casings, but no particles were observed to have bonded to the (relatively inert) stainless steel SSTs at both Shenton Park and Ledge Point (unsaturated sand sites) after being in the ground for a period of one month. The increasing shaft surface roughness tends to force the shearing failure to take place at a sand-sand interface rather than a sand-steel interface, which would give rise to a larger interface friction angle accompanied by a higher level of dilation. This may contribute to some small degree of set-up but is unlikely to be a major contributor especially for the large diameter full-scale piles.

Conclusions based on the entire database

The results obtained from both field and chamber tests, in concert with previous experimental observations, confirm that pile set-up is closely related to the level of pile installation disturbance. The increases in pile shaft resistance with time appear to be negligible for the buried/bored piles, rather small for the jacked piles and significantly larger for the impact driven piles. Detailed investigations, assisted greatly by a parallel series of tension load tests on driven piles at Shenton Park (noting the uncertainties of the re-tested capacities employed), lead to an improved characterisation of the set-up phenomenon as follows:

- Instead of capacity gain, the phenomenon of pile set-up is better defined as a process of strength and stiffness recovery following installation disturbance. In some cases, a stronger set-up response could simply be a reflection of more severe disturbance during pile installation.

- None of the pile design methods has considered the effects of time on pile shaft friction explicitly. The speculation of ICP predictions to match the medium-term capacity at around 50 days of pile age (Jardine and Chow, 1996) or more recently 10 days for the first-time loaded ‘fresh’ piles (Jardine *et al.*, 2005), for

instance, is tentative and likely to vary with factors such as the pile end conditions, driving procedures and local ground conditions.

- The existing characterisation approach (Skov and Denver, 1988), which employs a logarithmic time function and adopts an initial capacity measured shortly after installation as the reference, is flawed and could be misleading. The set-up factor A is highly sensitive to the initial reference time when the first reference test is conducted. Poorly defined t_o during EOID in the dynamic load tests aggravates the uncertainties.

- An alternative approach also assumes ageing to vary with the logarithm of time but normalises the shaft friction with the capacity estimated based on a pile design method, thereby accounting for the overall effects of local variations in ground conditions (Jardine *et al.*, 2006). The set-up factor B derived from this semi-log plot is more consistent but varies with the levels of installation disturbance assumed as a constant in a design method.

- A new characterisation approach is proposed here, which normalised the measured shaft friction by a projected upper limit of the shaft resistance estimated from the UWA-05 method. This UWA limit capacity (τ_{lim}) assumes a parameter c equal to -0.1, which represents the minimum anticipated friction fatigue for a displacement pile. The representation is consistent with the expectation that set-up is a recovery process and reveals distinctive trends for displacement piles subjected to differing degrees of (installation) disturbance.

- The new representation of pile set-up behaviour can be modelled using a (monomolecular) model for limited growth phenomenon (Seber and Wild, 2003) to represent the time-dependent relationship. The proposed correlation captures the degree of disturbance imparted from pile installation and the rate of recovery seen at Shenton Park (jacked and driven pile tests) and for the GOPAL project at Dunkirk (Jardine *et al.*, 2006). Moreover, it incorporates a *delay* of set-up during the initial period and a *limit* after full stress equilibration is reached, which experimental observations indicate to have occurred after about a year.

This research suggests a better definition for the phenomenon of pile set-up in sand and demonstrates some important characteristics of set-up with respect to the influence of installation method, ambient stress, environmental cyclic loading, sand mineralogy, diameter effects, etc. that greatly assists in the understanding of time effects on pile shaft friction. The principal underlying mechanism leading to the changes of pile shaft friction, which is the increase in constrained dilation over time following installation, is suggested and a new representation of capacity variation with time is proposed.

8.2.2 Scale Effects and the UWA-05 Method

The competing effects of dilation and friction fatigue complicate the assessment of scale effects on pile shaft friction. In spite of numerous studies were pursued, no satisfactory means of extrapolating the results from model piles to full-scale piles has emerged. Previous investigations were constrained by a limited range of pile diameters employed in each testing environment. In this research, a database comprising reliable load test results on driven piles with diameters differing by more than two orders of magnitude was established for assessment. The UWA-05 method is adopted as a base calculation approach and this is also compared with the existing CPT alpha methods. Results of the assessment suggest that:

- The $\tau_{avg}/q_{c\text{-}avg}$ ratios for all the test data vary with D and with L/D in a similar fashion to that predicted by UWA-05 method. However, $\tau_{avg}/q_{c\text{-}avg}$ ratios for the model scale piles are over-predicted by UWA-05 by a factor of about 2.

- While the difference between OEP and CEP is hardly discernible at the model scale, the $\tau_{avg}/q_{c\text{-}avg}$ ratios of OEPs are in general slightly lower than CEPs at prototype scale; this is in agreement with the UWA-05 prediction with respect to the plugging effect in OEPs. The UWA-05 prediction for OEPs in dense sand is reasonable and does not seem to be overly conservative as claimed by Gavin *et al.* (2011).

- Regardless of the end condition, the $\tau_{avg}/q_{c\text{-}avg}$ ratios of model piles are higher than those of prototype piles. The observation suggests that the scale effects as reported in the literatures do exist, but are over-predicted when extrapolated using the UWA-05 method to laboratory-scale piles. The high sensitivity of

predictions to the interface properties, the sand type, the assumed G value and its distribution, amongst other factors, are likely to have contributed to the discrepancy.

- The recommendations from CPT alpha methods (except Dutch practice) do not differ significantly from the UWA-05 predictions at typical L/D values adopted for most piling projects. However, the CPT alpha methods do not account for the scale effects explicitly, which may be un-conservative for large diameter piles.

- The recommendation, in many methods, of lower α_s values ($= q_c/\tau$) in sand deposits with low q_c values is in agreement with the tendency of decreasing $\tau_{avg}/q_{c\text{-}avg}$ with L/D predicted by the UWA-05 method (noting that q_c is generally lower where L or L/D is lower).

- At constant L, the $\tau_{avg}/q_{c\text{-}avg}$ ratios decrease with increasing D for the small-scale piles but increase with increasing D for the full-scale piles, with the transition taking place at around D = 200 mm and D = 90 mm in medium dense and dense sands, respectively. The changes predicted by the UWA-05 method are attributed to the complicating relative influence from stationary component (τ_s) and dilation component (τ_d) of the pile shaft friction at different diameters.

- At constant L/D, UWA-05 method predicts the $\tau_{avg}/q_{c\text{-}avg}$ ratio to decrease with increasing D for all scales of piles. The decreases, which are attributed to the dilation term, are remarkably large for the small-scale piles but become negligible for the full-scale piles. The increases in shaft capacity with diameter projected by Knudsen *et al.* (2012) for UWA-05 emerge because they assumed piles of constant length, L.

The assessment of scale and diameter effects on pile shaft friction using an expanded database comprising a wide range of pile scales provide further insights on the complex phenomenon. Amendments for time effects and for the varying influence of the installation method on data sets from different sources are crucial to the generalised interpretation presented here. Examination of the UWA-05 method indicates that the prediction of full-scale offshore piles is reasonable but the capacity of small-scale model

piles is over-predicted and requires a more complex treatment of the non-linear interaction between the shear zone and shear stiffness of the sand mass surrounding the pile shaft.

8.3 FURTHER RESEARCH

This research has demonstrated some new insights into the complex time and scale effects of displacement piles in sand. The hypotheses, however, involve various inferences and assumptions based on limited number of reliable data, which require further verification. Additional research necessary to advance the findings of this thesis is presented below:

- Observations of pile set-up derived from first-time statically loaded pile tests are scarce. More *reliable* pile tests (preferably at full-scale) are required to further corroborate the new characterisation approach proposed in this thesis and refine the set-up characteristics (defined as degree of disturbance and rate of recovery) for a variety of practical conditions.

- The experimental evidence suggests that for essentially the same pile type and dimension installed at the same site, the use of a different driving hammer could result in distinctively different short to medium term pile capacity and subsequent set-up behaviour. An investigation into the resultant penetration (and associated rebound) and the dynamic pile-soil interaction (loosening or densification effects) following each impact driving force, such as an advanced pile driveability analysis, may facilitate the quantification of pile installation disturbance.

- In contrast to driven piles, jacked piles are usually (*i*) installed in a significantly smaller number of loading-unloading cycles and (*ii*) subjected to much smaller vibrations. Discrepancies between the behaviour of jacked and driven piles are recognised and often attributed to the effects of installation method in general. It is important to clarify the relative influence of each component to unveil the governing mechanism of jacked and driven piles. Such research is beneficial to understanding the behaviour of vibratory driven piles that have gained recent popularity (e.g. Middendorp and Verbeek, 2012).

- Time effects for piles in sand have been treated separately from those in clay (e.g. Karlsrud, 2012). Although the underlying mechanisms and controlling parameters for piles installed in both materials are different, it is desirable to explore if their global responses following installation disturbance could be modelled using the same framework. This would facilitate the account of set-up effects for all natural soil deposits.

- High quality pile instrumentation is important to unveil the underlying processes of the pile set-up phenomenon. The local set-up concluded from the field tests at Shenton Park involved differing diameters of piles with single SSTs, each located at a different h/D. A more complete shaft stress distribution and its variation with time could be established by having multiple sensors fixed at several depths and monitored over a longer period.

- The current formulation of the UWA-05 method (similar to ICP-05 method) incorporates a dilation component that is deduced from a cavity expansion analogy, with assumptions that are known to incur compensating errors but result in reasonable estimates for full-scale piles. Calibration against the small-scale model piles in this thesis suggests that the UWA-05 method overestimates the shaft capacity of small diameter pile significantly. Further investigation is required to model the (non-linear) shear stiffness of the sand mass surrounding the pile shaft using a more complex representation.

APPENDIX A

This Appendix presents some details of the SST calibration and its performance. The SST was developed at Imperial College in collaboration with Cambridge Insitu. The 100 mm diameter SST was borrowed from Imperial College London (ICL) while two other new SSTs in the diameters of 65 mm and 135 mm were ordered from Cambridge Insitu for The University of Western Australia (UWA). The SSTs share the same design and were subjected to similar calibration procedures as described in the following. General description of the SSTs and other components of the instrumented piles are discussed in Section 4.2.

In order to apply both shearing and compression forces onto the loading platen simultaneously (to represent shear stress (τ) and radial stress (σ_r) respectively), a special calibration rig, similar to that employed by Bond (1989), was constructed with modifications made to accommodate the three different sizes of SSTs used in this study (Figure A1(a)).

The calibration procedures employed were in general similar to those outlined by Bond *et al.* (1991a). Given the loose to medium dense sand encountered at the testing sites visited for this research project and the shorter length (thus lower stress level) of the instrumented piles available, calibration for the eccentric loading condition and under high air/water pressure was considered optional. For the same reason, the transducers were calibrated to smaller maximum radial and shear stresses of 200 kPa and 100 kPa, respectively.

The calibration consisted of two main stages as described below. Before the calibration commenced, the SSTs were subjected to series of exercises under sustained loading and rapid cycling conditions to minimise the zero drift, non-linearity and hysteresis problems. After the calibration was completed, stability of the SSTs was further inspected by sustaining a presumed working load to a longer period to examine its potential of creep.

Figure A1. Calibration of the SSTs: (a) application of shearing and compression forces on the loading platen; (b) 135 mm, 100 mm and 65 mm diameter SSTs with top caps; (c) calibration of axial load sensitivity (in tension) using a Baldwin loading machine

Stage I: Shear Calibration

- Shear stress was varied between ±100% while keeping radial stress at 100%.
- Shear stress was varied between ±100% while keeping radial stress at 80%.
- Shear stress was varied between ±100% while keeping radial stress at 60%.
- Shear stress was varied between ±100% while keeping radial stress at 40%.

Stage II: Radial Calibration

- Radial stress was varied from 0 to 100% while keeping shear stress at 40%.
- Radial stress was varied from 0 to 100% with zero shear stress.

Considering the cross-sensitivity between the strain gauges distributed over the shear webs and radial pillars of the 'dogbone' Cambridge earth pressure cell, the relationship between the applied forces (represented as σ_r and τ) and the output signals (radial 1, radial 2 and shear) can be expressed by the following equations:

$$\sigma_r = c_{11}[0.5(V_o/V_i)_{r1} + 0.5(V_o/V_i)_{r2}] + c_{12}(V_o/V_i)_s \quad \text{(A-1)}$$

$$\tau = c_{21}[0.5(V_o/V_i)_{r1} + 0.5(V_o/V_i)_{r2}] + c_{22}(V_o/V_i)_s \quad \text{(A-2)}$$

where c_{ij} are the calibration coefficients; V_o and V_i are the output and input voltages respectively (V_i = 5 volts); and the subscripts *r* and *s* refer to the radial and shear circuits respectively. The calibration coefficients together with correcting factors, which are described below, are summarised in Table A1.

The stresses were further corrected for three factors: (*i*) zero drift, (*ii*) axial load sensitivity, and (*iii*) temperature sensitivity, which were known to influence the accuracy of the measurement. The zero readings of the transducers recorded during calibration (and later confirmed in field experiments) show that the mean zero drifts of radial stress measurements for the 65 mm, 100 mm and 135 mm diameter SSTs are approximately ±3.3 kPa, ±3.5 kPa and ±3.0 kPa, respectively. Accordingly, the mean zero drifts of shear stress measurements were recorded as ±1.3 kPa, ±0.8 kPa and ±0.7 kPa, respectively. These drifts are considered negligible in comparison to the measured stresses.

The operation of the model piles (i.e. installation and tension load test) involves axial loads that would affect the shear and radial signal outputs. Therefore, the SSTs were calibrated for axial load sensitivity (compression and tension) using a Baldwin loading machine (Figure A1(c)). The results showed that the 65 mm diameter SST is more sensitive than the 100 mm and 135 mm diameter SSTs, and the response was often non-linear and exhibited hysteresis. Instead of adopting average linear correction, which is sufficient for the bigger diameter instruments, the 65 mm diameter SST was corrected using a non-linear correcting factor (Figure A2). Slight hysteretic responses of the gauges during axial loading and unloading are believed to limit the resolutions of radial and shear stresses to not better than 2 and 1 kPa, respectively.

The temperature sensitivity was assessed by continuously logging the signal outputs without any forces under room temperature in the laboratory up to one week (repeated several times over the entire testing programme). The ambient temperature change is typically around 10^{o}C for a day, which spans larger than the range of temperature difference between ground surface and down to final embedment that typically differs by less than 5^{o}C. In the ground, the daily temperature fluctuation is much smaller and has less influence on the instruments. The linear and repeatable temperature calibration greatly assisted the data interpretation particularly on the penetration profiles during installation.

Table A1. Details of calibration for the SSTs

	Radial stress	Shear stress
65 mm diameter SST		
Direct sensitivity	750.9 kPa/V	116.5 kPa/V
Cross sensitivity	15.1 kPa/V	-8.3 kPa/V
Axial load sensitivity	-1.8 kPa/kN *	0.03 kPa/kN
Temperature sensitivity	-3.0 kPa/^{o}C	-0.1 kPa/^{o}C
100 mm diameter SST		
Direct sensitivity	483.9 kPa/V	85.4 kPa/V
Cross sensitivity	-1.4 kPa/V	-2.7 kPa/V
Axial load sensitivity	-0.4 kPa/kN	0.003 kPa/kN
Temperature sensitivity	-2.5 kPa/^{o}C	0.05 kPa/^{o}C
135 mm diameter SST		
Direct sensitivity	635.2 kPa/V	131.9 kPa/V
Cross sensitivity	-30.5 kPa/V	-8.8 kPa/V
Axial load sensitivity	-0.02 kPa/kN	0.04 kPa/kN
Temperature sensitivity	-2.8 kPa/^{o}C	0.1 kPa/^{o}C

Note:

* The value is only indicative – reflecting its higher sensitivity to axial load as compared to other SSTs. A non-linear correction factor was specified to give a more accurate result.

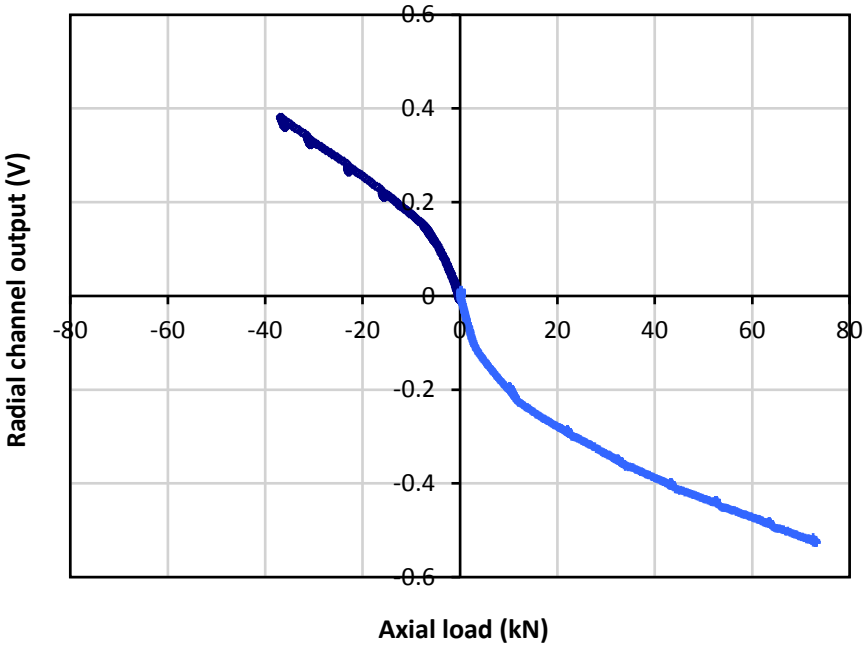

(a)

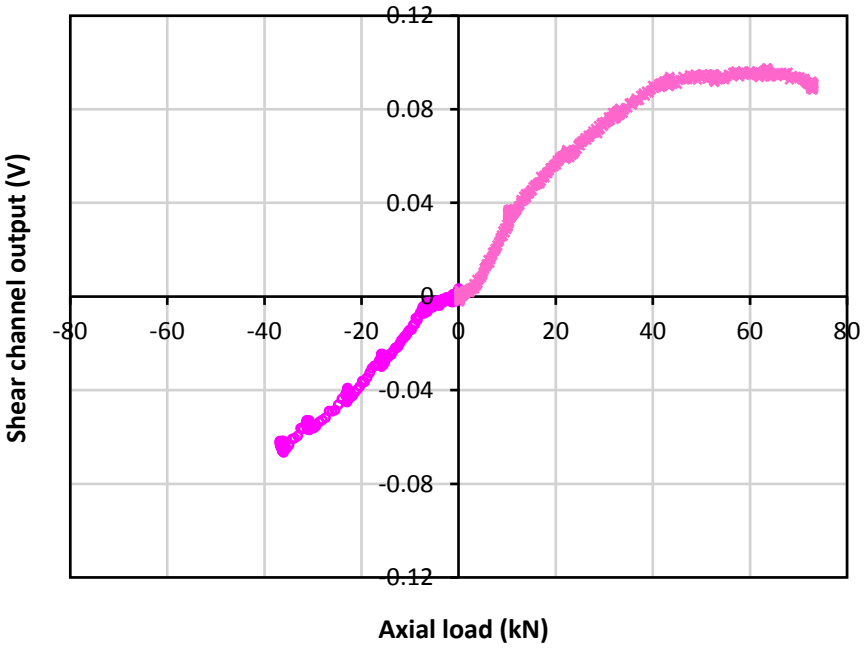

(b)

Figure A2. Calibration of axial load sensitivity for 65 mm diameter SST: (a) radial channel; (b) shear channel; positive axial load is in compression

It has been noted in Chapter 4 that model piles with a single SST will not provide a stress distribution along the pile shaft, and does not provide sufficient redundancy to identify any under-registration of SST measurements (due to cell action effects) as reported by Lehane (1992). Nevertheless, the problem is considered relatively small (e.g. ≈ 12% at Labenne) and only evident during installation and plunging failures in compression load tests. Most importantly, the systematic deficiency (if any) is unlikely to affect the time effects on pile shaft friction in this study.

APPENDIX B

As mentioned in Chapter 4, a short pile test programme involving two test piles was performed at Ledge Point – a test site that is composed of coastal dune sands with a calcium carbonate content of 90% – to investigate the behaviour of shaft friction for displacement piles in uncemented calcareous sand. The programme also comprised some assessment on the effects of sand mineralogy on pile set-up, which is further elaborated in this thesis. Findings of the investigation, which incorporated self-boring pressuremeter tests (SBPMTs) performed in close vicinity to the test piles and a parallel series of constant normal stiffness (CNS) interface tests, have been published and are provided in this Appendix.

Appendix B has been removed due to copyright restrictions.

APPENDIX C

The majority of the offshore piles worldwide are designed based on the recommended guidelines published by the American Petroleum Institute – API RP2A. Following some extensive investigations that highlighted the deficiencies of the conventional API design approach (e.g. Toolan *et al.*, 1990), four CPT-based pile design methods are now included in the commentary of the 22nd edition of the API RP 2A document (API, 2010). The four CPT-based methods are referred to as Fugro-05 (Kolk *et al.*, 2005a), ICP-05 (Jardine *et al.*, 2005), NGI-05 (Clausen *et al.*, 2005) and UWA-05 (Lehane *et al.*, 2005b). Schneider *et al.* (2008b) showed that the UWA-05 method generally has slightly better performance than others, and hence was selected for the assessment here. The ICP-05 and UWA-05 methods were employed in the analysis and interpretation in this thesis and therefore are described here for reference.

ICP Design Method

The ICP design method was developed at Imperial College London based mainly on the extensive experimental work of four consecutive PhD studies (Jardine, 1985; Bond, 1989; Lehane, 1992; Chow, 1997). The details relating to pile shaft friction in silica sand for piles loaded in tension is relevant to present study and is briefly described in the following.

In tension loading, the local shear stress acting on the pile shaft at failure follows a Coulomb failure criterion as:

$$\tau_f = \sigma'_{rf} \tan \delta_f = a(0.8\, \sigma'_{rc} + \Delta\sigma'_{rd}) \tan \delta_{cv} \qquad \text{(C-1)}$$

where σ'_{rf} is the radial effective stress at failure that depends on (*i*) σ'_{rc}, the equalised radial effective stress a few days after installation, and (*ii*) $\Delta\sigma'_{rd}$, the change in radial effective stress developed during pile loading; δ_f is the operational interface angle of friction, taken as δ_{cv} when shearing takes place at constant volume; the constant 0.8 is a reduction factor to account for smaller shaft friction when a pile is loaded in tension; and a is a correction factor for pile end condition (1 for closed-ended piles and 0.9 for open-ended piles).

The local radial effective stress after installation and equalisation is represented as:

$$\sigma'_{rc} = 0.029\, q_c \cdot \left(\frac{\sigma'_{vo}}{p_a}\right)^{0.13} \cdot \max\left(\frac{h}{R^*}, 8\right)^{-0.38} \quad \text{(C-2)}$$

$$R^* = \left(R_o{}^2 - R_i{}^2\right)^{0.5} \quad \text{(C-3)}$$

where q_c is the CPT cone tip resistance at the depth that σ'_{rc} acts, σ'_{vo}/p_a is the free-field vertical effective stress normalised by atmospheric pressure (p_a = 100 kPa), and h/R^* is the relative depth of the pile tip normalised by modified pile radius (R^*). The value of R^* depends on the outer radius (R_o) and inner radius (R_i) for open-ended pile; it equals R_o for closed-ended piles and is taken as an equivalent radius with the same end area for non-circular closed-ended piles.

The dilatant increase in local radial effective stress during pile loading is represented as:

$$\Delta\sigma'_{rd} = 2G_0 \cdot \frac{\Delta r}{R} \quad \text{(C-4)}$$

$$G_0 = q_c[0.0203 + 0.00125\eta - 1.216 \times 10^{-6}\eta^2]^{-1} \quad \text{(C-5)}$$

$$\eta = \frac{q_c}{(\sigma'_{vo} \cdot p_a)^{0.5}} \quad \text{(C-6)}$$

where G_0 is the small strain shear stiffness obtained from in-situ shear wave measurements or bender element tests in the laboratory, and Δr is the radial displacement developed in the thin interface shear zone during shearing which is a function of pile roughness (R_{cla}). In cases where reliable measurements of G_o are not available, estimates may be made from Baldi *et al.* (1989) correlation with CPT q_c as presented above. Δr is assumed equal to $2R_{cla}$ or about 0.02 mm for lightly rusted steel piles.

UWA Design Method

The UWA design method shares a similar framework with that of the ICP method but differs in a number of ways based on additional research findings such as that published by De Nicola and Randolph (1993), Gavin and Lehane (2003), Paik *et al.* (2003), White and Lehane (2004) and White *et al.* (2005). UWA-05 quantifies the influence of plugging on shaft friction for open-ended piles, allows for differing levels of friction

fatigue for jacked and driven piles and predicts a stronger reduction of radial stress than ICP-05 in tension loading.

The local shear stress at failure on the shaft of a displacement pile is expressed by UWA-05 as:

$$\tau_f = \sigma'_{rf} \tan \delta_f = \frac{f}{f_c} (\sigma'_{rc} + \Delta\sigma'_{rd}) \tan \delta_{cv} \qquad \text{(C-7)}$$

where σ'_{rf} is the radial effective stress at failure that can be separated into two major components: (*i*) σ'_{rc} is the equilibrium radial effective stress after installation and equalisation, and (*ii*) $\Delta\sigma'_{rd}$ is the increase in radial effective stress during pile loading; δ_f is the interface friction angle at failure, taken as the constant volume interface friction angle (δ_{cv}) (determined from interface shear testing or estimated from Figure C3); and f/f_c is a correction factor for the smaller shaft friction developed when a pile is loaded in tension relative to that in compression (1 for compression and 0.75 for tension).

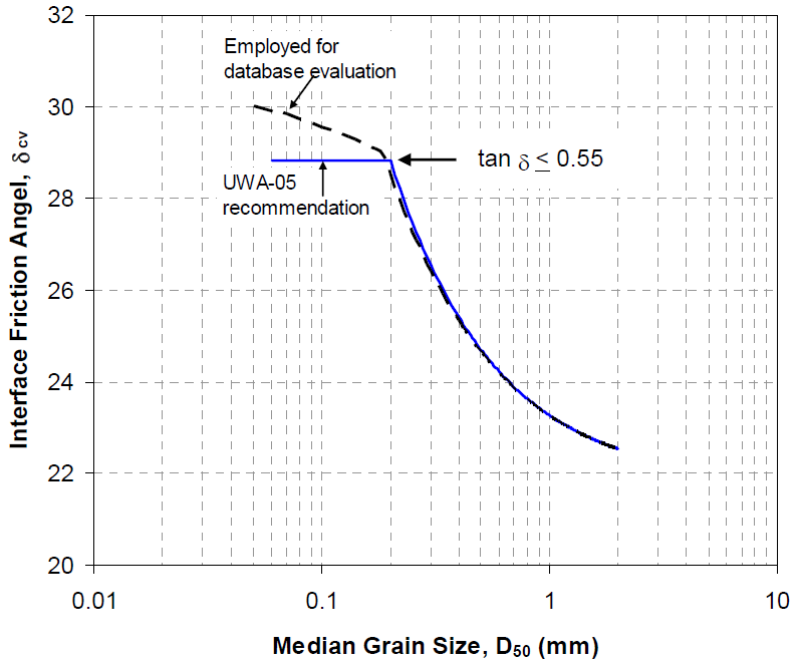

Figure C3. Variation of δ_{cv} with D_{50} (Lehane *et al.*, 2005b)

The radial effective stress after installation and equalisation is expressed as:

$$\sigma'_{rc} = \frac{q_c}{a} \cdot {A_{rs}}^{b} \cdot \max\left(\frac{h}{D}, 2\right)^{c} \quad \text{(C-8)}$$

$$A_{rs} = 1 - \mathrm{IFR}_{\mathrm{mean}} \left(\frac{D_i}{D}\right)^{2} \quad \text{(C-9)}$$

$$\mathrm{IFR}_{\mathrm{mean}} = \frac{\Delta h_p}{\Delta z_b} \text{ averaged over final } 20D \quad \text{or} \quad \mathrm{IFR}_{\mathrm{mean}} = \min\left[\left(\frac{D_i}{1.5}\right)^{0.2}, 1\right] \quad \text{(C-10)}$$

where q_c is the CPT cone tip resistance at the corresponding depth that σ'_{rc} acts, h/D is the relative depth of the pile tip (h) normalised by pile diameter (D), and A_{rs} is the effective area ratio to reflect the degree of plugging (1 for a fully plugged or closed-ended pile reducing to approximately 0.1 for fully 'coring' pile) which is a function of incremental filling ratio (IFR) and pile dimensions D and D_i (inner pile diameter, expressed in metres). The IFR is the ratio of incremental change in plug height (Δh_p) to the incremental increase in embedment depth (Δz_b), of which a mean value ($\mathrm{IFR}_{\mathrm{mean}}$) is computed as the average of IFR measured over the final 20 diameters of penetration (or estimated using the empirical correlation above in the absence of IFR measurements).

The three terms in the expression for σ'_{rc} and the associated empirical parameters a, b and c (taken as 33, 0.3 and -0.5, respectively for a driven pile) are introduced to explicitly allow for: (*i*) the effects of soil displacement as soil flows around the pile tip; (*ii*) the degree of plugging during penetration of an open-ended pile; and (*iii*) friction fatigue due to the shearing cycles imposed on given soil horizons as the pile tip penetrates to deeper level. The degree of friction fatigue for jacked piles is expected to be less severe and a value of c of -0.33 is proposed in place of the driven value of -0.5 (Lehane *et al.*, 2007).

The increase in radial effective stress during pile loading is expressed as:

$$\Delta\sigma'_{rd} = 4G \cdot \frac{\Delta r}{D} \quad \text{(C-11)}$$

$$G = q_c \cdot 185 \cdot {q_{c1N}}^{-0.7} \quad \text{(C-12)}$$

$$q_{c1N} = \frac{(q_c/p_a)}{(\sigma'_{vo}/p_a)^{0.5}} \quad \text{(C-13)}$$

where G is the operational shear stiffness of the surrounding soil that assumed to be equal to the in-situ very small strain shear modulus (G_o), and Δr is the dilation of the interface layer during shearing that approximates 2 times the pile roughness, R_{cla} (assumed as 0.02 mm for lightly rusted steel piles). The G_o value can be obtained from in-situ shear wave measurements or bender element tests in the laboratory. In the absence of reliable measurements, estimates of G_o may be made from the empirical correlation proposed by Baldi *et al.* (1989) as presented above. It is noted that these assumptions (i.e. $G = G_o$ and $\Delta r = 2R_{cla}$) are acknowledged to incur compensating errors, resulting in a reasonable estimate of $\Delta\sigma'_{rd}$.

At Shenton Park, the stiffness of the in-situ sand at various levels of strain has been evaluated by Schneider (2007) from self-boring presuremeter tests with small strain stiffnesses obtained from seismic cone and bender element tests. The ratio of shear modulus to cone tip resistance (G_o/q_c) plotted against normalised cone tip resistance (q_{c1N}) indicates that the sand exhibits some level of cementation and structuring (Rix and Stokoe, 1991; Fahey *et al.*, 2003). A site-specific correlation was derived in the form of $G_o = q_c \cdot 500 \cdot q_{c1N}^{-0.75}$. The δ_{cv} is assumed equal to 25°, estimated based on median grain size (D_{50}) and average roughness of the pile from Figure C3.

APPENDIX D

A complete description of the UWA-05 design method on pile shaft friction was provided in Appendix C. In general, the local shear stress at failure of a driven pile that is subjected to tension loading comprises two major components – the stationary term (τ_s) and the dilation term (τ_d) – which are expressed in the following:

$$\tau_f = \tau_s + \tau_d \tag{D-1}$$

$$\tau_s = 0.75\left[\frac{q_c}{33}\cdot {A_{rs}}^{0.3}\cdot\max\left(\frac{h}{D},2\right)^{-0.5}\right]\tan\delta_{cv} \tag{D-2}$$

$$\tau_d = 0.75\left[4G\cdot\frac{\Delta r}{D}\right]\tan\delta_{cv} \tag{D-3}$$

where q_c is the CPT cone tip resistance at the corresponding depth, A_{rs} is the effective area ratio that reflects the degree of plugging (1 for a fully plugged or closed-ended pile reducing to approximately 0.1 for a typical fully 'coring' pile) and h/D is the distance from the pile tip ($h = L - z$) normalised by pile diameter (D). L is the embedded length of pile and z is the depth from ground level. For full-scale offshore piles, a simplified form of UWA-05 method was proposed that omits the dilation term and assumes an unplugged condition (IFR = 1) for the open-ended piles (OEP).

The equations above indicate that τ_s and τ_d do not vary with diameter in the same way and that the relative magnitudes of these components also vary along the entire shaft length. As a result, the dominant component that governs the pile shaft resistance of small and large diameter piles is different. The relationship, however, has not been interrogated rigorously and therefore its suitability for the extrapolation to full-scale offshore piles has recently been questioned (Gavin *et al.*, 2011; Knudsen *et al.*, 2012).

The implied relationship between pile shaft friction, pile geometry and CPT-q_c value is examined in the following. Initially, this relationship is explored for a sand deposit where (*i*) q_c is constant with depth and (*ii*) q_c increases with the square root of the depth (i.e. a sand with a near constant relative density).

q_c is constant with depth

The average unit pile shaft resistance of the stationary term ($\tau_{s\text{-}avg}$) can be obtained by integrating the Equation (D-2) along the depth (z) from ground level ($z = 0$) to pile tip level ($z = L$; approximated as $0.99L$ since $h = 0$ is infinity in the base function) and divided by the pile length (L). A simple idealisation is made by assuming q_c is constant with depth and there is no limitation on the value of shear stress developed over the bottom $2D$ of the shaft (i.e. h/D $_{\text{minimum}}$ is approximating zero). The relationship for the stationary term is expressed as follows (where all the K used in the following derivations are constant):

$$\tau_{s-avg} = \left(0.75 \cdot \frac{q_c}{33} \cdot \tan\delta_{cv}\right) \cdot \frac{1}{L} \int_0^{0.99L} \left(\frac{L-z}{D}\right)^{-0.5} dz$$

$$= q_c \cdot K_1 \cdot \frac{D^{0.5}}{L} \int_0^{0.99L} \left(\frac{1}{L-z}\right)^{0.5} dz$$

$$= q_c \cdot K_1 \cdot \frac{D^{0.5}}{L} \left[-\frac{(L-z)^{0.5}}{0.5}\right]_0^{0.99L}$$

$$\cong q_c \cdot K_1 \cdot \frac{D^{0.5}}{L} [2 \cdot L^{0.5}]$$

$$\cong q_c \cdot 2K_1 \cdot \frac{1}{\left({}^{L}/_{D}\right)^{0.5}}$$

$$\frac{\tau_{s-avg}}{q_{c-avg}} \cong 2K_1 \cdot \frac{1}{\left({}^{L}/_{D}\right)^{0.5}}$$

$$\therefore \frac{\tau_{s-avg}}{q_{c-avg}} \propto \frac{1}{\left({}^{L}/_{D}\right)^{0.5}}$$

For constant q_c in this case, $q_{c\text{-}avg}$ is equal to q_c and the ratio of $\tau_{s\text{-}avg}$ or $\tau_{s\text{-}avg}/q_{c\text{-}avg}$ (a better representation which will be explained later) has the same relationship with respect to L, D and L/D. The expression, which represents shaft friction for full-scale

offshore piles (where the effects of dilation are ignored; $\tau_{avg} = \tau_{s\text{-}avg}$), suggests that, for UWA-05:

- $\tau_{avg}/q_{c\text{-}avg}$ is inversely proportional to L/D
- At constant L/D, $\tau_{avg}/q_{c\text{-}avg}$ remains unchanged with either D or L
- At constant D, $\tau_{avg}/q_{c\text{-}avg}$ is inversely proportional to L
- At constant L, $\tau_{avg}/q_{c\text{-}avg}$ is directly proportional to D

However, the effect of dilation for model-scale piles is significant and should be considered. As for constant q_c assumed in this case, an equivalent G value can be taken as a constant. The relationship of the dilation component can then be expressed as:

$$\tau_{d-avg} = \left(0.75 \cdot 4G \cdot \frac{\Delta r}{D} \cdot \tan\delta_{cv}\right) \cdot \frac{1}{L} \int_0^L dz$$

$$= K_2 \cdot \frac{1}{D \cdot L}[L]$$

$$= K_2 \cdot \frac{1}{D}$$

$$\frac{\tau_{d-avg}}{q_{c-avg}} = K_3 \cdot \frac{1}{D}$$

$$\therefore \frac{\tau_{d-avg}}{q_{c-avg}} \propto \frac{1}{D}$$

It can be seen that the normalised dilation term in UWA-05 is inversely proportional to D, regardless of L and L/D. The different relationship with D of the stationary term and the dilation term must therefore be compensatory, complicating the overall tendency.

q_c increases in proportion to the square root of depth

A more realistic idealisation is to assume q_c increases in proportion to the square root of depth, which approximates a constant relative density (D_r) based on many widely

adopted correlations (e.g. Jamiolkowski *et al.*, 2001). Following the same procedure and simplification, the relationship can be established as follows:

$$\tau_{s-avg} = (0.75 \cdot \tan\delta_{cv}) \cdot \frac{1}{L} \int_0^{0.99L} \left(\frac{K_4 \cdot z^{0.5}}{33}\right)\left(\frac{L-z}{D}\right)^{-0.5} dz$$

$$= K_1 \cdot K_4 \cdot \frac{D^{0.5}}{L} \int_0^{0.99L} \left(\frac{z}{L-z}\right)^{0.5} dz$$

$$= K_1 \cdot K_4 \cdot \frac{D^{0.5}}{L} \left[-L \sin^{-1}\left(\sqrt{1-\frac{z}{L}}\right) - \sqrt{z(L-z)}\right]_0^{0.99L}$$

$$\cong K_1 \cdot K_4 \cdot \frac{D^{0.5}}{L}\left[\frac{\pi}{2} \cdot L\right]$$

$$\cong \frac{\pi}{2} \cdot K_1 \cdot K_4 \cdot D^{0.5}$$

$$q_{c-avg} = \frac{1}{L} \int_0^{L} (K_4 \cdot z^{0.5}) dz$$

$$= \frac{K_4}{L} \int_0^{L} (z^{0.5}) dz$$

$$= \frac{K_4}{L}\left[\frac{L^{1.5}}{1.5}\right]$$

$$= \frac{K_4}{1.5} \cdot L^{0.5}$$

$$\frac{\tau_{s-avg}}{q_{c-avg}} \cong \frac{\pi}{2} \cdot 1.5K_1 \cdot \frac{D^{0.5}}{L^{0.5}}$$

$$\therefore \frac{\tau_{s-avg}}{q_{c-avg}} \propto \frac{1}{\left({}^{L}/_{D}\right)^{0.5}}$$

For q_c that increases with the square root of depth, the corresponding G value in the dilation term can be approximated as a function effective vertical stress (σ'_v), which is essentially a function of the square root of the depth as expressed in the following:

$$\tau_{d-avg} = \left(0.75 \cdot 4 \cdot \frac{\Delta r}{D} \cdot \tan\delta_{cv}\right) \cdot \frac{1}{L} \int_0^L (K_5 \cdot z^{0.5}) dz$$

$$= K_6 \cdot \frac{1}{D \cdot L}\left[\frac{L^{1.5}}{1.5}\right]$$

$$= \frac{K_6}{1.5} \cdot \frac{L^{0.5}}{D}$$

$$\because q_{c-avg} = \frac{K_4}{1.5} \cdot L^{0.5}$$

$$\frac{\tau_{d-avg}}{q_{c-avg}} = K_7 \cdot \frac{1}{D}$$

$$\therefore \frac{\tau_{d-avg}}{q_{c-avg}} \propto \frac{1}{D}$$

As q_c is increasing with depth at a constant D_r in this case, different length of interest corresponds to a different value of $q_{c\text{-}avg}$, and result in different values of τ_{avg}. Therefore, it is important to normalise the τ_{avg} with $q_{c\text{-}avg}$ to represent a more consistent relationship and ensure a valid comparison between different cases.

It is interesting to note that the assumption of q_c increasing in proportion to the square root of depth leads to exactly the same relationship (both stationary and dilation terms) seen earlier for the case of a constant q_c. However, the increasing q_c always leads to a higher ratio of $\tau_{s\text{-}avg}/q_{c\text{-}avg}$ than that of the constant q_c (at comparable $q_{c\text{-}avg}$) given the embedded power law degradation function that reserves more weightage to the lower section of pile shaft. In addition, the derivation shows that UWA-05, in the absence of effects of dilation, predicts no significant effect of relative density on the $\tau_{avg}/q_{c\text{-}avg}$ ratio.

REFERENCES

Afifi, S.S., and R.D. Woods (1971) "Long-term pressure effects on shear modulus of soils," *Journal of the Soil Mechanics and Foundations Division*, Vol. 97, No. 10, pp 1445-1460.

Airey, D.W., R.H. Al-Douri, and H.G. Poulos (1992) "Estimation of pile friction degradation from shearbox tests," *ASTM geotechnical testing journal*, Vol. 15, No. 4, pp 388-392.

Al-Douri, R.H., and H.G. Poulos (1992) "Static and cyclic direct shear tests on carbonate sands," *ASTM geotechnical testing journal*, Vol. 15, No. 2, pp 138-157.

Al-Mhaidib, A.I., and T.B. Edil (1998) "Model tests for uplift resistance of piles in sand," *ASTM geotechnical testing journal*, Vol. 21, No. 3, pp 213-221.

Alawneh, A.S., and A.I. Husein Malkawi (2000) "Estimation of post-driving residual stresses along driven piles in sand," *ASTM geotechnical testing journal*, Vol. 23, No. 3, pp 313-326.

Alawneh, A.S., A.I.H. Malkawi, and H. Al-Deeky (1999) "Tension tests on smooth and rough model piles in dry sand," *Canadian geotechnical journal*, Vol. 36, No. 4, pp 746-753.

Alawneh, A.S., O.K. Nusier, and M.S. Awamleh (2009) "Time dependent capacity increase for driven pile in cohesionless soil," *Jordan Journal of Civil Engineering*, Vol. 3, No. 1, pp 1-31.

Allersma, H.G.N. (1988) "Optical analysis of stress and strain surrounding the tip of a penetration probe," In: J. De Ruiter, Ed., *Proc. 1st Int. Symp. on Penetration Testing (ISOPT-1)*. Orlando, pp 615-620.

Anderson, D.G., and K.H. Stokoe (1978) "Shear modulus: A time-dependent soil property," *Dynamic Geotechnical Testing, ASTM STP 654*, pp 66-90.

API (2010) "Recommended Practice for Planning, Designing and Constructing Fixed Offshore Platform-Working Stress Design, API RP 2A-WSD, 21st Edition." Washington, DC: API Publishing Services.

AS-2159 (2009) "Piling–Design and Installation." Sydney, NSW: Standards Australia Limited.

Åstedt, B., L. Weiner, and G. Holm (1992) "Increase in bearing capacity with time for friction piles in silt and sand," *Proc. Nordic Geotech. Meeting*, pp 411–416.

Åstedt, B., L. Weiner, and G. Holm (1994) "Friktionspålar: bärförmågans tillväxt med tiden," *Rapport 91*. Sweden: Commission on Pile Research.

ASTM-D4945 (2012) "Standard Test Method for High-Strain Dynamic Testing of Deep Foundations." West Conshohocken, PA: ASTM International.

Attwooll, W.J., D.M. Holloway, K.M. Rollins, M.I. Esrig, S. Sakhai, and D. Hemenway (1999) "Measured pile setup during load testing and production piling: I-15 Corridor Reconstruction Project in Salt Lake City, Utah," *Transportation Research Record: Journal of the Transportation Research Board*, Vol. 1663, No. 1, pp 1-7.

Axelsson, G (2000) "Long-term set-up of driven piles in sand." Stockholm, Sweden: Royal Institute of Technology.

Axtell, P.J., J.W. Owen, and S.D. Vollink (2004) "Increase in pile capacity with time in Missouri River alluvium," In: S. Prakash, Ed., *Proc. 5th Int. Conf. on Case Histories in Geotech. Engng*. New York, NY: Center for Infrastructure Engineering Studies, University of Missouri-Rolla, p Paper No. 1.47.

Baldi, G., R. Belottini, V.N. Ghionna, M. Jamiolkowski, and D.C.F. Lo Presti (1989) "Modulus of sand from CPT's and DMT's," *Proc. 12th Int. Conf. on Soil Mech. Foundation Engng*. Rio de Janeiro, pp 165-170.

Baxter, C.D.P., and J.K. Mitchell (2004) "Experimental study on the aging of sands," *Journal of Geotechnical and Geoenvironmental Engineering*, Vol. 130, No. 10, pp 1051-1062.

BCP_Committee (1971) "Field tests on piles in sand," *Soils and foundations*, Vol. 11, No. 2, pp 29-49.

BD (2004) "Code of Practice for Foundations." Kowloon, Hong Kong: Buildings Department, The Government of the Hong Kong Special Administrative Region.

Beringen, F.L., D. Windle, and W.R. Van Hooydonk (1979) "Results of loading tests on driven piles in sand," *Recent developments in the design and construction of piles*. ICE, London, England, pp 213-225.

Bolton, M.D., and C.K. Lau (1988) "Scale effects arising from particle size," *Centrifuge 88*. Paris, pp 127-131.

Bolton, MD, MW Gui, J. Garnier, JF Corte, G. Bagge, J. Laue, and R. Renzi (1999) "Centrifuge cone penetration tests in sand," *Géotechnique*, Vol. 49, No. 4, pp 543-552.

Bond, A.J. (1989) "Behaviour of displacement piles in overconsolidated clays." London: University of London (Imperial College).

Bond, A.J., R.J. Jardine, and J.C.P. Dalton (1991a) "Design and performance of the Imperial College instrumented pile," *ASTM geotechnical testing journal*, Vol. 14, No. 4, pp 413-424.

Bond, AJ, RJ Jardine, and JCP Dalton (1991b) "Design and performance of the Imperial College instrumented pile," *ASTM geotechnical testing journal*, Vol. 14, No. 4, pp 413-424.

Boulon, M., and P. Foray (1986) "Physical and numerical simulation of lateral shaft friction along offshore piles in sand," *Proc. 3rd Int. Conf. on Numerical Methods in Offshore Piling*. Nantes, France, pp 127-147.

Bowman, E.T., and K. Soga (2003) "Creep, ageing and microstructural change in dense granular materials," *Soils and foundations*, Vol. 43, No. 4, pp 107-117.

Bowman, E.T., and K. Soga (2005) "Mechanisms of setup of displacement piles in sand: laboratory creep tests," *Canadian geotechnical journal*, Vol. 42, No. 5, pp 1391-1407.

Briaud, J.L., and L.M. Tucker (1984) "Piles in sand: a method including residual stresses," *Journal of Geotechnical Engineering*, Vol. 110, No. 11, pp 1666-1680.

Bruno, D. (1999) "Dynamic and static load testing of driven piles in sand," *School of Civil and Resource Engineering*. Perth, Australia: The University of Western Australia.

Bullock, P.J. (1999) "Pile friction freeze: A field and laboratory study." Gainesville, Fla: University of Florida.

Bullock, P.J., J.H. Schmertmann, M.C. McVay, and F.C. Townsend (2005a) "Side shear setup. I: Test piles driven in Florida," *Journal of Geotechnical and Geoenvironmental Engineering*, Vol. 131, No. 3, pp 292-300.

Bullock, P.J., J.H. Schmertmann, M.C. McVay, and F.C. Townsend (2005b) "Side shear setup. II: Results from Florida test piles," *Journal of Geotechnical and Geoenvironmental Engineering*, Vol. 131, No. 3, pp 301-310.

Bustamante, M., and L. Gianeselli (1982) "Pile bearing capacity prediction by means of static penetrometer CPT," In: Verruijt, Beringen, and De Leeuw, Eds., *Proc. 2nd European Symp. on Penetration Testing (ESOPT-II)*. Amsterdam: A.A. Balkema, pp 493-500.

Campanella, R.G., and P.K. Robertson (1981) "Applied cone research," *Proc. Symp. on Cone Penetration Testing and Experience*: ASCE, pp 343-362.

Chambers, H., and B.M. Lehane (2011) "An assessment of the geotechnical strength reduction factors specified in the new Australian piling standard," *Australian Geomechanics*, Vol. 46, No. 4, p 71.

Chapman, T.J.P., B. Marsh, and A. Foster (2001) "Foundations for the future," *Proceedings of the Institution of Civil Engineers-Civil Engineering*, Vol. 144, No. 1, pp 36-41.

Charlie, W.A., M.F.J. Rwebyogo, and D.O. Doehring (1993) "Time-dependent cone penetration resistance due to blasting," *Journal of Geotechnical Engineering*, Vol. 118, No. 8, p 1992.

Chin, F.K. (1970) "Estimation of the ultimate load of piles not carried to failure," *Proc. 2nd Southeast Asian Conf. on Soil Engng*, pp 81-90.

Chin, J.T., and H.G. Poulos (1996) "Tests on model jacked piles in calcareous sand," *ASTM geotechnical testing journal*, Vol. 19, No. 2, pp 164-180.

Chong, M.K. (1988) "Density changes of sand on cone penetration resistance," In: J. De Ruiter, Ed., *Proc. 1st Int. Symp. on Penetration Testing (ISOPT-1)*. Orlando, pp 707-714.

Chow, F.C. (1997) "Investigations into the behaviour of displacement piles for offshore structures." London: University of London (Imperial College).

Chow, F.C., R.J. Jardine, F. Brucy, and J.F. Nauroy (1998) "Effects of time on capacity of pipe piles in dense marine sand," *Journal of Geotechnical and Geoenvironmental Engineering*, Vol. 124, No. 3, pp 254-264.

Chow, F.C., R.J. Jardine, J.F. Nauroy, and F. Brucy (1997) "Time-related increases in the shaft capacities of driven piles in sand," *Géotechnique*, Vol. 47, No. 2, pp 353-361.

Chow, F.C., R.J. Jardine, J.F. Nauroy, and F. Brucy (2001) "Discussion-Time-related increases in the shaft capacities of driven piles in sand," *Géotechnique*, Vol. 51, No. 5, pp 475-476.

Clausen, C.J.F., P.M. Aas, and K. Karlsrud (2005) "Bearing capacity of driven piles in sand, the NGI approach," In: S. Gourvenec, and M. Cassidy, Eds., *Proc. 1st Int. Symp. on Frontiers in Offshore Geotechnics (ISFOG)*. Perth, Australia: Balkema, pp 574-580.

Coop, M.R., E.U. Klotz, and L. Clinton (2005) "The influence of the in situ state of sands on the load-deflection behaviour of driven piles," *Géotechnique*, Vol. 55, No. 10, pp 721-730.

Coop, M.R., and I.K. Lee (1993) "The behaviour of granular soils at elevated stresses," *Predictive soil mechanics*, pp 186-198.

Corfdir, A., P. Lerat, and I. Vardoulakis (2004) "A cylinder shear apparatus," *ASTM geotechnical testing journal*, Vol. 27, No. 5, pp 447-455.

Coyle, H.M., and I.H. Sulaiman (1967) "Skin friction for steel piles in sand," *Journal of the Soil Mechanics and Foundations Division*, Vol. 93, No. SM6, pp 261-278.

Daramola, O. (1980) "Effect of consolidation age on stiffness of sand," *Géotechnique*, Vol. 30, No. 2, pp 213-216.

Davidson, W.A. (1995) "Hydrogeology and groundwater resources of the Perth region, Western Australia," Geological Survey of Western Australia Perth.

De Cock, F., C. Legrand, and N. Huybrechts (2003) "Overview of design methods of axially loaded piles in Europe-Report of ERTC3-Piles, ISSMGE Subcommittee," *Proc. 8th European Conf. on Soil Mech. and Geotech. Engng*. Prague, pp 663-715.

De Nicola, A., and M.F. Randolph (1993) "Tensile and compressive shaft capacity of piles in sand," *Journal of Geotechnical Engineering*, Vol. 119, No. 12, pp 1952-1973.

De Nicola, A., and M.F. Randolph (1997) "The plugging behaviour of driven and jacked piles in sand," *Géotechnique*, Vol. 47, No. 4, pp 841-856.

De Nicola, A., and M.F. Randolph (1999) "Centrifuge modelling of pipe piles in sand under axial loads," *Géotechnique*, Vol. 49, No. 3, pp 295-318.

De Ruiter, J., and F.L. Beringen (1979) "Pile foundations for large North Sea structures," *Marine Georesources & Geotechnology*, Vol. 3, No. 3, pp 267-314.

DeJong, J.T. (2001) "Investigation of particulate-continuum interface mechanisms and their assessment through a multi-friction sleeve penetrometer attachment." Atlanta, GA: Georgia Institute of Technology.

DeJong, J.T., R.A. Jaeger, R.W. Boulanger, M.F. Randolph, and D.A.J. Wahl (2012) "Variable penetration rate cone testing for characterization of intermediate soils," In: R.Q. Coutinho, and P.M. Mayne, Eds., *Proc. 4th Int. Conf. on Site Characterization (Keynote Paper)*. Porto de Galinhas, Brazil, pp 25-42.

DeJong, J.T., M.F. Randolph, and D.J. White (2003) "Interface load transfer degradation during cyclic loading: A microscale investigation," *Soils and foundations*, Vol. 43, No. 4, pp 81-93.

DeJong, J.T., and Z.J. Westgate (2009) "Role of initial state, material properties, and confinement condition on local and global soil-structure interface behavior," *Journal of Geotechnical and Geoenvironmental Engineering*, Vol. 135, No. 11, pp 1646-1660.

DeJong, J.T., D.J. White, and M.F. Randolph (2006) "Microscale observation and modeling of soil-structure interface behavior using particle image velocimetry," *Soils and foundations*, Vol. 46, No. 1, pp 15-28.

Desai, C.S., E.C. Drumm, and M.M. Zaman (1985) "Cyclic testing and modeling of interfaces," *Journal of Geotechnical Engineering*, Vol. 111, No. 6, pp 793-815.

Desrues, J., and G. Viggiani (2004) "Strain localization in sand: an overview of the experimental results obtained in Grenoble using stereophotogrammetry," *International Journal for Numerical and Analytical Methods in Geomechanics*, Vol. 28, No. 4, pp 279-321.

Dietz, M.S., and M.L. Lings (2006) "Postpeak strength of interfaces in a stress-dilatancy framework," *Journal of Geotechnical and Geoenvironmental Engineering*, Vol. 132, No. 11, pp 1474-1484.

Dunnicliff, J. (1993) *Geotechnical instrumentation for monitoring field performance*: Wiley-Interscience.

EN-1997 (2009) "Eurocode 7: Geotechnical design," *Part 1: General rules*. Brussels: European Committee for Standardisation (CEN).

Erbland, P.J., and R.T. McGillivray (2004) "Incorporating set-up and support cost distributions into driven pile design," In: J.A. DiMaggio, and M.H. Hussein, Eds., *Current Practices and Future Trends in Deep Foundations (GSP 125)*: ASCE, pp 66-76.

Eriksson, H., L. Hellman, T. Nilsson, and L. Weiner (1993) "Ny järnvägsbro vid Öre älv: Påldimensionering med hjälp av stötvågsmätning vid hejarsondering," *Bygg & Teknik 8/93*. Sweden, pp 12-17.

Eslaamizaad, S., and P.K. Robertson (1997) "Evaluation of settlement of footings on sand from seismic in-situ tests," *Proc. 50th Canadian Geotech. Conf.* Ottawa, Ont.: BiTech Publishers, Richmond, B.C., pp 755-764.

Eslami, A., and B.H. Fellenius (1997) "Pile capacity by direct CPT and CPTu methods applied to 102 case histories," *Canadian geotechnical journal*, Vol. 34, No. 6, pp 886-904.

Evgin, E., and K. Fakharian (1996) "Effect of stress paths on the behaviour of sand steel interfaces," *Canadian geotechnical journal*, Vol. 33, No. 6, pp 853-865.

Fahey, M., B.M. Lehane, and D. Stewart (2003) "Soil stiffness for shallow foundation design in the Perth CBD," *Australian Geomechanics*, Vol. 38, No. 3, pp 61-90.

Fellenius, B.H. (1980) "The analysis of results from routine pile load tests," *Ground Engineering*, Vol. 13, No. 6, pp 19-31.

Fellenius, B.H. (2002) "Determining the true distributions of load in instrumented piles," In: M.W. O'Neill, and F.C. Townsend, Eds., *Deep Foundations 2002: An International Perspective on Theory, Design, Construction, and Performance (GSP 116)*. Orlando, Florida, pp 1455-1470.

Fellenius, B.H., and A. Altaee (2002) "Pile dynamics in geotechnical practice - Six case histories," In: M.W. O'Neill, and F.C. Townsend, Eds., *Deep Foundations 2002: An International Perspective on Theory, Design, Construction, and Performance (GSP 116)*. Orlando, Florida: ASCE, pp 619-631.

Fellenius, B.H., W.G. Brusey, and F. Pepe (2000) "Soil set-up, variable concrete modulus, and residual load for tapered instrumented piles in sand," *Specialty Conference on Performance Confirmation of Constructed Geotechnical Facilities (GSP94)*. University of Massachusetts, Amherst: ASCE, p 16.

Fellenius, B.H., R.E. Riker, A.J. O'Brien, and G.R. Tracy (1989) "Dynamic and static testing in soil exhibiting set-up," *Journal of Geotechnical Engineering*, Vol. 115, No. 7, pp 984-1001.

Fioravante, V. (2002) "On the shaft friction modelling of non-displacement piles in sand," *Soils and foundations*, Vol. 42, No. 2, pp 23-33.

Fleming, W.G.K. (1992) "A new method for single pile settlement prediction and analysis," *Géotechnique*, Vol. 42, No. 3, pp 411-425.

Fleming, W.G.K., and S. Thorburn (1983) "Recent piling advances," *Proc. Conf. on Advances in Piling and Ground Treatment for Foundations*, pp 1-16.

Fleming, W.G.K., A. Weltman, M.F. Randolph, and W.K. Elson (2008) *Piling engineering*, Oxon, UK: Taylor & Francis.

Foray, P. (1991) "Scale and boundary effects on calibration chamber pile tests," In: A.-B. Huang, Ed., *Proc. 1st Int. Symp. on Calibration Chamber Testing*. Potsdam, New York: DTIC Document, pp 147-160.

Foray, P., L. Balachowski, and G. Rault (1998) "Scale effects in shaft friction due to the localisation of deformations," *Centrifuge 98*. Tokyo, pp 211-216.

Foray, P., J.M. Genevois, S. Labanieh, and A. Goulois (1989) "Effect of pile installation on the bearing capacity of piles in sand," *Proc. 12th Int. Conf. on Soil Mech. Foundation Engng*, pp 913-914.

Foray, P.Y., C.H.C. Tsuha, M. Silva, R.J. Jardine, and Z.X. Yang (2010) "Stress paths measured around a cyclically loaded pile in a calibration chamber," In: S.M. Springman, J. Laue, and L. Seward, Eds., *Proc. 7th Int. Conf. of Physical Modelling in Geotechnics*. Zurich, Switzerland: Taylor & Francis Group, pp 933-939.

Foyn, T., and M. Alstad (1999) "Langtids baereevne av friksjon speler. Eksempel med PDA målinger og CAPWAP-analyse," *Geoteknikdagen*. Norway.

Frost, J.D., and J.T. DeJong (2005) "In situ assessment of role of surface roughness on interface response," *Journal of Geotechnical and Geoenvironmental Engineering*, Vol. 131, No. 4, pp 498-511.

Frost, J.D., J.T. DeJong, and M. Recalde (2002) "Shear failure behavior of granular-continuum interfaces," *Engineering fracture mechanics*, Vol. 69, No. 17, pp 2029-2048.

Garnier, J., C. Gaudin, S.M. Springman, P.J. Culligan, D.J. Goodings, D. Konig, B.L. Kutter, R. Phillips, M.F. Randolph, and L. Thorel (2007) "Catalogue of scaling laws and similitude questions in geotechnical centrifuge modelling," *International Journal of Physical Modelling in Geotechnics*, Vol. 7, No. 3, pp 1-23.

Garnier, J., and D. König (1998) "Scale effects in piles and nails loading tests in sand," *Centrifuge 98*. Tokyo, pp 205-210.

Gavin, K.G., D. Igoe, and P. Doherty (2011) "Piles for offshore wind turbines: a state-of-the-art review," *Proceedings of the Institution of Civil Engineers-Geotechnical Engineering*, Vol. 164, No. 4, pp 245-256.

Gavin, K.G., D.J.P. Igoe, and L. Kirwan (2013) "The effect of ageing on the axial capacity of piles in sand," *Proceedings of the Institution of Civil Engineers-Geotechnical Engineering*, Vol. 166, No. 2, pp 122-130.

Gavin, K.G., and B.M. Lehane (2003) "The shaft capacity of pipe piles in sand," *Canadian geotechnical journal*, Vol. 40, No. 1, pp 36-45.

Hannigan, P.J., G.G. Goble, G. Thendean, G.E. Likins, and F. Rausche (1997) "Design and Construction of Driven Pile Foundations," *FHWA-HI-97-013*. Washington, DC: Federal Highway Administration.

Hebeler, G.L. (2005) "Multi-scale behavior at geomaterial interfaces." Atlanta, GA: Georgia Institute of Technology.

Hettler, A. (1982) "Approximation formulae for piles under tension," *Proc. IUTAM Conf. on Deformation and Failure of Granular Materials* Delft, pp 603-608.

Ho, T.Y.K., R.J. Jardine, and N. Anh-Minh (2011) "Large-displacement interface shear between steel and granular media," *Géotechnique*, Vol. 61, No. 3, pp 221-234.

Holloway, D.M., G.W. Clough, and A.S. Vesic (1978) "The effects of residual driving stresses on pile performance under axial loads," *Proc. 10th Annual Offshore Tech. Conf.* Houston, Texas, pp 2225-2236.

Holm, G. (1992) "Piling in Sweden, Denmark, Norway and Finland," *Proc. Conf. on Piling in Europe*. London: ICE, pp 25-31.

Houlsby, G.T., and R. Hitchman (1988) "Calibration chamber tests of a cone penetrometer in sand," *Géotechnique*, Vol. 38, No. 1, pp 39-44.

Howie, J.A., T. Shozen, and Y.P. Vaid (2002) "Effect of ageing on stiffness of very loose sand," *Canadian geotechnical journal*, Vol. 39, No. 1, pp 149-156.

Hussein, M.H., M.R. Sharp, and W.F. Knight (2002) "The use of superposition for evaluating pile capacity," In: M.W. O'Neill, and F.C. Townsend, Eds., *Deep Foundations 2002: An International Perspective on Theory, Design, Construction, and Performance (GSP 116)*. Orlando, Florida: ASCE, pp 6-21.

Jamiolkowski, M., C.C. Ladd, J.T. Germaine, and R. Lancellotta (1985) "New developments in field and laboratory testing of soils," *Proc. 11th Int. Conf. on Soil Mech. Foundation Engng*. San Francisco, pp 57-153.

Jamiolkowski, M., D.C.F. LoPresti, and M. Manassero (2001) "Evaluation of relative density and shear strength of sands from CPT and DMT," *Soil Behavior and Soft Ground Construction (GSP119)*. Reston, Va: ASCE, pp 201-238.

Jardine, R.J. (1985) "Investigation of pile-soil behaviour with special reference to the foundations of offshore structures." London: University of London (Imperial College).

Jardine, R.J., and F.C. Chow (1996) "New design methods for offshore piles," *MTD Publication 96/103*. London: Marine Technology Directorate.

Jardine, R.J., F.C. Chow, R. Overy, and J.R. Standing (2005) *ICP design methods for driven piles in sands and clays*: Thomas Telford.

Jardine, R.J., B.M. Lehane, and S.J. Everton (1992) "Friction coefficients for piles in sands and silts," *Proc. Conf. on Offshore Site Investigation and Foundation Behaviour*. London, pp 661-677.

Jardine, R.J., and J.R. Standing (2000) "Pile Load Testing Performed for HSE Cyclic Loading Study at Dunkirk, France Volumes 1 & 2," *Offshore Technology Report OTO 2000 008 & 007*. Health Safety Executive, London.

Jardine, R.J., J.R. Standing, and F.C. Chow (2006) "Some observations of the effects of time on the capacity of piles driven in sand," *Géotechnique*, Vol. 56, No. 4, pp 227-244.

Jardine, R.J., B. Zhu, P. Foray, and C.P. Dalton (2009) "Experimental arrangements for investigation of soil stresses developed around a displacement pile," *Soils and foundations*, Vol. 49, No. 5, pp 661-673.

Jewell, R.A. (1989) "Direct shear tests on sand," *Géotechnique*, Vol. 39, No. 2, pp 309-322.

Jewell, R.J., and M.F. Randolph (1989) "Cyclic rod shear tests in calcareous sediments," *Engineering for Calcareous Sediments*, Vol. 2, pp 837-857.

Joshi, R.C., G. Achari, S.R. Kaniraj, and H. Wijeweera (1995) "Effect of aging on the penetration resistance of sands," *Canadian geotechnical journal*, Vol. 32, No. 5, pp 767-782.

Karimpour, H., and P.V. Lade (2010) "Time effects relate to crushing in sand," *Journal of Geotechnical and Geoenvironmental Engineering*, Vol. 136, No. 9, pp 1209-1219.

Karlsrud, K. (2012) "Prediction of load-displacement behaviour and capacity of axially loaded piles in clay based on analyses and interpretation of pile load test results." Trondheim, Norway: Norwegian University of Science and Technology.

Kelly, R. (2001) "Development of a large diameter ring shear apparatus and its use." Sydney: The University of Sydney.

Kishida, H., and M. Uesugi (1987) "Tests of the interface between sand and steel in the simple shear apparatus," *Géotechnique*, Vol. 37, No. 1, pp 45-52.

Klotz, E.U., and M.R. Coop (2001) "An investigation of the effect of soil state on the capacity of driven piles in sands," *Géotechnique*, Vol. 51, No. 9, pp 733-751.

Knudsen, S., T. Langford, S. Lacasse, and P.M. Aas (2012) "Axial capacity of offshore piles driven in sand using four CPT-based methods," *Proc. 7th Int. Conf. on Offshore Site Investigation and Geotechnics*. London, UK, pp 449-457.

Kolk, H.J., A.E. Baaijens, and M. Senders (2005a) "Design criteria for pipe piles in silica sands," In: S. Gourvenec, and M. Cassidy, Eds., *Proc. 1st Int. Symp. on Frontiers in Offshore Geotechnics (ISFOG)*. Perth, Australia: Balkema pp 711-716.

Kolk, H.J., A.E. Baaijens, and P. Vergobbi (2005b) "Results of axial load tests on pipe piles in very dense sands: The EURIPIDES JIP," In: S. Gourvenec, and M. Cassidy, Eds., *Proc. 1st Int. Symp. on Frontiers in Offshore Geotechnics (ISFOG)*. Perth, Australia: Balkema, pp 661-667.

Komurka, V.E. (2004) "Incorporating set-up and support cost distributions into driven pile design," In: J.A. DiMaggio, and M.H. Hussein, Eds., *Current Practices and Future Trends in Deep Foundations (GSP 125)*: ASCE, pp 16-49.

Komurka, V.E., A.B. Wagner, and T. Edil (2003) "Estimating soil/pile set-up," *Report No. 03-05*: Wisconsin Highway Research Program.

Koutsoftas, D.C. (2002) "High capacity piles in very dense sands," In: M.W. O'Neill, and F.C. Townsend, Eds., *Deep Foundations 2002: An International Perspective on Theory, Design, Construction, and Performance (GSP 116)*. Orlando, Florida: ASCE, pp 632-646.

Kuo, C., G. Cao, A.L. Guisinger, and P. Passe (2007) "A case history of pile freeze effects in dense Florida sands," *Proc. Transportation Research Board (TRB) Annual Meeting*. Washington, DC.

Lade, P.V., and H. Karimpour (2010) "Static fatigue controls particle crushing and time effects in granular materials," *Soils and foundations*, Vol. 50, No. 5, pp 573-583.

Lebêgue, N.Y. (1964) "Etude experimental des efforts d'arrachage et de frottement négatif sur les pieux en milieu pulvérulent'," *Annales de l'Institut technique du bâtiment et des travaux publics, Serie soils et fondations*, Vol. 17, No. 199-200, pp 808-822.

Lee, W., D. Kim, R. Salgado, and M. Zaheer (2010) "Setup of driven piles in layered soil," *Soils and foundations*, Vol. 50, No. 5, pp 585-598.

Lehane, B.M. (1992) "Experimental investigation of pile behaviour using instrumented field piles." London: University of London (Imperial College).

Lehane, B.M. (2008) "Relationships between axial capacity and CPT qc for bored piles in sand," *Proc. 5th Int. Symp. on Deep Foundations on Bored and Auger Piles (BAP V)*. Ghent, Belgium: CRC, pp 61-76.

Lehane, B.M., J.P. Doherty, and J.A. Schneider (2008) "Settlement prediction for footings on sand," In: Susan E. Burns, Paul W. Mayne, and J. Carlos Santamarina, Eds., *Proc. 4th Int. Symp. on Deformation Characteristics of Geomaterials (IS Atlanta)*. Atlanta, Georgia, USA, pp 133-150.

Lehane, B.M., C. Gaudin, and J.A. Schneider (2005a) "Scale effects on tension capacity for rough piles buried in dense sand," *Géotechnique*, Vol. 55, No. 10, pp 709-720.

Lehane, B.M., M.A. Ismail, and M. Fahey (2004) "Seasonal dependence of in situ test parameters in sand above the water table," *Géotechnique*, Vol. 54, No. 3, pp 215-218.

Lehane, B.M., and R.J. Jardine (1994) "Shaft capacity of driven piles in sand: a new design approach," *Proc. Conf. on Behaviour of Offshore Structures*. Boston, MA, pp 23-36.

Lehane, B.M., R.J. Jardine, A.J. Bond, and R. Frank (1993) "Mechanisms of shaft friction in sand from instrumented pile tests," *Journal of Geotechnical Engineering*, Vol. 119, No. 1, pp 19-35.

Lehane, B.M., J.A. Schneider, J.K. Lim, and G. Mortara (2012) "Shaft friction from instrumented displacement piles in an uncemented calcareous sand," *Journal of Geotechnical and Geoenvironmental Engineering*, Vol. 138, No. 11, pp 1357-1368.

Lehane, B.M., J.A. Schneider, and X. Xu (2005b) "CPT based design of driven piles in sand for offshore structures," *Report GEO:05345*. Perth: The University of Western Australia.

Lehane, B.M., J.A. Schneider, and X. Xu (2005c) "A review of design methods for offshore driven piles in siliceous sand," *Report GEO:05358*. Perth: The University of Western Australia.

Lehane, B.M., J.A. Schneider, and X. Xu (2005d) "The UWA-05 method for prediction of axial capacity of driven piles in sand," In: S. Gourvenec, and M. Cassidy, Eds., *Proc. 1st Int. Symp. on Frontiers in Offshore Geotechnics (ISFOG)*. Perth, Australia: Balkema, pp 683-689.

Lehane, B.M., J.A. Schneider, and X. Xu (2007) "CPT-based design of displacement piles in siliceous sands," In: Kikuchi, Otani, Kimura, and Morikawa, Eds., *Advances in Deep Foundations*. Yokosuka, Japan: Taylor & Francis Group, pp 69-86.

Lehane, B.M., and D.J. White (2005) "Lateral stress changes and shaft friction for model displacement piles in sand," *Canadian geotechnical journal*, Vol. 42, No. 4, pp 1039-1052.

Li, A.Z., and B.M. Lehane (2010) "Embedded cantilever retaining walls in sand," *Géotechnique*, Vol. 60, No. 11, pp 813-823.

Lings, M.L., and M.S. Dietz (2004) "An improved direct shear apparatus for sand," *Géotechnique*, Vol. 54, No. 4, pp 245-256.

Lings, M.L., and M.S. Dietz (2005) "The peak strength of sand-steel interfaces and the role of dilation," *Soils and foundations*, Vol. 45, No. 6, pp 1-14.

Long, J.H., J.A. Kerrigan, and M.H. Wysockey (1999) "Measured time effects for axial capacity of driven piling," *Transportation Research Record: Journal of the Transportation Research Board*, Vol. 1663, No. -1, pp 8-15.

Lumb, P. (1962) "The properties of decomposed granite," *Géotechnique*, Vol. 12, No. 3, pp 226-243.

Lumb, P. (1965) "The residual soils of Hong Kong," *Géotechnique*, Vol. 15, No. 2, pp 180-194.

Lunne, T., P.K. Robertson, and J.J.M. Powell (1997) *Cone penetration testing in geotechnical practice*, London: Taylor & Francis Group.

Luzzani, L., and M.R. Coop (2002) "On the relationship between particle breakage and the critical state of sands," *Soils and foundations*, Vol. 42, No. 2, pp 71-82.

Marchetti, S. (1980) "In situ tests by flat dilatometer," *Journal of the Geotechnical Engineering Division*, Vol. 106, No. 3, pp 299-321.

Marchetti, S., P. Monaco, G. Totani, and M. Calabrese (2001) "The flat dilatometer test (DMT) in soil investigations. A report by the ISSMGE Committee TC 16.," *Proc. Int. Conf. on In Situ Measurement of Soil Properties (IN-SITU 2001)*. Bali, Indonesia, pp 95-131.

Mello, J.R.C., and N.S. Galgoul (1992) "Piling and monitoring of large diameter closed-toe pipe piles," *Proc. 4th Int. Conf. on the Application of Stress-Wave Theory to Piles*: AA Balkema, Rotterdam, The Netherlands, pp 443-448.

Mesri, G., TW Feng, and JM Benak (1990) "Postdensification penetration resistance of clean sands," *Journal of Geotechnical Engineering*, Vol. 116, No. 7, pp 1095-1115.

Mesri, G., and M.M. Smadi (2001) "Discussion: Time-related increases in the shaft capacities of driven piles in sand," *Géotechnique*, Vol. 51, No. 5, pp 475-476.

Meyerhof, G.G. (1956) "Penetration tests and bearing capacity of cohesionless soils," *Journal of the Soil Mechanics and Foundations Division*, Vol. 82, No. 1, pp 1-19.

Meyerhof, G.G., and G. Ranjan (1972) "The bearing capacity of rigid piles under inclined loads in sand. I: Vertical piles," *Canadian geotechnical journal*, Vol. 9, No. 4, pp 430-446.

Michalowski, R.L., and S.S. Nadukuru (2012) "Static fatigue, time effects, and delayed increase in penetration resistance after dynamic compaction of sands," *Journal of Geotechnical and Geoenvironmental Engineering*, Vol. 138, No. 5, pp 564-574.

Middendorp, P., and G.E.H. Verbeek (2012) "At the cutting edge of pile foundations and pile testing," In: T. Matsumoto, Ed., *Proc. 9th Int. Conf. on Testing and Design Methods for Deep Foundations*. Kanazawa, Japan, pp 931-937.

Mikasa, M., and N. Takada (1973) "Significance of centrifugal model test in soil mechanics," *Proc. 8th Int. Conf. on Soil Mech. Foundation Engng*. Moscow, pp 273-278.

Mitchell, J.K. (2008) "Aging of sand - A continuing enigma?," *Proc. 6th Int. Conf. on Case Histories in Geotech. Engng*. Arlington, VA, pp 1-21.

Mitchell, J.K., and Z.V. Solymar (1984) "Time-dependent strength gain in freshly deposited or densified sand," *Journal of Geotechnical Engineering*, Vol. 110, No. 11, pp 1559-1576.

Monzón, J.C. (2006) "Review of CPT based design methods for estimating axial capacity of driven piles in siliceous sand." Cambridge, MA: Massachusetts Institute of Technology.

Mortara, G., D. Ferrara, and G. Fotia (2010) "Simple model for the cyclic behavior of smooth sand-steel interfaces," *Journal of Geotechnical and Geoenvironmental Engineering*, Vol. 136, No. 7, pp 1004-1009.

Mortara, G., A. Mangiola, and V.N. Ghionna (2007) "Cyclic shear stress degradation and post-cyclic behaviour from sand-steel interface direct shear tests," *Canadian geotechnical journal*, Vol. 44, No. 7, pp 739-752.

Nauroy, J., and P. LeTirant (1985) "Driven piles and drilled and grouted piles in calcareous sands," *Proc. 17th Offshore Tech. Conf.* Houston, USA, pp 83-91.

Ng, E.S., J.L. Briaud, and L.M. Tucker (1988) "Pile foundations: the behavior of piles in cohesionless soils," *Report FHWA-RD-88-081*. McLean, VA: Federal Highway Administration.

Ng, N., P. Berner, and C. Covil (1998) "The ageing effects of sands," *Ground Engineering*, Vol. 10, No. Suppl., p 21.

Nottingham, L.C. (1975) "Use of quasi-static friction cone penetrometer data to predict load capacity of displacement piles," *Department of Civil Engineering*. Gainesville: University of Florida.

O'Neill, M.W., and R.D. Raines (1991) "Load transfer for pipe piles in highly pressured dense sand," *Journal of Geotechnical Engineering*, Vol. 117, No. 8, pp 1208-1226.

Ozkahriman, F., and J. Wartman (2007) "Investigation of 1-g similitude laws by "modeling-of-models" exercise," *Advances in Measurement and Modeling of Soil Behavior (GSP 173)*: ASCE, pp 1-9.

Paik, K., and R. Salgado (2004) "Effect of pile installation method on pipe pile behavior in sands," *ASTM geotechnical testing journal*, Vol. 27, No. 1, pp 78-88.

Paik, K., R. Salgado, J. Lee, and B. Kim (2003) "Behavior of open-and closed-ended piles driven into sands," *Journal of Geotechnical and Geoenvironmental Engineering*, Vol. 129, No. 4, pp 296-306.

Paikowsky, S.G., C.M. Player, and P.J. Connors (1995) "A dual interface apparatus for testing unrestricted friction of soil along solid surfaces," *ASTM geotechnical testing journal*, Vol. 18, No. 2, pp 168-193.

Parkin, A.K., and T. Lunne (1982) "Boundary effects in the laboratory calibration of a cone penetrometer for sand," In: Verruijt, Beringen, and De Leeuw, Eds., *Proc. 2nd European Symp. on Penetration Testing (ESOPT-II)*. Amsterdam: Balkema, Rotterdam, pp 761-768.

Parsons, J.D. (1966) "Piling difficulties in the New York area," *Journal of the Soil Mechanics and Foundations Division*, Vol. 92, No. 1, pp 43-64.

Peck, R.B., W.E. Hanson, and T.H. Thornburn (1974) *Foundation engineering*: Wiley New York.

Playford, P.E., A.E. Cockbain, and G.H. Low (1976) "Geology of the Perth Basin, Western Australia," Geological Survey of Western Australia.

Porcino, D., V. Fioravante, V.N. Ghionna, and S. Pedroni (2003) "Interface behavior of sands from constant normal stiffness direct shear tests," *ASTM geotechnical testing journal*, Vol. 26, No. 3, pp 289-301.

Potyondy, J.G. (1961) "Skin friction between various soils and construction materials," *Géotechnique*, Vol. 11, No. 4, pp 339-353.

Preim, M.J., R. March, and M. Hussein (1989) "Bearing capacity of piles in soils with time dependent characteristics," *Proc. 3rd Int. Conf. on Piling and Deep Foundations*. Brookfield, VT: Balkema, pp 363-370.

Rad, N.S., and M.T. Tumay (1987) "Factors affecting sand specimen preparation by raining," *ASTM geotechnical testing journal*, Vol. 10, No. 1, pp 31-37.

Randolph, M.F. (2003) "Science and empiricism in pile foundation design," *Géotechnique*, Vol. 53, No. 10, pp 847-876.

Randolph, M.F., J.P. Carter, and C.P. Wroth (1979) "Driven piles in clay—the effects of installation and subsequent consolidation," *Géotechnique*, Vol. 29, No. 4, pp 361-393.

Rausche, F., G.E. Likins, and M.H. Hussein (2008) "Analysis of post-installation dynamic load test data for capacity evaluation of deep foundations," In: J.E. Laier, D.K. Crapps, and M.H. Hussein, Eds., *From Research to Practice in Geotechnical Engineering (GSP 180)*. Reston, Virginia, pp 312-330.

Rausche, F., G. Thendean, H. Abou-matar, G.E. Likins, and G.G. Goble (1997) "Determination of pile driveability and capacity from penetration tests. Volume I: Final report," *FHWA-RD-96-179*. Washington, DC: Federal Highway Administration.

Reddy, E.S., D.N. Chapman, and M. O'Reilly (1998) "Design and performance of soil-pile-slip test apparatus for tension piles," *ASTM geotechnical testing journal*, Vol. 21, No. 2, pp 132-139.

Rimoy, S., R. Jardine, M. Silva, P. Foray, C.H.C. Tsuha, and Z.X. Yang (2012) "Local and global behaviour of axial cyclic loaded instrumented model displacement piles in sand," *Proc. 7th Int. Conf. on Offshore Site Investigation and Geotechnics*. London, UK, pp 279-286.

Rix, G.J., and K.H. Stokoe (1991) "Correlation of initial tangent modulus and cone penetration resistance," In: A.B. Huang, Ed., *Proc. Int. Symp. on Calibration Chamber Testing*: Elsevier Publishing, New York, pp 351-362.

Robertson, P.K. (1990) "Soil classification using the cone penetration test," *Canadian geotechnical journal*, Vol. 27, No. 1, pp 151-158.

Robertson, P.K. (2009) "Interpretation of cone penetration tests - a unified approach," *Canadian geotechnical journal*, Vol. 46, No. 11, pp 1337-1355.

Robertson, P.K., R.G. Campanella, D. Gillespie, and A. Rice (1986) "Seismic CPT to measure in situ shear wave velocity," *Journal of Geotechnical Engineering*, Vol. 112, No. 8, pp 791-803.

Robertson, P.K., and C.E. Wride (1998) "Evaluating cyclic liquefaction potential using the cone penetration test," *Canadian geotechnical journal*, Vol. 35, No. 3, pp 442-459.

Robinsky, E.I., and C.F. Morrison (1964) "Sand displacement and compaction around model friction piles," *Canadian geotechnical journal*, Vol. 1, No. 2, pp 81-93.

Robinsky, E.I., W.L. Sagar, and C.F. Morrison (1964) "Effect of shape and volume on the capacity of model piles in sand," *Canadian geotechnical journal*, Vol. 1, No. 4, pp 189-204.

Sadrekarimi, A., and S.M. Olson (2010) "Particle damage observed in ring shear tests on sands," *Canadian geotechnical journal*, Vol. 47, No. 5, pp 497-515.

Salgado, R., JK Mitchell, and M. Jamiolkowski (1998) "Calibration chamber size effects on penetration resistance in sand," *Journal of Geotechnical and Geoenvironmental Engineering*, Vol. 124, No. 9, pp 878-888.

Samson, L., and J. Authier (1986) "Change in pile capacity with time: case histories," *Canadian geotechnical journal*, Vol. 23, No. 2, pp 174-180.

Saxena, D.S. (2004) "Case histories of a five-story printing press foundation with zero movement criterion," *Proc. 57th Canadian Geotech. Conf.*

Schmertmann, J.H. (1978) "Guidelines for Cone Penetration Test (Performance and Design)," *FHWA-TS-78-209*: U.S. Federal Highway Administration.

Schmertmann, J.H. (1987) "Discussion of "Time-dependent strength gain in freshly deposited or densified sand"," *Journal of Geotechnical Engineering*, Vol. 113, No. 2, pp 173-175.

Schmertmann, J.H. (1991) "The mechanical aging of soils," *Journal of Geotechnical Engineering*, Vol. 117, No. 9, pp 1288-1330.

Schnaid, F., B.M. Lehane, and M. Fahey (2004) "In situ test characterization of unusual geomaterials," *Proc. 2nd Int. Conf. on Site Characterization (ISC)*. Porto, Portugal: Millpress, pp 49-74.

Schneider, J.A. (2007) "Analysis of piezocone data for displacement pile design," *School of Civil and Resource Engineering*. Perth, Australia: The University of Western Australia.

Schneider, J.A., M. Fahey, and B.M. Lehane (2008a) "Characterisation of an unsaturated sand deposit by in situ testing," *Proc. 3rd Int. Conf. on Site Characterization (ISC)*, pp 633-638.

Schneider, J.A., X. Xu, and B.M. Lehane (2008b) "Database assessment of CPT-based design methods for axial capacity of driven piles in siliceous sands," *Journal of Geotechnical and Geoenvironmental Engineering*, Vol. 134, No. 9, pp 1227-1244.

Seber, George A.F., and Christopher John Wild (2003) *Nonlinear regression*: Wiley-Interscience.

Sedran, G., D.F.E. Stolle, and R.G. Horvath (2001) "An investigation of scaling and dimensional analysis of axially loaded piles," *Canadian geotechnical journal*, Vol. 38, No. 3, pp 530-541.

Seidel, J.P., I.J. Haustorfer, and S. Plesiotis (1988) "Comparison of dynamic and static testing for piles founded into limestone," In: B.G. Fellenius, Ed., *Proc. 3rd Int. Conf. on the Application of Stress-Wave Theory to Piles*. Ottawa, Canada: Vancouver, BC, Canada: BiTech Publishers, pp 717-723.

Seidel, J.P., and M. Kalinowski (2000) "Pile set-up in sands," *Proc. 6th Int. Conf. on the Application of Stress-Wave Theory to Piles*. Sao Paulo, Brazil, pp 267-274.

Sharma, S.S. (2004) "Characterisation of cyclic behaviour of calcite cemented calcareous soils," *School of Civil and Resource Engineering*. Perth, Australia: The University of Western Australia.

Shek, L.M.P., L.M. Zhang, and H.W. Pang (2006) "Set-up effect in long piles in weathered soils," *Proceedings of the Institution of Civil Engineers-Geotechnical Engineering*, Vol. 159, No. 3, pp 145-152.

Shibuya, S., T. Mitachi, and S. Tamate (1997) "Interpretation of direct shear box testing of sands as quasi-simple shear," *Géotechnique*, Vol. 47, No. 4, pp 769-790.

Silva, M.F., and M.D. Bolton (2005) "Interpretation of centrifuge piezocone tests in dilatant, low plasticity silts," *Proc. Int. Conf. on Problematic Soils*. Eastern Mediterranean University, Famagusta, N. Cyprus, pp 27-34.

Simpson, B., and F. Tatsuoka (2008) "Geotechnics: the next 60 years," *Géotechnique*, Vol. 58, No. 5, pp 357-368.

Skov, R., and H. Denver (1988) "Time-dependence of bearing capacity of piles," In: B.G. Fellenius, Ed., *Proc. 3rd Int. Conf. on the Application of Stress-Wave Theory to Piles*. Ottawa, Canada: Vancouver, BC, Canada: BiTech Publishers, pp 879-888.

Soderberg, L.O. (1962) "Consolidation theory applied to foundation pile time effects," *Géotechnique*, Vol. 12, No. 3, pp 217-225.

Stevens, R.F. (2000) "Pile acceptance based on combined CAPWAP analyses," In: S. Niyama, and J. Beim, Eds., *Proc. 6th Int. Conf. on the Application of Stress-Wave Theory to Piles*. Sao Paulo, Brazil: A.A. Balkema Publishers, pp 17-27.

Svinkin, M.R. (2002) "Engineering judgement in determination of pile capacity by dynamic methods," In: M.W. O'Neill, and F.C. Townsend, Eds., *Deep*

Foundations 2002: An International Perspective on Theory, Design, Construction, and Performance (GSP 116). Orlando, Florida: ASCE, pp 898-914.

Svinkin, M.R. (2004) "Some uncertainties in high-strain dynamic pile testing," *Geotechnical Engineering for Transportation Projects (GSP 126)*: ASCE, pp 705-714.

Svinkin, M.R., C.M. Morgano, and M. Morvant (1994) "Pile capacity as a function of time in clayey and sandy soils," *Proc. 5th Int. Conf. Piling and Deep Foundations*. Bruges.

Symes, M.J.P. (1983) "Rotation of principal stresses in sand." London: Imperial College London (University of London).

Tabucanon, J.T. (1997) "Shaft resistance of piles in sand." Sydney: The University of Sydney.

Tabucanon, J.T., D.W. Airey, and H.G. Poulos (1995) "Pile skin friction in sands from constant normal stiffness tests," *ASTM geotechnical testing journal*, Vol. 18, No. 3, pp 350-364.

Tan, S.L., J. Cuthbertson, and R.E. Kimmerling (2004) "Prediction of pile set-up in non-cohesive soils," In: J.A. DiMaggio, and M.H. Hussein, Eds., *Current Practices and Future Trends in Deep Foundations (GSP 125)*: ASCE, pp 50-65.

Tavenas, F., and R. Audy (1972) "Limitations of the driving formulas for predicting the bearing capacities of piles in sand," *Canadian geotechnical journal*, Vol. 9, No. 1, pp 47-62.

Tejchman, A., and J. Tejchman (1994) "Scale effect in pile model tests due to different pile and grain diameters," *Proc. 13th Int. Conf. on Soil Mech. Foundation Engng*. New Delhi, India: Balkema, pp 717-720.

Thomann, T.G., and R.D. Hryciw (1992) "Stiffness and strength changes in cohesionless soils due to disturbance," *Canadian geotechnical journal*, Vol. 29, No. 5, pp 853-861.

Thomassen, K., L.V. Andersen, and L.B. Ibsen (2012) "Comparison of design methods for axially loaded driven piles in cohesionless soil," *Proc. 22nd Int. Offshore and Polar Engng Conf.* Rhodes, Greece, pp 705-712.

Tika, T.E. (1999) "Ring shear tests on a carbonate sandy silt," *ASTM geotechnical testing journal*, Vol. 22, No. 4, pp 342-355.

Tomlinson, M.J. (1996) "Recent advances in driven pile design," *Ground Engineering*, Vol. 29, No. 10, pp 31-33.

Tomlinson, M.J., and J. Woodward (2007) *Pile design & construction practice*, New York: Taylor & Francis.

Toolan, F.E., M.L. Lings, and U.A. Mirza (1990) "An appraisal of API RP2A recommendations for determining skin friction of piles in sand," *Proc. 22nd Offshore Tech. Conf.* Houston, TX, pp 33-42.

Tsuha, C.H.C., P.Y. Foray, R.J. Jardine, Z.X. Yang, M. Silva, and S. Rimoy (2012) "Behaviour of displacement piles in sand under cyclic axial loading," *Soils and foundations*, Vol. 52, No. 3, pp 393-410.

Uesugi, M., and H. Kishida (1986a) "Frictional resistance at yield between dry sand and mild steel," *Soils and foundations*, Vol. 26, No. 4, pp 139-149.

Uesugi, M., and H. Kishida (1986b) "Influential factors of friction between steel and dry sands," *Soils and foundations*, Vol. 26, No. 2, pp 33-46.

Uesugi, M., H. Kishida, and Y. Tsubakihara (1988) "Behavior of sand particles in sand-steel friction," *Soils and foundations*, Vol. 28, No. 1, pp 107-118.

Uesugi, M., H. Kishida, and Y. Tsubakihara (1989) "Friction between sand and steel under repeated loading," *Soils and foundations*, Vol. 29, No. 3, pp 127-137.

Wang, Y.H., and K.Y. Tsui (2009) "Experimental characterization of dynamic property changes in aged sands," *Journal of Geotechnical and Geoenvironmental Engineering*, Vol. 135, No. 2, pp 259-270.

Wesley, L.D. (2002) "Interpretation of calibration chamber tests involving cone penetrometers in sands," *Géotechnique*, Vol. 52, No. 4, pp 289-293.

White, D., T. Finlay, M. Bolton, and G. Bearss (2002) "Press-in piling: Ground vibration and noise during pile installation," In: M.W. O'Neill, and F.C. Townsend, Eds., *Deep Foundations 2002: An International Perspective on Theory, Design, Construction, and Performance (GSP 116)*. Orlando, Florida, pp 363-371.

White, D.J. (2002) "An investigation into the behaviour of pressed-in piles," University of Cambridge.

White, D.J. (2005) "A general framework for shaft resistance on displacement piles in sand," In: S. Gourvenec, and M. Cassidy, Eds., *Proc. 1st Int. Symp. on Frontiers*

in Offshore Geotechnics (ISFOG). Perth, Australia: Taylor and Francis, pp 697-704.

White, D.J., and M.D. Bolton (2004) "Displacement and strain paths during plane-strain model pile installation in sand," *Géotechnique*, Vol. 54, No. 6, pp 375-397.

White, D.J., and A.D. Deeks (2007) "Recent research into the behaviour of jacked foundation piles," In: Kikuchi, Otani, Kimura, and Morikawa, Eds., *Advances in Deep Foundations*. Yokosuka, Japan: Taylor & Francis Group, pp 3-26.

White, D.J., and B.M. Lehane (2004) "Friction fatigue on displacement piles in sand," *Géotechnique*, Vol. 54, No. 10, pp 645-658.

White, D.J., J.A. Schneider, and B.M. Lehane (2005) "The influence of effective area ratio on shaft friction of displacement piles in sand," In: S. Gourvenec, and M. Cassidy, Eds., *Proc. 1st Int. Symp. on Frontiers in Offshore Geotechnics (ISFOG)*. Perth, Australia: Taylor and Francis, pp 741-748.

White, D.J., and Y. Zhao (2006) "A model-scale investigation into 'set-up' of displacement piles in sand," In: Charles W.W. Ng, L.M. Zhang, and Y.H. Wang, Eds., *Proc. 6th Int. Conf. of Physical Modelling in Geotechnics*. Hong Kong: Taylor & Francis Group, pp 889-894.

Wood, D.M. (2007) "The magic of sands-The 20th Bjerrum Lecture presented in Oslo, 25 November 2005," *Canadian geotechnical journal*, Vol. 44, No. 11, pp 1329-1350.

Xu, X., and B.M. Lehane (2008) "Pile and penetrometer end bearing resistance in two-layered soil profiles," *Géotechnique*, Vol. 58, No. 3, pp 187-197.

Yang, J., L.G. Tham, P.K. Lee, and F. Yu (2006a) "Observed performance of long steel H-piles jacked into sandy soils," *Journal of Geotechnical and Geoenvironmental Engineering*, Vol. 132, No. 1, pp 24-35.

Yang, J., L.G. Tham, P.K.K. Lee, S.T. Chan, and F. Yu (2006b) "Behaviour of jacked and driven piles in sandy soil," *Géotechnique*, Vol. 56, No. 4, pp 245-259.

Yang, L.Y.L., and R.L.R. Liang (2009) "Incorporating setup into load and resistance factor design of driven piles in sand," *Canadian geotechnical journal*, Vol. 46, No. 3, pp 296-305.

Yang, N.C. (1970) "Relaxation of piles in sand and inorganic silt," *Journal of the Soil Mechanics and Foundations Division*, Vol. 96, No. 2, pp 395-409.

Yang, Z.X., R.J. Jardine, B.T. Zhu, P. Foray, and C.H.C. Tsuha (2010) "Sand grain crushing and interface shearing during displacement pile installation in sand," *Géotechnique*, Vol. 60, No. 6, pp 469-482.

Yasufuku, N., and A.F.L. Hyde (1995) "Pile end-bearing capacity in crushable sands," *Géotechnique*, Vol. 45, No. 4, pp 663-676.

York, D.L., W.G. Brusey, F.M. Clemente, and S.K. Law (1994) "Setup and relaxation in glacial sand," *Journal of Geotechnical Engineering*, Vol. 120, No. 9, pp 1498-1513.

Yoshimi, Y., and T. Kishida (1981) "A ring torsion apparatus for evaluating friction between soil and metal surfaces," *ASTM geotechnical testing journal*, Vol. 4, No. 4, pp 145-152.

Zai, J. (1988) "Pile dynamic testing experiences in Shanghai," In: B.G. Fellenius, Ed., *Proc. 3rd Int. Conf. on the Application of Stress-Wave Theory to Piles*. Ottawa, Canada: Vancouver, BC, Canada: BiTech Publishers, pp 781-792.

Zhang, G., P.K. Robertson, and R.W.I. Brachman (2002) "Estimating liquefaction-induced ground settlements from CPT for level ground," *Canadian geotechnical journal*, Vol. 39, No. 5, pp 1168-1180.

Zhang, L.M., C.W. Ng, F. Chan, and H.W. Pang (2006) "Termination criteria for jacked pile construction and load transfer in weathered soils," *Journal of Geotechnical and Geoenvironmental Engineering*, Vol. 132, No. 7, pp 819-829.

Zhang, L.M., and H. Wang (2009) "Field study of construction effects in jacked and driven steel H-piles," *Géotechnique*, Vol. 59, No. 1, pp 63-69.

Zuidberg, H., and P. Vergobbi (1996) "EURIPIDES, load tests on large driven piles in dense silica sands," *Proc. Offshore Tech. Conf.* Houston, pp 193-206.